

UNCLASSIFIED

AD NUMBER

AD367584

CLASSIFICATION CHANGES

TO: UNCLASSIFIED

FROM: CONFIDENTIAL

LIMITATION CHANGES

TO:
Approved for public release; distribution is unlimited.

FROM:
Distribution authorized to U.S. Gov't. agencies and their contractors;
Administrative/Operational Use; 11 NOV 1965.
Other requests shall be referred to Air Force Rocket Propulsion Lab, Edwards AFB, CA.

AUTHORITY

Oct 30, 1977 per document markings and DoD 5200.1r. .

THIS PAGE IS UNCLASSIFIED

GENERAL DECLASSIFICATION SCHEDULE

**IN ACCORDANCE WITH
DOD 5200.1-R & EXECUTIVE ORDER 11652**

THIS DOCUMENT IS:

**Subject to General Declassification Schedule of
Executive Order 11652-Automatically Downgraded at
2 Years Intervals- DECLASSIFIED ON DECEMBER 31, 1972**

BY

**Defense Documentation Center
Defense Supply Agency
Cameron Station
Alexandria, Virginia 22314**

SECURITY

MARKING

The classified or limited status of this report applies to each page, unless otherwise marked.

Separate page printouts MUST be marked accordingly.

THIS DOCUMENT CONTAINS INFORMATION AFFECTING THE NATIONAL DEFENSE OF THE UNITED STATES WITHIN THE MEANING OF THE ESPIONAGE LAWS, TITLE 18, U.S.C., SECTIONS 793 AND 794. THE TRANSMISSION OR THE REVELATION OF ITS CONTENTS IN ANY MANNER TO AN UNAUTHORIZED PERSON IS PROHIBITED BY LAW.

NOTICE: When government or other drawings, specifications or other data are used for any purpose other than in connection with a definitely related government procurement operation, the U. S. Government thereby incurs no responsibility, nor any obligation whatsoever; and the fact that the Government may have formulated, furnished, or in any way supplied the said drawings, specifications, or other data is not to be regarded by implication or otherwise as in any manner licensing the holder or any other person or corporation, or conveying any rights or permission to manufacture, use or sell any patented invention that may in any way be related thereto.

CONFIDENTIAL

NO. C27-5C68.68A
DOCUMENT CONTROL

367584

(Unclassified Title)

**AN INTEGRATED RESEARCH EFFORT ON
HIGH-ENERGY HYBRID PROPELLANTS**

**TECHNICAL DOCUMENTARY
REPORT NO. AFRPL-TR-65-184**

OCTOBER 1965

**AIR FORCE ROCKET PROPULSION LABORATORY
RESEARCH AND TECHNOLOGY DIVISION
AIR FORCE SYSTEMS COMMAND
UNITED STATES AIR FORCE
EDWARDS AFB, CALIFORNIA**

PROJECT NO. 305804



**(PREPARED UNDER CONTRACT NO. AF 04(611)-8516
BY UNITED TECHNOLOGY CENTER, SUNNYVALE, CALIFORNIA)**

AUTHOR: C.W. VICKLAND

CONFIDENTIAL

**Group 4
DOWNGRADED AT 3 YEAR INTERVALS
DECLASSIFIED AFTER 12 YEARS**

NOTICES

Qualified requesters may obtain copies from the Defense Documentation Center.

When U. S. Government drawings, specifications, or other data are used for any purpose other than a definitely related government procurement operation, the government thereby incurs no responsibility nor any obligation whatsoever; and the fact that the government may have formulated, furnished, or in any way supplied the said drawings, specifications, or other data is not to be regarded by implication or otherwise, as in any manner licensing the holder or any other person or corporation, or conveying any rights or permission to manufacture, use, or sell any patented invention that may in any way be related thereto.

CONFIDENTIAL
United Technology Center

DIVISION OF UNITED AIRCRAFT CORPORATION

**U
A
C**

11 November 1965

BKF-2121-65-F

Air Force Rocket Propulsion Laboratory
Edwards Air Force Base, California

Attention: RPRE

Subject: AFRPL-TR-65-184 (UTC Report No. 2098-FR)

Reference: Contract AF 04(611)-8516, Supplemental Agreement
No. 3, dated 30 June 1964

Gentlemen:

United Technology Center submits three (3) copies of the subject report
in accordance with the referenced contract.

It is requested that the Contracting Officer provide UTC with an acceptance
of this Final Report.

Yours very truly,

UNITED TECHNOLOGY CENTER
A Division of United Aircraft Corporation


B. K. Forman, Manager
Contract Management

BKF:erb

Enclosures

cc: AFFTC, Edwards AFB, California 93523
Attn: FTMKR-4 (w/encl)
AFPRO, UTC, Sunnyvale, California 94088
Attn: CMRQK (w/encl)
Air Force Designated Government Agency and
Corporate Distribution (w/encls)

This letter down-
graded to unclassi-
fied if detached
from accompanying
material.

SUNNYVALE, CALIFORNIA 94088

CONFIDENTIAL

Phone 739-4880

FOREWORD

(C) Under Contract No. AF 04(611)-8516, United Technology Center (UTC) has been conducting an applied research and development program on high-energy hybrid propellant systems. The program was initiated in August 1962 with an effort directed toward high-energy space-storable propellant systems. The original objectives included the development of a 5000-lb thrust hybrid motor capable of a specific impulse in excess of 300 sec (1000/14.7) with space storable propellants, 20 sec of full thrust operation, multiple start operation, and thrust modulation over at least a 12:1 range.

(C) Prior to initiation of the present follow-on effort, all of the objectives except throttling had been demonstrated with a propellant system consisting of OF_2 and a fuel containing 25% lithium, 10% lithium hydride, and 65% binder. The throttleable motor development studies were, therefore, completed using this same fuel system.

(C) In December 1964 a portion of the program was redirected toward the investigation of prepackaged hybrid propellant systems suitable for application in air-launched tactical missiles so that the program objectives would be consistent with current Air Force studies. The revised Phase II program objectives included the selection and evaluation of candidate propellants applicable to a prepackaged tactical missile system. This system requires a propellant system which is storable between -65° and $+165^\circ$ F, is nonsustaining so that motor shutdown and restart are achievable, and which produces an exhaust plume with favorable radar attenuation and reflection properties. A propellant system consisting of an oxidizer containing either chlorine pentafluoride (ClF_5) and/or bromine pentafluoride (BrF_5) and/or perchloryl fluoride (ClO_3F) with a fuel containing triaminoguanidine azide (TAZ), boron, ammonium perchlorate (AP), and binder have the potential of meeting these objectives.

(U) The research activity reported in this publication (UTC Publication No. 2098-FR) was supported by the Advanced Research Projects Agency.

ABSTRACT

(C) A lightweight 12-in. hybrid test motor has been developed which is capable of delivering 5000-lb thrust for 20-sec duration and up to 90-sec duration at reduced thrust. The motor has consistently delivered a specific impulse in excess of 300 sec (1000/14.7), with a high value of 316 sec, is capable of multiple restarts, and can be throttled over a 13.8:1 ratio while maintaining a nearly constant mixture ratio. The propellant system, which consists of OF_2 and a fuel containing lithium, lithium hydride, and a binder has demonstrated its suitability to space storable mission requirements. Further development of this propulsion system would now require the application of the technology achieved to lightweight motor designs and to statistical evaluation of fuel utilization and motor performance in multiple tests of flight configuration motors.

(C) Injector development studies have resulted in several injector designs which will eliminate the requirement for injector shielding and reduce or eliminate the requirement for a splash block. Other successful injector designs include poppet-type injectors which allow injector-face oxidizer shutoff, a dual manifold injector which permits dual thrust operation, and regeneratively cooled multiple stream injectors which operate fully exposed to the combustion chamber environment.

(C) Fuel system studies were conducted with a fuel containing 50% THA and 50% binder which, because of its pressure-sensitive behavior, showed promise as a substitute for the Li/LiH/binder fuel system. In scaling from laboratory to 5.0-in. motors it became apparent that the pressure sensitivity is reduced by many motor and operating parameters. Thus, the usefulness of pressure sensitivity to control mixture ratio during throttling would be limited without considerable additional study. Therefore, further work on the development of a throttleable motor was conducted using the nonpressure sensitive Li/LiH fuel system.

(C) A thrust control system that includes a thrust control valve, an oxidizer flow-divider valve, and a control network has been designed and successfully tested. This system distributes the oxidizer to primary and aft injectors in such a manner as to produce a 50:1 throttling ratio.

CONFIDENTIAL

(C) Formulations studies have resulted in the selection of a potential pre-packaged hybrid propellant system that consists of ClF_5 and a fuel containing triaminoguanidine azide (TAZ) or tetraformaltrisazine (TFTA), boron or aluminum, ammonium perchlorate, and a binder. This propellant system was selected because it has high theoretical specific and density impulse levels. Processing studies have produced castable blends of the four components with solid loadings as high as 80%.

(C) Fifty-six 3.5-in. motor tests were conducted using ClF_3 to evaluate and screen the fuel systems. Forty 5.0-in. motor tests were conducted with five fuel blends using the components previously mentioned. These tests evaluated the regression characteristics of pelletized and homogeneous fuel blends and demonstrated the feasibility of pelletized non-sustaining hybrid fuel grains.

(C) In addition, a fuel containing 35% TFTA, 20% aluminum, 15% AP, and 30% binder was used in six 12-in. motor tests, delivering up to 95% of the theoretical specific impulse. Two tests were conducted with this fuel for durations of 30 sec using an oxidizer consisting of 18% ClO_3F and 72% ClF_3 . Another motor was tested and restarted three times using ClF_3 as the oxidizer.

(U) Publication of this Technical Documentary Report does not constitute Air Force approval of the report's findings or conclusions. It is published only for the exchange and stimulation of ideas.

(U) Catalog cards with an unclassified abstract may be found in the back of this document.

CONFIDENTIAL

CONTENTS

<u>Section</u>	<u>Page</u>
FOREWORD	ii
ABSTRACT	iii
1.0 THROTTLING STUDIES – HIGH-ENERGY PROPELLANTS (PHASE I)	1
1.1 Pressure-Sensitive Fuels	1
1.1.1 Laboratory Motor Studies	8
1.1.2 5.0-In. Motor Studies	10
1.2 Injector Development	17
1.2.1 Hollow-Cone Injectors	18
1.2.2 Aeration	21
1.2.3 Subscale Aeration Motor Tests	24
1.2.4 Regenerative-Cooled Injectors	33
1.2.5 Variable-Area Injectors	33
1.2.6 Poppet Injectors	42
1.3 Control System Development	47
1.4 Throttleable Motor Development	56
1.4.1 Motor Design	61
1.4.2 Throttleable Motor Test Program	66
1.5 Qualitative Prediction of the Reliability and Maintainability of Space-Storable Motors	99
2.0 PREPACKAGED HYBRID PROPELLANT SYSTEMS (PHASE II)	101
2.1 Prepackaged Hybrid Propellant Studies	101
2.1.1 Propellant Evaluation	102
2.1.2 Temperature Effects	104
2.1.3 Fuel Components	107
2.1.4 Formulation and Processing	110
2.2 Subscale Motor Test Program	114
2.2.1 3.5-In. Motor Tests	114
2.2.2 5.0-In. Motor Tests	118
2.3 Twelve-In. Motor Tests	127
2.3.1 Motor No. 008	130
2.3.2 Motor No. 009	136
2.3.3 Motor No. 010	140

CONTENTS (Continued)

<u>Section</u>	<u>Page</u>
2.4 Qualitative Prediction of the Reliability and Maintainability of Storable Prepackaged Motors	142
APPENDIX I: Implications of Pressure-Sensitive Hybrid Fuel Systems	147
APPENDIX II: Method for Determining Regression Rate Equation for Pressure-Sensitive Fuel System	153
APPENDIX III: Thermochemistry of a High-Nitrogen Propellant Ingredient	157
APPENDIX IV: Assembly Drawing of 12-In. Filament-Wound Hybrid Motor	167
APPENDIX V: Summary of Motor Tests	171

ILLUSTRATIONS

<u>Figure</u>		<u>Page</u>
1	Theoretical Performance of Space Storable Hybrid Propellants	3
2	Laboratory Survey Motor	4
3	5.0-In. Hybrid Test Motor	5
4	Regression Rate as a Function of Chamber Pressure for Fuels with THA	6
5	Regression Rate as a Function of Chamber Pressure for TAZ-Containing Fuels	7
6	Regression Behavior of Pressure Sensitive Fuel in Survey Motor	9
7	Initial Regression Rate of Pressure-Sensitive Fuel in Survey Motor	9
8	Regression Behavior of Li/LiH/Binder Fuel in Survey Motor	11
9	Regression Rate as a Function of Chamber Pressure for Conventional Fuel in Survey Motor Tests	11
10	Average Regression Rate as a Function of Chamber Pressure, 5.0-In. Motor Data	12
11	Fuel Regression versus Burning Time for 50% THA/50% Binder Fuel (C)	14
12	Fuel Flow Rate versus Oxidizer Flow Rate for the THA/Binder Fuel	15
13	Regression Behavior of 50% THA/50% Binder Fuel in Small-Port Motor (C)	16
14	Hollow-Cone Injector	19
15	5.0-In. Fuel Grain After Test Using Hollow-Cone Injector	20
16	Grain Tapering at Low G_0	20

ILLUSTRATIONS (Continued)

<u>Figure</u>		<u>Page</u>
17	Effect of Oxidizer Spray-Cone Angle on Fuel Grain Regression	21
18	5000-lb-Thrust Motor Injector	22
19	5000-lb-Thrust Motor Injector (Modified)	23
20	Cold-Flow Aeration Test Using Water	25
21	Cold-Flow Aeration Tests Using LOX	27
22	Comparison of LOX and Water Flow Aeration Tests	28
23	Aerated Hollow-Cone Injector	29
24	Solid-Cone Injector	29
25	Typical Fuel Grain Profiles After Firing with Aerated Hollow-Cone Injector	30
26	Effect of Helium Aeration Flow Rate on Fuel Grain Tapering	31
27	Typical Fuel Grain Profiles After Firing with Solid-Cone Injector	32
28	Impinging Streams Injector	34
29	Showerhead Injector	35
30	Spray Pattern of Impinging Streams Injector	30
31	Showerhead Injector After Test	37
32	Grain Fired with Showerhead Injector	38
33	Variable-Area Hollow-Cone Injector	39
34	Movable Poppet Injector	40
35	Injector Spray-Cone Angle as a Function of Injector Orifice Area	41
36	Spray Pattern of Variable-Area Poppet Injector	41
37	Variable-Area Poppet Injector	43
38	Poppet Injector	44
39	Spray Pattern of Poppet Injector	45
40	Shutoff Orifice Injector	46

ILLUSTRATIONS (Continued)

<u>Figure</u>		<u>Page</u>
41	Oxidizer Flow Rate as a Function of Motor Thrust	48
42	Schematics of Control Systems	49
43	Selected Flow-Control System	50
44	Thrust Control Valve	52
45	Flow Divider Valve	53
46	Hybrid Thrust Control Circuit	55
47	Oxidizer Flow Control Valve	57
48	Thrust Control Valve Assembly	58
49	Full-Scale Filament-Wound Motor	59
50	5000-lb-Thrust Motor Designs	60
51	Full-Scale Test Motor Schematic	63
52	Mixer Assembly	65
53	Three-Spoke Fuel Grain	67
54	Filament Winding a 12-in. Motor Case	67
55	Lightweight Nozzle	68
56	Motor 001 Components After Test	71
57	Splash Block from Motor 001	72
58	Fuel Grain of Motor 001 After Test	73
59	Original Injector Installation	74
60	Modified Injector Installation	74
61	Nozzle Assembly After Test	75
62	Injector After Test	77
63	Failed Injector	78
64	Test Sequence Showing Aft Injector Manifold Failure	79
65	Throttled Motor Oscillograph Record, Motor 004	81
66	Mixture Ratio vs Thrust for Full-Scale Motor	82
67	Full-Scale Motor Aft Injector Design	83

ILLUSTRATIONS (Continued)

<u>Figure</u>		<u>Page</u>
68	Full-Scale Motor Injector After Test	86
69	Full-Scale Motor 005 After Test	87
70	Full-Scale Motor 001 After Test	88
71	Splash Block After Test	89
72	Sectioned Mixer Plenum with Aft Injector After Test	90
73	Mixer Assembly After Test	91
74	Close-up View of Mixer Wall	92
75	Thrust Trace of Throttled Motor 006	93
76	Fuel Grain from Motor 006 After Test	94
77A	Fuel Grain from Motor 007 After Test	95
77B	Fuel Grain from Motor 007 After Test	96
78A	Carbon Cloth-Phenolic Nozzle	97
78B	Carbon Cloth-Phenolic Nozzle	98
79	Estimated Oxidizer Vapor Pressures	105
80	Effect of Temperature on Oxidizer Density	107
81	Performance of Four-Component Fuels	108
82	Fuel Compatibility Samples	113
83	3.5-In. Hybrid Motor	115
84	5.0-In. Hybrid Motor	116
85	Effect of AP Loading on Fuel Regression Rate	116
86	3.5-In. Homogeneous Fuel Grain After Test	117
87	3.5-In. Pelletized Fuel Grain After Test	117
88	Light Sensing Probes	120
89	Regression Behavior of Fuel Containing 35% TFTA/20% Boron/15% AP/30% Binder (C)	121
90	Typical 5.0-In. Hybrid Fuel Grain After Test	122
91	Regression Behavior of Fuel Containing 35% TFTA/20% Al/15% AP/30% Binder (C)	123

ILLUSTRATIONS (Continued)

<u>Figure</u>		<u>Page</u>
92	5.0-In. Fuel Grain, Postfire, Containing Boron and Pelletized AP	124
93	Pressure Effects on Pelletized Hybrid Fuels	125
94	Regression Behavior of Fuel Containing 22% TFTA/20% Al/38% AP (Pelletized)/20% Binder	128
95	Regression Behavior of Fuel Containing 45% TFTA (Compacted)/20% Al/35% Binder	129
96	Three-Component Fuel System with Compacted TFTA	130
97	12-In. Hybrid Fuel Grain	131
98	12-In. Hybrid Motor Firing	132
99	Photo Sequence of Motor 008 - Fuel Grain After 5, 10, and 15 sec Duration	134
100	Fuel Grain From Motor 008 After Test	135
101	Splash Block From Motor 008 After Test	137
102	Mixer Assembly From Motor 008 After Test	138
103	Poppet Injector Assembly	139
104	Splash Block From Motor 010 After Test	141
105	Mixer Assembly From Motor 010 After Test	143
106	Phenolic Mixer Baffle After Test	144
107	Dust Orifice Injector Assembly	145

TABLES

<u>Table</u>		<u>Page</u>
I	Oxidizer Flow-Control Valve Requirements	54
II	High-Performance, Full-Thrust Motor Tests	61
III	Test Summary Phase I Full-Scale Motor Test Program	69
IV	Calculated Specific Impulse Performance	85
V	Hybrid Propellant Combinations Selected for Evaluation	102
VI	Theoretical Performance of Storable Hybrid-Propellant Systems	103
VII	Oxidizer Physical Properties	106
VIII	Relative Performance Levels	133

SYMBOLS

	Proportionality constant
A_p	Fuel port area, in. ²
A_t	Nozzle throat area
c^*	Characteristic velocity, ft/sec
ϵ	Nozzle expansion ratio = area of nozzle exit divided by area of nozzle throat
F_n	Motor thrust, lb
g	Gravitational constant, ft/sec ²
G_o	Oxidizer mass flux $\left(\frac{\dot{w}_{ox}}{A_p}\right)$, lb/sec-in. ²
I_{sp}	Specific impulse, sec
L	Fuel grain length, in.
m	Pressure-sensitivity exponent
n	Oxidizer mass flux exponent
O/F	Mixture ratio (gravimetric)
P_b	Burning perimeter of fuel grain, in.
P_c	Combustion chamber pressure, psia
R	Fuel port radius, in.
\dot{r}	Regression rate, in./sec
\bar{r}	Average regression rate, in./sec
ρ_f	Fuel density, lb/in. ³
\dot{w}_f	Fuel flow rate, lb/sec
\dot{w}_{ox}	Oxidizer flow rate, lb/sec

1.0 THROTTLING STUDIES - HIGH-ENERGY PROPELLANTS (PHASE I)

(C) Original program objectives included the development of a 5000-lb thrust hybrid motor capable of delivering a specific impulse in excess of 300 sec (1000/14.7) with space-storable propellants, a full thrust duration of 20 sec, start-stop-restart operation, and thrust modulation over the widest possible range. A goal of 50:1 throttling ratio was set with an objective of achieving a ratio of at least 12:1.

(C) Throttling studies were completed using a propellant system consisting of $F_2 + 1/2 O_2$ (FLOX) and the 25% lithium, 10% lithium hydride, 65% hydrocarbon binder fuel. The studies have included pressure-sensitive fuel investigation, injector development, control system development, and throttleable motor development tests.

(U) As a result of these studies, a lightweight 5000-lb thrust filament-wound hybrid test motor has been developed which demonstrated throttling ratios in excess of 13:1, was fired for individual test durations of 60 sec and cumulative durations of 90 sec, and demonstrated its restart capability on several occasions. The motor has demonstrated a high level of performance in eleven tests and has provided substantial qualitative design data that can now be incorporated into flightweight motor designs. It is left to subsequent programs to statistically evaluate motor performance and demonstrate fuel utilization in multiple tests of flight configuration motors.

(C) Two fuel systems were evaluated for use with OF_2 , representing two concepts in throttleable hybrid motors. The Li/LiH/binder fuel requires that oxidizer be injected at the aft end of the motor to maintain optimum mixture ratio during throttled operation. The second fuel system contains a pressure-sensitive additive, THA, which had the potential for producing a linear fuel/oxidizer flow relationship, thereby eliminating the need for aft injection. When the pressure-sensitive fuel system proved unsuccessful, the throttleable motor studies were completed using the Li/LiH/binder fuel system.

1.1 PRESSURE-SENSITIVE FUELS

(C) A new family of hybrid fuels were investigated as a possible substitute for the Li/LiH/binder fuel system. The fuels consist of various blends of binder and TAZ or its double salt, THA. These fuels were of interest

because, under certain conditions, they show a pronounced regression rate dependency on combustion chamber pressure. The implications of this pressure effect include the possible development of a hybrid fuel system which does not require aft-end injection of oxidizer to maintain an optimum mixture ratio during throttled operation.

(C) It can be shown (see appendix I) that if the fuel regression rate is expressed by the anticipated form

$$\dot{r} = a P_c^m G_o^n \quad (1)$$

where:

\dot{r} = regression rate (in./sec)

a = constant

G_o = oxidizer mass flux (lb/sec-in.²)

P_c = combustion chamber pressure (psi)

n = oxidizer mass flux exponent

m = pressure sensitivity,

a constant oxidizer/fuel (O/F) ratio can be maintained if the sum of the exponents ($m + n$) equal 1.0.

(C) The lithium fuel has an exponent, n , equal to 0.5 and laboratory motor data obtained from fuels containing 50% THA and 50% binder produced pressure exponents (m) nearly equal to 0.5. A fuel system possessing a combination of exponents equal to these would produce the desired effect.

(C) Both fuel systems deliver a high specific impulse with oxygen difluoride (OF₂) and are potentially suitable for space applications. As shown in figure 1, the theoretical specific impulse of the lithium fuel system with OF₂ is 345 sec (1000/14.7) as compared to 341 sec for the 50% THA/50% binder fuel. In a full-scale motor, the slightly lower performance would be offset by simplification of the oxidizer distribution system, elimination of aft injectors, and flow control valves.

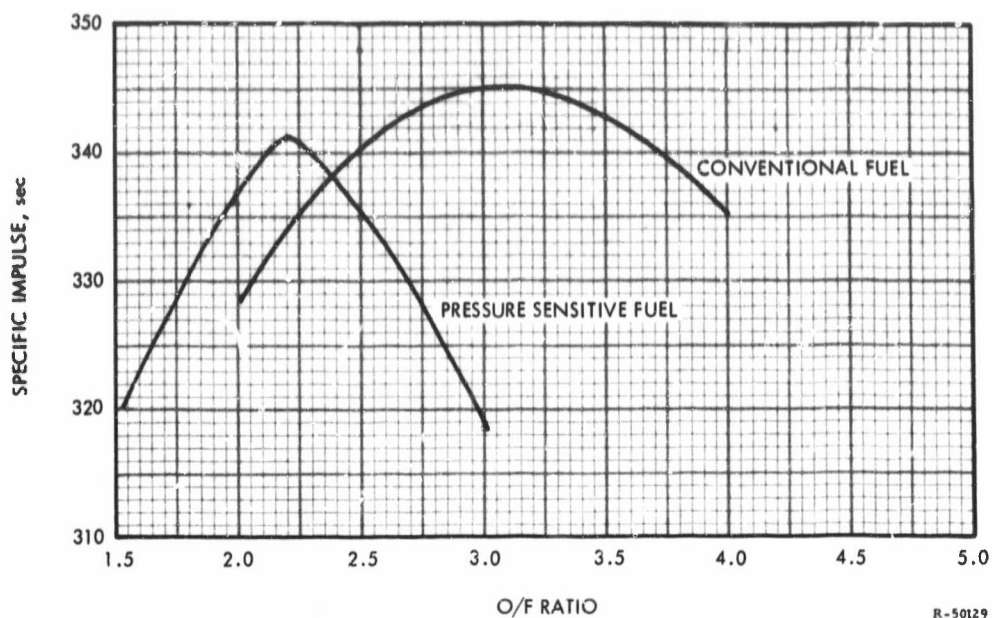


Figure 1. (U) Theoretical Performance of Space Storable Hybrid Propellants

(U) Two motor sizes were used in the evaluation of pressure-sensitive fuels: the laboratory survey motor shown in figure 2 and the 5.0-in. motor shown in figure 3. Laboratory survey motors were used to screen fuel samples for effects of variation in formulation and chamber pressure on grain regression. The 5.0-in. -diameter subscale motors were used with 2.0-in. port fuel grains to obtain data to develop the empirical relations that characterize the fuels.

(C) Preliminary data were initially obtained in a UTC-sponsored program in which laboratory survey motor tests were used to determine average regression rate as a function of pressure for various percentages of THA and TAZ at a constant oxidizer mass flux of $0.270 \text{ lb/sec-in.}^2$. Figures 4 and 5 indicate this relative sensitivity by the slope of the curves. From these curves it is apparent that the fuel system may be altered to obtain the pressure exponent desired. However, these average regression-rate data are obtained from small motors with short firing durations (up to 4 sec) and are indicative of relative effects only. Studies conducted in the laboratory survey motors on this program yielded pressure exponents (m) equal to 0.46 in tests using gaseous oxygen as oxidizer. An exponent of 0.46 is an extremely useful degree of pressure sensitivity if coupled with a high mass flux exponent (n). However, 5.0-in. motor tests conducted with FLOX resulted in a negligible pressure exponent. Further testing

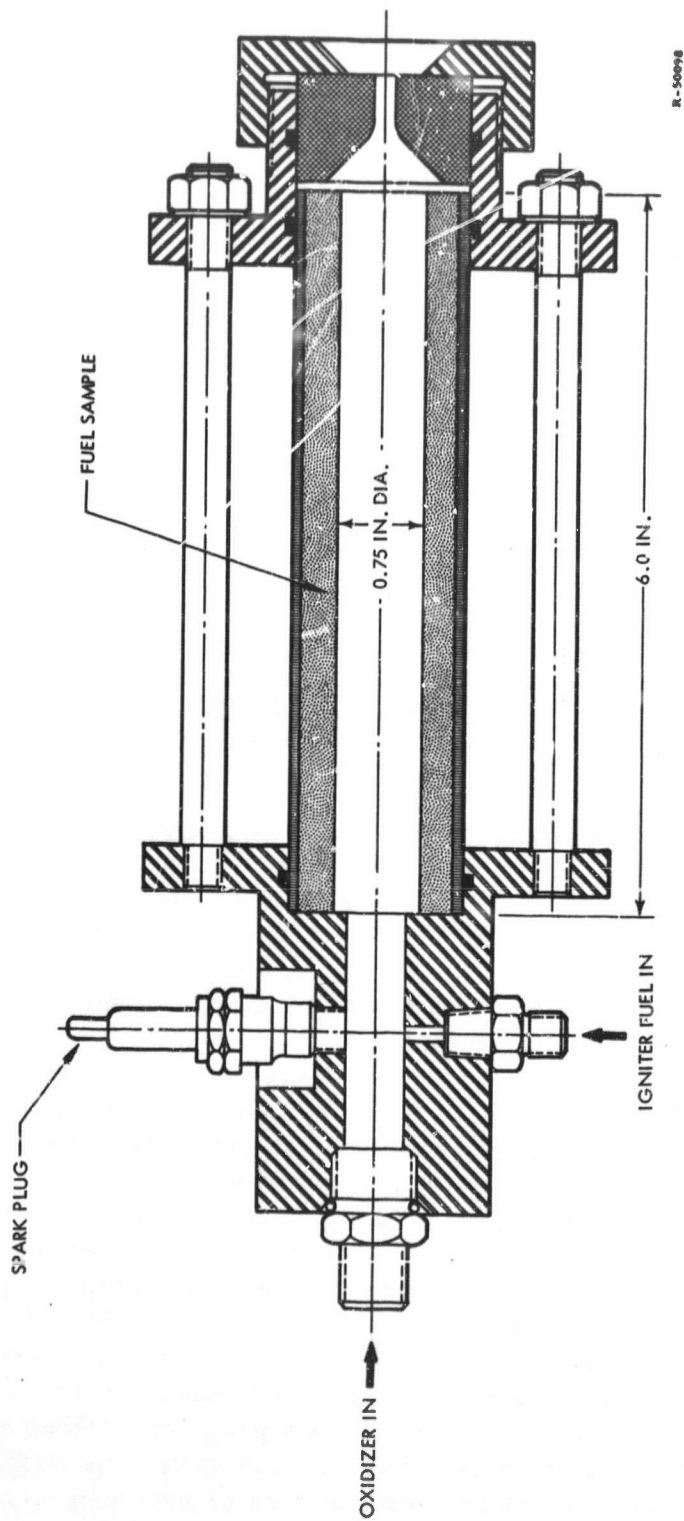


Figure 2. (U) Laboratory Survey Motor

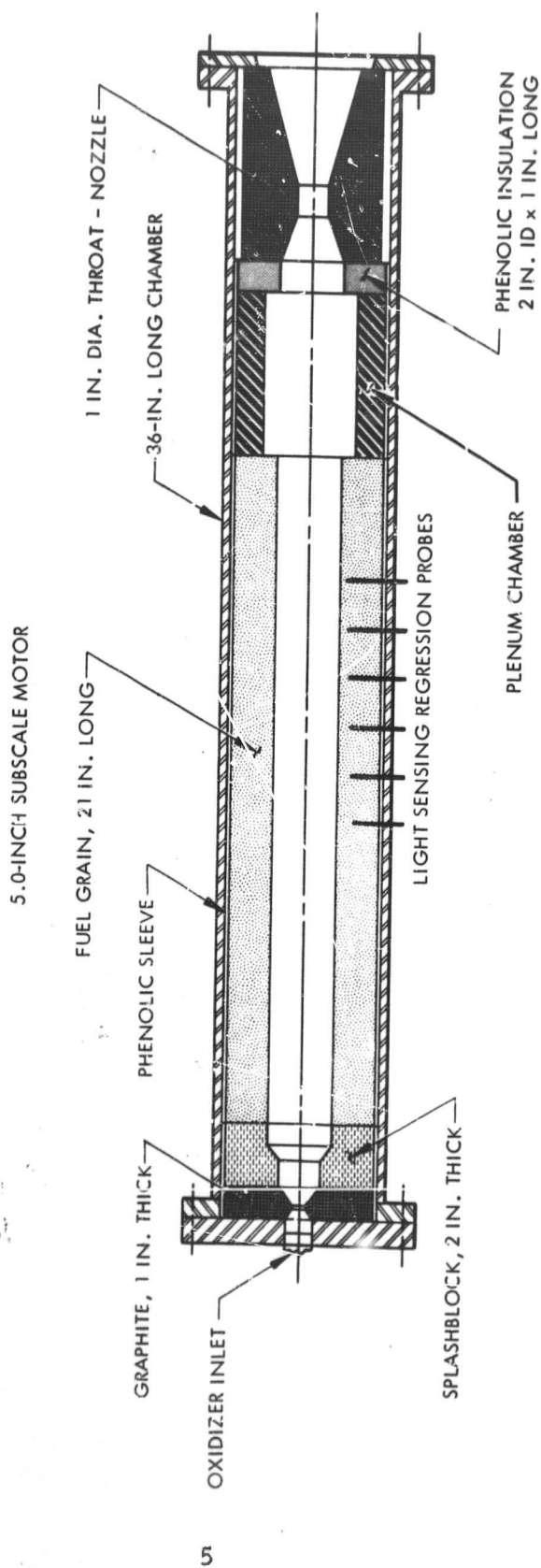


Figure 3. (U) 5.0-in. Hybrid Test Motor

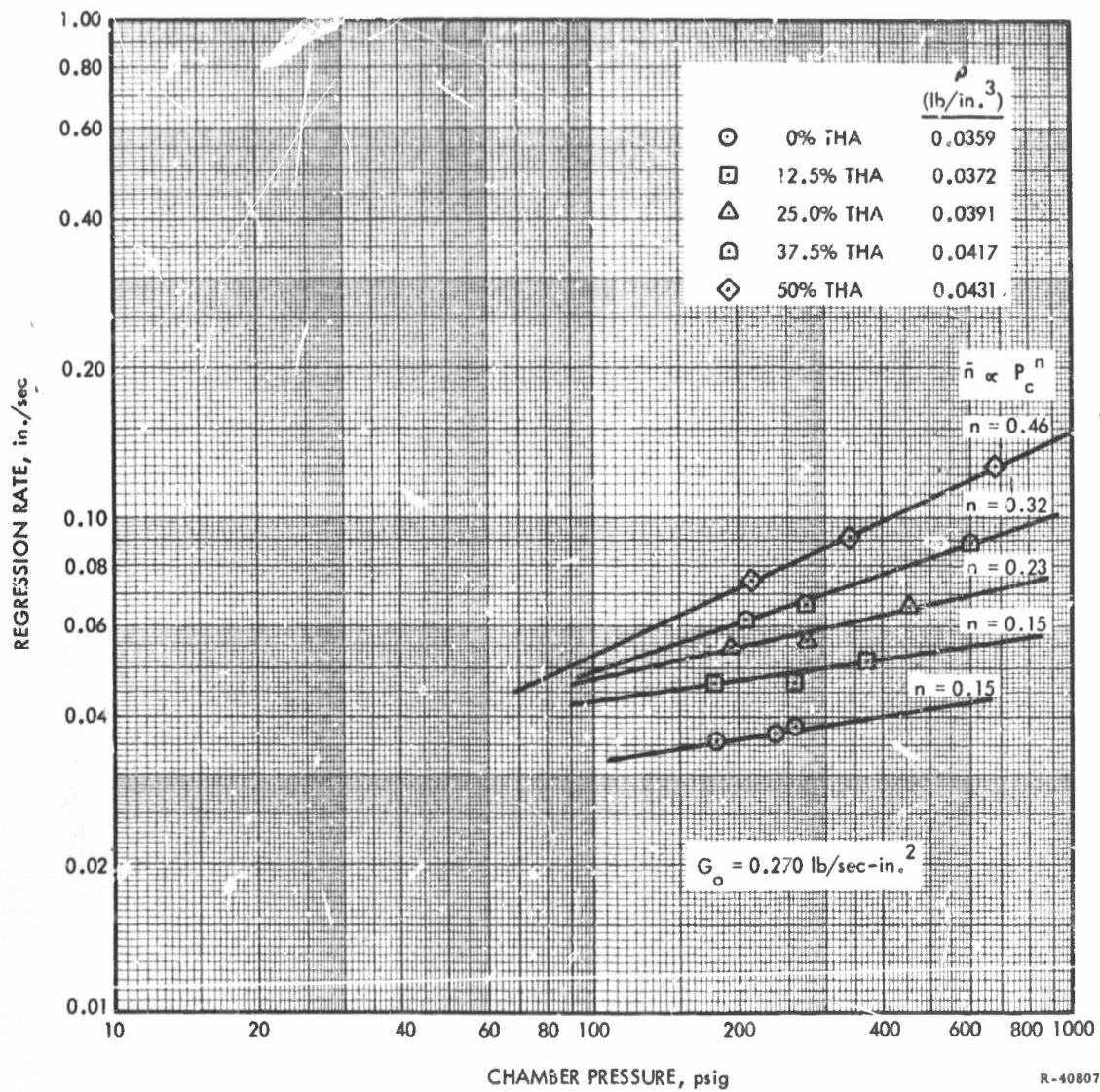


Figure 4. (U) Regression Rate as a Function of Chamber Pressure for Fuels with THA

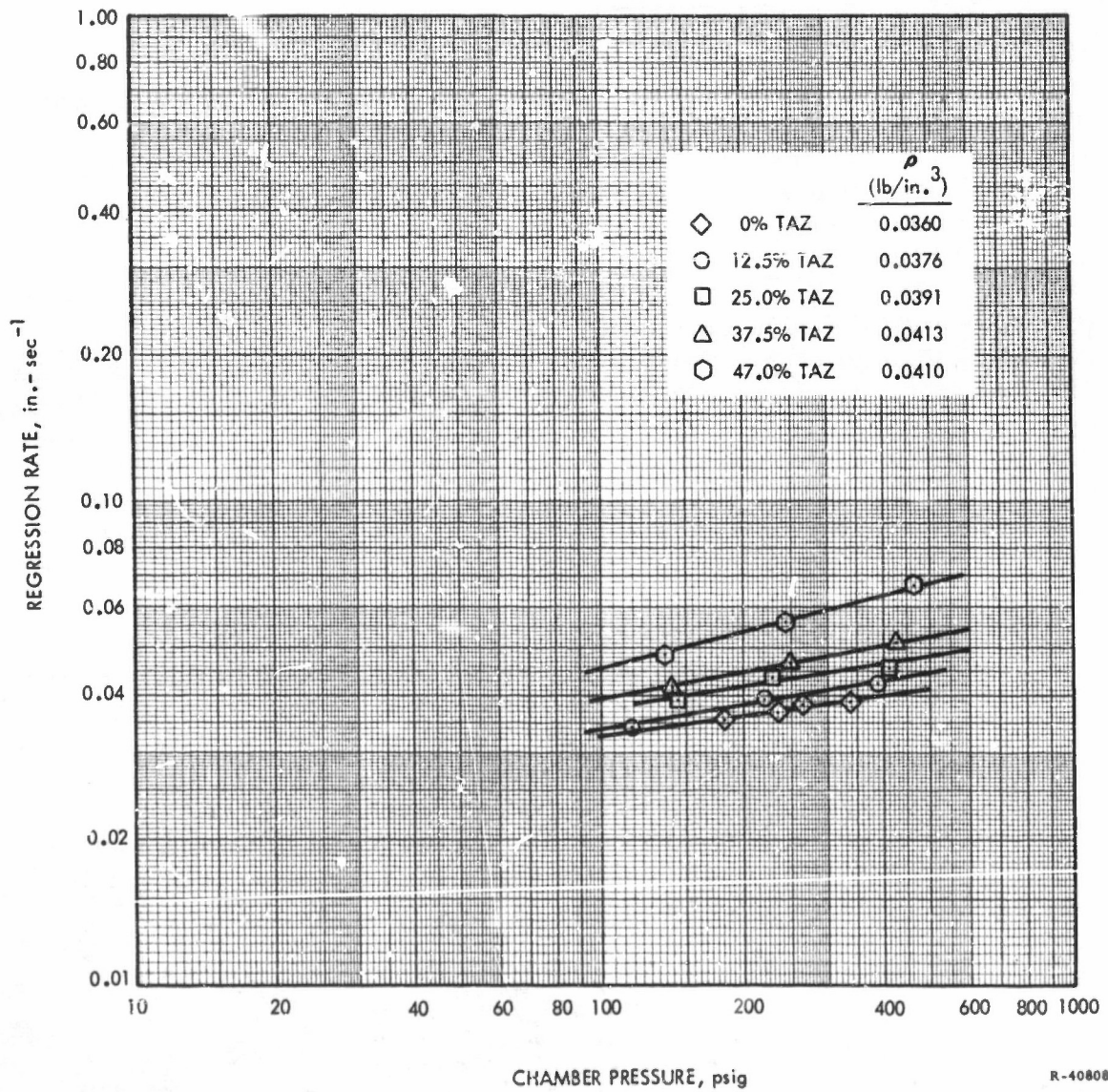


Figure 5. (U) Regression Rate as a Function of Chamber Pressure for TAZ-Containing Fuels

with liquid oxygen instead of FLOX yielded an exponent of 0.39, implying that oxygen concentration in the oxidizer may be a significant parameter. Further tests in 5.0-in. motors also demonstrated that motor dimensions play a significant part. The results indicated that additional fundamental work was needed before TAZ and THA fuels could be used in full-scale motors. The investigation was therefore discontinued.

1.1.1 Laboratory Motor Studies

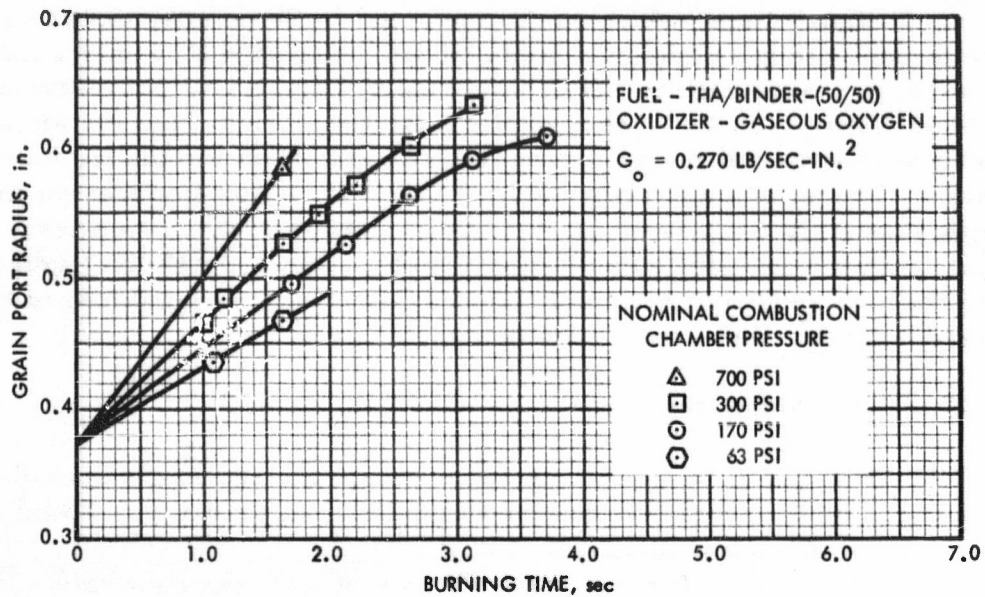
(C) Laboratory survey motor studies have demonstrated a high degree of pressure sensitivity with fuels containing 50% THA and 50% polybutadiene. These studies were conducted to verify the test results obtained under a program sponsored by UTC because these tests showed a definite pressure-sensitive effect that was not present in previous 5.0-in. motor tests with a similar fuel formulation. (The results of these 5-in. motor tests are discussed in paragraph 1.12.)

(C) Twenty-four additional survey motor tests were conducted during this study to determine accurately the degree of pressure sensitivity of the 50% THA fuel system and to investigate possible motor size effects indicated by differences between the survey motor data and the 5.0-in. motor data. Fifteen survey motor tests were conducted with the 50% THA/50% binder fuel and gaseous oxygen. The gaseous oxygen flow rate was held constant at 0.12 lb/sec and chamber pressure and test durations were varied to obtain curves of port radius as a function of burning time and chamber pressures.

(U) The results of laboratory survey motor tests, shown in figure 6, disclose a definite pressure effect in this size motor. Regression rate is essentially constant to a burned radius of approximately 0.575 in. The curve of regression rate versus chamber pressure, shown in figure 7, is taken from the initial slopes of the curves in figure 6. Included on this curve are some of the data points obtained in the initial screening tests of THA fuels. These data would indicate that if the regression behavior is expressed by an equation of the form

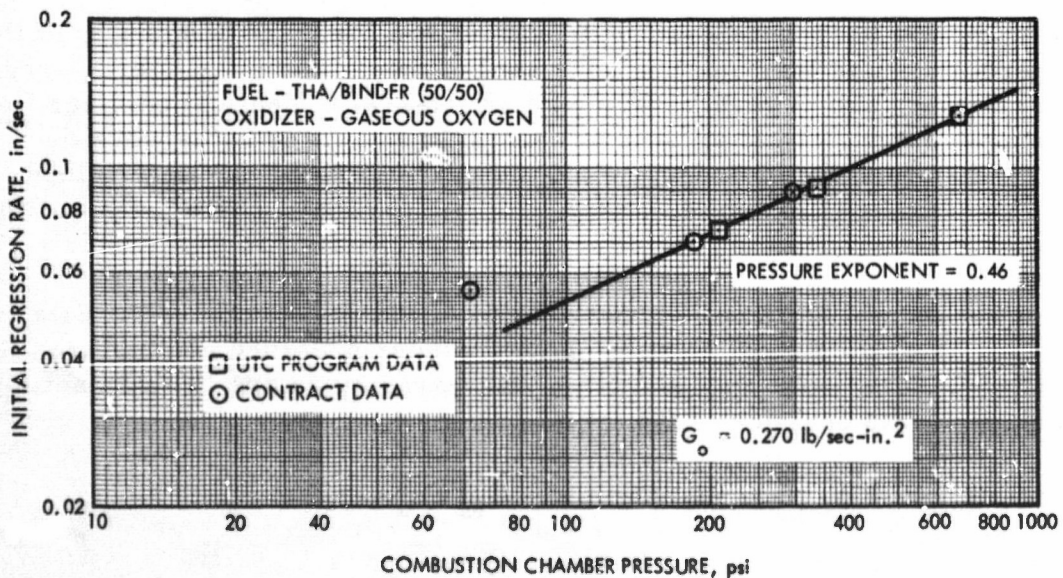
$$\dot{r} = a G_o^n P_c^m$$

then the value of m is approximately 0.46, which is a useful degree of pressure sensitivity.



R-50099

Figure 6. (U) Regression Behavior of Pressure Sensitive Fuel in Survey Motor



R-50290 A

Figure 7. (U) Initial Regression Rate of Pressure-Sensitive Fuel in Survey Motor

CONFIDENTIAL

(U) Additional tests, which were conducted in the survey motor using the conventional lithium composite fuel system, indicated that only a minor degree of pressure sensitivity can be expected in typical conventional fuels. The data taken from the survey motor with the lithium fuel system agree exactly with the established regression rate equation for the lithium fuel system. These data are presented in figure 8. A pressure exponent, m , of approximately 0.09 is obtained for this fuel when data from tests with equal durations are plotted as a function of chamber pressure (figure 9). The pressure sensitivity of the lithium system is not considered to be significant enough to influence grain design.

1.1.2 5.0-In. Motor Studies

(C) The 50% THA/50% binder fuel was characterized in a series of thirty-two 5.0-in. motor tests summarized in table I, appendix V. Twenty-four tests were conducted with FLOX to characterize the fuel system. The motors were tested at various combinations of oxidizer flow rate and chamber pressures to determine the regression rate sensitivity to pressure and oxidizer mass flux.

(U) Fuel regression probes were used to record the passing of burning fuel surface. The probes were located at various depths so that a history of the fuel grain surface could be obtained as a function of burning time.

(U) Two methods were used to determine the pressure sensitivity of the fuel system. The first method consisted of determining the average regression rate for each of several firings conducted with identical oxidizer flow rates and varying chamber pressures. These average rates were then plotted as a function of pressure and the pressure exponent determined from the slope of this curve (figure 10). An exponent of 0.11 was obtained, indicating a negligible degree of pressure sensitivity.

(U) The second method involved the use of the regression probe data from a series of motor firings in which both chamber pressure and oxidizer flow rate vary. The probe data and other test parameters are fit to an anticipated regression rate equation of the form

$$\dot{r} = a P_c^m G_o^n$$

CONFIDENTIAL

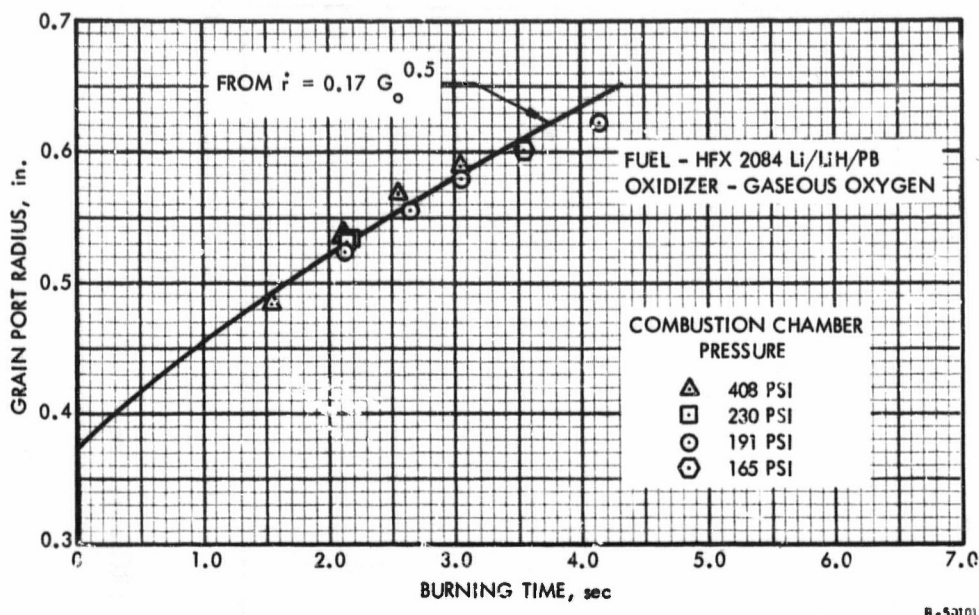


Figure 8. (U) Regression Behavior of Li/LiH/Binder Fuel in Survey Motor

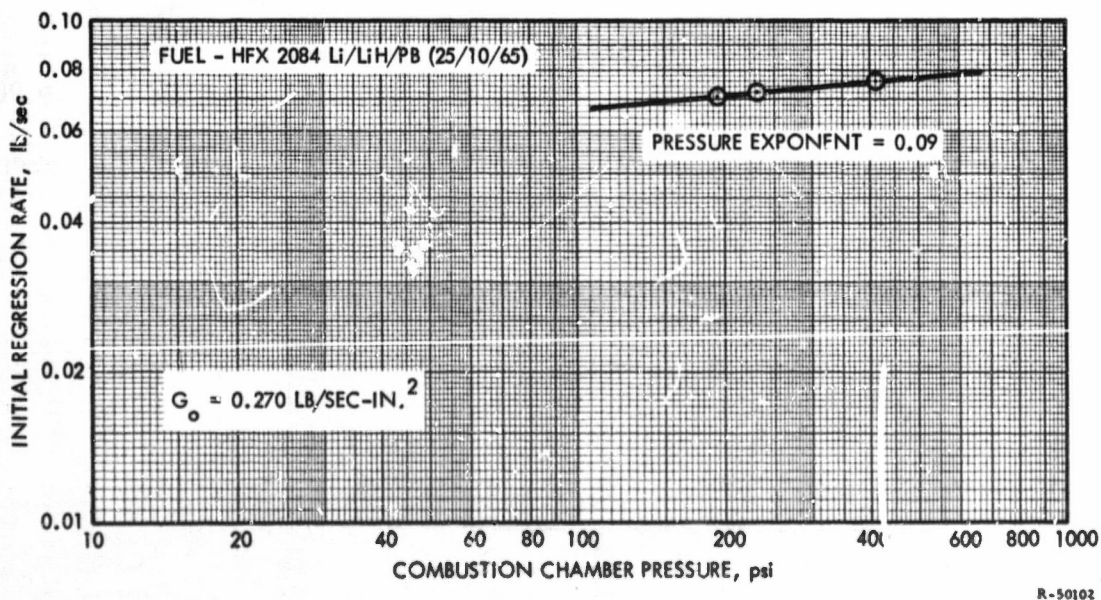
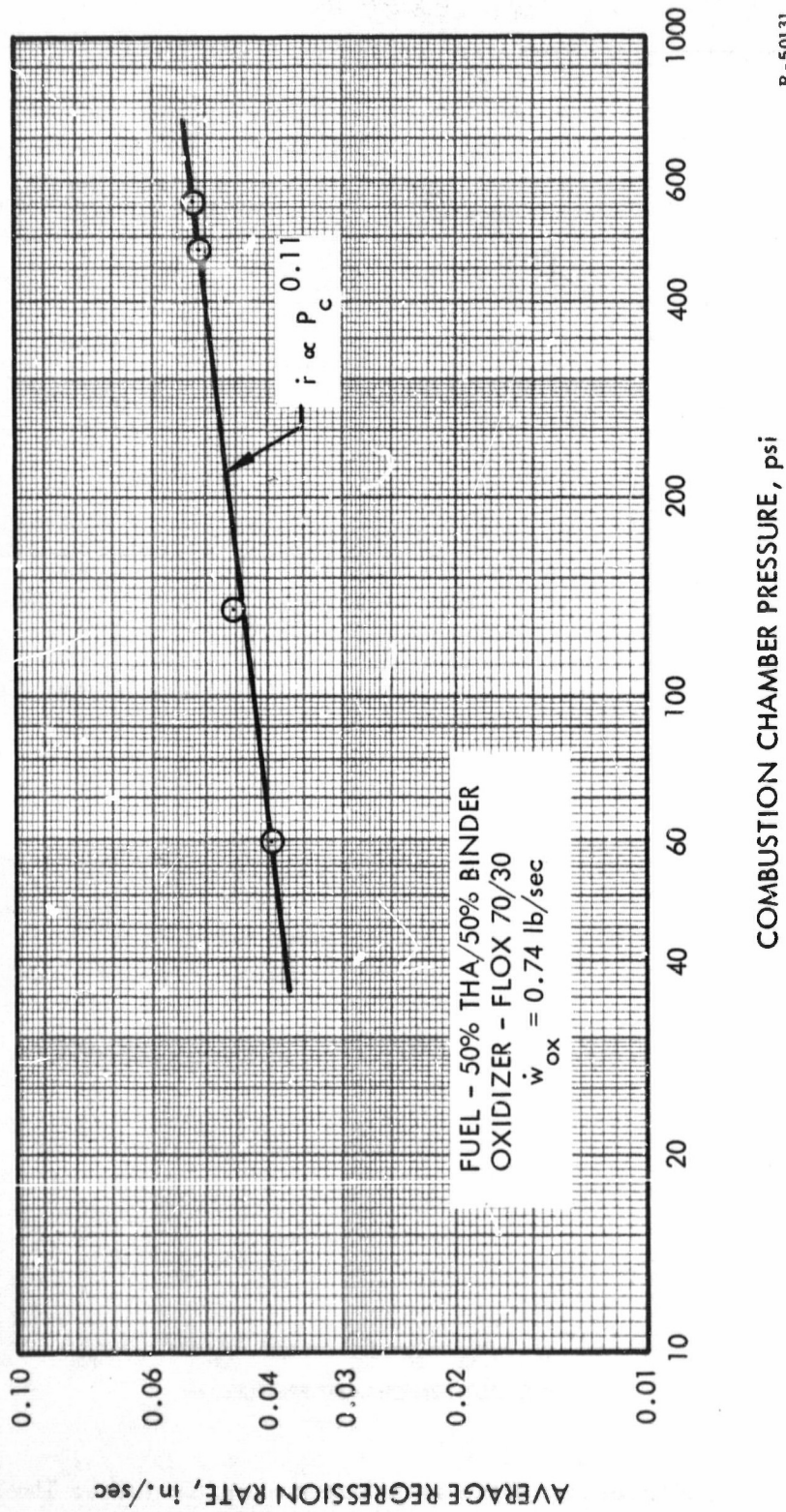


Figure 9. (U) Regression Rate as a Function of Chamber Pressure for Conventional Fuel in Survey Motor Tests

PRESSURE SENSITIVE FUELS INVESTIGATION
5.0-INCH MOTOR DATA



R-50131

Figure 10. (U) Average Regression Rate as a Function of Chamber Pressure, 5.0-In. Motor Data

(U) From the data obtained from the initial 16 tests the regression behavior was expressed by the equation

$$\dot{r} = 0.0572 P_c^{0.072} G_o^{0.278} \quad (2)$$

where:

\dot{r} = instantaneous regression rate.

(U) This method is described in detail in appendix II. The value of the pressure exponent, m , lies between the limits of 0.072 and 0.145. Because these exponents indicate negligible sensitivity, further refinement of data was not attempted. The pressure exponents obtained by both methods indicate no useful pressure effect.

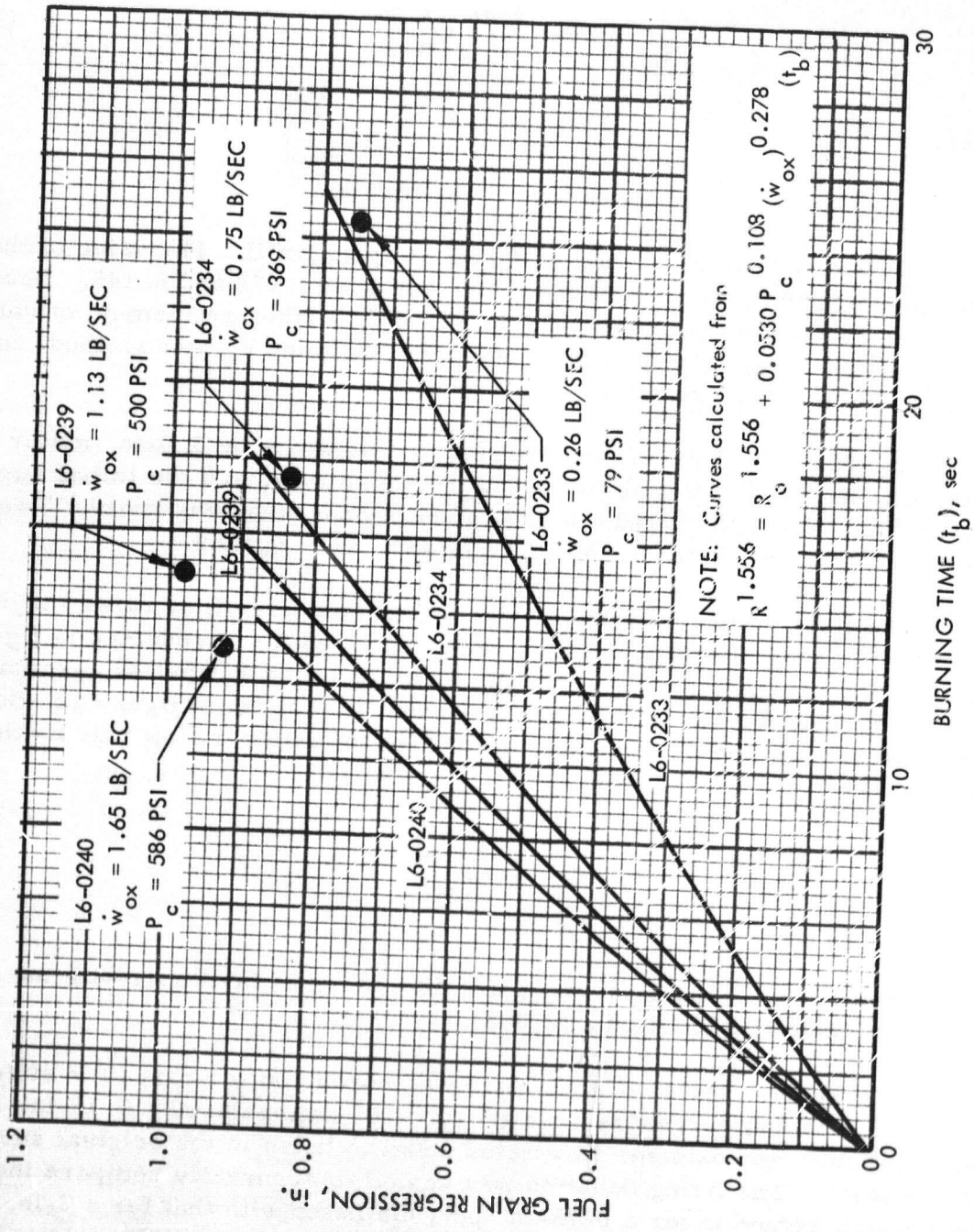
(U) An unexplained difference still existed between the 5.0-in. motor data, which indicated negligible pressure sensitivity, and the initial survey motor data, which indicated a high degree of pressure sensitivity. Twelve additional tests were conducted to explain the discrepancy.

(U) The first four tests were conducted with oxidizer flow rates varying over a wide range (0.26 to 1.65 lb/sec). The results, presented in figure 11, indicate reasonable agreement with equation 2. Better agreement is seen between the actual and predicted fuel flow rates in figure 12. Because fuel flow rate can be expressed as a function of oxidizer flow rate by the proportionality

$$\dot{w}_f \propto \dot{w}_{ox}^{m+n}$$

the exponent (0.42) indicated by figure 12 compares favorably with the sum of the exponents of equation 2 (0.388).

(U) The second series of four tests was conducted to search for effects of motor size upon pressure sensitivity. The motors used a 0.75-in. fuel-port diameter and oxidizer flow rates equal to those in the original survey motor tests. The firing duration was varied to accurately compare the regression behavior for a 0.75-in. port diameter with that for a 2-in. port diameter. The initial regression rates reproduce those of the original survey motor tests as shown in figure 13. However, the regression rate diminished rapidly after reaching a port diameter of approximately 1.25 in.



R-50103

Figure 11. (C) Fuel Regression versus Burning Time for 50% THA/50% Binder Fuel

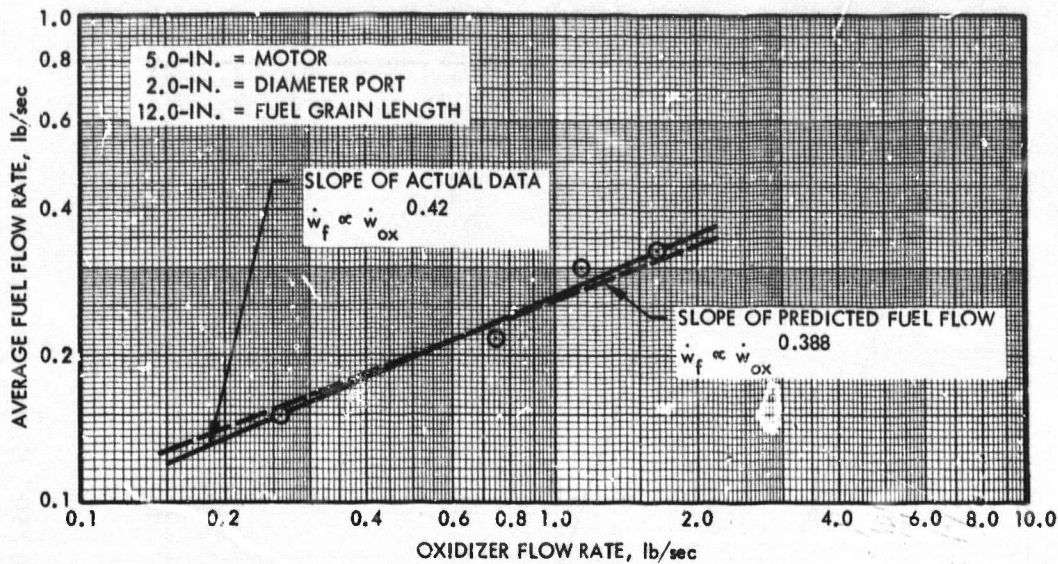


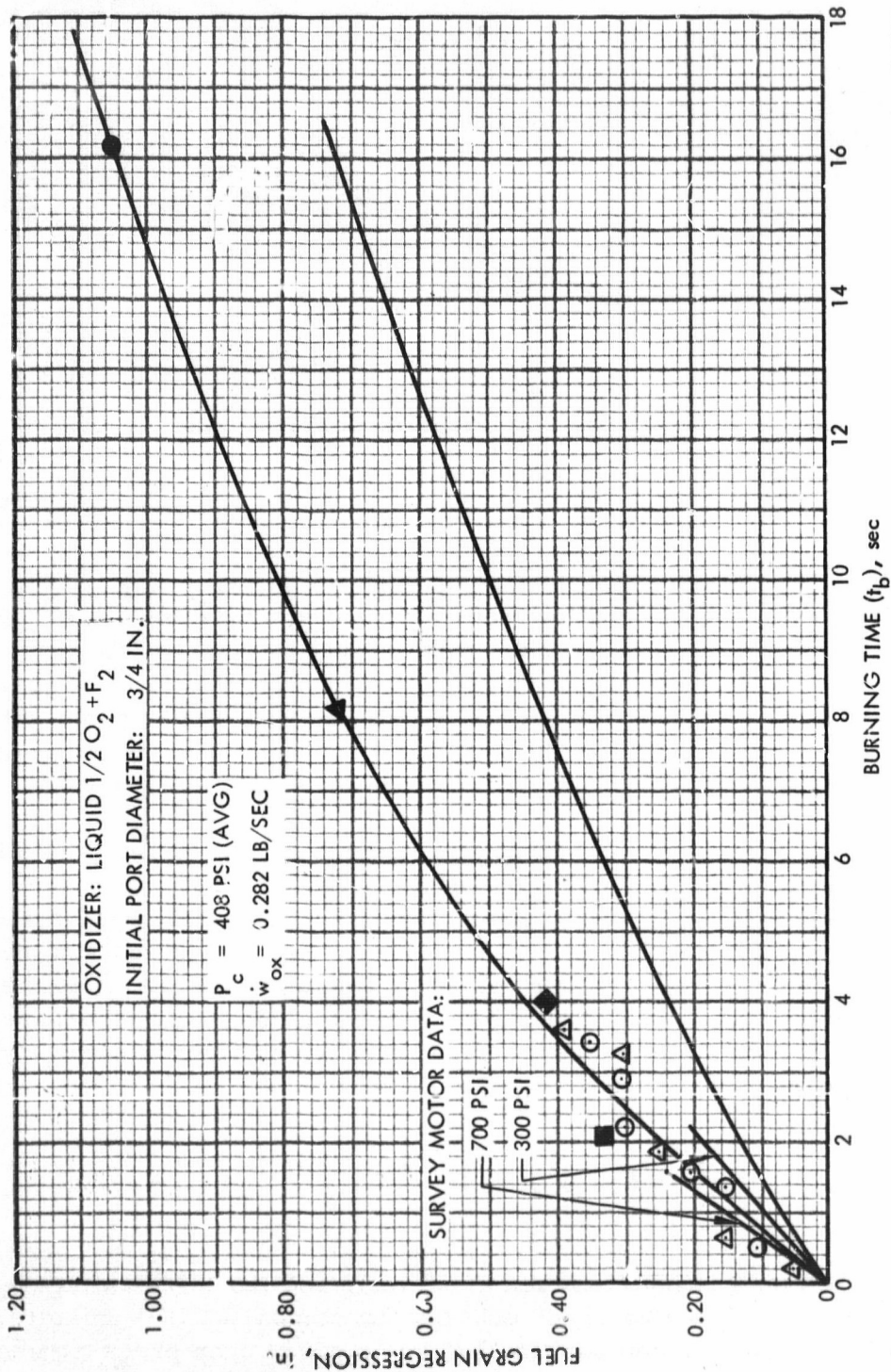
Figure 12. (U) Fuel Flow Rate versus Oxidizer Flow Rate for the THA/Binder Fuel

Thereafter, the regression rates were consistent with the 5.0-in. motor data. The data validated the results of the survey motor tests and established the existence of a port size effect upon pressure sensitivity.

(U) The final series of four tests were conducted to determine the effects of the oxidizer composition and state upon pressure sensitivity. The original survey motor tests were made with gaseous oxygen and the 5.0-in. motor tests used the cryogenic FLOX mixture. These four tests were conducted at identical oxidizer flow rates using liquid oxygen (LOX) as the oxidizer. Examination of the data disclosed a high degree of pressure sensitivity. The data yielded regression rates which correlate closely with the equation

$$\dot{r} = 0.0081 P_c^{0.388} G_o^{0.278} \quad (3)$$

(U) Since the only change between these tests and those indicating negligible sensitivity was the substitution of LOX for the standard FLOX mixture, it is implied that oxidizer composition has some effect upon pressure sensitivity. It appeared that further investigation would depend upon use of LOX, which is not space storable and would not yield results in time for final full-scale motor tests; consequently, the investigation was terminated and the full-scale motor design was based upon the HFX 2084 fuel system.



R-50105

Figure 13. (C) Regression Behavior of 50% THA/50% Binder Fuel in Small-Port Motor

1.2 INJECTOR DEVELOPMENT

(U) Injector design studies were conducted during the past year to meet specific requirements associated with continuous throttling over a 12:1 thrust range (Phase I), and step throttling over a 2:1 range (Phase II). These design studies have resulted in the development of an aerated injector that maintains a uniform oxidizer distribution over thrust ratios of at least 50:1 and that has permitted several restarts in full-scale motor tests. The studies have resulted in the development of several other injector concepts applicable to dual-thrust operation. These injector designs have been evaluated in 5.0-in. motor tests conducted under Contract No. AF 04(611)-10789 and have led directly to the development of a dual-thrust injector with a face-shutoff capability. The studies have also resulted in the elimination of injector shielding and reduction in the weight of splash-block systems, which is essential for lightweight motor development.

(U) Although each of the systems being considered have different specific requirements, the development problems are similar. Basically, the problem is to design an injector to provide an oxidizer spray pattern that will result in uniform fuel regression throughout the port with a minimum of heat shielding.

(U) The objective of that portion of the injector development program, which is related to Phase I of this contract, is to deliver a satisfactory spray pattern as the oxidizer is throttled over a thrust ratio of 50:1.

(U) To achieve a throttling ratio of 12:1, as was done in Phase I, the oxidizer flow ratio at the primary injector must vary by the square of the throttling ratio, or 144:1. The injector pressure drop varies with the square of the flow rate with a fixed-area injector; therefore, some supplementary means must be used to maintain adequate injection velocity.

(U) The requirements of typical advanced tactical missile designs include two thrust levels, boost and sustain, of approximately a 2:1 ratio. Using typical hybrid propellants, the ratio of boost to sustain oxidizer flow rates would be approximately 4:1. With conventional injectors, this would result in a 16:1 change in injector pressure drop. Such a change would result either in deterioration of the spray pattern at low flow rates or excessive tank pressures at the high flow rate.

(U) Restarting hybrid motors using aft injection also presents a problem in phasing the oxidizer distribution to prevent back flow of fuel vapors and subsequent injector failure as a result of reaction with the oxidizer when oxidizer flow in one injector may lead the other.

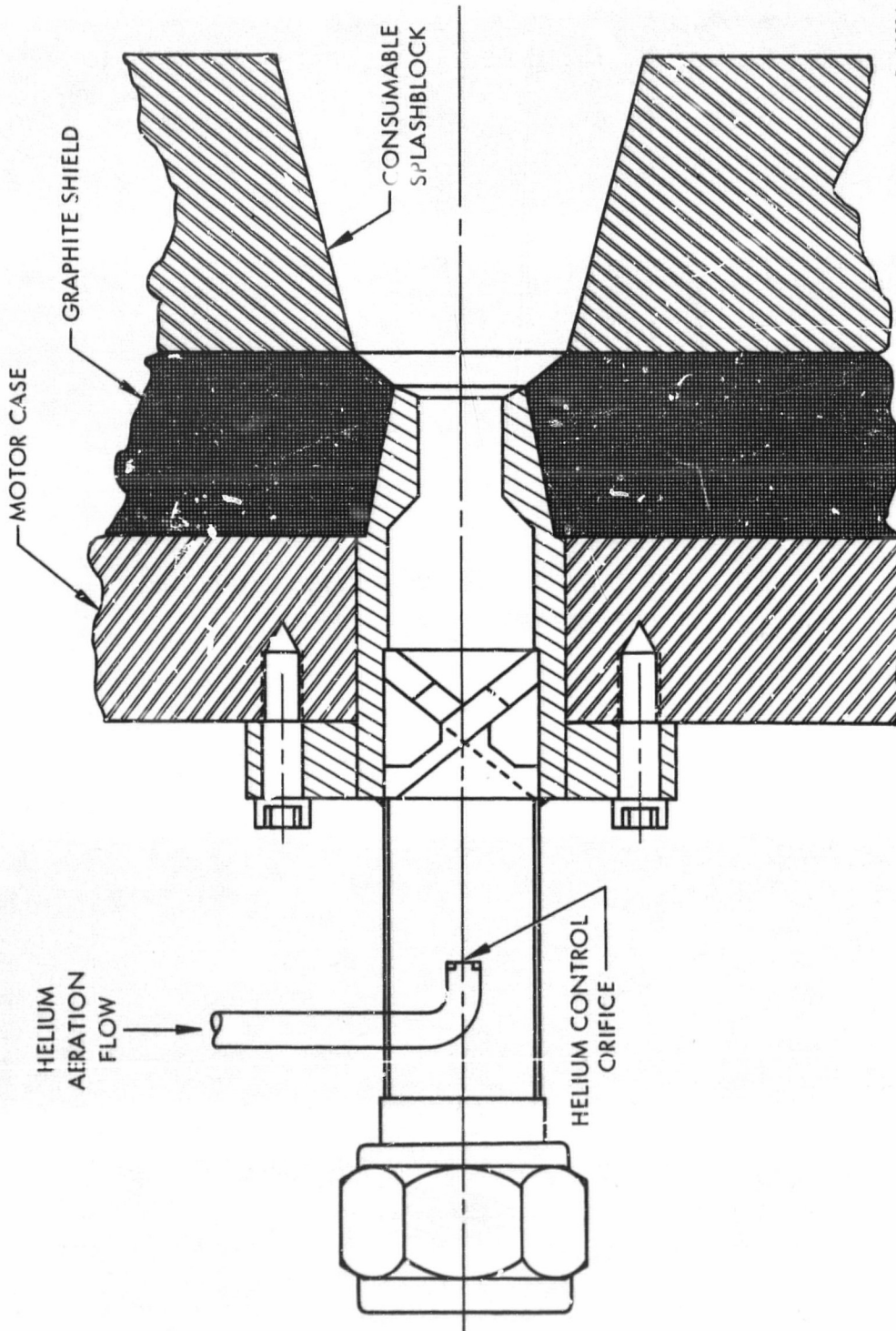
(U) The injector development program discussed in the following paragraphs has solved these and other development problems.

1.2.1 Hollow-Cone Injectors

(U) The hollow-cone injector design has been used almost exclusively for investigating hybrid internal ballistics and performance during this program because of its simple and inexpensive design. However, the hollow-cone injector has two undesirable qualities which tend to inhibit its potential for use on a prototype motor. In its present configuration, shown in figure 14, this type of injector requires both a graphite shield to protect it from the intense radiant heat source in the combustion chamber and a splash block to absorb the radial component of oxidizer momentum. At nominal flow rates the injector produces uniform fuel utilization as shown in figure 15; however, a fuel-grain tapering effect has been observed at oxidizer mass fluxes (G_o) of less than 0.05 lb/sec-in², such as those which would be encountered in deep throttling. This grain tapering effect is illustrated in figure 16. The injector development program was initiated to study these problems and to determine the injector design best suited to meet the objectives of this program.

(U) The elimination of the injector splash block is desirable from the standpoint of reducing motor weight. With a hollow-cone injector, the consumption rate of a splash block is almost independent of oxidizer flow rates, which means that at low thrust levels the splash block can be consumed long before the fuel, thus limiting the motor firing duration. Therefore, practical hybrid motor design requires that the splash block be eliminated. There are two possible methods of eliminating the excessive splash block erosion: reduction in cone angle to reduce the radial momentum of the oxidizer, or use of an alternative oxidizer spray pattern. Test firings were conducted with hollow-cone injectors having spray cone angles of 20°, 30°, and 40° to determine the effect of spray cone angle on grain regression profile. All tests were conducted at an oxidizer mass flux (G_o) of 0.15 lb/in²-sec. As can be seen in figure 17, the direction of taper was reversed between oxidizer spray cone angles of 40° and 20°, with regression almost uniform at a 30° spray cone angle. This demonstrates that uneven regression obtained at low oxidizer mass flux can be controlled by proper injector design and that the effect of the injector upon fuel regression is not necessarily restricted to the head end of the grain.

(U) Experience had shown that an injector heat shield was required to permit survival of injectors in the intense combustion chamber environment. It was also observed that a splash block was required to prevent nonuniform fuel utilization resulting from direct impingement of oxidizer on the fuel. Because of the desirability of retaining the relatively simple hollow-cone injector, emphasis was placed on reducing the heat shield and splash block requirements. Some shielding is still required, but the total weight of the full-scale motor injector heat shield has been reduced to an insignificant amount. Figures 18 and 19 show relative size of the heat shields for the full-scale hollow-cone injectors.



R-40824

Figure 14. (U) Hollow-Cone Injector

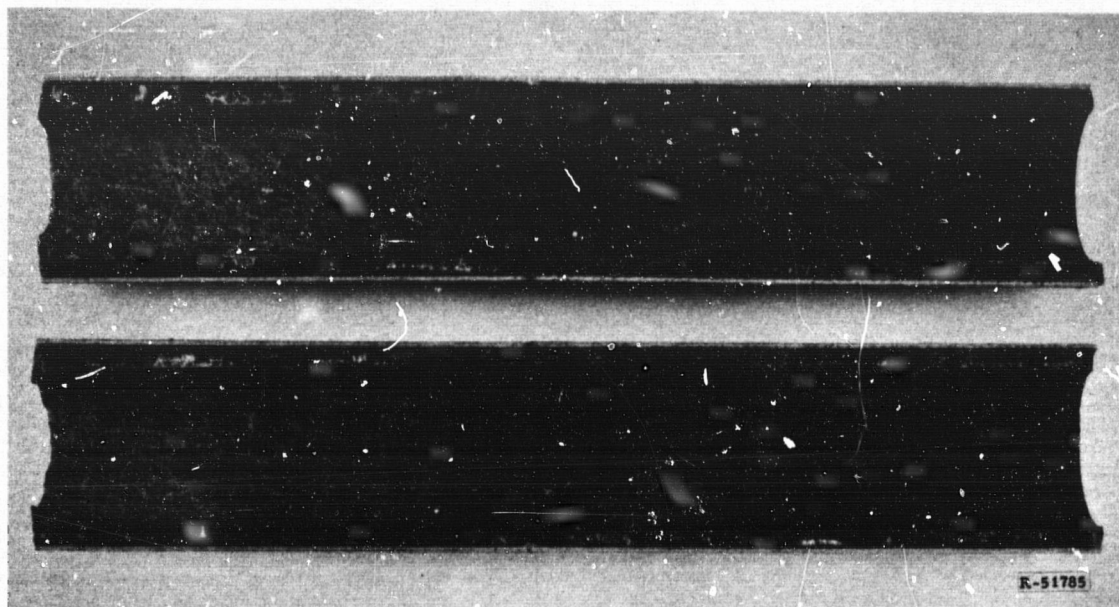


Figure 15. (U) 5.0-In. Fuel Grain After Test Using Hollow-Cone Injector

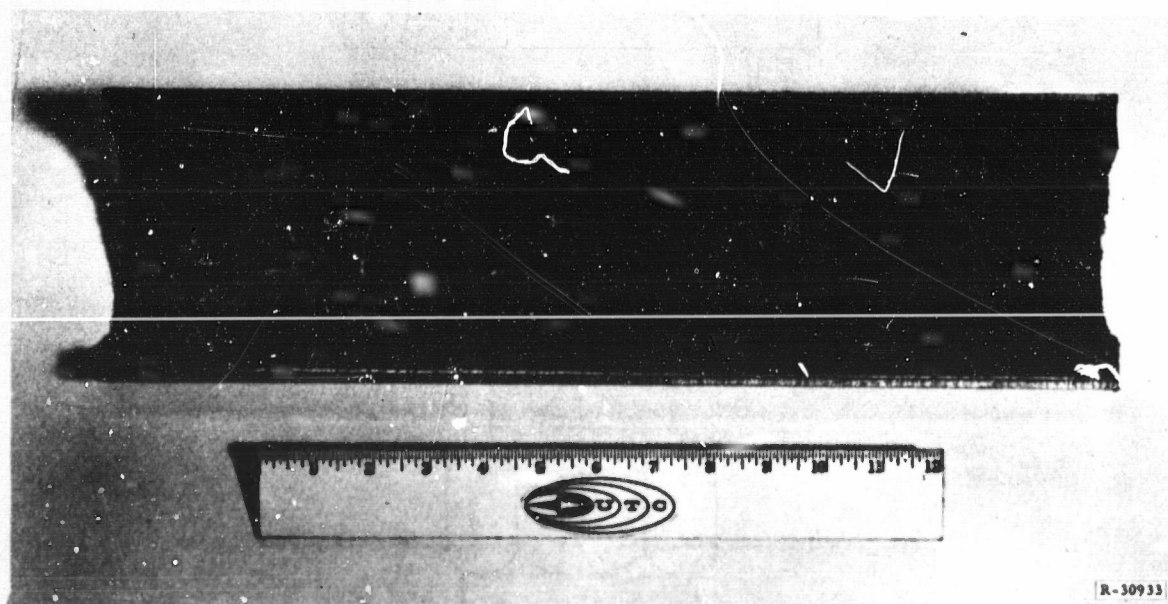
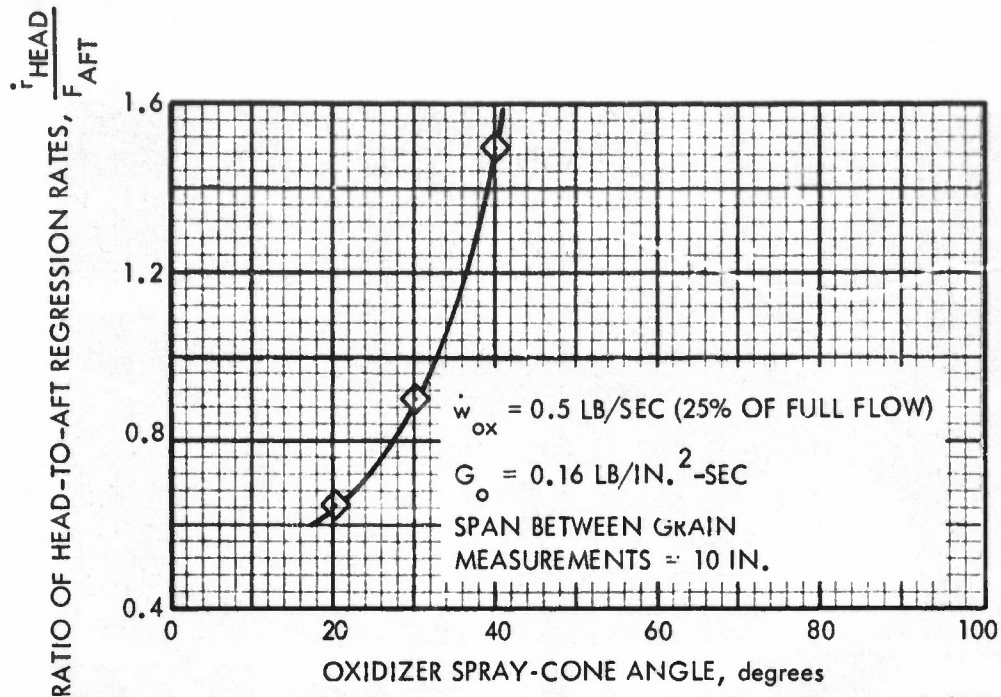


Figure 16. (U) Grain Tapering at Low G_0



R-50107

Figure 17. (U) Effect of Oxidizer Spray-Cone Angle on Fuel Grain Regression

1.2.2 Aeration

(U) Aeration provides a means of maintaining the injector spray pattern at the very low oxidizer flow rates encountered when throttling over a ratio of more than 3:1. Aeration consists of injecting a gas, usually helium, into the oxidizer feed system at the injectors to maintain a high volumetric flow through the injector. The resulting spray pattern remains intact and finely atomized over turndown ratios of 100:1.

(U) Two series of aeration tests were conducted with the injector shown in figure 14 to determine minimum helium flow requirements. The initial tests used water to simulate the FLOX and provided cursory data on helium flow requirements and the properties of the resulting spray patterns. The data was refined in the second test series using LOX to simulate FLOX.

(U) The second test series was required because the effect of a cryogenic injectant upon helium requirements and the effects of vaporization upon the resulting spray pattern were far from negligible. Two opposing effects were observed: the decreased effectiveness of a given quantity of helium due to the cooling effect of the oxidizer and the augmentation effects resulting from vaporization of the oxidizer during injection. The net change in helium requirements was minimal.

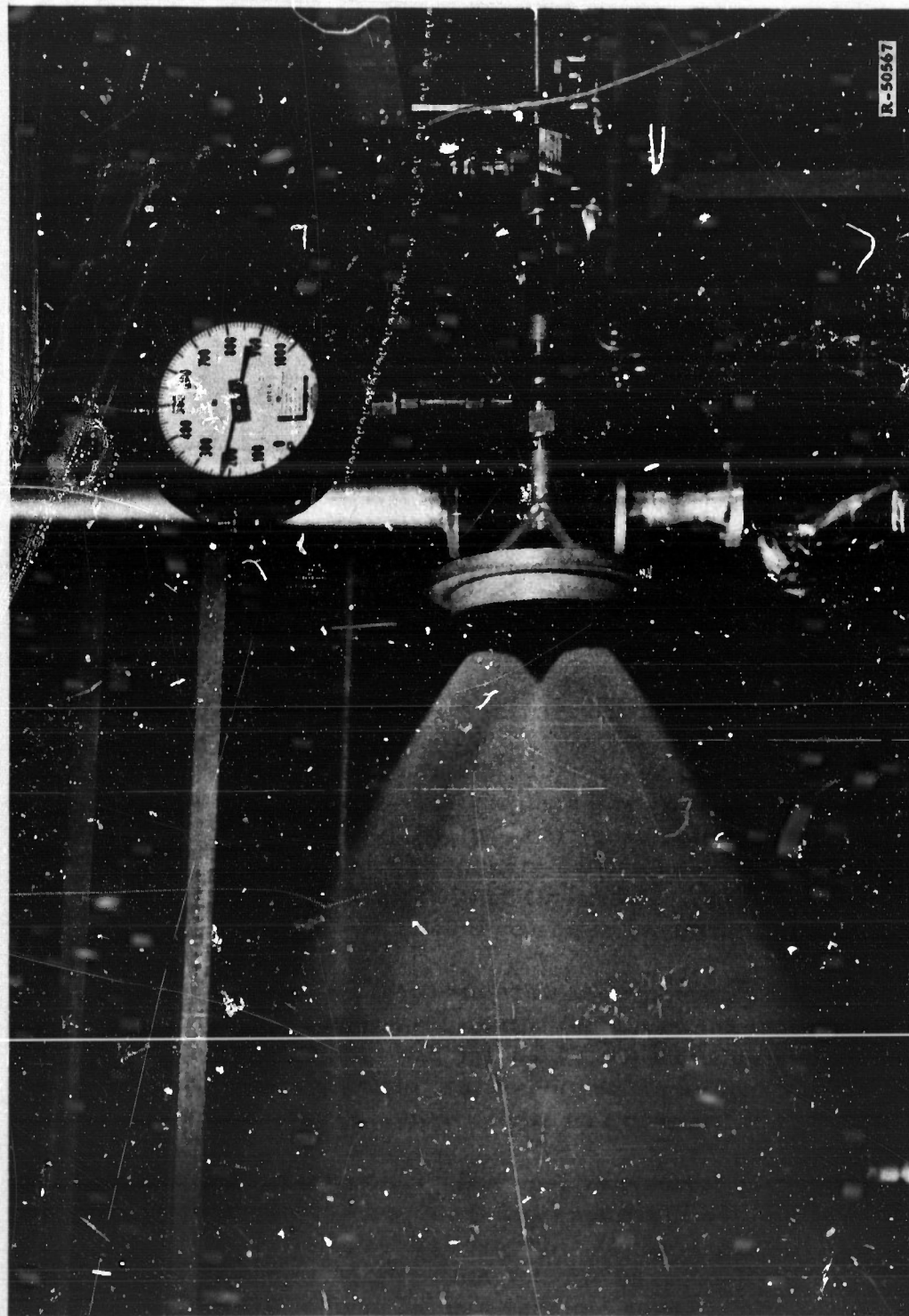


Figure 18. (11) 5000-lb-Thrust Motor Injector



Figure 19. (U) 5000-lb-Thrust Motor Injector (Modified)

(U) The water flow tests (figure 20) indicated that a suitable spray pattern is maintained over the entire range of simulated oxidizer and helium flow rates and that at injector pressure differentials under 5 psi, the pattern begins to deteriorate.

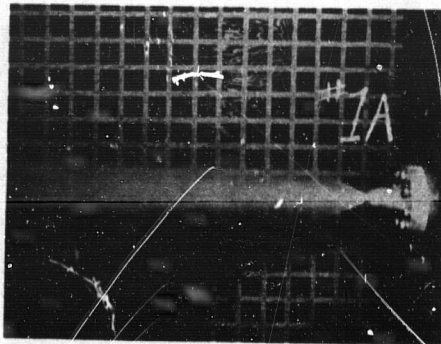
(U) In the tests with liquid oxygen, the spray pattern is improved at low oxidizer flow rates, presumably because of the additional benefit of vaporizing liquid oxygen. Calculations indicated that a 25% increase in gas flow effectiveness may result from oxygen vaporization. Figure 21 compares the liquid oxygen tests with water flow tests and shows the improvement in injector spray pattern observed with liquid oxygen. Figure 22 illustrates the departure of liquid oxygen pressure differentials from water flow data. The increased effectiveness with LOX is evident, and additional data points with LOX flow rates in the vicinity of 0.1 lb/sec indicated that a higher injection pressure drop occurs. The closer correlation of LOX and water flow data is evident at higher flow rates.

(U) The results of the cold flow tests were verified later in full-scale motor tests when a 5000-lb-thrust motor was throttled to 380 lb thrust. Essentially, no injector pressure drop (≈ 2 psi) existed, and yet stable combustion and uniform cross-sectional regression behavior was obtained. The results of these tests indicate that the aeration concept is feasible. However, individual mission analyses must be used to determine the relative merits of aeration in specific propulsion systems.

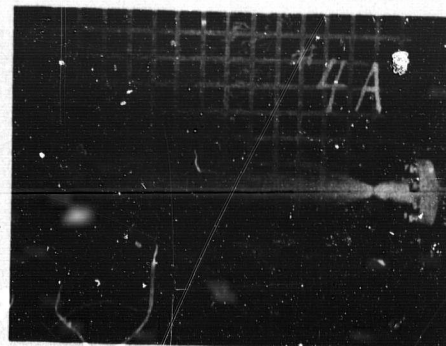
1.2.3 Subscale Aeration Motor Tests

(U) Standard 70° hollow-cone and solid-cone injectors were designed and fabricated for use in subscale aeration tests. The injectors were designed for a full-thrust flow rate of 2 lb/sec, and were designed to be throttled to 0.02 lb/sec by line throttling, using aeration to maintain injection velocity. The hollow-cone and solid-cone injector designs are shown in figures 23 and 24.

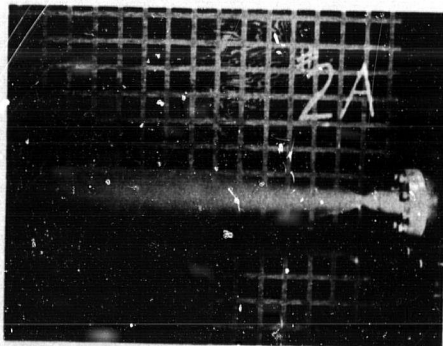
(U) A series of five firings were made with the aerated hollow-cone injector. The first four firings were made at an oxidizer mass flux of 0.064 lb/in²-sec, corresponding to about 30% at full thrust. Helium flow supplied to the aeration system was diminished and grain effects were noted. Figure 25 shows three typical fuel grains sectioned after firing. Figure 26 shows the effect of helium flow on uniformity of grain regression. A marked improvement in uniformity of regression is evident as helium flow is diminished. Helium flows were varied between 0.011 and 0.001 lb/sec for these firings, corresponding to 0.7 and 0.1% of the full-thrust oxidizer flow rates. Helium flows below 0.001 lb/sec could not be used without loss of measurable pressure drop across the injector. Minimum injector pressure drops used were approximately 2 psi. An additional test was made at an oxidizer mass flux of 0.006 lb/in²-sec (corresponding to 10% thrust).



WATER FLOW = 0.93 lb/sec
HELIUM FLOW = 0.0078 lb/sec
PRESSURE DROP = 17 psi



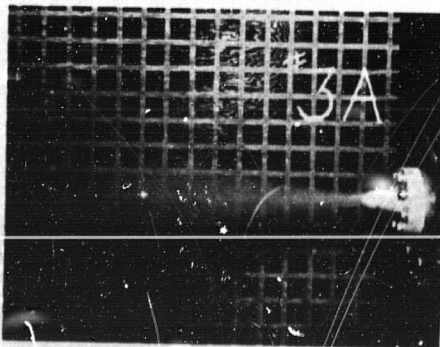
WATER FLOW = 0.93 lb/sec
HELIUM FLOW = 0.0050 lb/sec
PRESSURE DROP = 13 psi



WATER FLOW = 0.50 lb/sec
HELIUM FLOW = 0.0078 lb/sec
PRESSURE DROP = 9 psi



WATER FLOW = 0.50 lb/sec
HELIUM FLOW = 0.0050 lb/sec
PRESSURE DROP = 6.5 psi



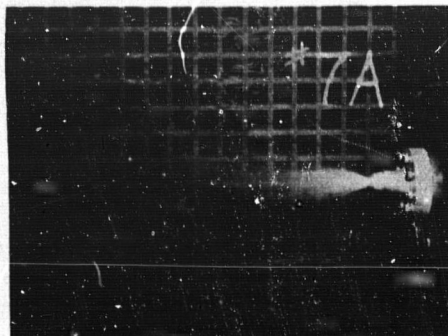
WATER FLOW = 0.10 lb/sec
HELIUM FLOW = 0.0078 lb/sec
PRESSURE DROP = 3 psi



WATER FLOW = 0.10 lb/sec
HELIUM FLOW = 0.0050 lb/sec
PRESSURE DROP = 2 psi

R-40827

Figure 20. (U) Cold-Flow Aeration Test Using Water (Sheet i of 2)



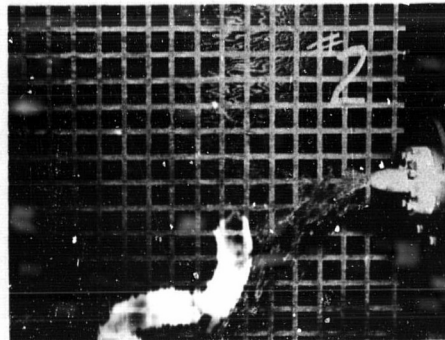
WATER FLOW = 0.93 lb/sec
 HELIUM FLOW = 0.0038 lb/sec
 PRESSURE DROP = 8 psi



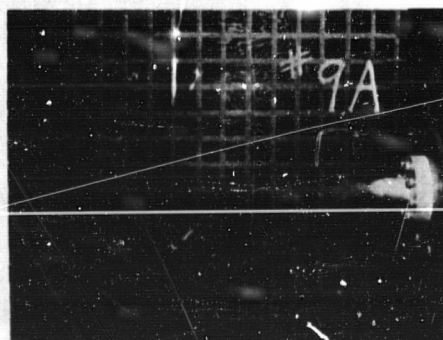
WATER FLOW = 0.93 lb/sec
 HELIUM FLOW = -
 PRESSURE DROP = 2 psi



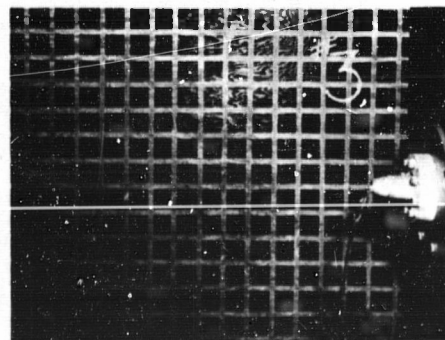
WATER FLOW = 0.50 lb/sec
 HELIUM FLOW = 0.0038 lb/sec
 PRESSURE DROP = 4 psi



WATER FLOW = 0.50 lb/sec
 HELIUM FLOW = -
 PRESSURE DROP = 0.5 psi



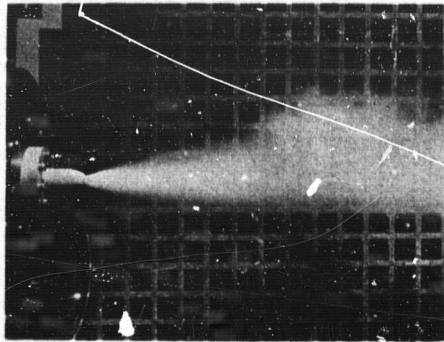
WATER FLOW = 0.10 lb/sec
 HELIUM FLOW = 0.0038 lb/sec
 PRESSURE DROP = 0.5 psi



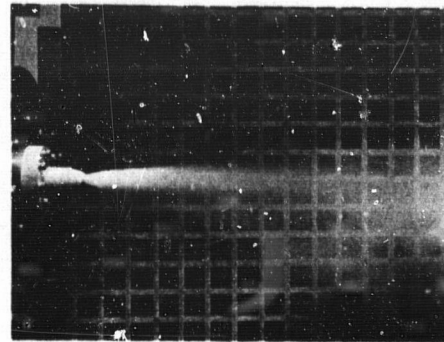
WATER FLOW = 0.10 lb/sec
 HELIUM FLOW = -
 PRESSURE DROP = 0 psi

R-40828

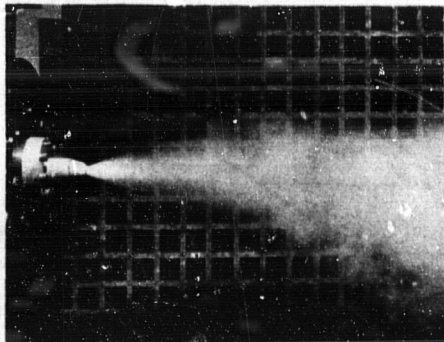
Figure 20. (U) Cold-Flow Aeration Test Using Water (Sheet 2 of 2)



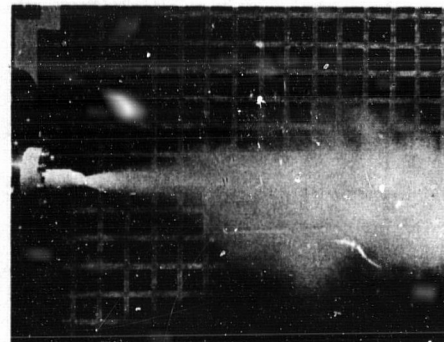
LOX FLOW = 0.99 lb/sec
 HELIUM FLOW = 0.0078 lb/sec
 PRESSURE DROP = 20 psi



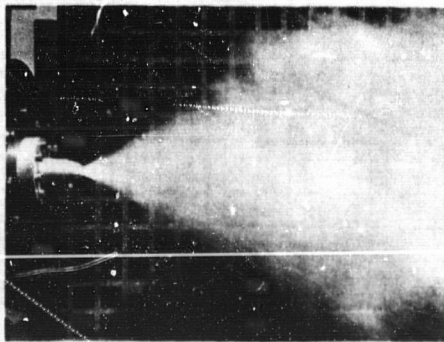
LOX FLOW = 0.54 lb/sec
 HELIUM FLOW = 0.0078 lb/sec
 PRESSURE DROP = 13.5 psi



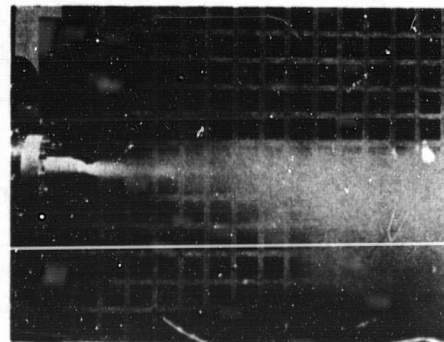
LOX FLOW = 0.99 lb/sec
 HELIUM FLOW = 0.0038 lb/sec
 PRESSURE DROP = 9.5 psi



LOX FLOW = 0.54 lb/sec
 HELIUM FLOW = 0.0038 lb/sec
 PRESSURE DROP = 9.0 psi



LOX FLOW = 0.99 lb/sec
 HELIUM FLOW = -
 PRESSURE DROP = 5.0 psi



LOX FLOW = 0.54 lb/sec
 HELIUM FLOW = -
 PRESSURE DROP = 6.5 psi

R-40825

Figure 21. (U) Cold-Flow Aeration Tests Using LOX

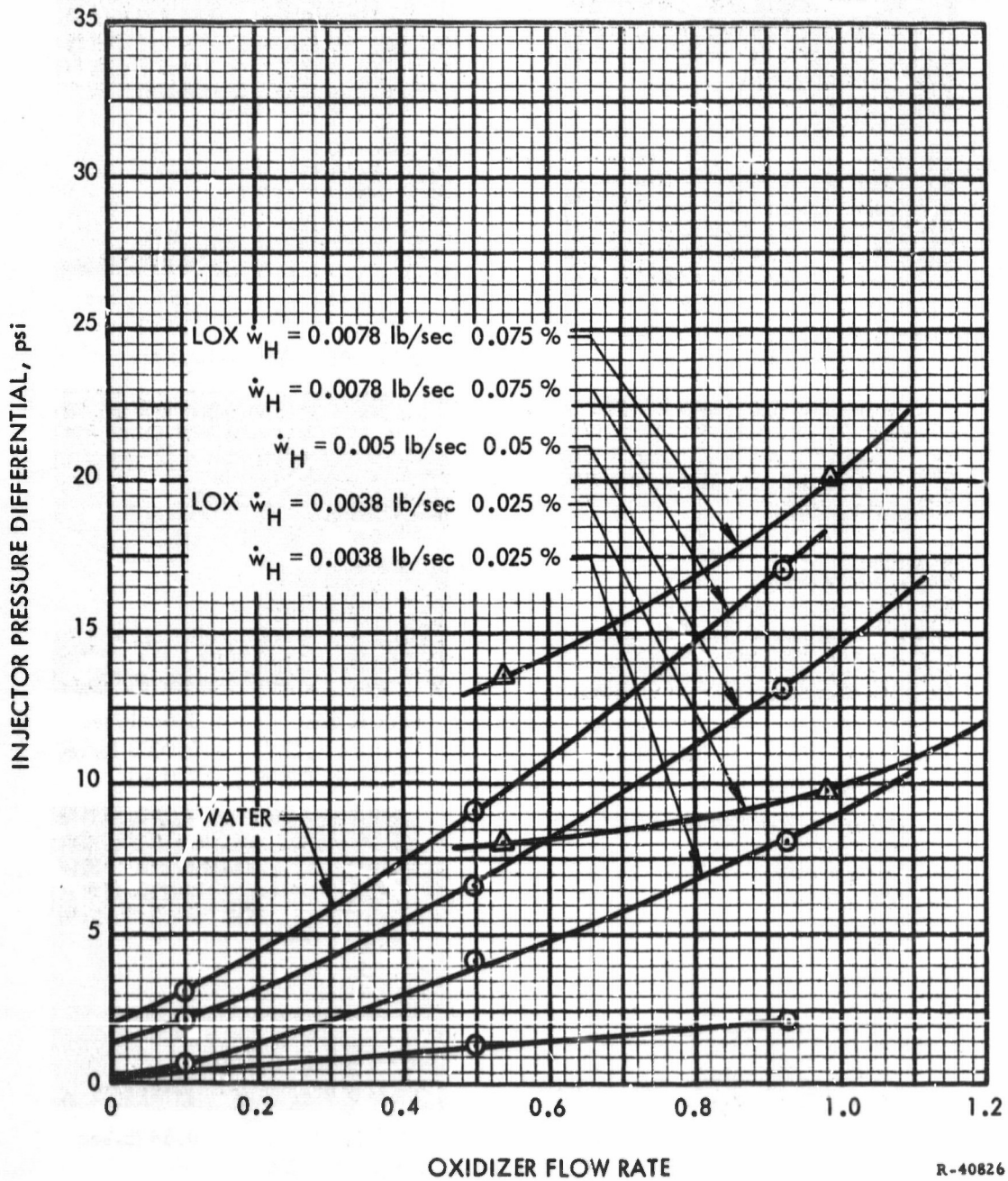
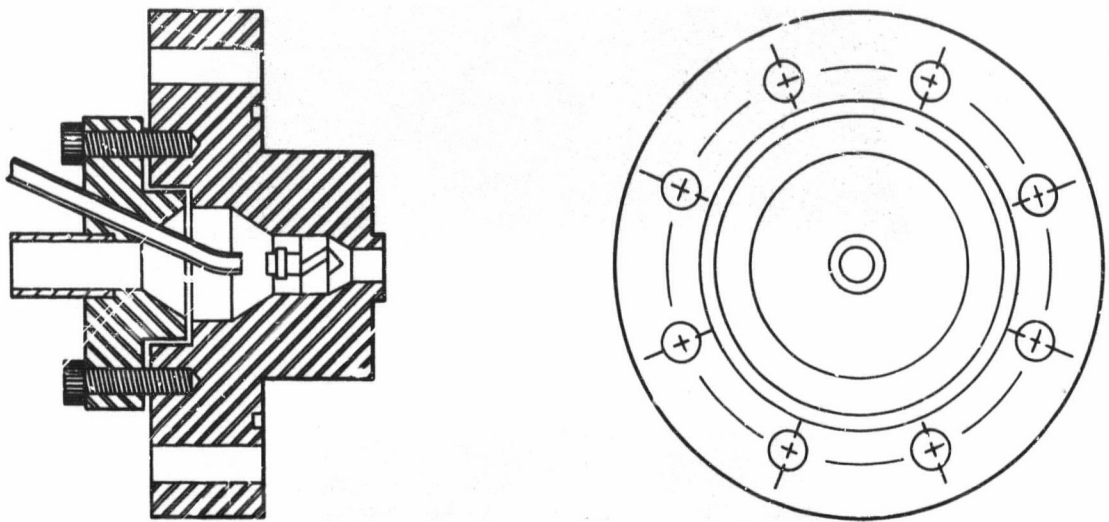
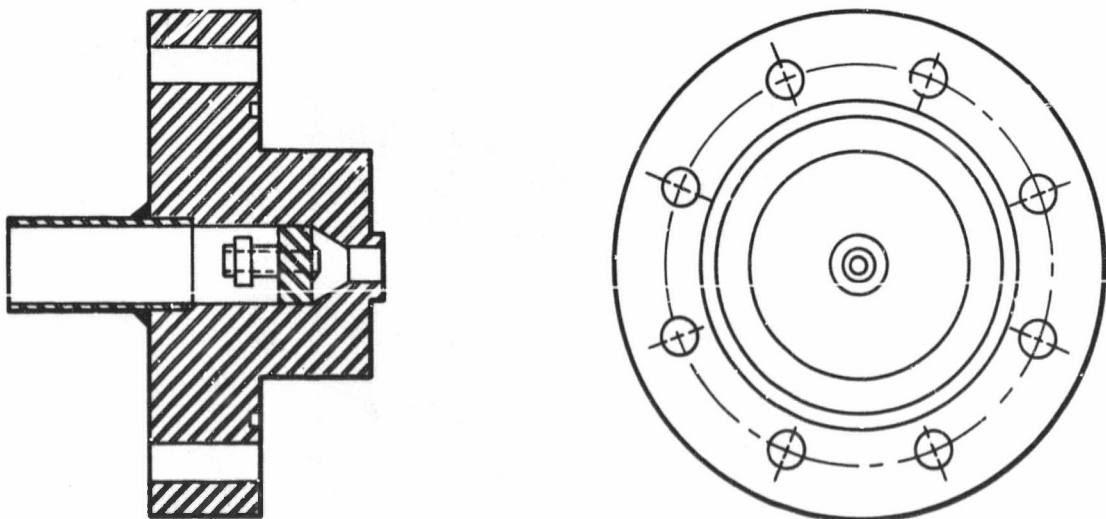


Figure 22. (U) Comparison of LOX and Water Flow Aeration Tests



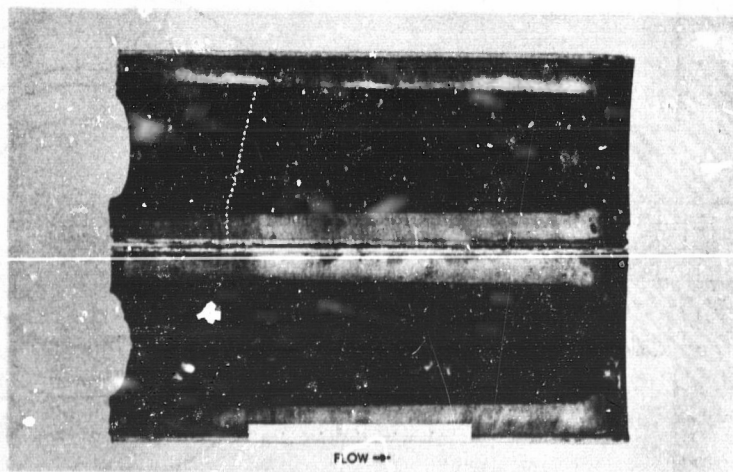
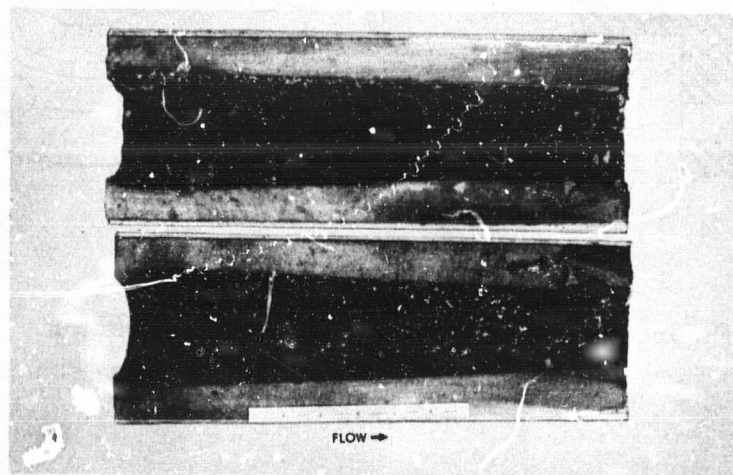
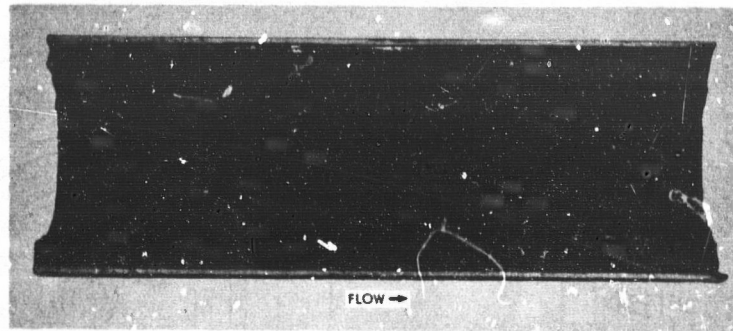
R-50110

Figure 23. (U) Aerated Hollow-Cone Injector



R-50111

Figure 24. (U) Solid-Cone Injector



R-50112

Figure 35. (U) Typical Fuel Grain Profiles After Firing with Aerated Hollow-Cone Injector

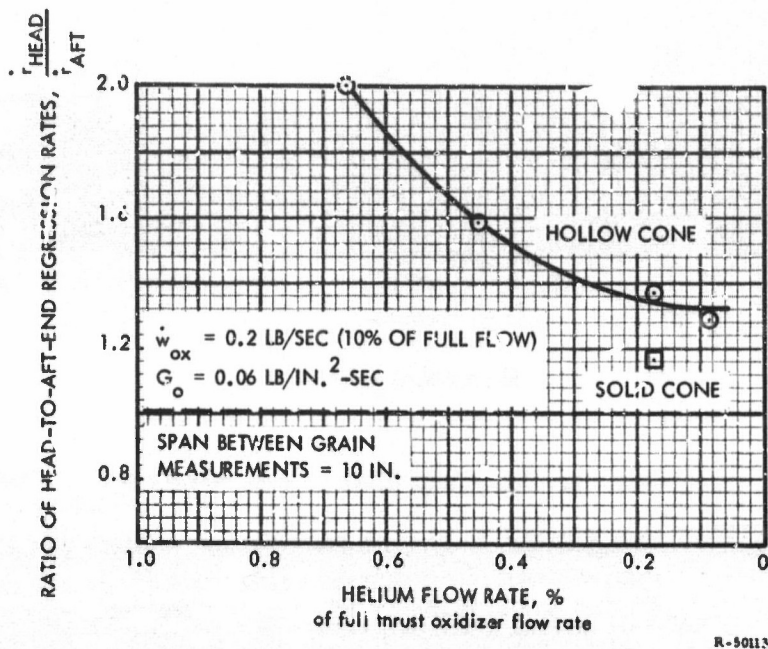
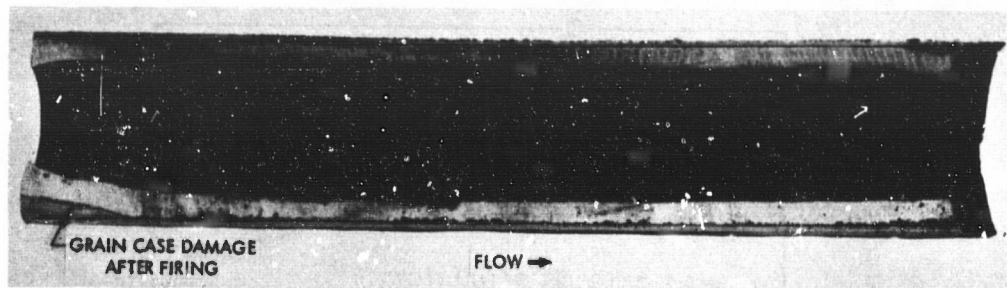


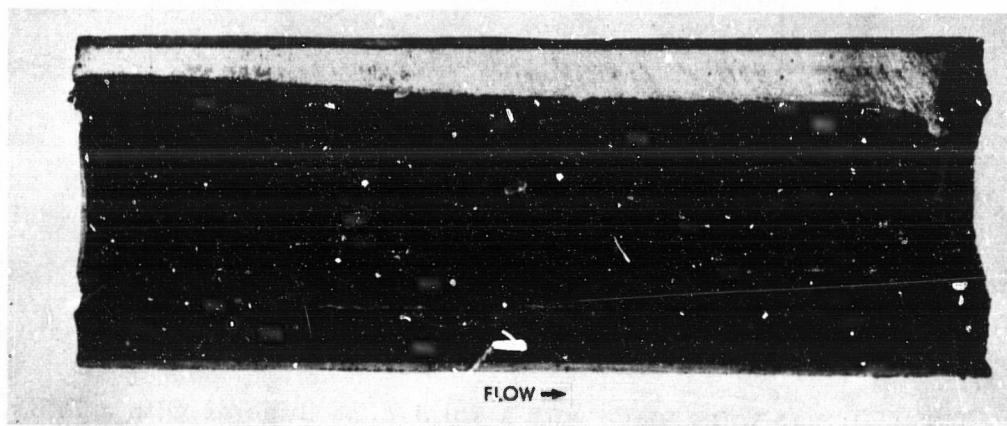
Figure 26. (U) Effect of Helium Aeration Flow Rate on Fuel Grain Tapering

(U) Three firings were made with a solid-cone injector with a 75° spray-cone angle. The first firing, made at full thrust ($G_o = 0.6 \text{ lb/in.}^2\text{-sec}$) indicated a marked improvement over the conventional hollow-cone design. Further investigations were made at reduced thrust (approximately 10%) to obtain a meaningful comparison of solid-cone injector performance. Aeration was used to maintain injector pressure drop and good atomization, with chosen helium and oxidizer flows duplicating conditions of the aerated hollow-cone injector tests described above. Postfire grain measurements indicate that the solid-cone injection pattern provides a more uniform regression profile than the hollow-cone pattern. Figure 27 shows three sectioned fuel grains obtained from this test series.

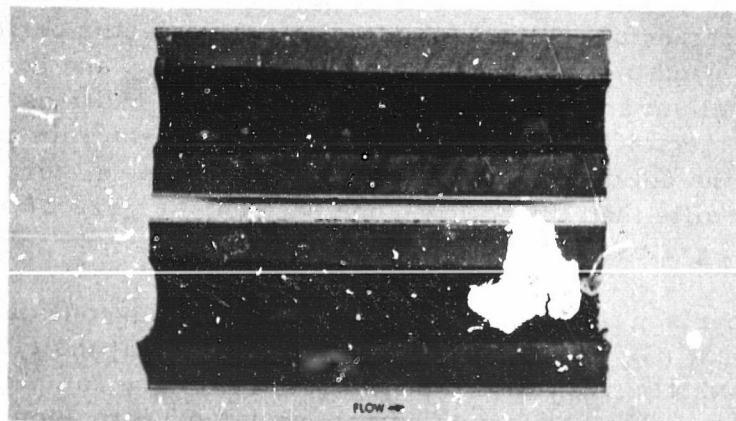
(U) A comparison of aerated hollow-cone and solid-cone patterns at minimum thrust ($G_o = 0.006 \text{ lb/in.}^2\text{-sec}$) indicates that the effects of excess fuel (approximately five times the oxidizer flow) have completely eliminated injector effects. The absence of any appreciable regression rate at the aft end of the grain indicates that with this 75° spray-cone angle, essentially no oxidizer was available to the grain at this point. This lack of oxidizer, coupled with the low gas temperature at the exit of the grain, caused the aft-end regression rate to lag far behind the head-end regression rate (figure 27 bottom photo).



MAXIMUM THRUST



INTERMEDIATE THRUST



MINIMUM THRUST

R-50114

Figure 27. (U) Typical Fuel Grain Profiles After Firing with Solid-Cone Injector

1.2.4 Regenerative-Cooled Injectors

(U) Two regeneratively-cooled subscale injectors were tested to prove feasibility of an injector design with a predominately axial flow requiring no shielding or splash block.

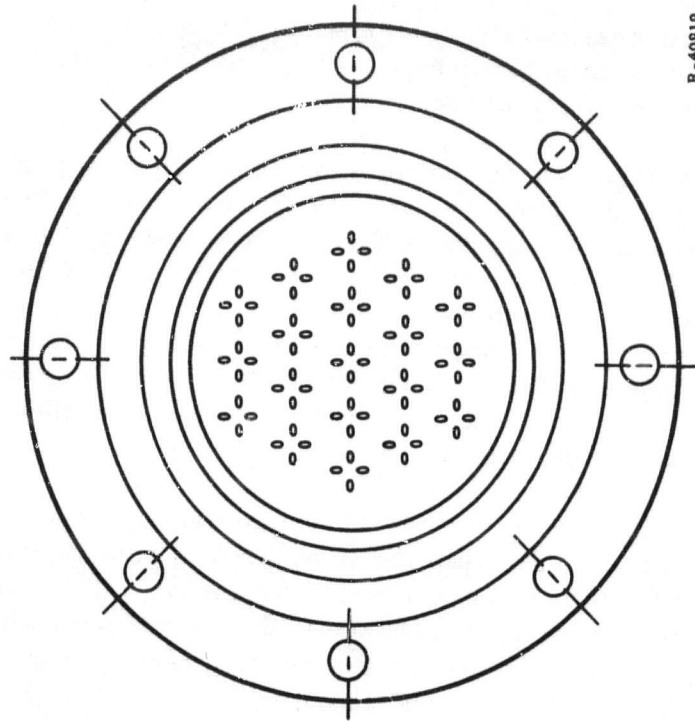
(U) An impinging-streams injector shown in figure 28 and a showerhead injector shown in figure 29, were both fabricated of OFHC copper. The spray pattern of the injector is shown in figure 30. Both injectors were tested in 5.0-in. motors for durations of 15 sec at flow rates of 2.0 lb/sec. Both injectors failed after a duration of 2 sec. The failure resulted in a localized burnthrough that occurred in a poorly cooled section near the edge of the injector face. (See figure 31.) In both cases the injectors continued to operate for the entire duration (15 sec) without further damage. The fuel grain fired with the showerhead injector is shown in figure 32.

(U) The concept of a regeneratively cooled injector was attractive; therefore, the manifolding within the injector was redesigned to eliminate the hot spot, and another injector was fabricated. The modified design utilized a 6061-T6 aluminum body and face with a 0.0015-in. -thick hard anodized coating on the face to increase the melting temperature of the surface. Again, no splash block or shielding was used. The modified injector was successfully tested under Contract No. AF 04(611)-10789 in a 10-sec test with an oxidizer (FLOX) flow rate of 2.0 lb/sec and a pressure drop of 50 psi. No face erosion or deterioration was observed. With feasibility demonstrated, further development was discontinued because other injector designs described in the following paragraphs can better accomplish the dual thrust requirements of Phase II of this program. Because the design can provide uniform axial flow of oxidizer without shielding and can be aerated to allow throttling, it has application in fixed-thrust hybrids and hybrid propulsion systems requiring continuous throttling.

1.2.5 Variable-Area Injectors

(U) Variable-area injector designs provide the only practical alternative to aeration of fixed-area injectors for use in high throttle-ratio applications. To provide a variable oxidizer flow rate over a thrust ratio in excess of 3:1 (without aeration), it is necessary to vary the discharge area of the injection port to maintain adequate injection velocity.

(U) Two types of variable-area injectors have been designed: the variable-area hollow-cone injector (figure 33) and movable-poppet injector (figure 34). Both injectors can be hydraulically or mechanically operated to control oxidizer flow.



R-40819

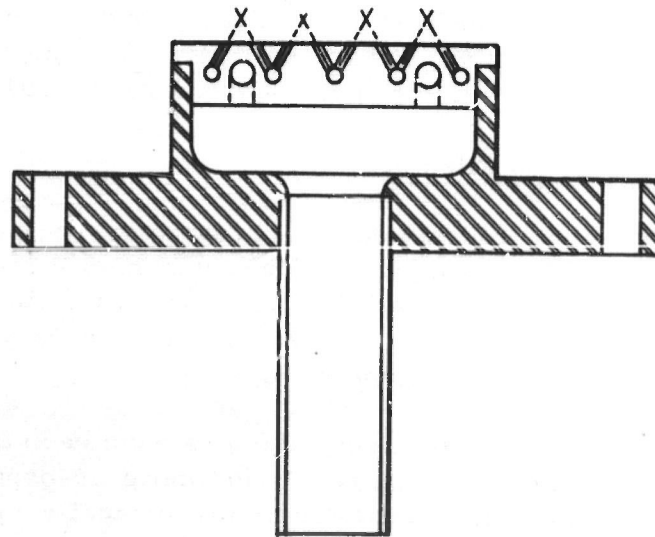
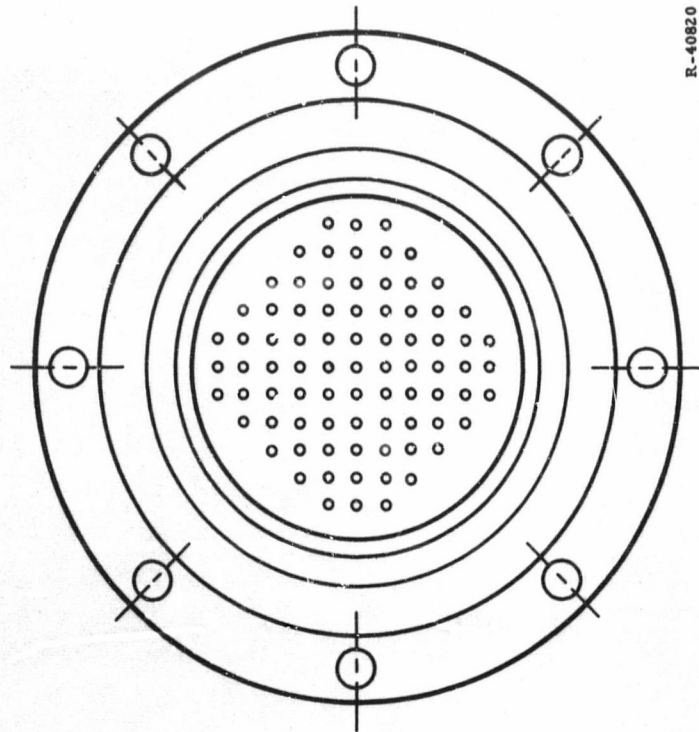


Figure 28. (U) Impinging Streams Injector



R-40820

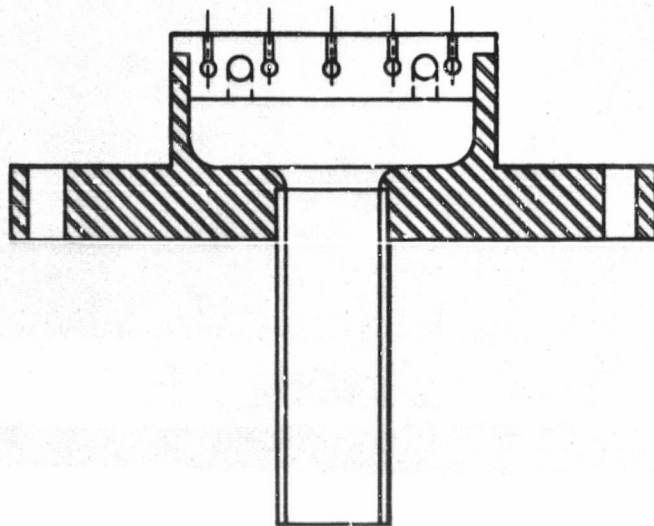


Figure 29. (U) Showerhead Injector

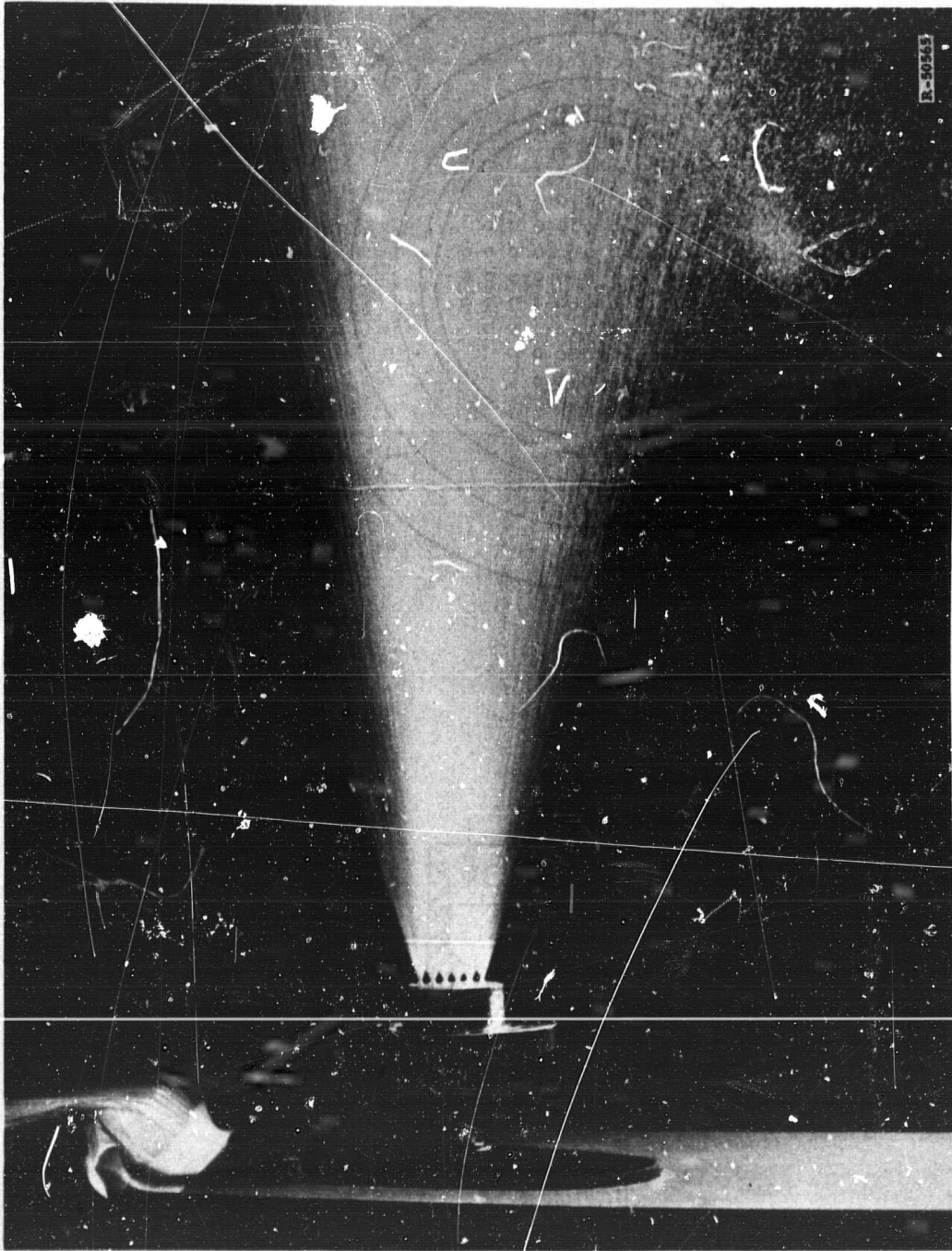


Figure 30. (U) Spray Pattern of Impinging Streams Injector



Figure 31. (U) Showerhead Injector After Test

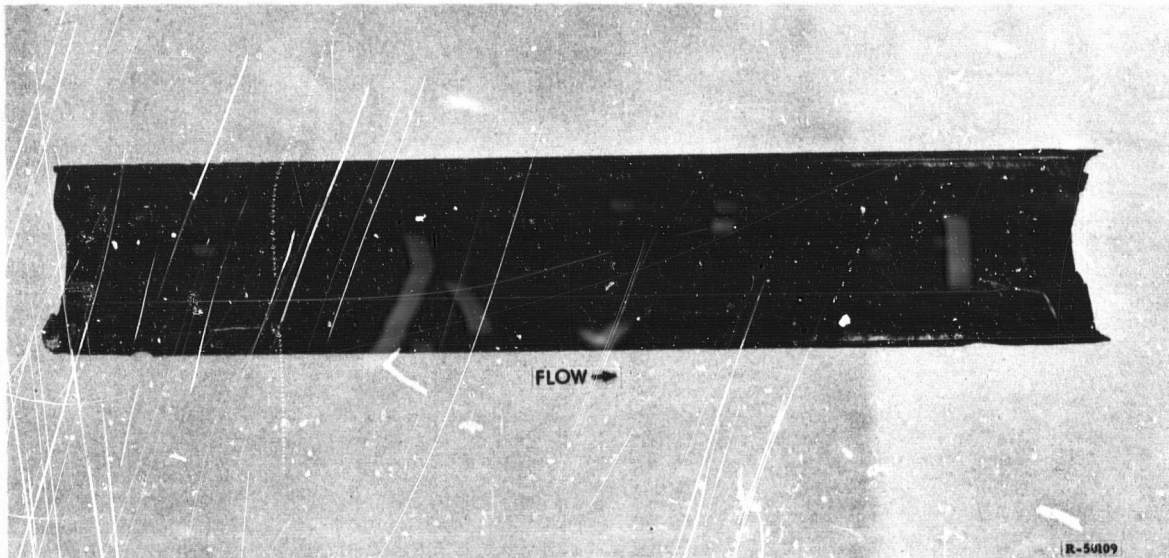
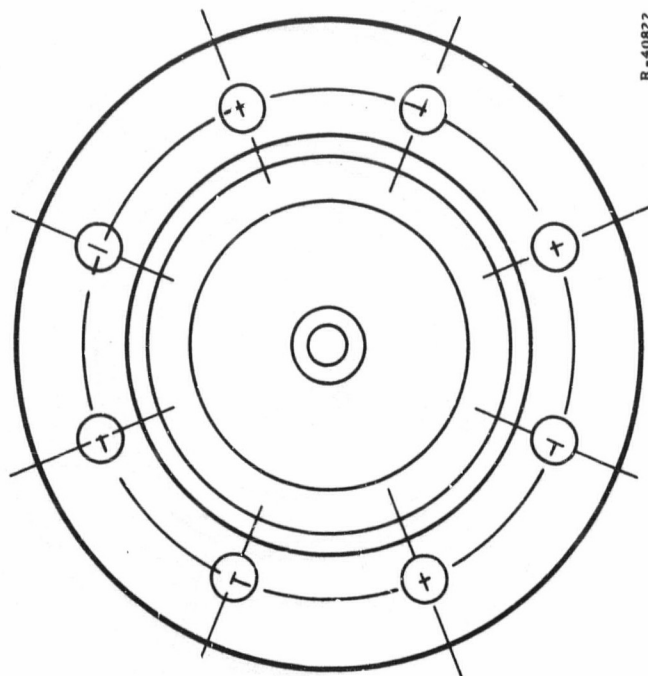


Figure 32. (U) Grain Fired with Showerhead Injector

(U) The hollow-cone injector was designed with a dual purpose: to investigate the feasibility of injector face throttling and to determine the effects of spray-cone angle on fuel regression. This injector consists of an impeller pintle assembly and an injector body. The flow rate through the injector is controlled by injection port area which, in turn, is controlled by the axial position of the pintle. The included angle of the conical spray can be varied by proper choice of impeller slot and injection port areas as shown in figure 35. Thus, for any chosen impeller area, the included angle of the conical spray is at some maximum value (usually 75°) at full thrust, and is reduced by throttling. It is, therefore, possible to counteract tapering of the fuel grain at low oxidizer flow rates by reducing the spray-cone angle at low thrust.

(U) The variable hollow-cone was successfully tested in three 5.0-in. motor firings with durations up to 20 sec.

(U) The second variable-area injector employs a movable poppet to control injection port area and a contoured nozzle to direct the flow parallel to the surface of the fuel grain, as shown in figure 36. This injector was also tested in 5.0-in. motor firings with durations of 20 sec.



R-40822

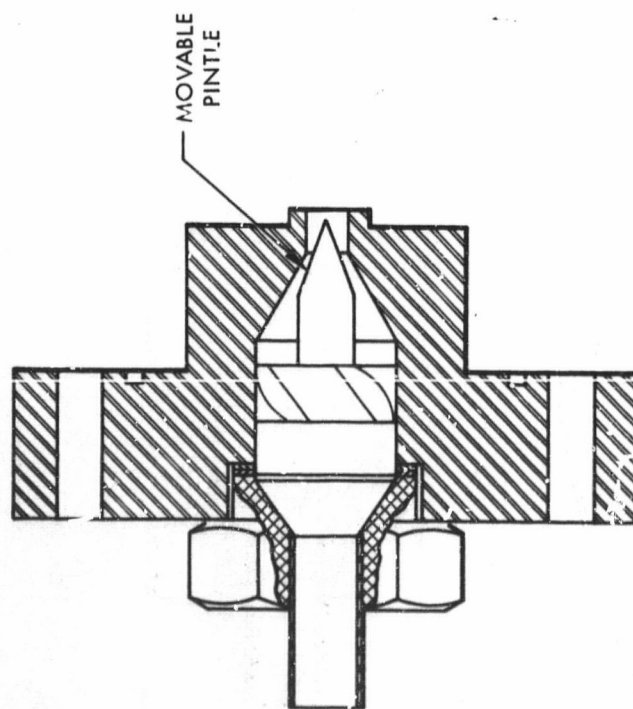
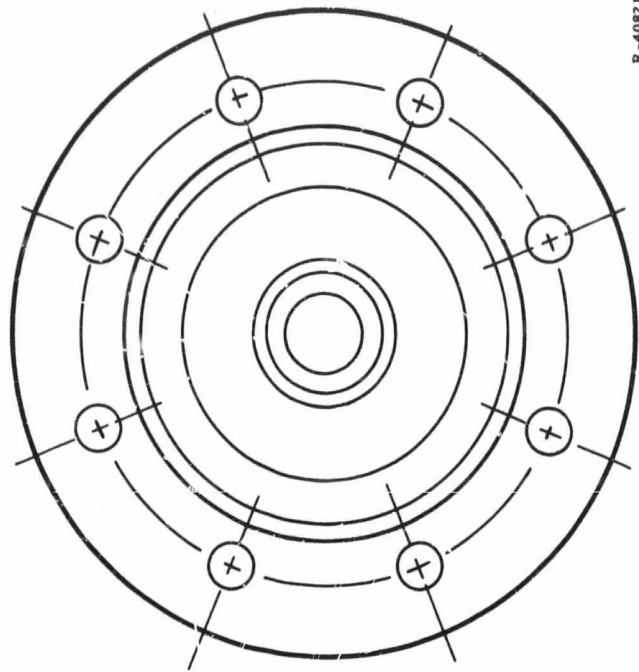


Figure 33. (U) Variable-Area Hollow-Cone Injector



R-40821

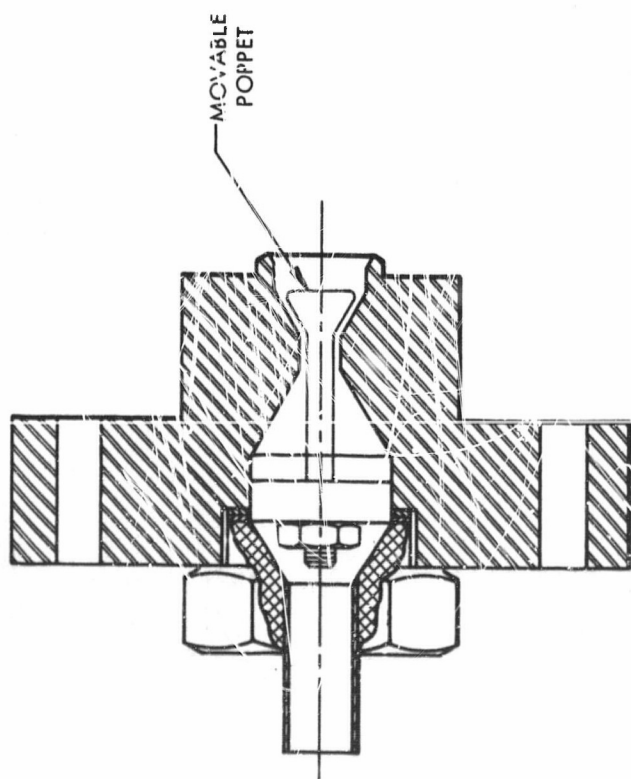


Figure 34. (U) Movable Poppet Injector

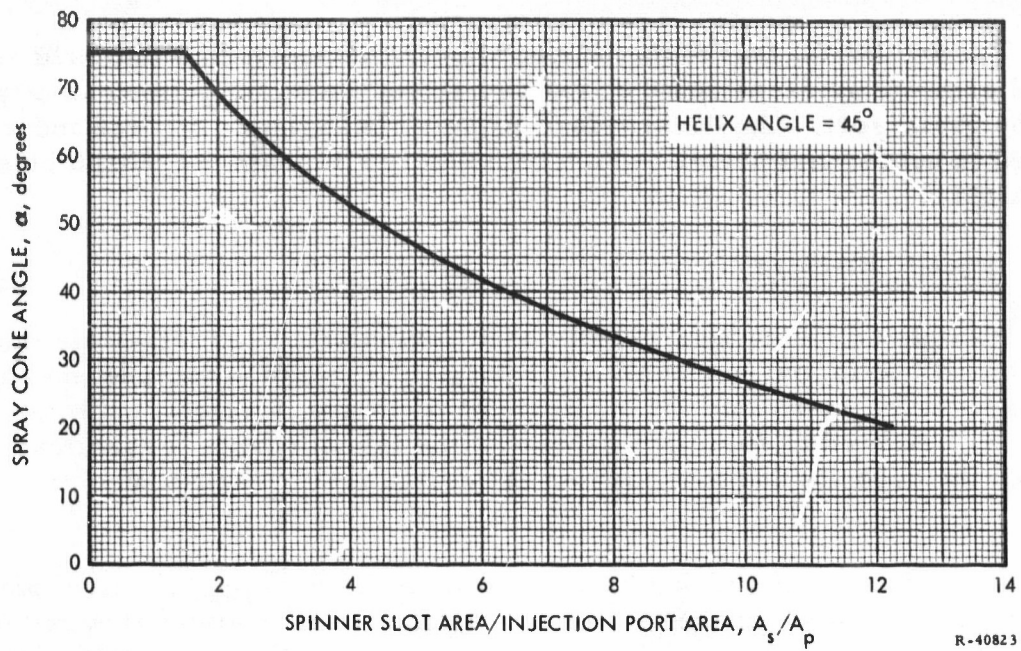


Figure 35. (U) Injector Spray-Cone Angle as a Function of Injector Orifice Area

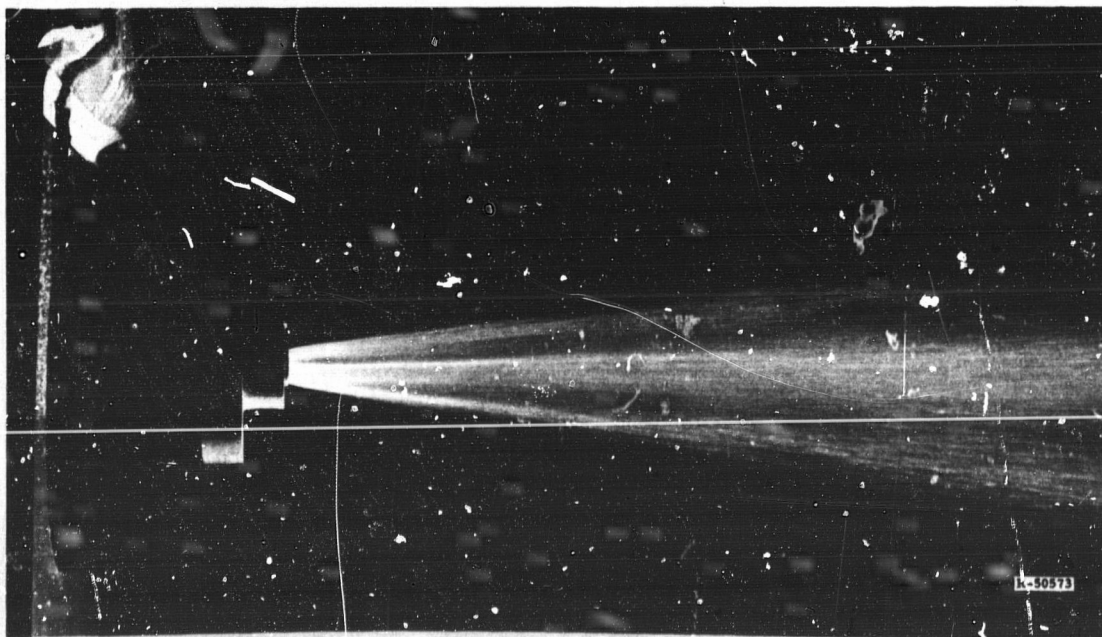


Figure 36. (U) Spray Pattern of Variable-Area Poppet Injector

(U) The successful test of the poppet injector demonstrated that oxidizer-cooled external surfaces could be used to direct the spray pattern axially into the grain port. This design feature, visible in figure 37, was incorporated in subsequent designs which completely eliminate the splash block and shield.

1.2. Poppet Injectors

(U) Multiple starts have frequently been demonstrated on full-scale motors, but a small helium purge has always been used at shutdown to prevent back-flow of fuel rich gases into the oxidizer manifold and injectors. If these vapors are allowed to enter and deposit in the injector port, a reaction between the deposits and the oxidizer at restart could result in injector failure.

(U) The necessity of purging has been eliminated by a poppet valve injector design which seals at the face of the injector when oxidizer flow is terminated by upstream valves. Two such designs have been completed: the first design (figure 38) is a simple spring-loaded poppet valve similar to the variable-area poppet. The injector spring load is overcome by oxidizer injection pressure when flow is initiated by upstream control valves, and the poppet opens against a stop, preset to give the required port area. This particular injector is not designed for continuous throttling. However, this poppet design and the design discussed in the following paragraph were combined in a dual manifold poppet injector to be used for dual thrust operation with the new storable hybrid, which is to be fired under Contract No. AF 04(611)-10789.

(U) The oxidizer flow and injector pressure drop are adjustable by present stops and eliminate any tendency toward the oscillating action typical of spring-loaded poppet valves. In addition to providing injector protection at restart motor shutoff, the injector will eliminate ignition phasing problems between primary and aft oxidizer injectors.

(U) The poppet injector produces a radial spray fan (figure 39) and, in this form, would require a splash block to absorb the radial momentum. However, previous work with the variable-area poppet injector and subsequent designs indicate that the radial flow can be turned by a film-cooled metal surface. This surface is machined into the injector body, thereby eliminating the need for a splash block.

(U) The second injector design shown in figure 40 also provides oxidizer shutoff at the injector face. In this design a greater spring force is used to guarantee positive shutoff. To operate the injector with the heavier spring loads, dynamic fluid pressures assist in holding the valve open. The injector also incorporates fixed-area drilled orifices to control the oxidizer flow.

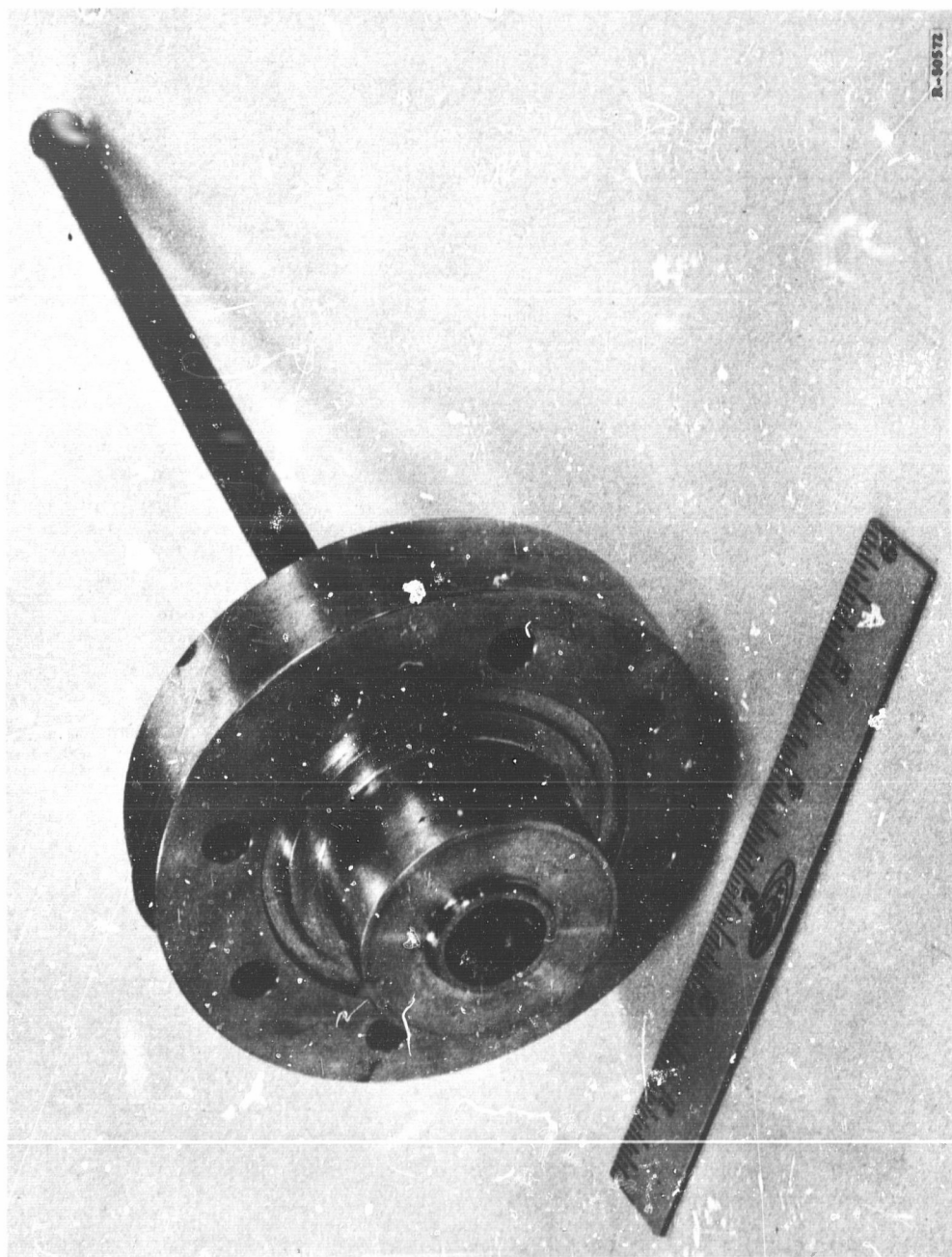
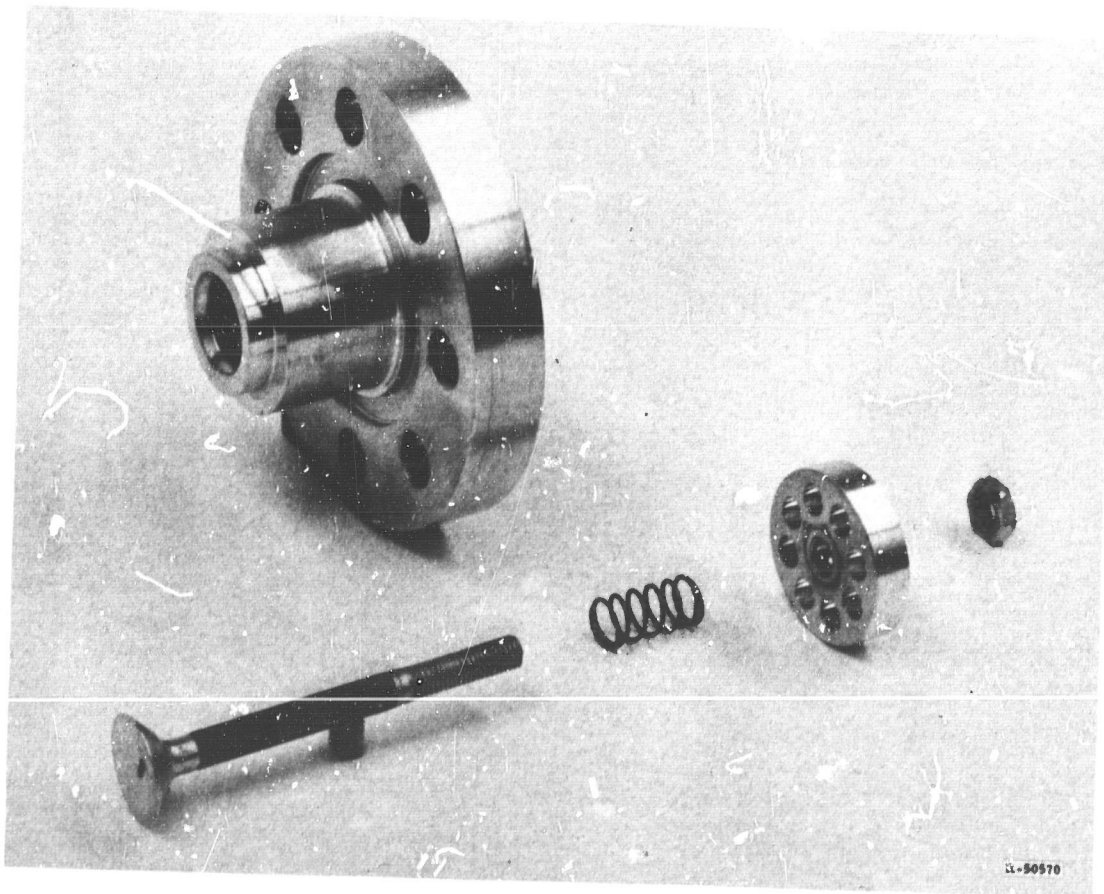
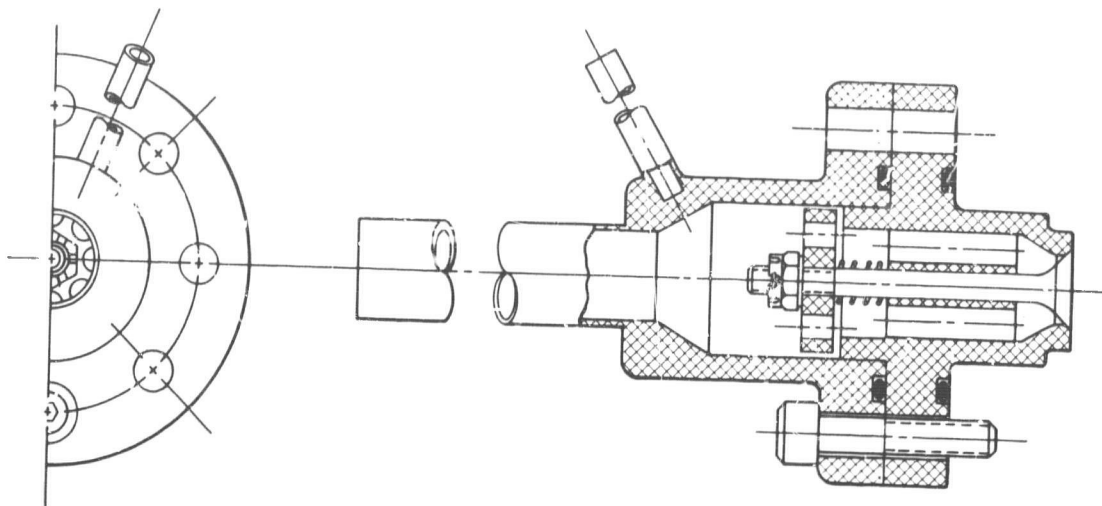


Figure 37. (U) Variable-Area Poppet Injector



U-50570

R-51779

Figure 38. (U) Poppet Injector

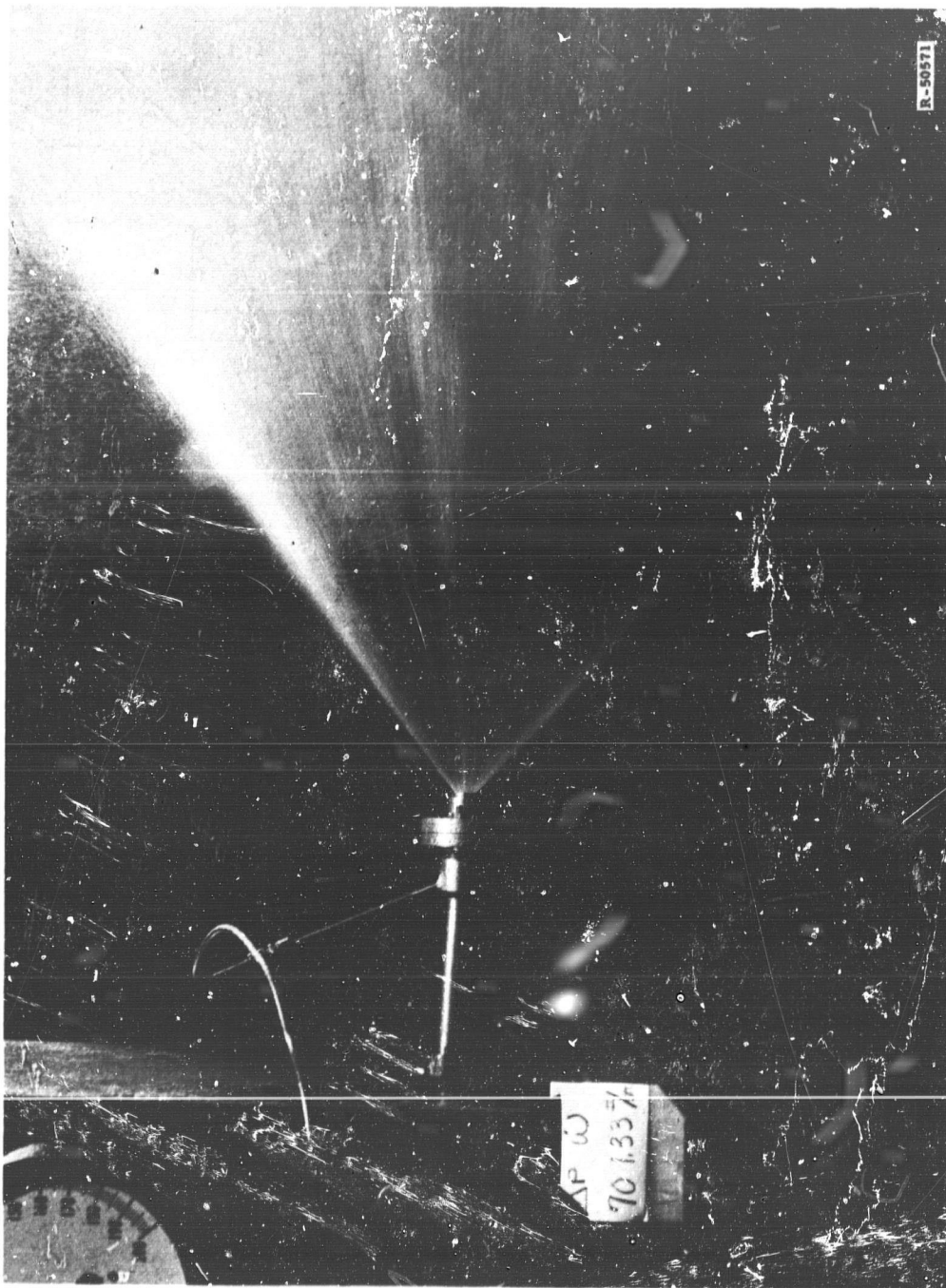
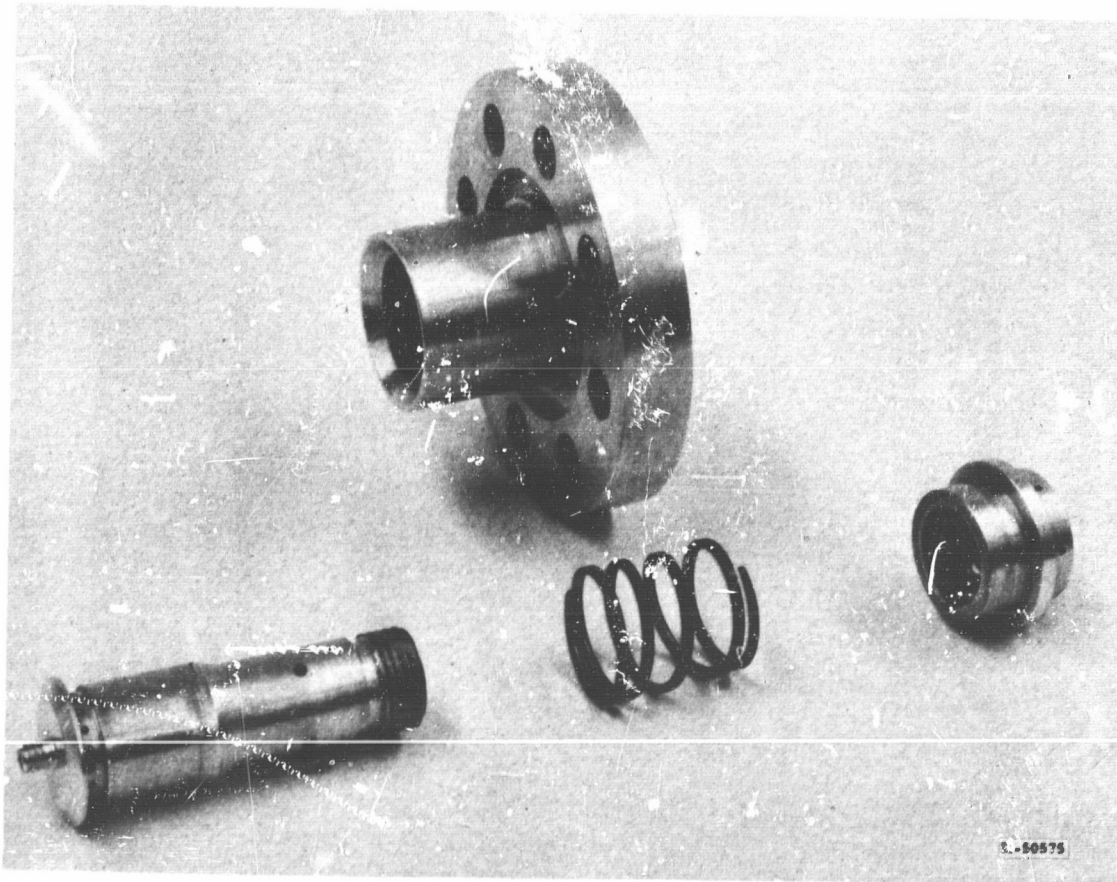
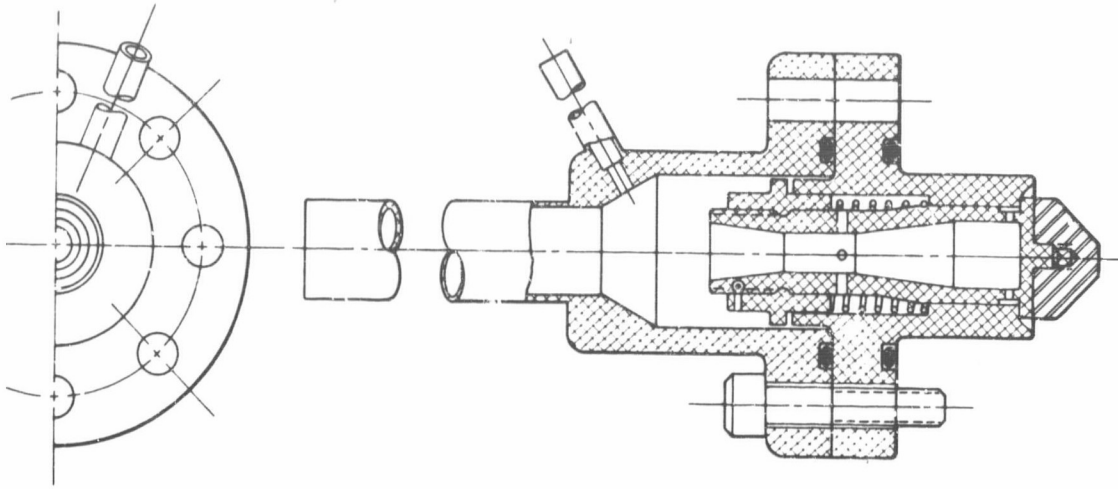


Figure 39. (U) Spray Pattern of Poppet Injector



R-51780

Figure 40. (U) Shutoff Orifice Injector

(U) Both injectors have been tested successfully, the former under this Contract and the latter under Contract No. AF 04(611)-10789. The concepts employed on both are being used in a dual manifold poppet injector being developed under Contract No. AF 04(611)-10789.

1.3 CONTROL SYSTEM DEVELOPMENT

(U) The development of an oxidizer flow control system was undertaken on Phase I of this program to provide a continuously changing distribution of primary and aft oxidizer flow rates as the motor is throttled. The objective of this program includes the achievement of a throttling ratio of 12:1 with a long-range goal of 50:1.

(C) Because the flow rate of the selected fuel system* varies with the square of the primary oxidizer** flow rate, the primary oxidizer flow must be varied with the square of the thrust ratio. To maintain a constant mixture ratio during throttling, oxidizer must then be injected at the aft end of the motor. The required primary and aft oxidizer flow rates for a 5000-lb-thrust motor are shown as a function of motor thrust in the flow schedule, figure 41. Aft-end oxidizer flow is maintained at a minimum of 1.0 lb/sec at full thrust to provide for cooling of the aft injectors.

(U) The practical limit of flow variation in fluid flow control devices is approximately 150:1, and is determined by the machining tolerances that can be used; hence, with a single fluid control device controlling the primary oxidizer flow rate, a throttling ratio of approximately 12:1 is available. A throttling ratio goal of 50:1 was established; therefore, studies were conducted to design a control system that could throttle the primary oxidizer flow rate over a range of 2500:1, the required range for a thrust ratio of 50.

(U) A preliminary design analysis has been conducted to evaluate several means of controlling thrust with a combined forward and aft injection system. The analysis included consideration of valve location in the circuit, the use of fixed-area injectors with aeration, the use of variable-area injectors, and the use of constant pressure-drop injector designs. Figure 42 shows the schematics of the control circuits considered and rejected in favor of the system used in figure 43, which has been tentatively chosen as the best control system with respect to minimum valve turndown ratio, simplicity, and accuracy.

* 25% lithium, 40% lithium hydride, 65% binder

** OF₂ or FLOX, 70% fluorine, 30% oxygen

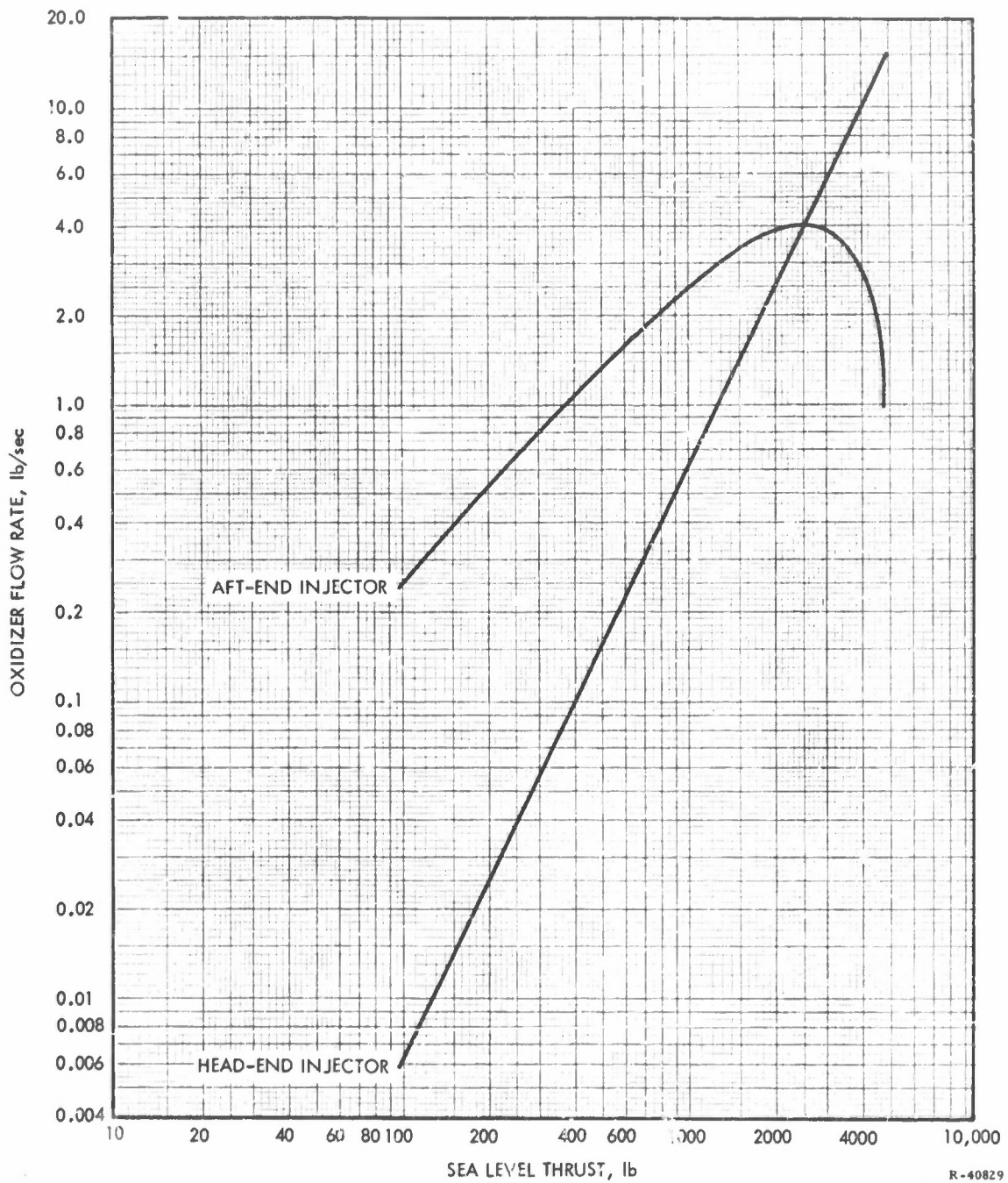


Figure 41. (U) Oxidizer Flow Rate as a Function of Motor Thrust

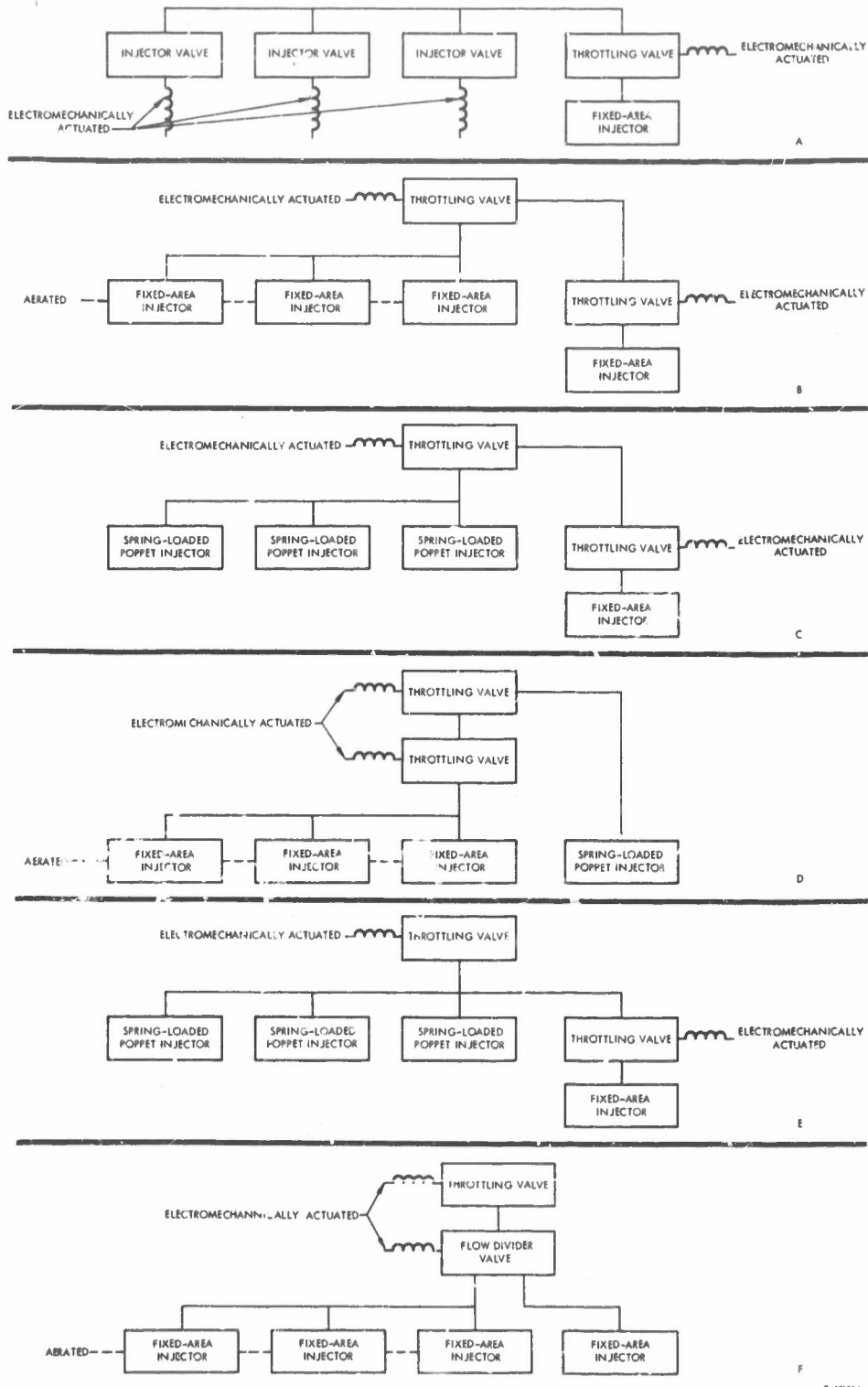


Figure 42. (U) Schematics of Control Systems

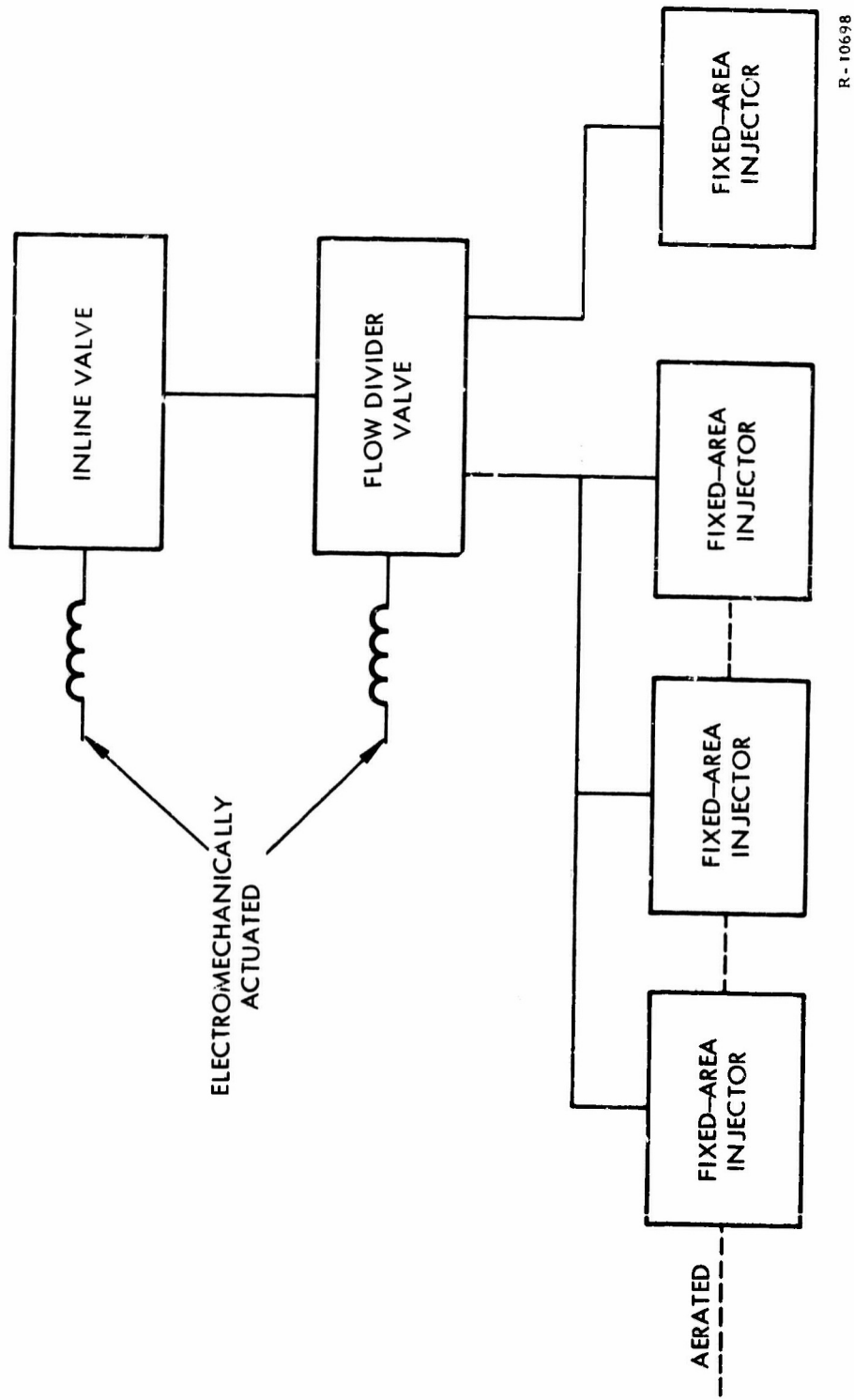


Figure 43. (U) Selected Flow-Control System

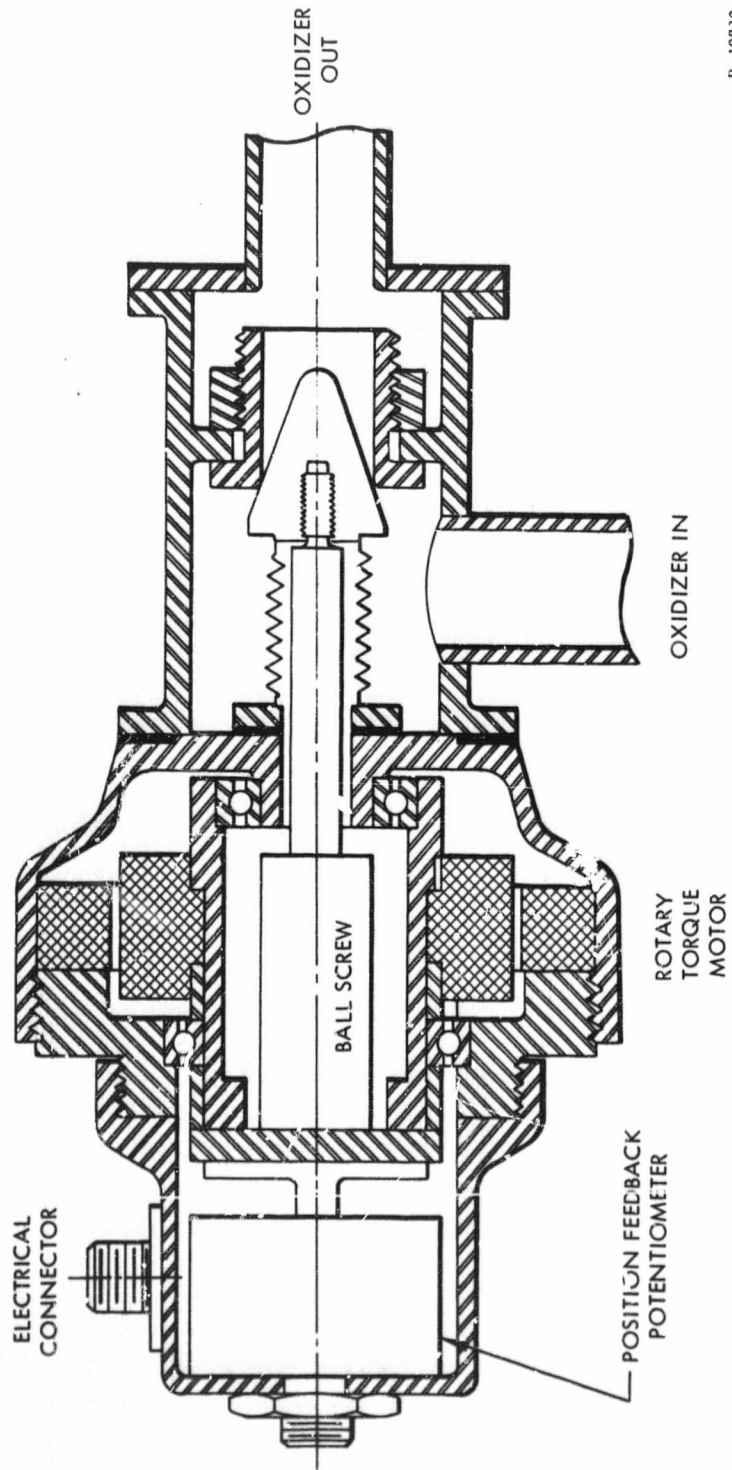
(U) The system chosen utilizes a main oxidizer flow control valve to throttle the oxidizer in proportion to thrust, a flow divider valve to distribute the oxidizer according to the schedule shown in figure 41, and an electronic network with a flow schedule function generator, which would allow continuous throttling on command.

(U) The control system selected has the following advantages:

- A. Thrust is controlled by one valve.
- B. Nonlinear aft-to-forward flow distribution can be controlled by a single flow-divider valve independently of the main throttle valve.
- C. It requires the lowest valve area turndown ratio with fixed area injectors.
- D. The control system requires only two feedback signals to control thrust and flow distribution.
- E. The choice of a flow-divider valve eliminates flow distribution errors caused by unpredicted errors in valve pressure differentials and oxidizer density.
- F. The primary oxidizer flow ratio that exhibits the greatest variation is indirectly controlled and is not used for feedback control.
- G. The system can be used with either fixed-area or spring-loaded constant pressure-drop injectors and can be developed independently of the final injector design.

(U) The flow-control valve (figure 44) is a pintle-type valve with a bellows for the pintle shaft seal. The actuator uses three rotary torque motors to drive the pintle through a ball-screw assembly. The flow-divider valve (figure 45) also uses a bellows shaft seal and the same actuator as the main control valve. Each valve will weigh approximately 5 lb.

(U) The throttling requirements of the two valves are shown in table I as a function of thrust. Both valves require a turndown ratio of approximately 50:1 to obtain the flow distribution and achieve 50:1 throttling ratios. These ratios do not introduce any significant fabrication tolerance problems.



R-40830

Figure 44. (U) Thrust Control Valve

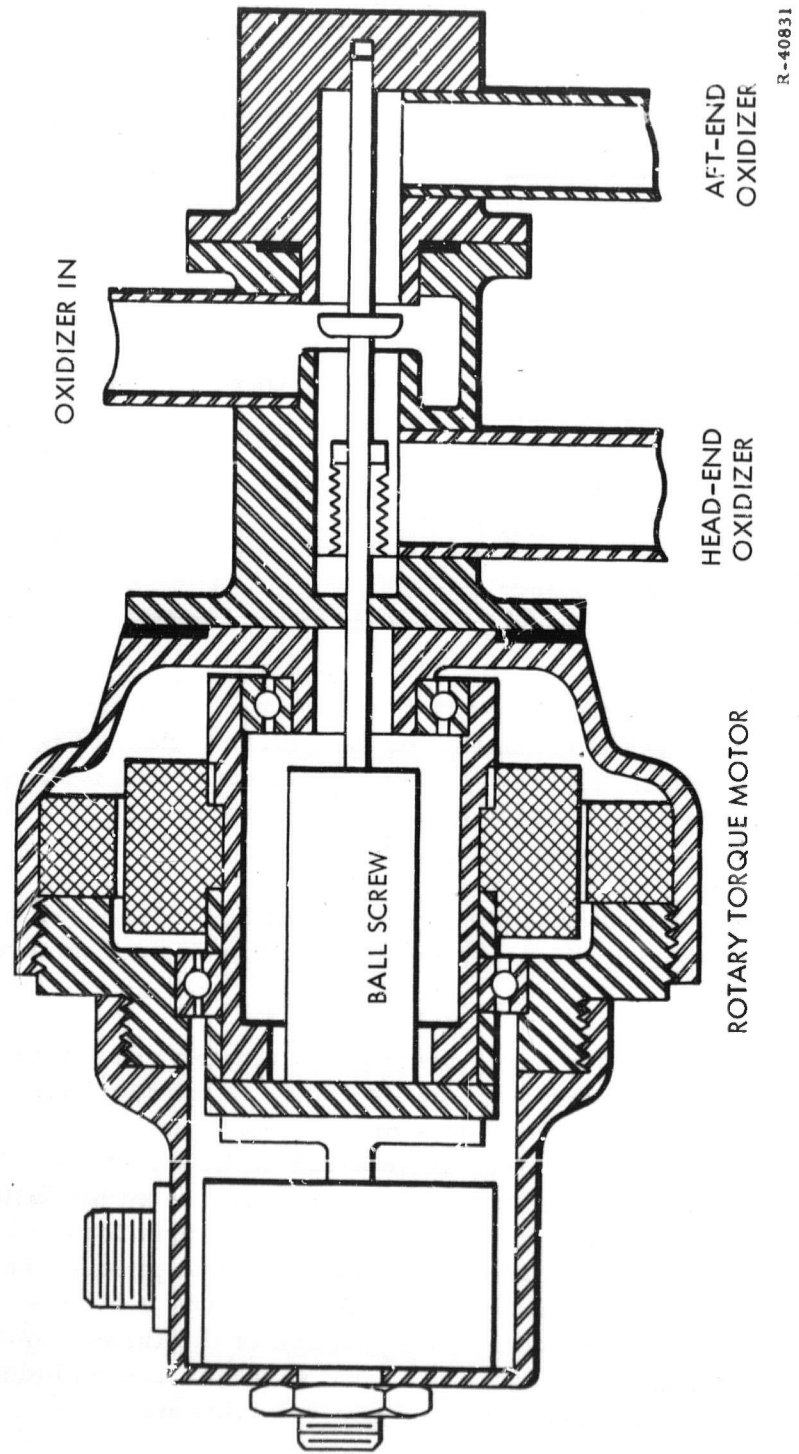


Figure 45. (U) Flow Divider Valve

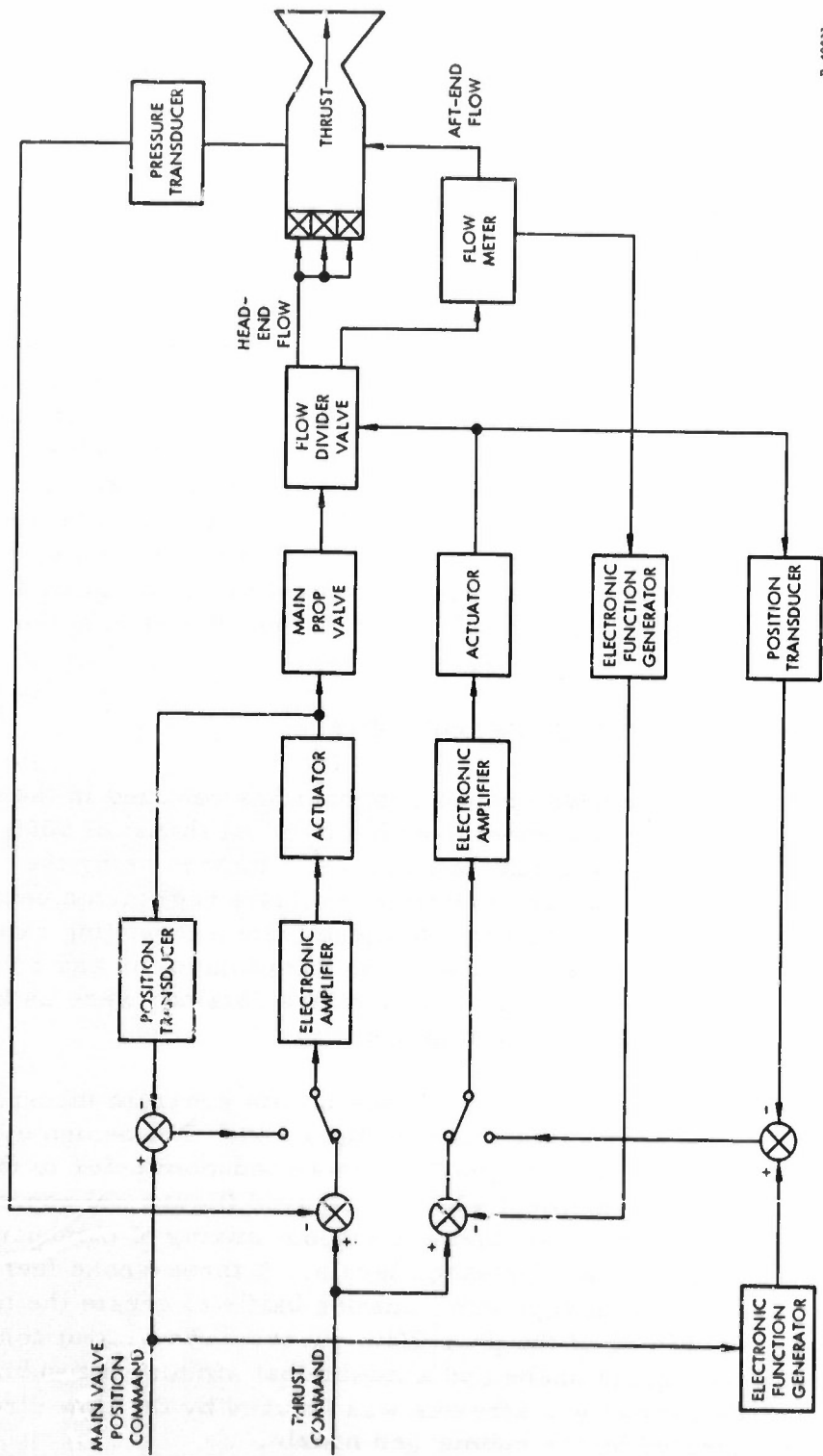
TABLE I
OXIDIZER FLOW-CONTROL VALVE REQUIREMENTS

<u>Thrust lb</u>	<u>Throttling Ratio</u>	<u>Main Oxidizer Control Ratio</u>	<u>Flow Divider Ratio Aft/Primary</u>
5000	1:1	1:1	0.079:1
2500	2:1	2:1	1:1
1000	5:1	5:1	4.4:1
500	10:1	10:1	9.8:1
100	50:1	50:1	40:1
50	100:1	100:1	106:1

(U) The control circuit consists of two control loops, one for controlling the main valve and one controlling flow distribution. Figure 46 shows the chamber-pressure control system planned for initial testing. The thrust-control loop is closed around chamber pressure and its error signal is used to control the main throttling valve.

(U) The flow-divider valve is positioned by a signal from a function generator, designed to match the flow ratio required as a function of engine thrust.

(U) The flow divider valve control system can use either valve position feedback or the aft-end oxidizer flow rate as the feedback signal. The former method should provide a more reliable feedback source because, once the valve is calibrated, little error in flow ratio will occur with changes in oxidizer temperature and density. With the latter method, at low thrust levels, the aft flow rate is greater than forward-end flow and small errors in aft-end flow-rate control would produce relatively large errors in forward-end flow rates. A secondary control system is incorporated to separately control the position of the thrust-control valve independently of chamber pressure. Two switches are included for selection between thrust and valve position control systems.



R-40832

Figure 46. (U) Hybrid Thrust Control Circuit

CONFIDENTIAL

AFRPL-TR-65-184

(U) This control system was selected because it did not have any limitations imposed by fabrication tolerances. Fixed-area injectors with aeration were selected as the most feasible means of obtaining deep throttling ratios. The desirability of using aeration would, of course, depend on the mission of the motor and the volume of helium required.

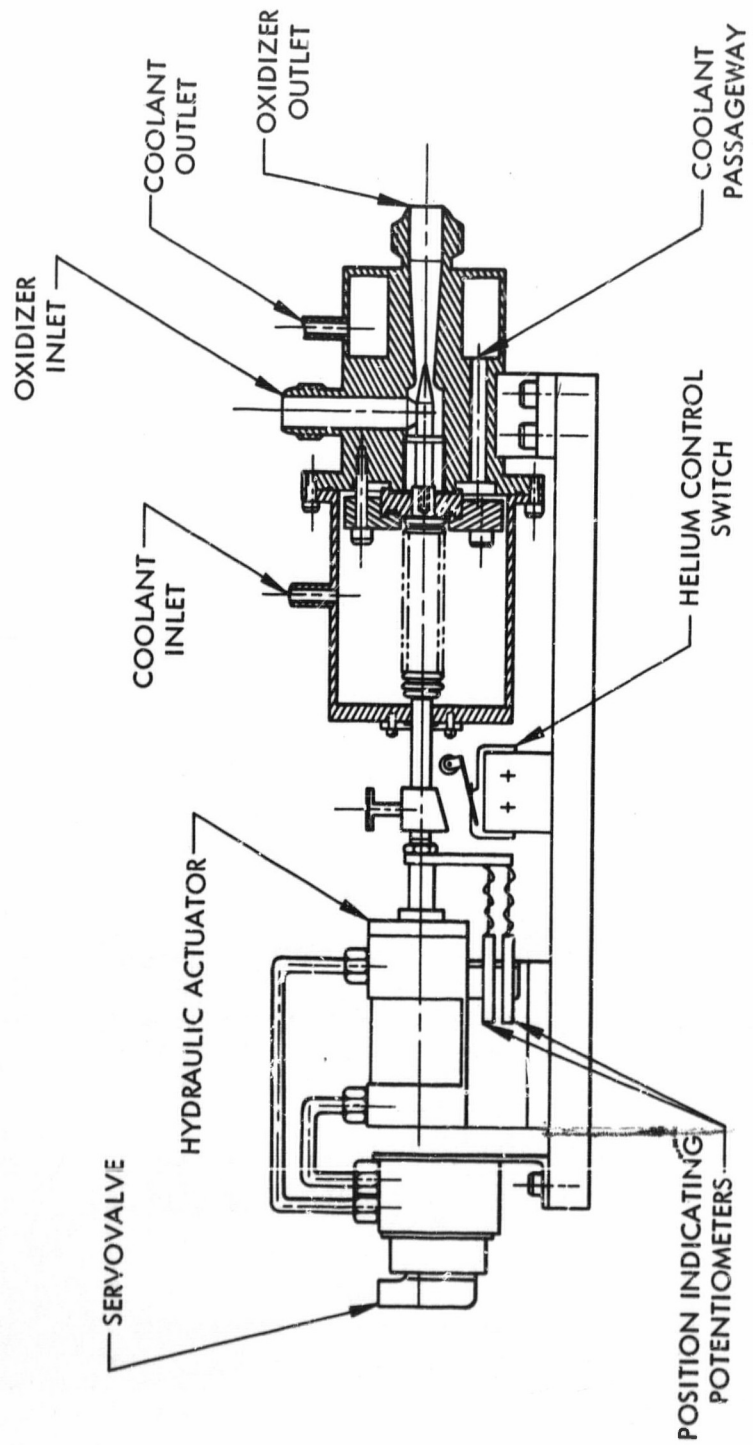
(U) Although designs were completed on the thrust control valve and flow divider valve, only the flow divider valve shown in figure 45 has been fabricated during this program.

(U) Development work on the valves was discontinued when the program was redirected toward a dual-thrust tactical hybrid propulsion system. The remaining throttleable motor development tests used the two existing venturi flow control valves shown in figure 47 to control primary and aft-end oxidizer flow separately. As a result, the maximum achievable throttling ratio was approximately 13:1. Development of the flow control system was continued at UTC under Contract No. NAS 7-311, which is directed toward the development of throttleable, space-storable propulsion systems. The flow divider valve, shown mounted to the control valve in figure 48, was successfully tested on full-scale motor tests conducted during the NASA program.

1.4 THROTTLEABLE MOTOR DEVELOPMENT

(C) The throttleable motor development program has resulted in the test firing of 7 lightweight hybrid test motors with a nominal thrust of 5000 lb. Twelve development tests were conducted with the 7 motors using the FLOX/lithium composite propellant system to evaluate regression behavior and performance at high and low thrust. In these tests a throttling ratio of 13.7:1 was demonstrated. Low-thrust firing durations of 30 and 60 sec were obtained on one motor and performance values obtained were as high as 94% of theoretical shifting specific impulse.

(U) The full-scale motor used in both phases of this program incorporated a lightweight fiberglass case design shown in figure 49. The design evolved from heavyweight steel-case motors used in tests conducted prior to this program. Two heavyweight motor designs were used (figure 50) representing two different concepts in achieving complete mixing of combustion chamber gases to obtain high performance levels. A three-spoke fuel grain motor was used in one design with a mixing baffle to create the turbulence necessary for mixing of the propellant gases. The second concept used a hubbed cartwheel grain shape and a mixer that simulated a submerged nozzle. Mixing of the coaxial gas streams was induced by the flow direction change in a plenum created by the submerged nozzle.



R-40487

Figure 47. (U) Oxidizer Flow Control Valve

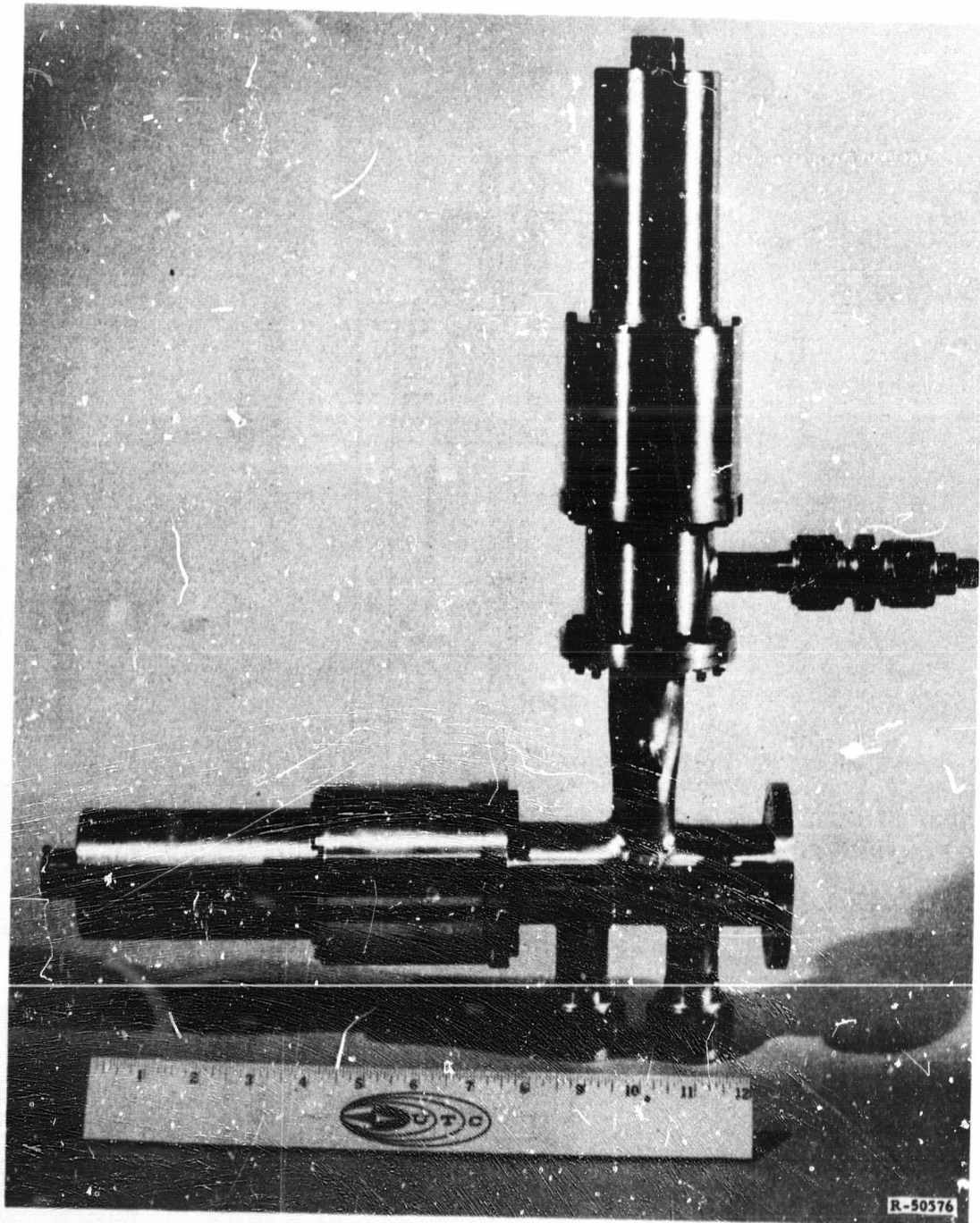


Figure 48. (U) Thrust Control Valve Assembly

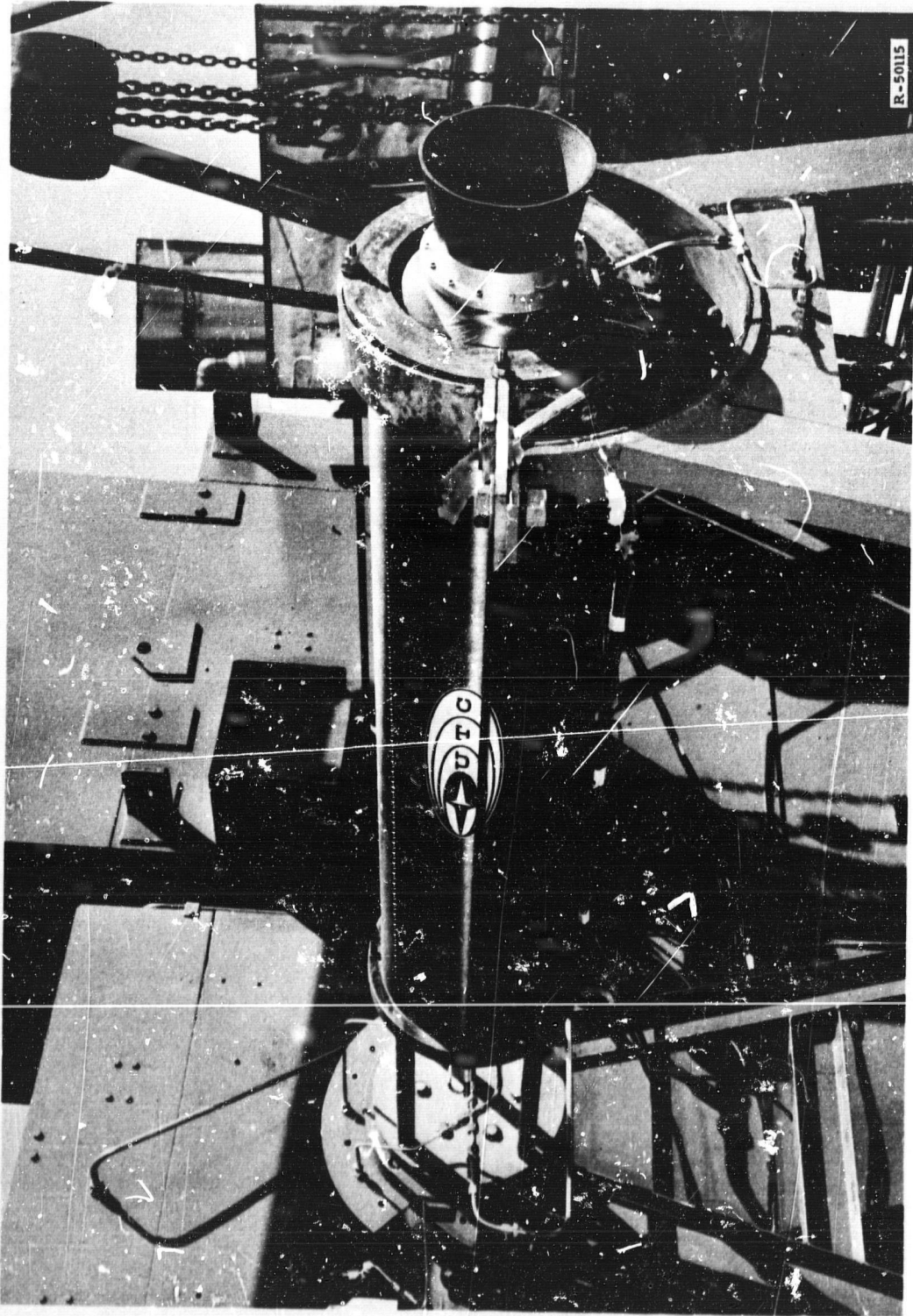
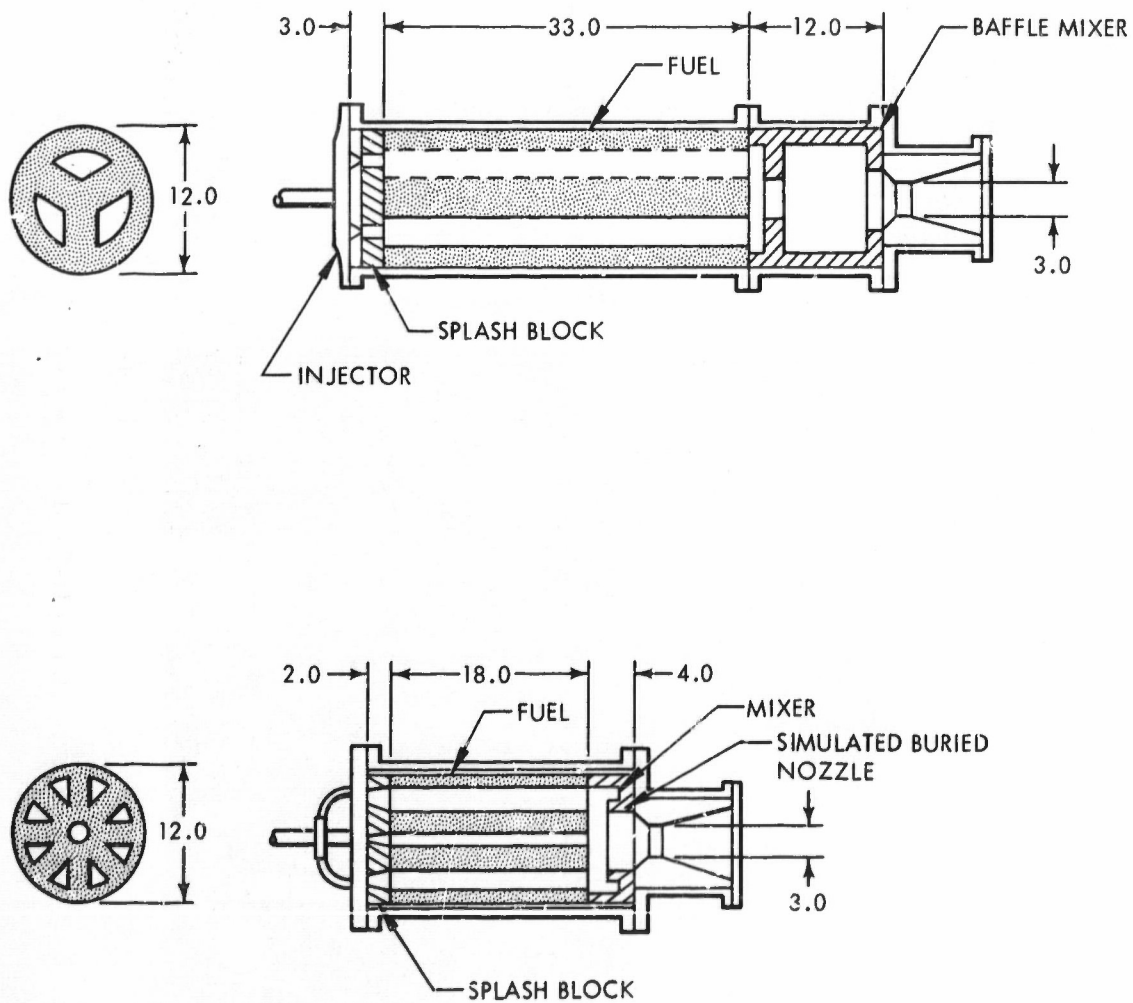


Figure 49. (U) Full-Scale Filament-Wound Motor



NOTE: All dimensions are in inches.

#-51781

Figure 50. (U) 5000-lb-Thrust Motor Designs

(C) Four tests were conducted prior to the present effort with the two motor configurations using FLOX and the lithium composite fuel. The test results are given in table II.

TABLE II
HIGH-PERFORMANCE, FULL-THRUST MOTOR TESTS

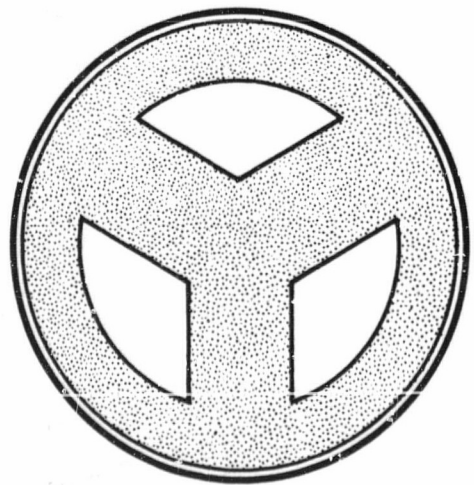
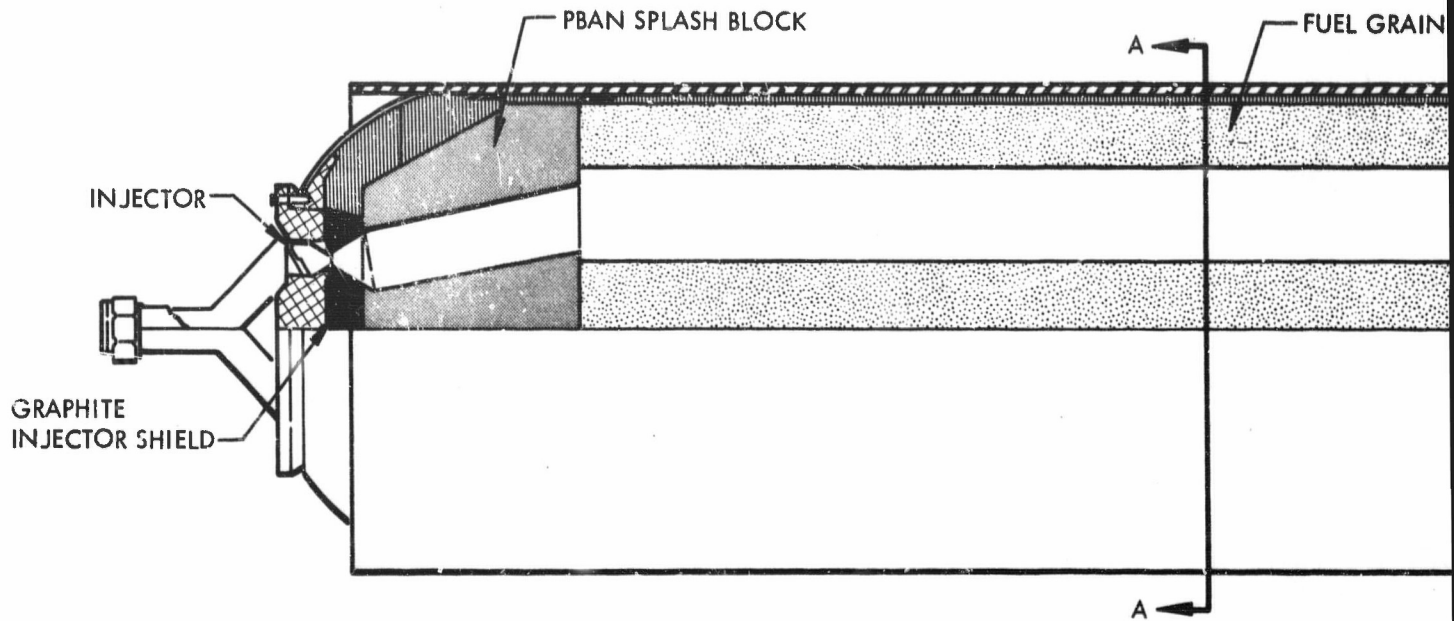
<u>Test No.</u>	<u>Grain Configuration</u>	<u>Delivered I_{sp} (Corrected to 1000/14.7 sec)</u>		<u>Characteristic Velocity (c*) ft/sec</u>	
L6-0170	Three spoke	315	94%	6510	99%
L6-0183	Three spoke	302	92%	6305	98%
L6-0184	Hubbed cartwheel	315	91%	6880	98%
L6-0215	Hubbed cartwheel	305	86%	6150	88%

(C) Both designs exceeded the performance goal of 300 sec. The three-spoke design produced slightly higher performance levels and a less complex system to conduct development testing and the submerged nozzle approach presented a more practical flight configuration design. The three-spoke design was selected for initial development testing.

(C) Flightweight motor development was to have been initiated in Phase II of the program with multiple test firings to statistically evaluate motor performance and fuel utilization. However, this phase of the program was redirected toward tactical missile propulsion systems in order to be more consistent with current Air Force requirements.

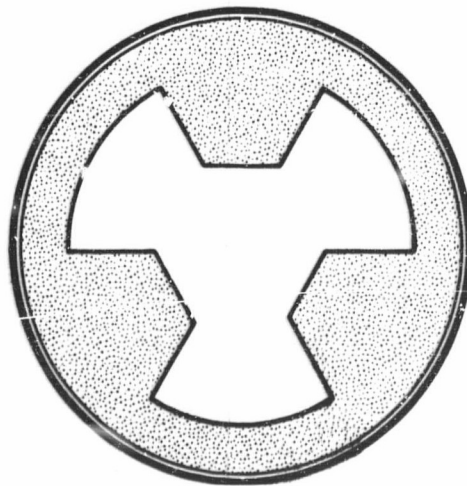
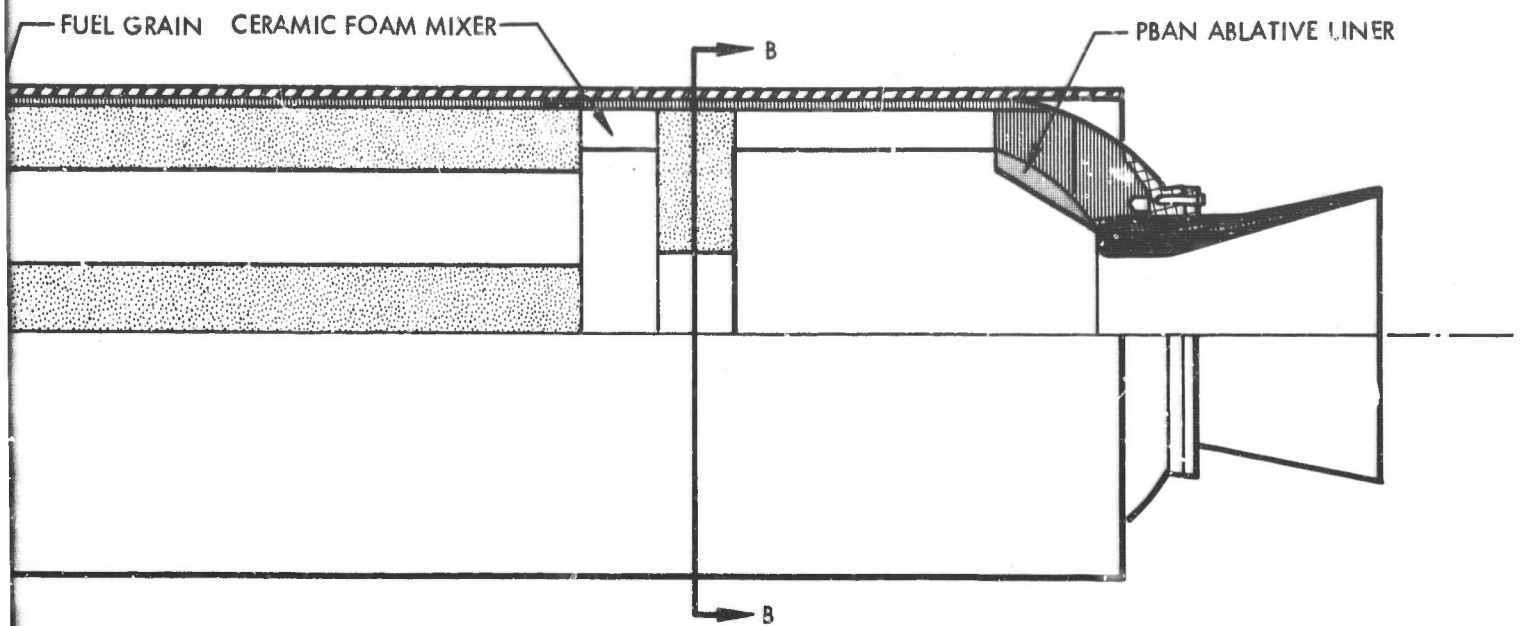
1.4.1 Motor Design

(C) The lightweight motor design is shown in figure 51. A detailed design drawing is presented in appendix IV. The motor uses a three-spoke grain shape and a star mixer which is fabricated of ceramic foam. The heavy-weight mixer assembly is shown in figure 52. Both the grain and mixer are similar to those previously tested in steel-case motor hardware, delivering specific impulse levels of up to 315 sec. Although the filament-wound motor weighs only 170 lb, it is not considered flightweight. It does, however, provide a less expensive motor case that is more easily handled than the 700-lb steel case motor.



SECTION A-A

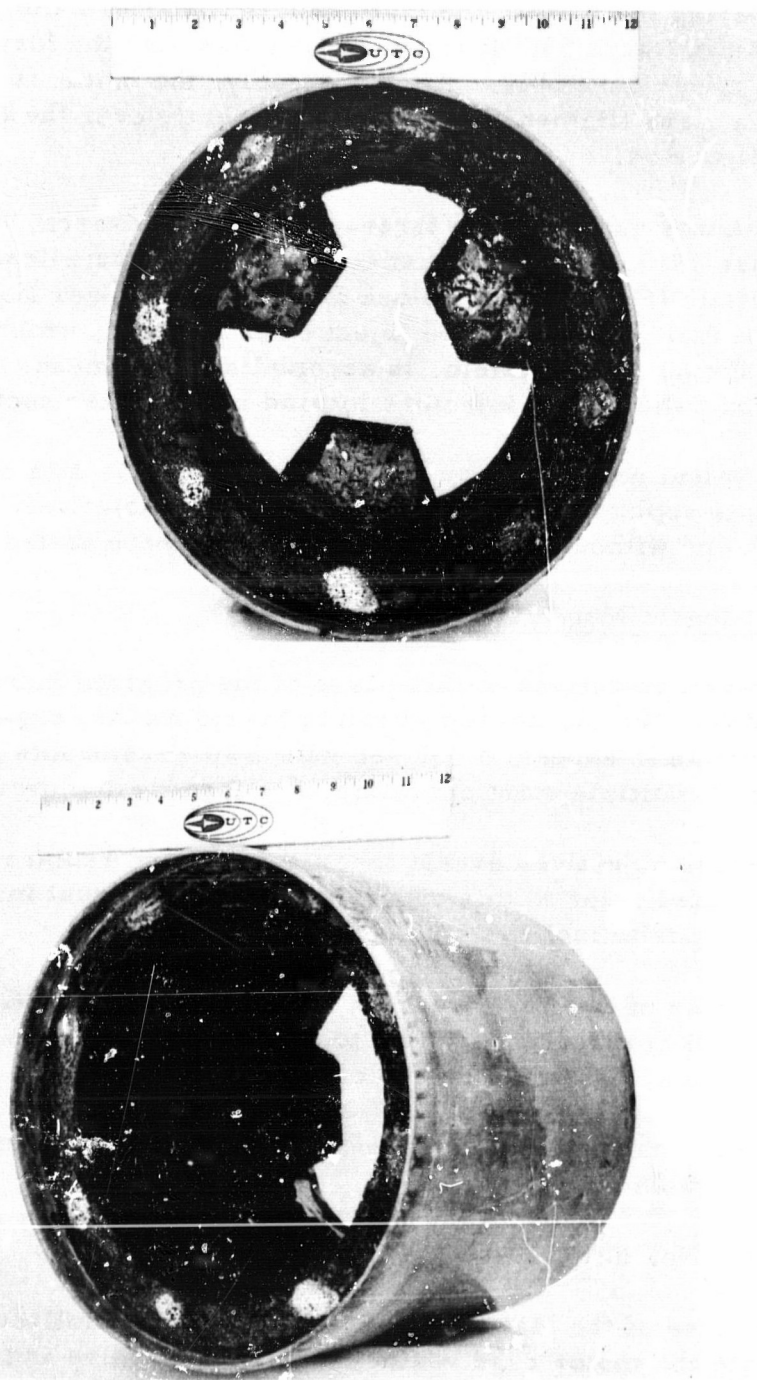
CONFIDENTIAL



SECTION B-B

P-50030

Figure 51. (U) Full-Scale Test Motor Schematic



R-50116

Figure 52. (U) Mixer Assembly

CONFIDENTIAL

(U) In preparing the motor, the fuel grain is cast into a thin phenolic liner as shown in figure 53. It is then assembled with the forward and aft closures and mixer assembly. After assembly, the motor is mounted on a mandrel and a glass filament case is wound directly over the components, as shown in figure 54.

(U) Aeration was used with the three-element, fixed-area, hollow-cone injector (figure 19) to provide thrust control. A polybutadiene acrylic-acid acrylonitrile (PBAN) splash block directs the oxidizer flow from the injector to the fuel grain. Aft-end injection of oxidizer, which is needed with the conventional fuel system, is accomplished by means of three equally spaced hollow-cone injectors located in the mixer section.

(U) A lightweight nozzle (figure 55) is used to provide data on nozzle design concepts applicable to flightweight motors. Ablatively cooled nozzles, with and without graphite throat inserts, were tested.

1.4.2 Throttleable Motor Test Program

(C) The overall objectives of this phase of the program include the development of a 5000-lb-thrust, 20-sec-duration hybrid motor, capable of delivering a specific impulse in excess of 300 sec with a space-storable propellant system, capable of multiple start operation, and throttleable over a 12:1 ratio.

(U) All of these objectives except throttleability and restart operation were demonstrated prior to this program in 5000-lb-thrust motors using the lithium composite fuel system and FLOX.

(U) The purpose of this test program was to evaluate throttled behavior of the motor with respect to performance and regression rate and to obtain empirical data to assist in the design of flightweight motors.

(U) A summary describing the essential parameters and purpose of each test is given in table III.

1.4.2.1 Motor No. 001

(U) The purpose of the test firings involving the first full-scale motor was to evaluate the motor case venturi flow control valve and the aeration system. The motor was to be fired for 20 sec while oxidizer flow was varied from 5 to 100% of the full flow rate. (The full flow rate corresponds to 5000-lb thrust.) A sea-level thrust range in excess of 15:1 was covered during this first test. However, because aft injection was not used, the mixture ratio shifted to fuel rich during throttling, resulting in reduced performance. A valve control calibration error resulted in the achievement

CONFIDENTIAL

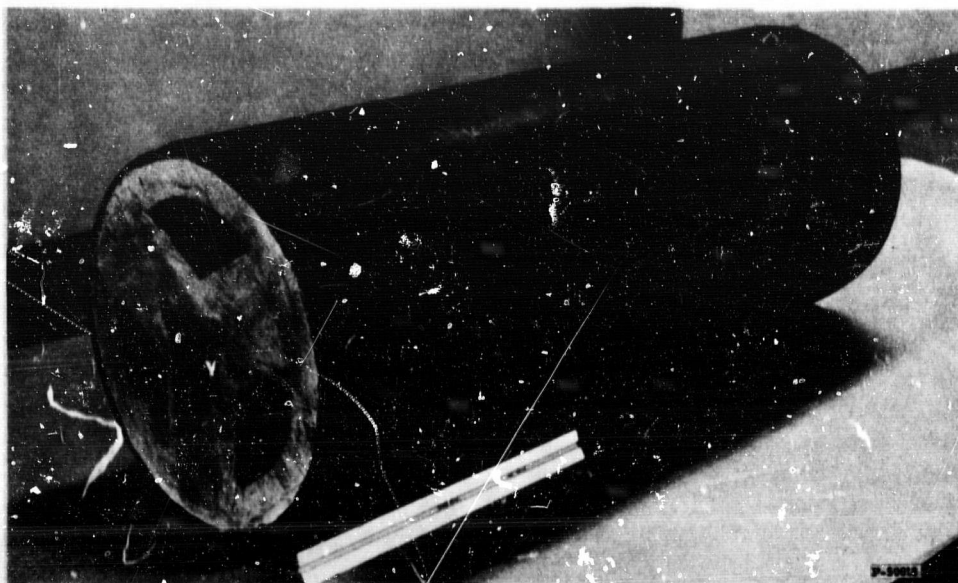


Figure 53. (U) Three-Spoke Fuel Grain

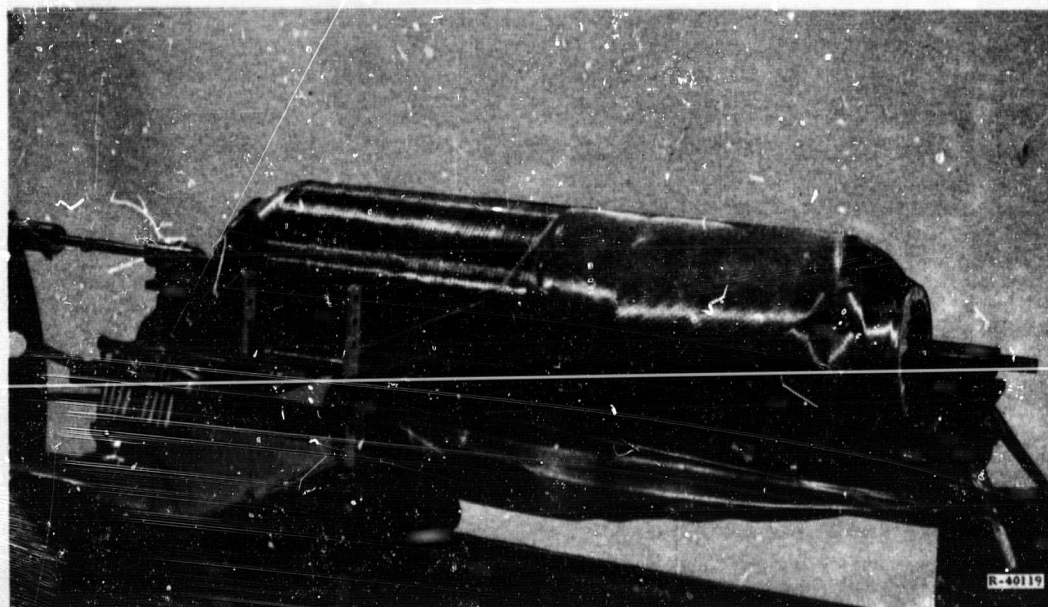


Figure 54. (U) Filament Winding a 12-in. Motor Case

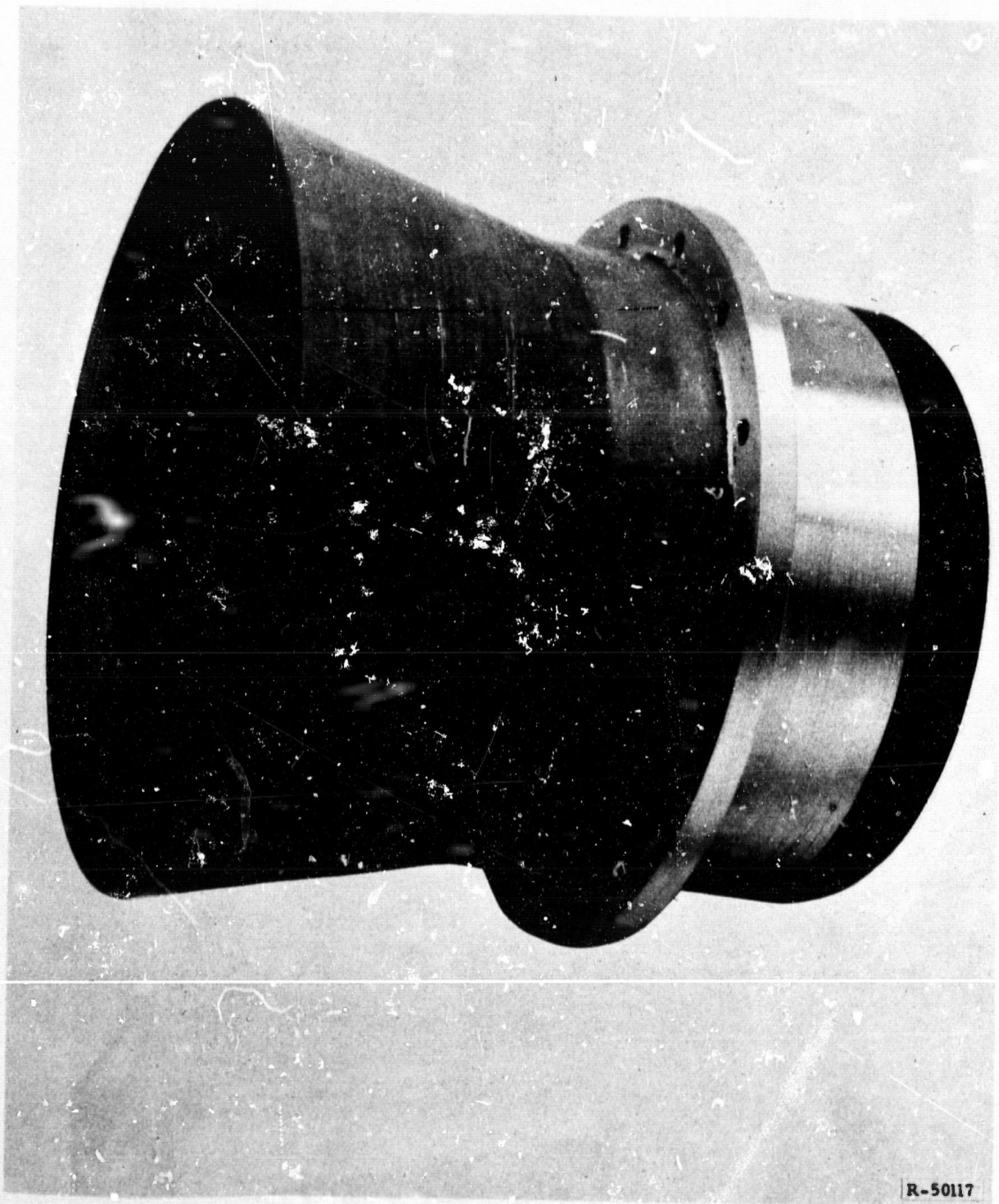


Figure 55. (U) Lightweight Nozzle

TABLE III
 TEST SUMMARY PHASE I
 FULL-SCALE MOTOR TEST PROGRAM

Motor No.	Fuel	Oxidizer	P _c psia	Thrust lb	Duration sec	Performance %	Purpose
001	HFX 2084	FLOX	117 → 17	4310 → 8C	20	-	Throttled primary injector 10 thrust levels
001	HFX 2084	FLOX	215 → 69	4690 → 1760	8.5	-	Restarted, 7 thrust levels
002	HFX 2084	FLOX	269	5777	12.4	-	Full-thrust evaluation with aft injectors
003	HFX 2084	FLOX	285	4800	1.4	-	Full-thrust evaluation with aft injectors
003	HFX 2084	FLOX	-	-	3.0	-	Full-thrust evaluation with aft injectors
003	HFX 2084	FLOX	-	-	5.0	-	Ignition test, 20% thrust level
004	HFX 2084	FLOX	-	-	-	-	
005	-	--	-	-	30.0	-	Low-thrust evaluation
005	-	--	-	-	60.0	90	Low-thrust evaluation
006	HFX 2084	FLOX	285	-	14.0	-	Throttled 13.7:1 with variable aft injection
007	HFX 2084	OF ₂	285	-	14.0	90	OF ₂ full-thrust, no mixer

of a maximum of 4200-lb thrust during this firing. The motor was reignited, after valve calibration, for an additional 8.5-sec duration and oxidizer flow was again varied from 5 to 100% of full flow. The second firing was conducted without cleaning the injector or servicing the motor or control valve system.

(U) Aeration was successfully demonstrated to be a simple and reliable means of throttling with a fixed-area injector; however, minor oscillations occurred on the first test when aeration was turned off for higher thrust levels. The oscillations, which were attributed to insufficient helium pressure, were eliminated during the second test by aerating at all thrust levels in which the injection pressure was less than the helium supply pressure. Postfire inspection of the motor components (figure 56) indicated the design of the motor to be sound.

(U) The erosion rate of the consumable PBAN splash block (shown in figure 57) was comparable to that predicted by earlier 5.0-in. motor tests.

(U) The regression behavior of the fuel grain (shown in figure 58) indicated the need for injector modifications in future motor designs. A web of 1/4 in. can be seen near the aft end of the motor, while the grain has been burned to the case liner material at the head end. The higher regression rate at the head end on the outer web was attributed to the radial component of oxidizer momentum imparted by the splash block. Figure 59 shows the oxidizer flow path. A design change was made which solved the problem by aligning the injectors with the fuel grain port. The change is shown in figure 60. Further benefit is obtained by reducing the weight of the splash block and eliminating the grain undercutting seen in figure 58.

(U) Performance information was not obtained for the throttled tests because the tests involved only head-end oxidizer control, and the O/F ratio varied widely as thrust was decreased. It is apparent from these test results that the design of the mixer section is conservative and can be reduced by more than 20 lb. Further weight reduction can be achieved when the mixer is redesigned to a more compact size for lightweight motors.

(U) Equally important qualitative data was obtained for future hybrid nozzle design. The lightweight nozzle used on this test is fabricated from silica-phenolic cloth and a graphite insert. After 28.5-sec duration at various thrust levels, the nozzle showed only minor throat erosion, although some erosion occurred just downstream of the nozzle throat. The nozzle is shown in figure 61.

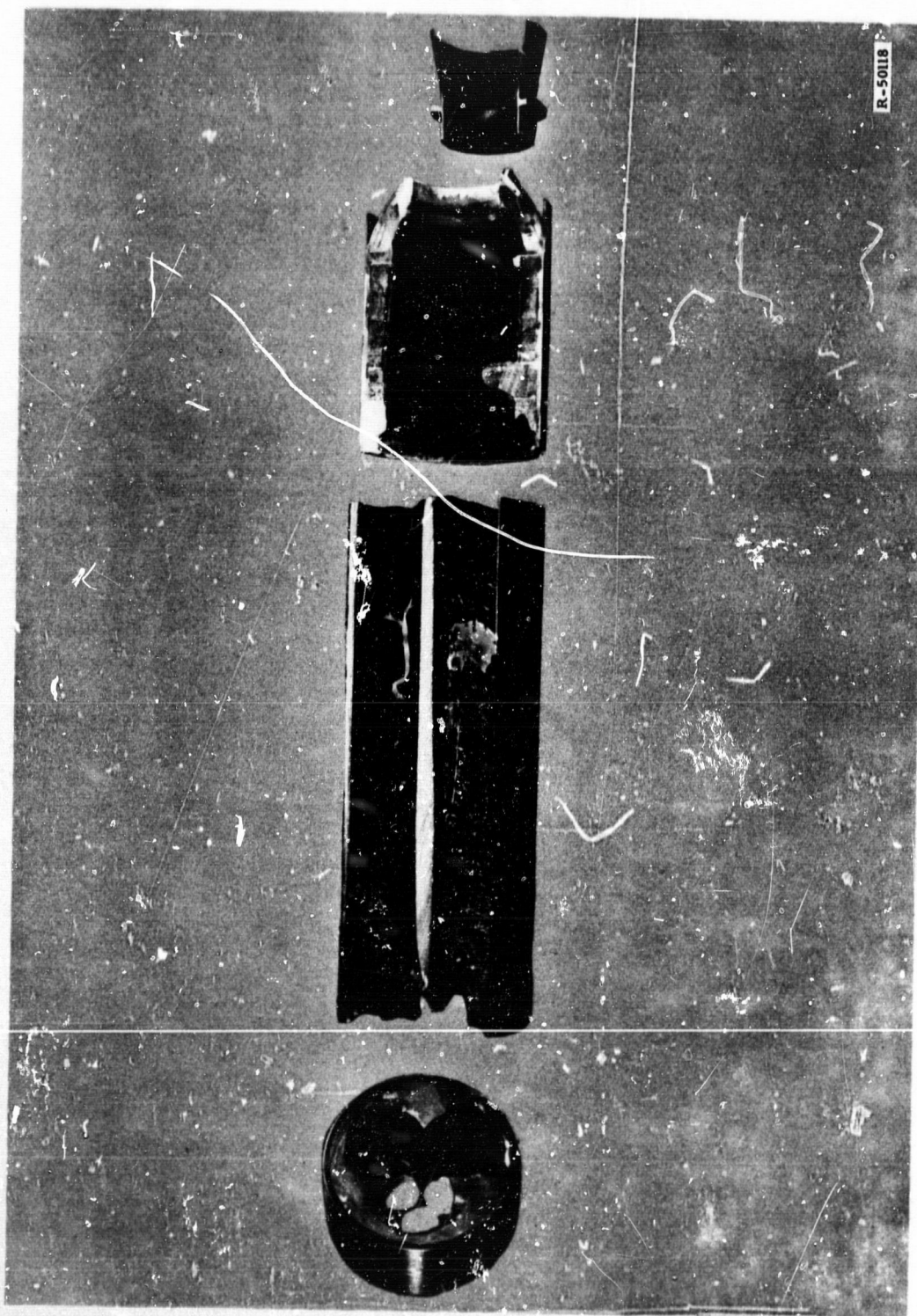


Figure 56. (U) Motor 001 Components After Test

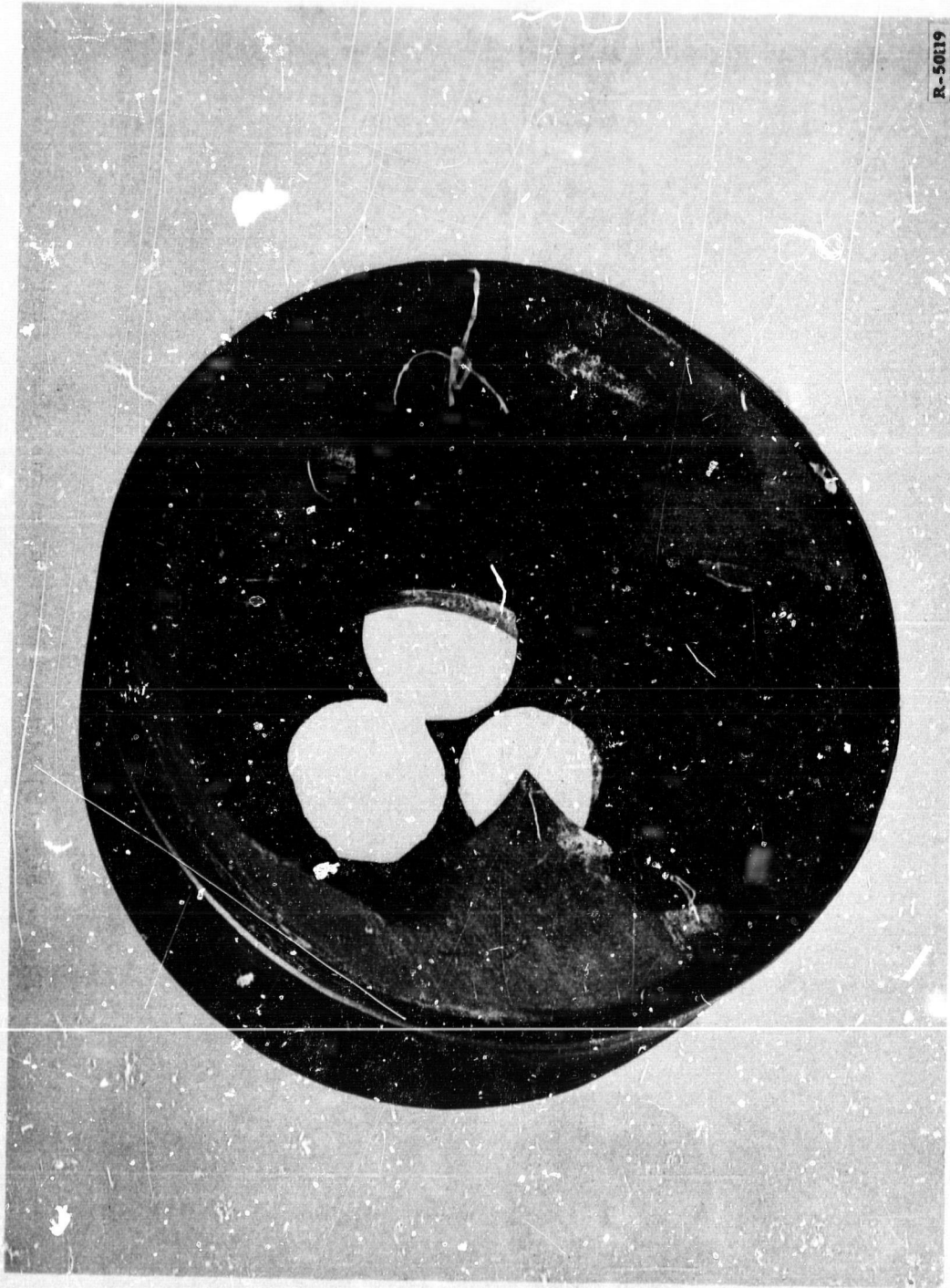
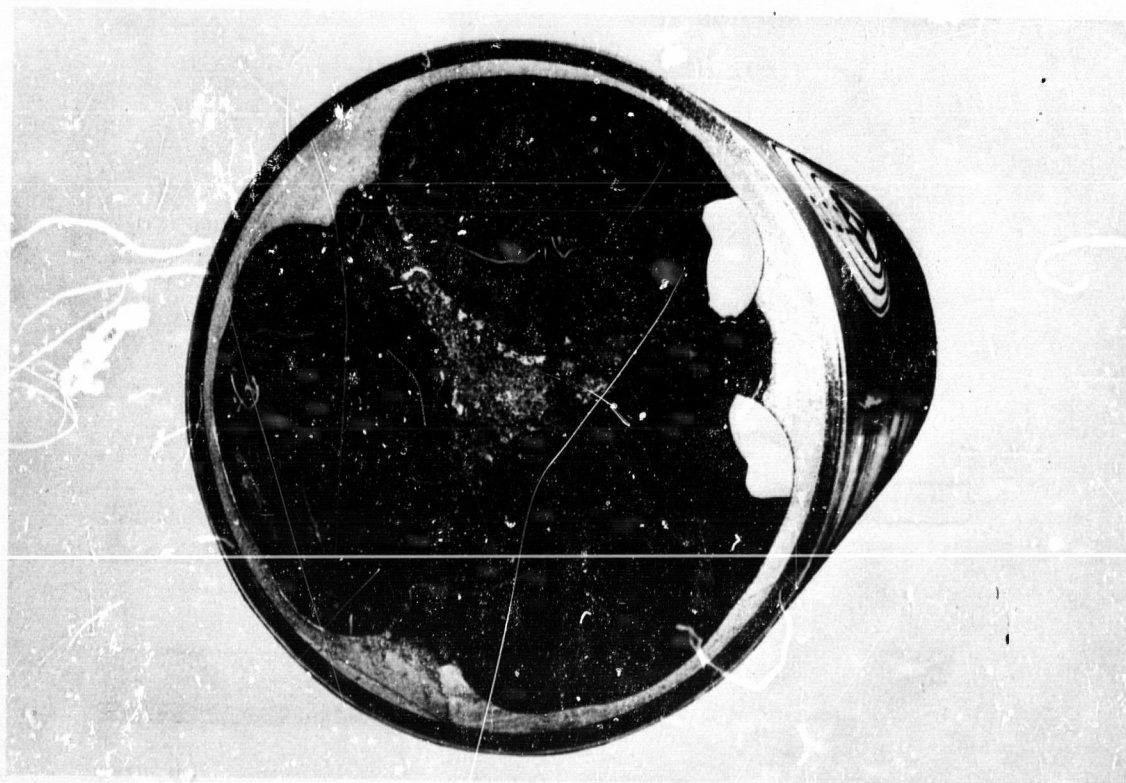
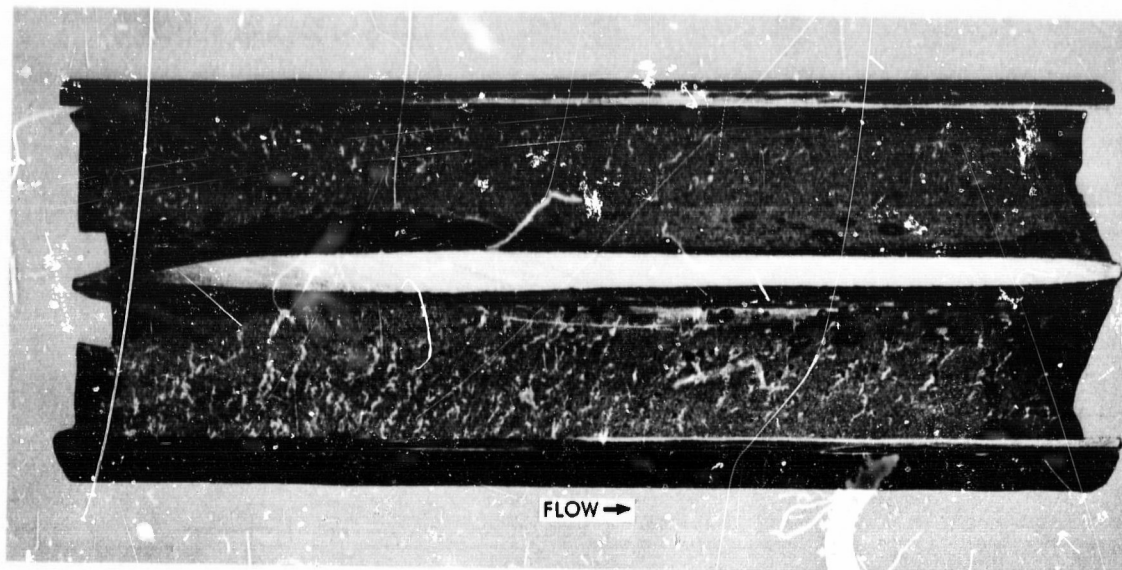


Figure 57. (U) Splash Block from Motor 001



R-50120

Figure 58. (U) Fuel Grain of Motor 001 After Test

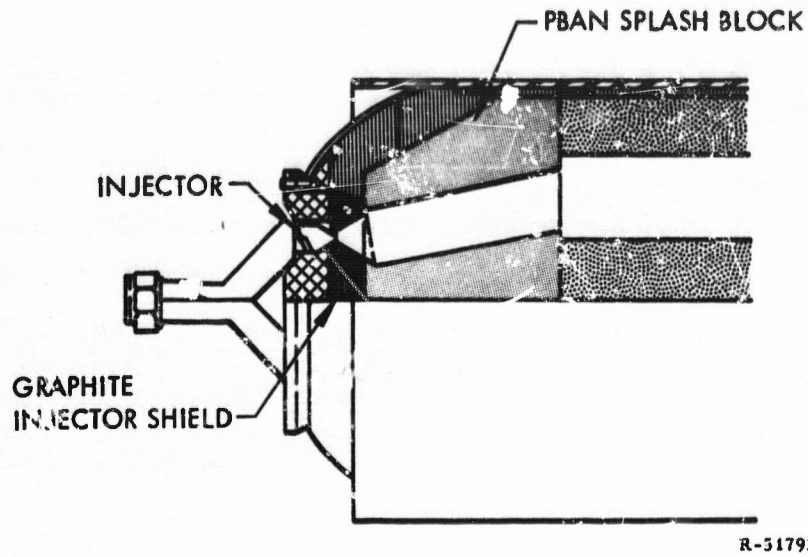


Figure 59. (U) Original Injector Installation

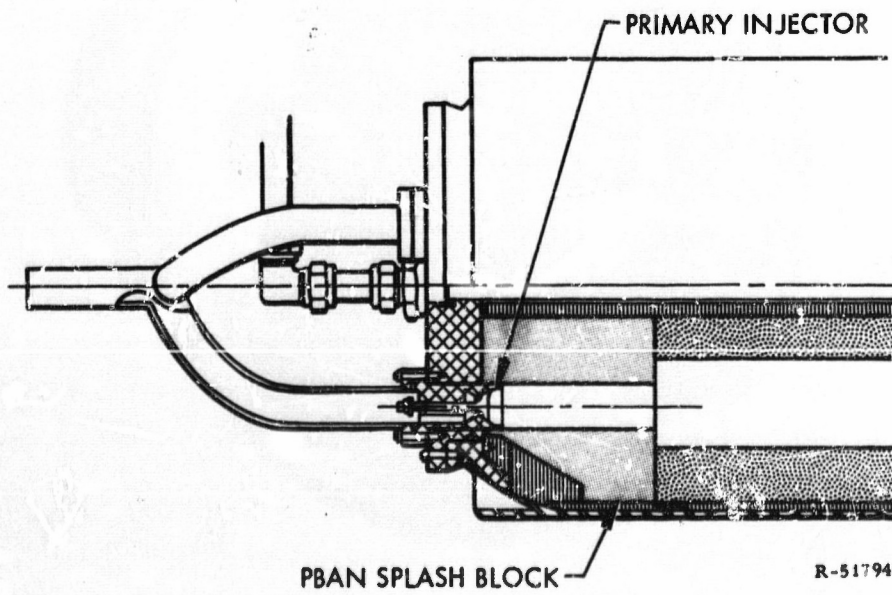


Figure 60. (U) Modified Injector Installation

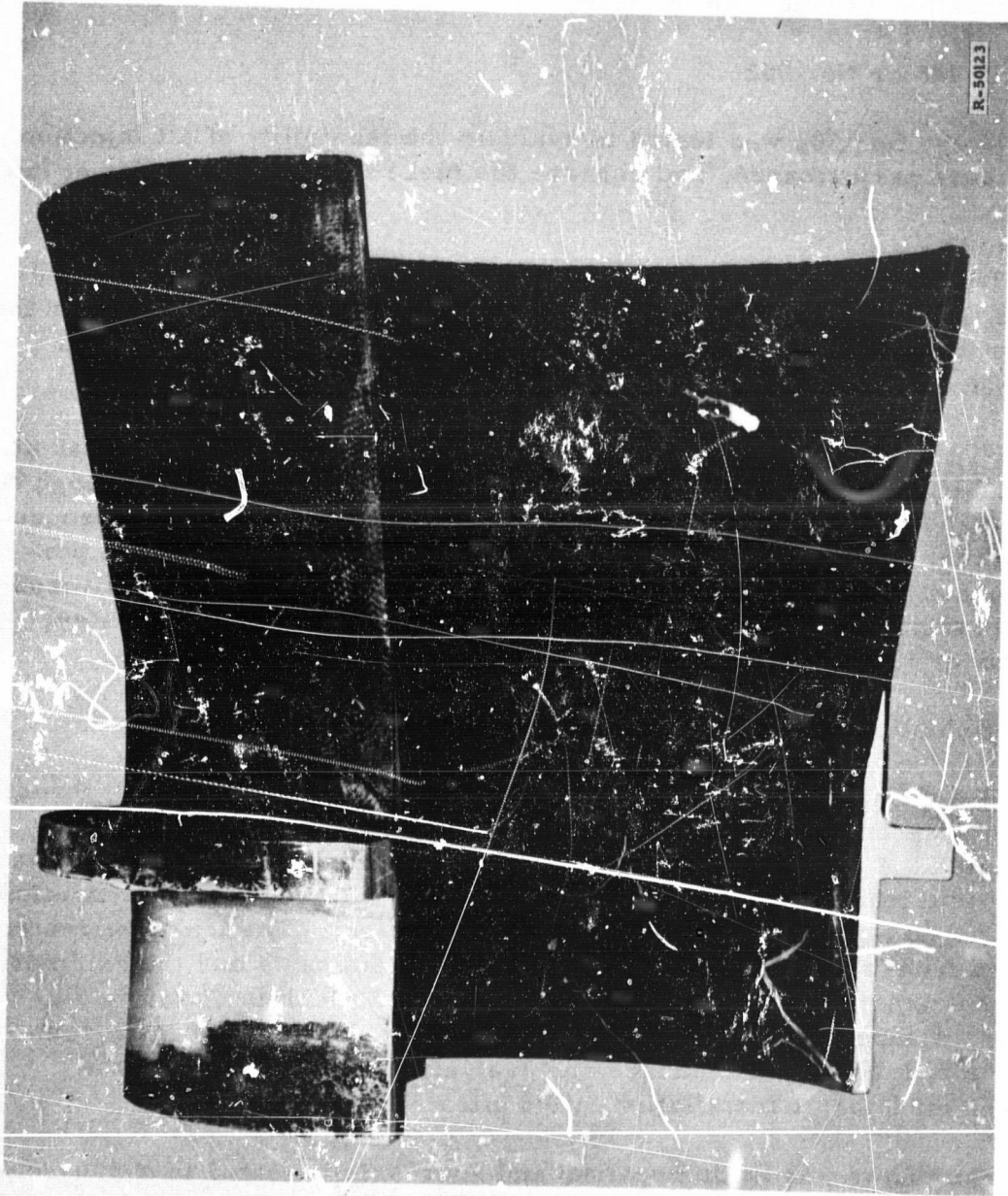


Figure 61. (U) Nozzle Assembly After Test

CONFIDENTIAL

(U) Reignition of the motor without servicing and the excellent condition of the lightweight injector after the second test indicate that multiple restarts pose no problem. The injector is shown in figure 62 with deposits of combustion products on the face.

1.4.2.2 Motor No. 002

(U) Motor No. 002 was tested to evaluate the feasibility of aft injection, to measure performance, and observe the fuel regression behavior at full thrust.

(U) The test was conducted at 5700-lb thrust for 14.2 sec of a planned 15-sec test. Termination of the test was planned at 15 sec rather than the full duration of 20 sec to allow sufficient fuel web to observe localized regression rates due to injector effects, etc.

(C) However, an O-ring failure at the injector caused a hot-gas leak at the head end of the motor. The injector is seen in figure 63. Although no performance data were obtained because of the case failure and subsequent loss of fuel, it is estimated from calculated fuel flow rates that the performance of this motor exceeded, by a substantial margin, the delivered specific impulse of 315 sec (1000/14.7) delivered by an identical steel case motor without aft injection.

1.4.2.3 Motor No. 003

(U) The firing of motor No. 003 was an attempt to repeat the full thrust performance test of motor 002. The motor was ignited but the test was terminated 0.5 sec after ignition when the aft oxidizer injection manifold developed a leak. The fluorine/oxygen mixture sprayed from the manifold and damaged an aft injector as well as the manifold. The leak apparently resulted from an internal reaction between contaminants and the oxidizer. Sequence camera coverage recorded the failure, which is shown in figure 64. A subsequent attempt was made to fire motor No. 003 to complete the full thrust performance and evaluation test. However, the repaired aft injector installation failed after 3.5 sec duration.

(U) The motor was again repaired and successfully tested in a 5.0-sec ignition test at 20% thrust without benefit of the gaseous fluorine lead used for ignition in previous tests. The test was conducted to verify safe ignition with FLOX for the impending throttleable motor test (motor No. 004). Smooth and rapid ignition was observed with FLOX at -310° F. In 5-in. motor tests conducted in previous years, ignition spikes have been observed with FLOX at low oxidizer temperatures and stronger ignition spikes were observed with OF₂. The spikes occurred at intermediate flow rates and diminished or disappeared as tests were conducted with extremely low or higher oxidizer flow rates.

CONFIDENTIAL

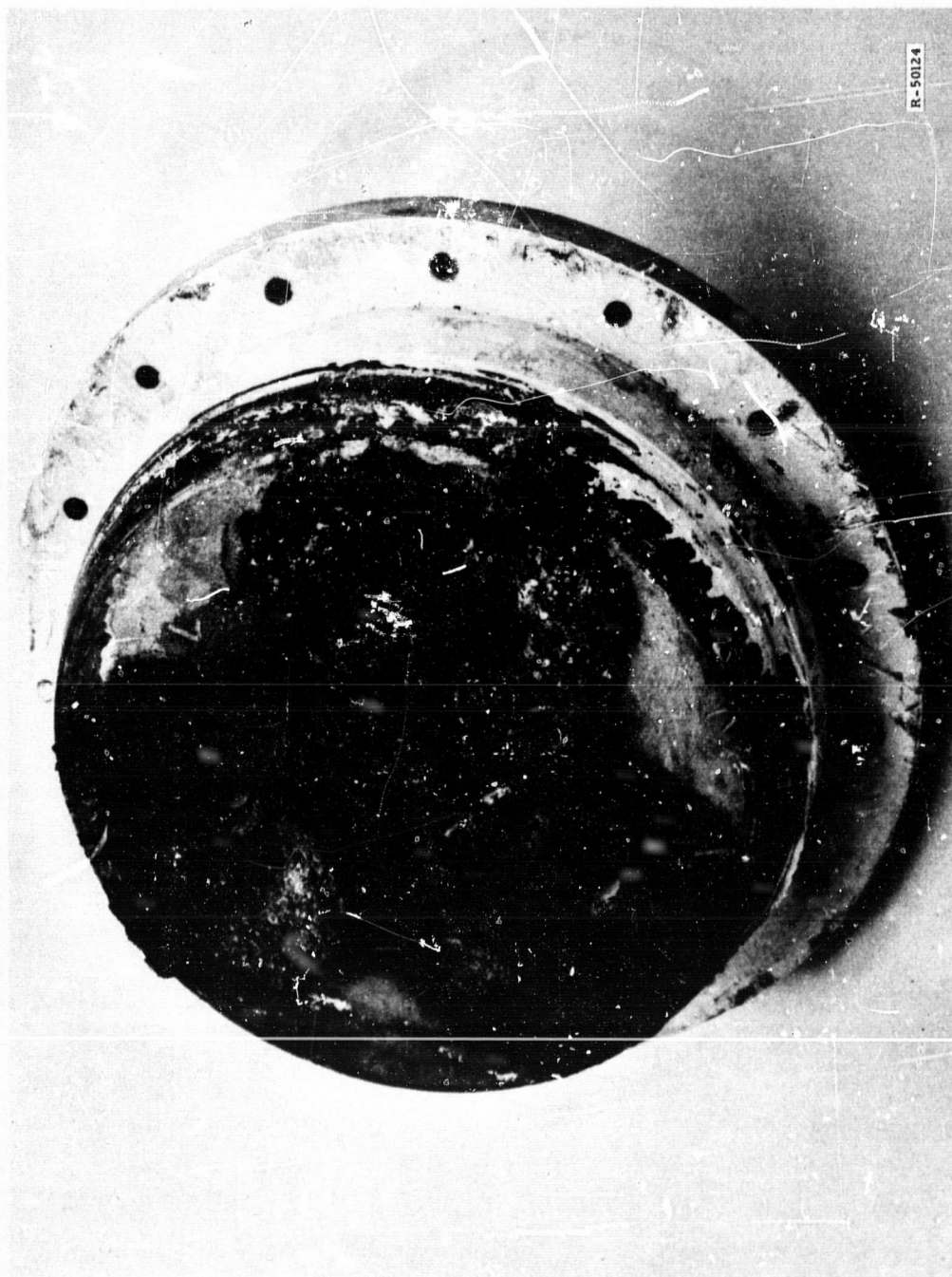


Figure 62. (U) Injector After Test

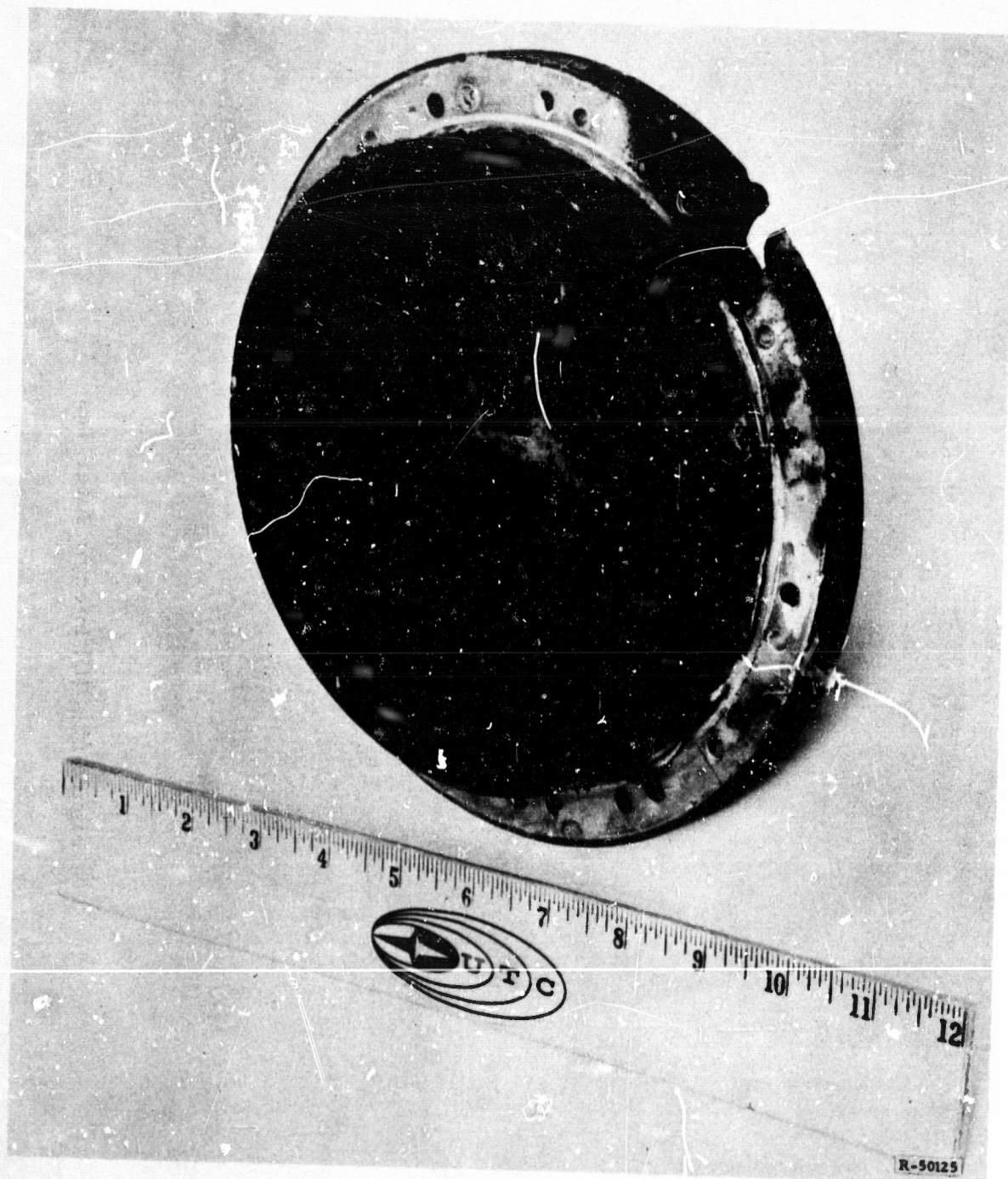
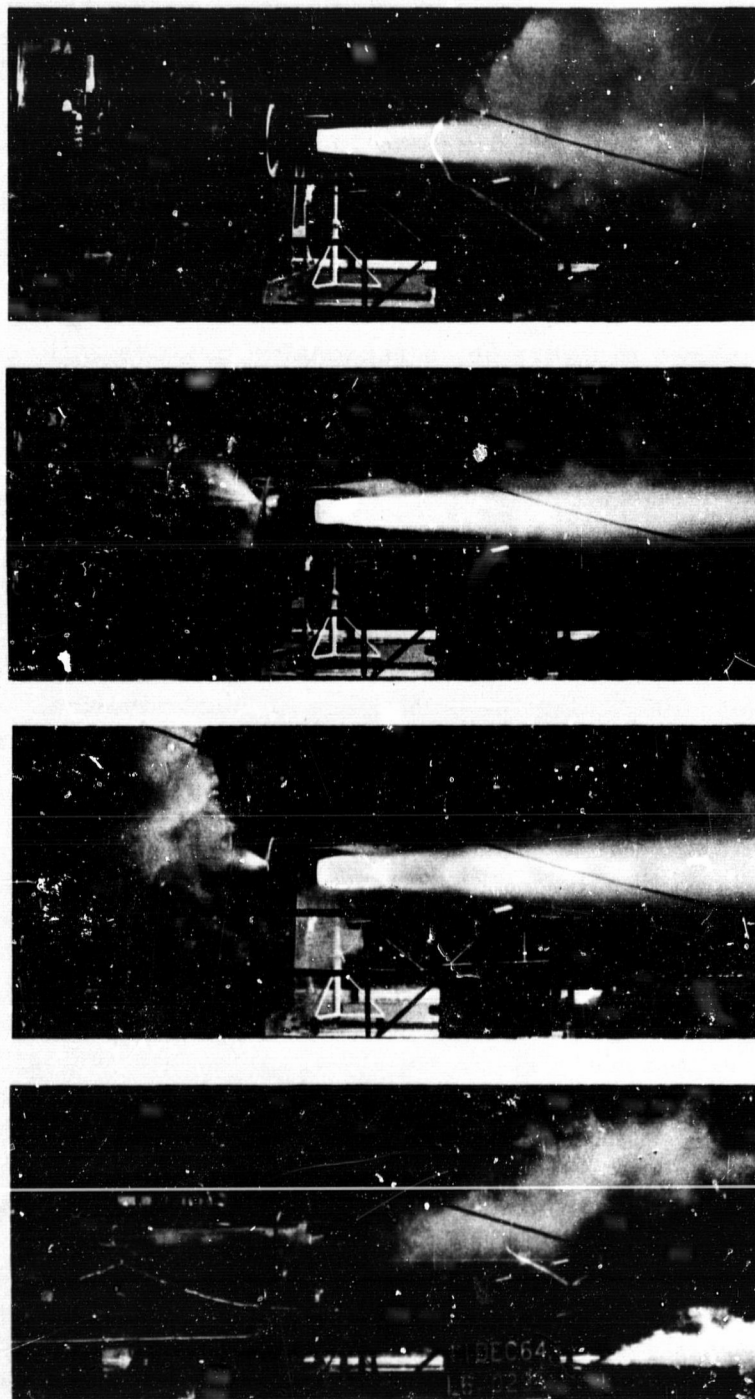


Figure 63. (U) Failed Injector



R-50126

Figure 64. (U) Test Sequence Showing Aft Injector Manifold Failure

1.4.2.4 Motor No. 004

(U) Variable thrust over a throttling range of 6:1 was demonstrated with motor No. 004. Motor thrust was varied in five steps of 3 sec each (figure 65) from 750 to 4500 lb for a total duration of 15 sec. Primary oxidizer flow was varied between 0.53 and 13.2 lb/sec. The flow divider valve discussed in section 1.0 was not fully developed at the time of this test; therefore a fixed oxidizer flow rate of 1.2 lb/sec was supplied to the aft injectors. The resulting mixture ratio shift over the thrust range was considerably reduced.

(U) As shown in figure 66, a reasonable mixture ratio can be maintained at an oxidizer flow rate of approximately 1.0 lb/sec and, because that flow rate provided a nearly optimum mixture ratio at the limits of the intended throttling range, it was selected for the aft-end oxidizer flow rate for this test. The design of motor No. 004 included an improved aft injector design as shown in figure 67.

(U) This improved injector is a conventional hollow-cone type with an injection port extension to direct the flow into the combustion chamber. The injector is threaded to facilitate installation and removal on the test stand, thus minimizing the possibility of contamination. A nozzle with an area ratio of 1.0 was used to allow operation at a chamber pressure of 30 psia without nozzle flow separation. Chamber pressures as low as 51 psia were obtained during the test.

(U) Specific impulse calculations were conducted to determine the relative performance of motor No. 004 at each thrust level. In these calculations, all of the motor weight loss (including consumed splash block material, the fuel grain, mixer, and insulation materials) were treated as fuel. The calculated motor performance at fixed thrust (where an essentially constant mixture ratio is obtained) is not significantly affected, although the conservative design of the test motor produces a significant quantity of nonpropellant combustible materials. These include splash block, mixer, and insulation. An accurate calculation of performance for each thrust step of a variable thrust test is extremely difficult because the distribution of these nonpropellant fuels as a function of thrust level and duration cannot be treated analytically. The problem is further complicated by the difficulty in ascertaining the mixture ratio and hence theoretical performance, especially at low thrust values where small differences between actual and assumed distribution of nonpropellant fuels can produce large errors in calculated performance.

(U) Performance was calculated three times using three different assumptions concerning the consumption of the nonpropellant fuels. The fuel grain

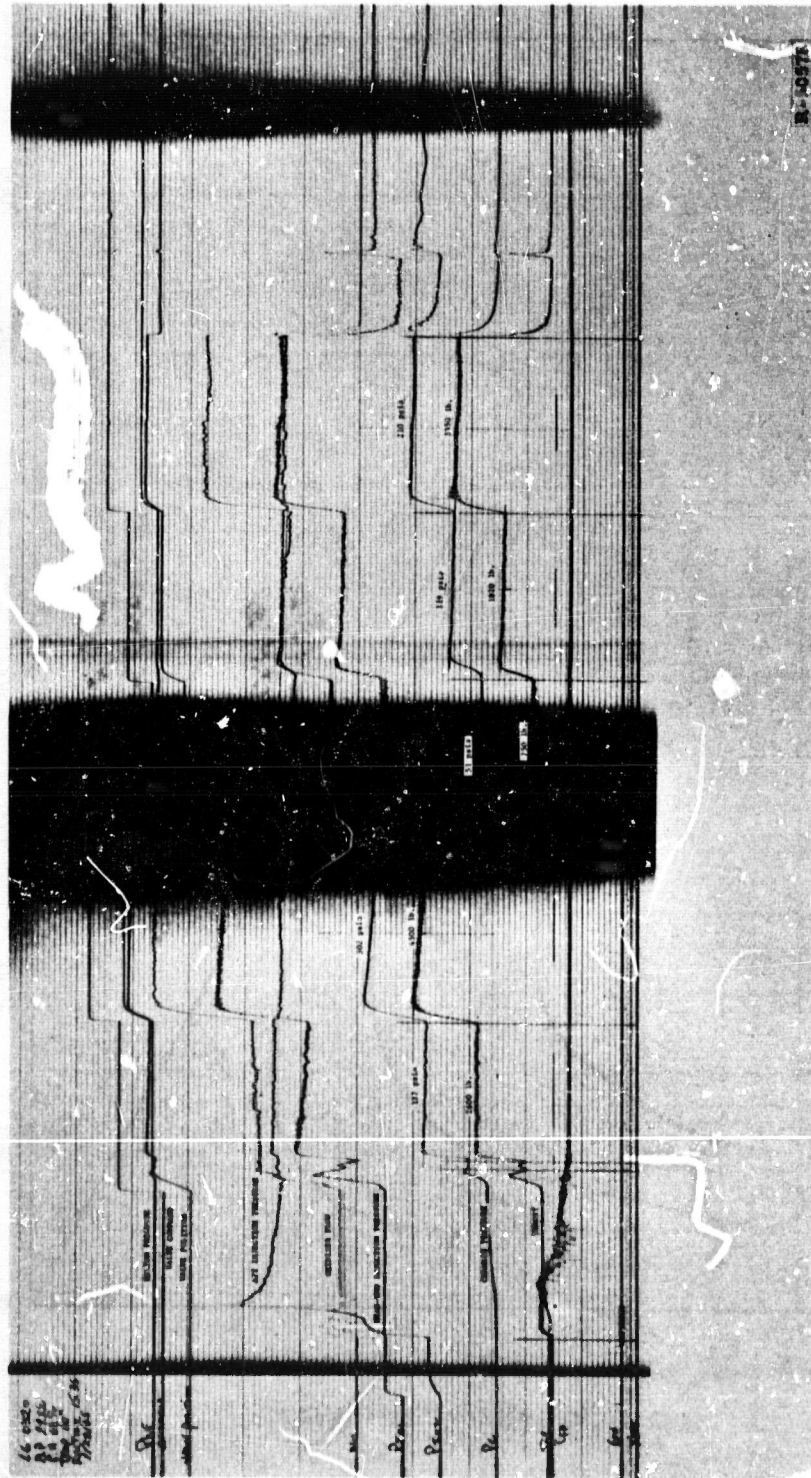
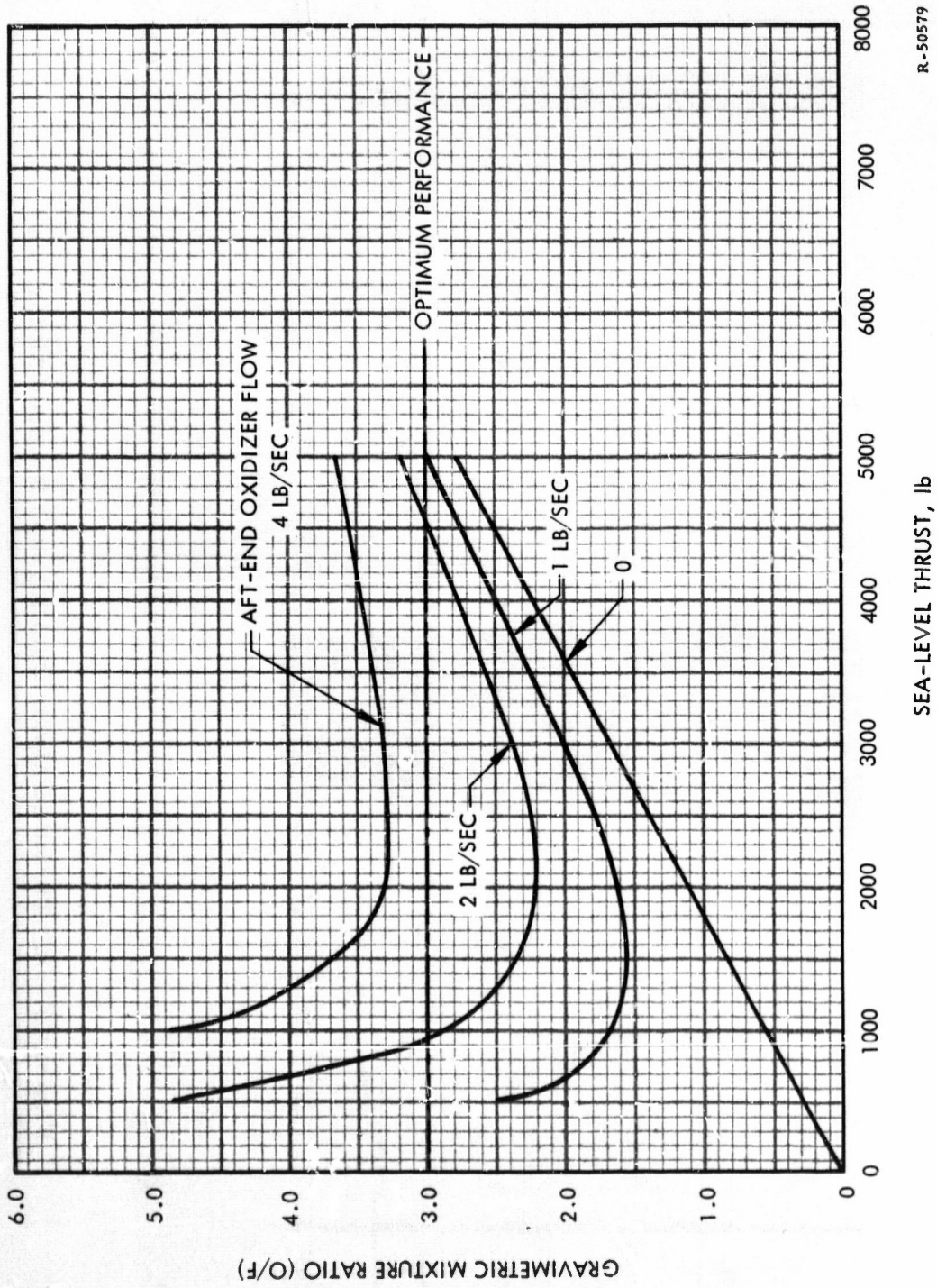
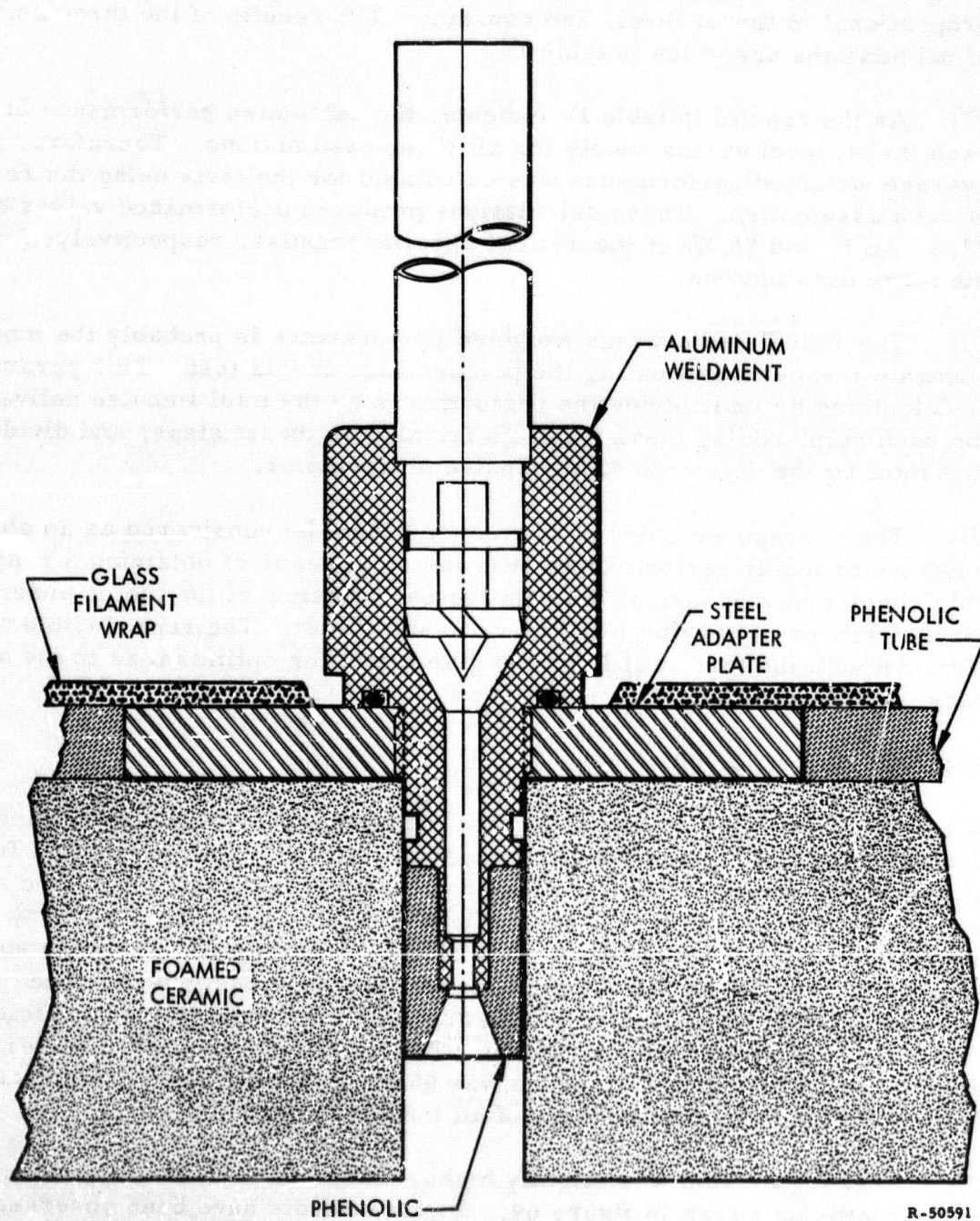


Figure 65. (U) Throttled Motor Oscillograph Record, Motor 004



R-50579

Figure 66. (U) Mixture Ratio vs Thrust for Full-Scale Motor



R-50591

Figure 67. (U) Full-Scale Motor Aft Injector Design

consumption rate was calculated with the regression rate equation of the lithium fuel system $\dot{r} = 0.17 G_o^{0.5}$ where G_o is the oxidizer flow rate divided by the fuel port area. The three assumptions were that the rate of consumption of the nonpropellant fuels is proportional to oxidizer flow rate, proportional to thrust level, and constant. The results of the three sets of calculations are given in table IV.

(C) As the results in table IV indicate, the calculated performance at each thrust level varies widely for all three assumptions. Therefore, an average weighted performance was calculated for the tests using the results of each assumption. These calculations produced performance values of 92.6, 93.7, and 93.9% of theoretical specific impulse, respectively, for the three assumptions.

(U) The calculated average weighted performance is probably the most accurate means of estimating the performance of this test. This parameter is calculated by multiplying the performance by the total impulse delivered for each step, adding these products for all five thrust steps, and dividing that total by the delivered total impulse of the motor.

(U) The average weighted performance cannot be considered as an absolute measure of motor performance; it is the only means of obtaining a reasonably consistent measure of the relative performance of the motor under the circumstances of varying mixture ratio and thrust. The reproducible results obtained with the three assumptions give cause for optimism as to the accuracy of these results.

1.4.2.5 Motor No. 005

(C) Two motor tests were conducted with motor No. 005 to determine performance and regression behavior at low thrust. This motor was fired at a chamber pressure of 32 psi (approximately 10% thrust) for 30 sec and was restarted for another 60 sec without servicing the injectors in any way. This injector is shown in figure 68. Phenolic injector shields were substituted on these tests for the graphite inserts previously used. The phenolic shields were almost completely consumed but retained sufficient thickness to prevent injector failure. The motor produced a characteristic velocity (c^*) of 6150 ft/sec, which was 95% of theoretical. Thrust data from both tests was lost because of an instrumentation failure.

(U) Fuel regression was slightly higher than normal at the injector end of the motor as shown in figure 69. Similar effects have been observed in subscale motor tests conducted with comparable oxidizer mass fluxes. This problem is not serious with the oxidizer mass flux values encountered over a 12:1 throttling range because the effect can be controlled by reducing the injector cone angle.

TABLE IV
CALCULATED SPECIFIC IMPULSE PERFORMANCE

<u>Thrust</u> lb	<u>Delivered</u> <u>Specific Impulse</u> sec	<u>Theoretical</u> <u>Specific Impulse</u> sec ($\epsilon = 1.0$)	<u>Percent</u> <u>of Theoretical</u>
I. Assuming Nonpropellant Fuel Flow Rate Proportional to Oxidizer			
2600	234	234	100
4500	216	250	86
740	257	188	137
1780	204	228	89
3350	210	239	88
II. Assuming Nonpropellant Fuel Flow Rate Proportional to Thrust Level			
2600	229	232	99
4500	221	252	88
730	247	186	133
1780	210	222	95
3350	213	241	88
III. Assuming Constant Nonpropellant Fuel Flow Rate			
2600	232	232	100
4500	229	253	91
730	189	165	113
1780	204	221	92
3350	218	243	90

CONFIDENTIAL

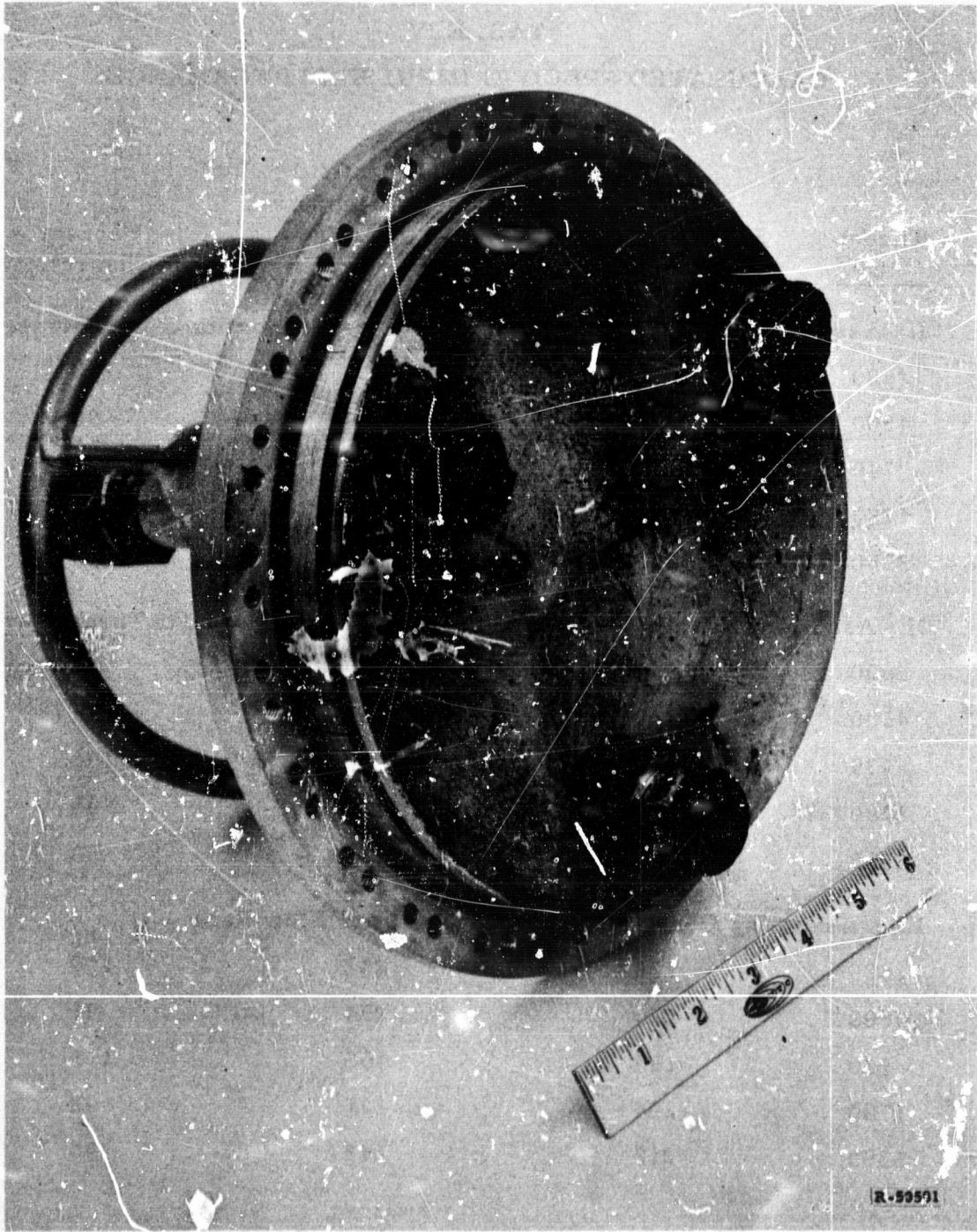


Figure 68. (U) Full-Scale Motor Injector After Test

CONFIDENTIAL



Figure 69. (U) Full-Scale Motor 005 After Test

(U) Aft injection in full-scale motor tests has resulted in increased end burning of the fuel grain, as can be seen by comparing the photo of motor No. 005 in figure 69 to motor No. 001 in figure 70, which did not use aft injection. However, the addition of low regression rate fuel or a thin sheet of insulation material to the aft end of the grain eliminates the problem.

(U) The splash block in motor No. 005 performed perfectly during the 90-sec test. Figure 71 shows the splash block after test. Although the consumption of the PBAN splash block material does not seriously penalize performance when burned with FLOX, large splash blocks make efficient fuel utilization difficult and, therefore, will be greatly reduced or eliminated in lightweight motor designs.

(U) Charring of foamed-ceramic plenum chamber walls after 90 sec was less than $3/16$ in. Figure 72 shows the section of the mixer with one aft injector in position. Figure 73, showing the mixer after test, indicates that only a trace of the spoke still exists. This figure also shows the effect of erosion on the mixer caused by the burning fuel. It has been observed in previous tests that the leading edge of a mixer plenum changer is consumed at about the same rate as the fuel, producing a tapered appearance. A close-up view of the ceramic-foam plenum wall is shown in figure 74 which clearly shows a postfire cross section of the wall. The original uncharred thickness was 1.0 in., which indicates that a char buildup has actually taken place.

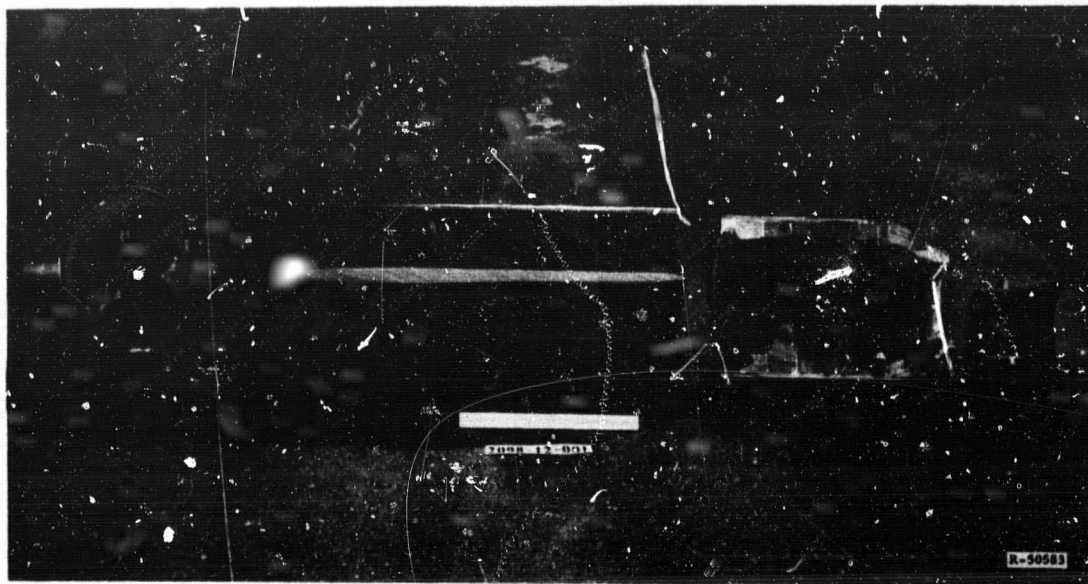


Figure 70. Full-Scale Motor 001 After Test

(U) An ATJ graphite nozzle with an expansion ratio equal to 1.0 was again used. Figure 73 shows the nozzle that survived the total 90-sec duration without erosion or cracking.

1.4.2.6 Motor No. 006

(U) A throttling ratio of 13.7:1 was successfully demonstrated with motor No. 006 in a 14-sec-duration firing in which the thrust was varied from 388 to 5300 lb. The motor was ignited with FLOX at 1000 lb thrust. The chamber pressure at the lowest thrust step was 32 psi. The throttling ratio was the largest that can be achieved at sea-level pressure without increasing the maximum chamber pressure. The thrust trace is shown in figure 75.

(C) The calculation of motor performance is again hampered by variation in the nonpropellant flow rates as described in the discussion on motor No. 004. However, if motor specific impulse is calculated on an overall basis (i. e. , by dividing the total impulse delivered by the weight flow rate of all materials passing out the nozzle), a specific impulse of 208 sec is calculated which, with an expansion ratio of 1.0, is 90% of theoretical. Characteristic exhaust velocity is 5933 ft/sec or 92.8% of theoretical.

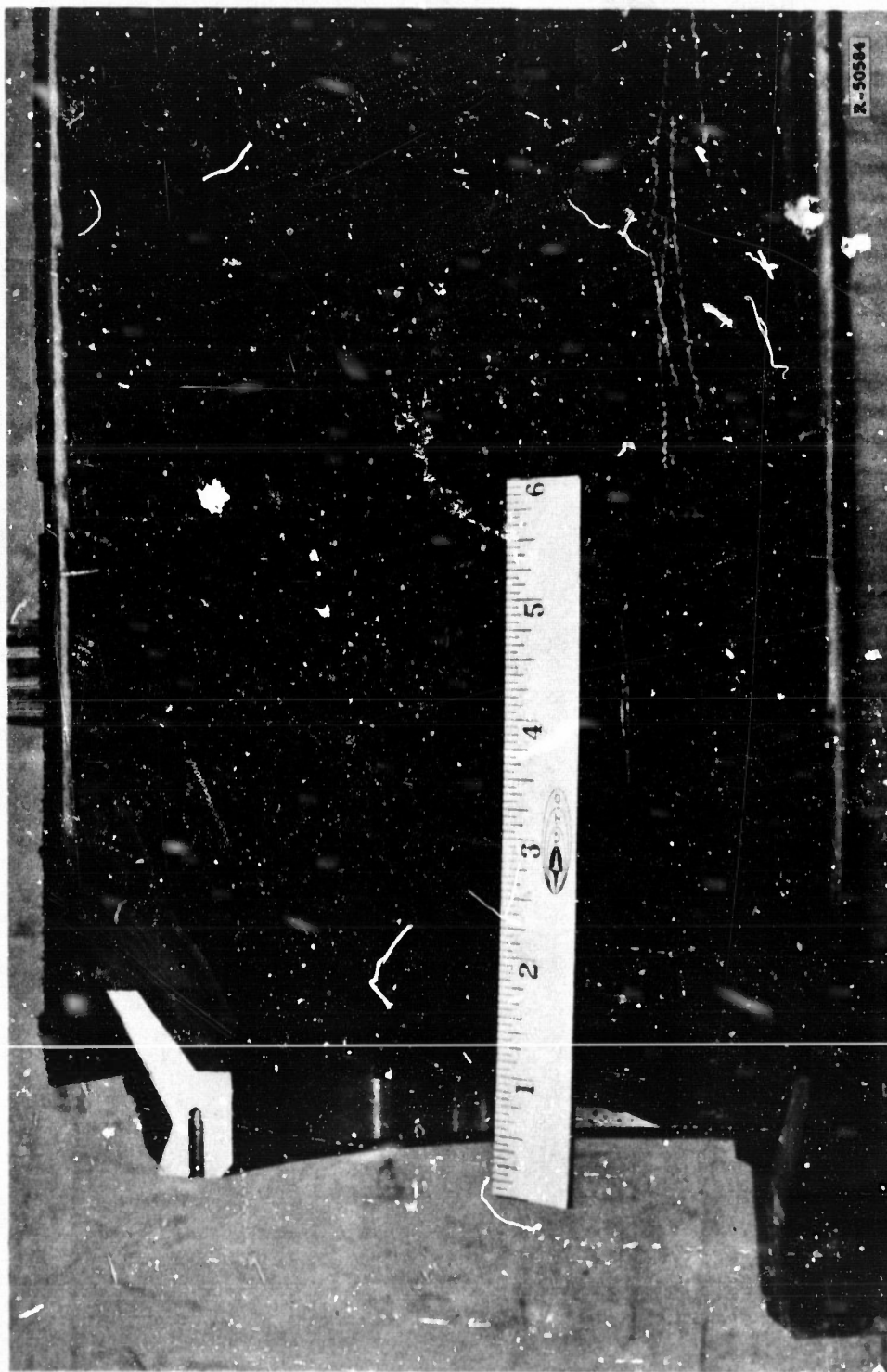


Figure 71. (U) Splash Block After Test

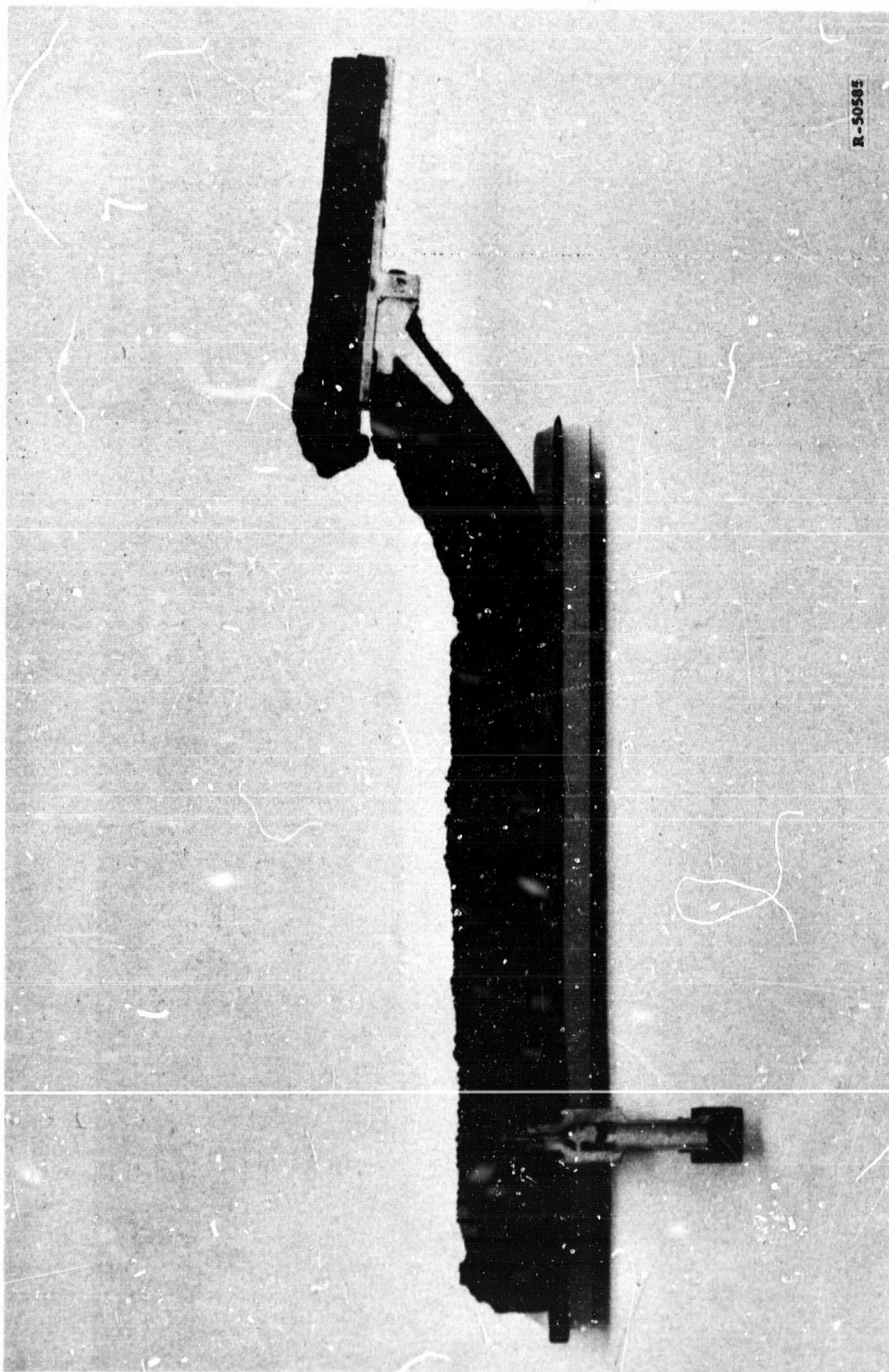


Figure 72. (U) Sectioned Mixer Plenum with Aft Injector After Test

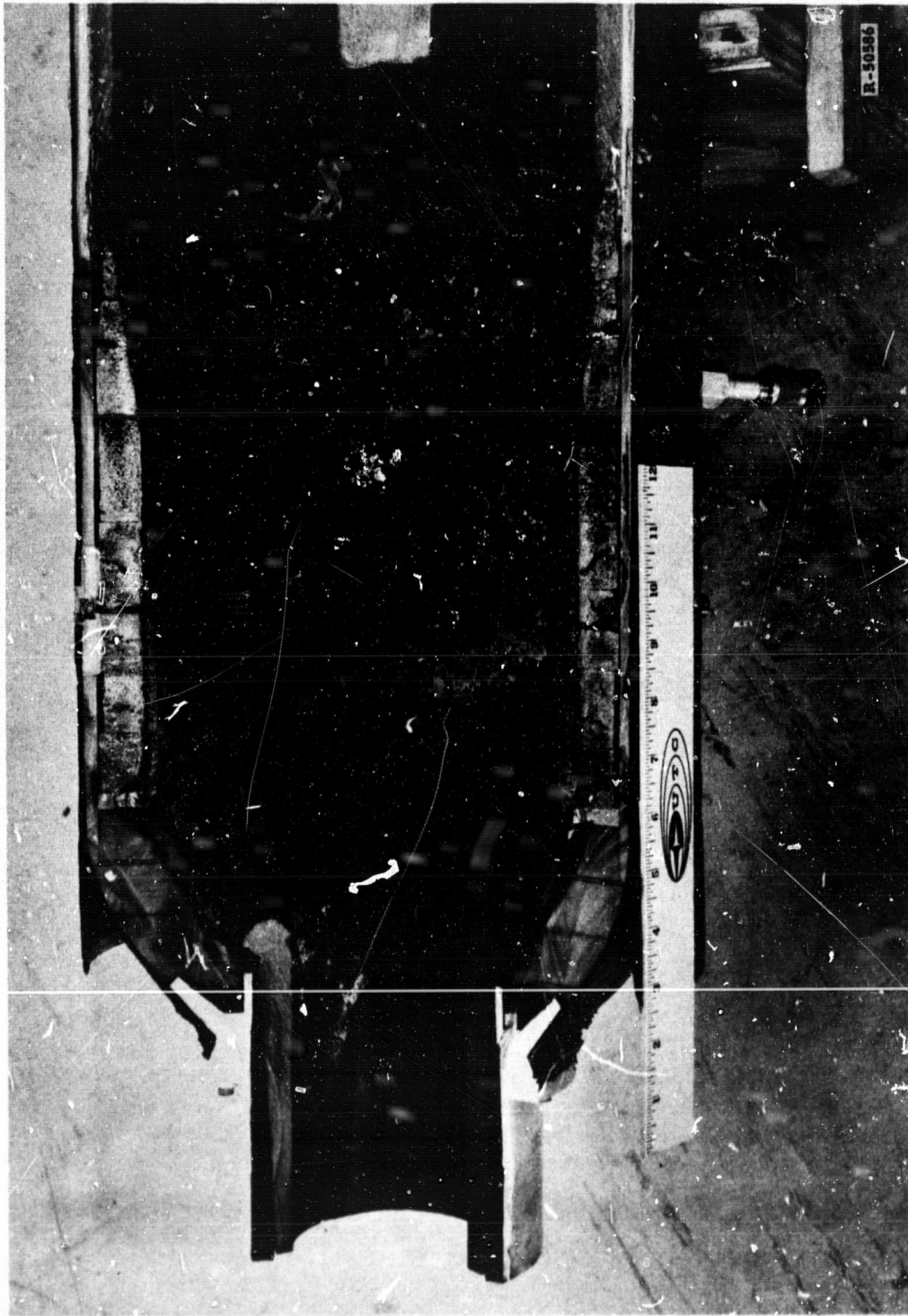


Figure 73. (U) Mixer Assembly After Test

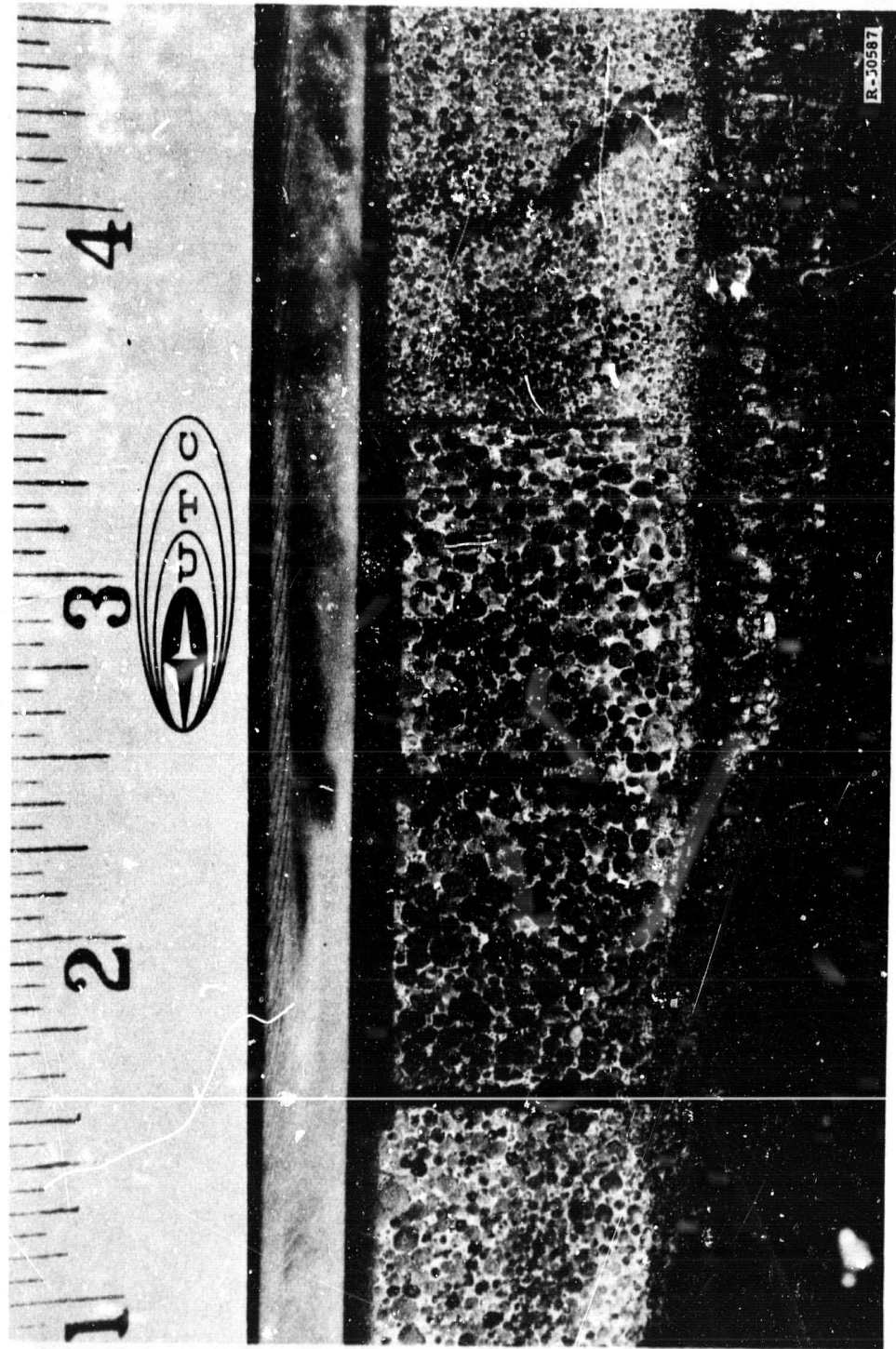


Figure 74. (U) Close-up View of Mixer Wall

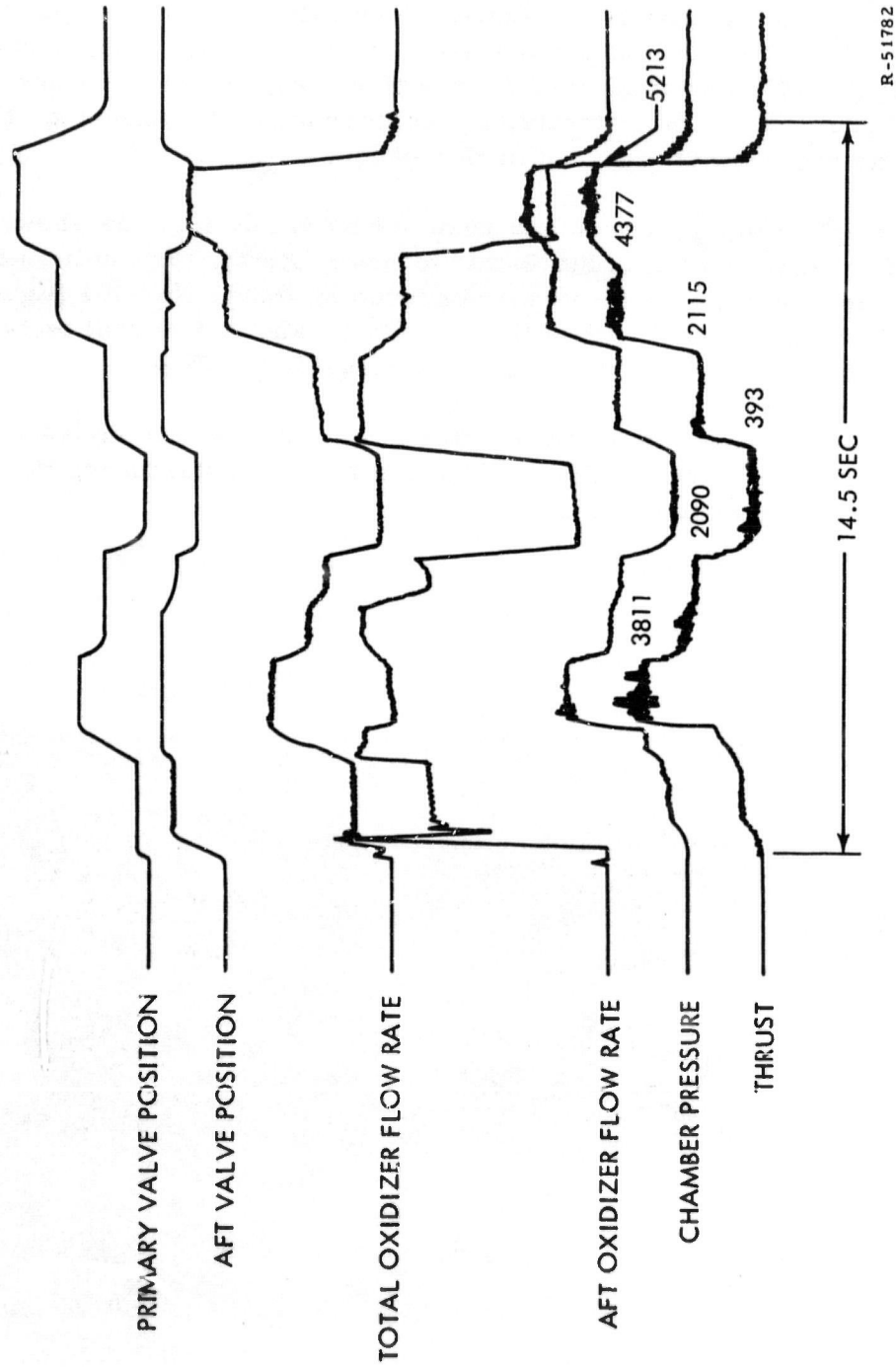


Figure 75. (U) Thrust Trace of Throttled Motor 006

(C) If performance is determined as described previously, where fuel flow rate is predicted by the regression rate equation $\dot{r} = 0.17 G_O^{0.5}$, and the nonpropellant combustibles are assumed to be consumed (1) at a constant rate, (2) in proportion to oxidizer flow rate, or (3) in proportion to thrust level, the calculated performance values are 95.5, 93.2, and 93.2%, respectively, of theoretical specific impulse. Again, these values are not intended to relate, with certainty, the performance of this motor; they indicate an approximate level of performance.

(U) A rippled fuel grain surface resulted from this test, as shown in figure 76. This rippling is attributed to inadvertently high helium flow rates. The rippling effect was not observed in motor No. 001 (figure 58), which was also throttled with helium aeration, and subsequent tests with the same injector at fixed thrust did not result in rippling.

(U) Postfire inspection of the injector revealed an error in installation of the sonic orifices controlling the helium flow, substantiating the suspicion of an excessively high flow rate.

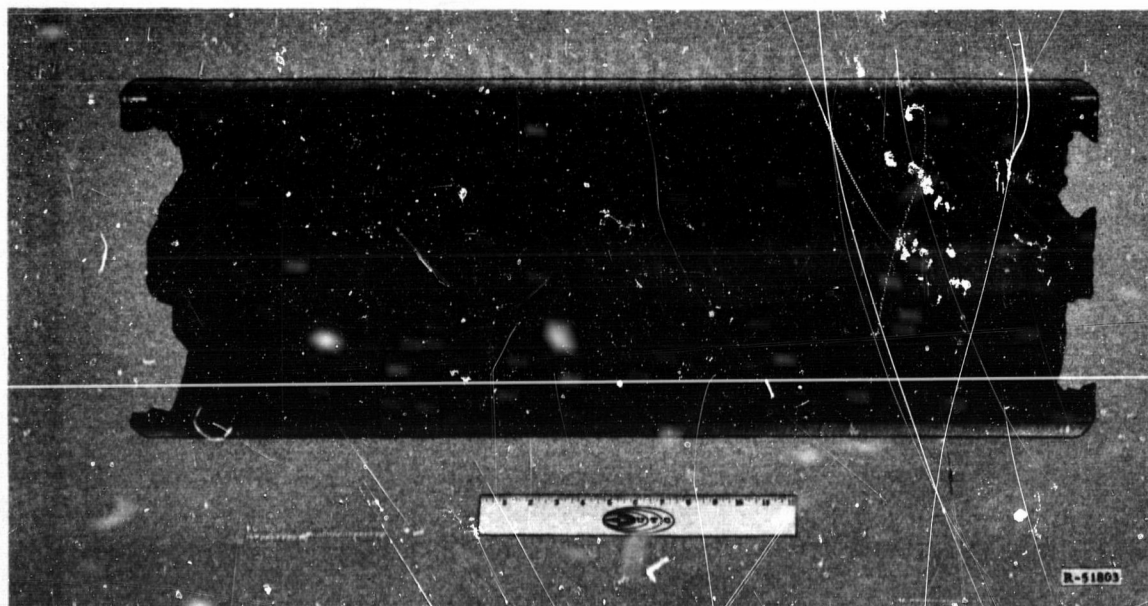


Figure 76. (U) Fuel Grain from Motor 006 After Test

1.4.2.7 Motor No. 007

(C) The final motor test of this phase was conducted using OF_2 as oxidizer in a full-thrust performance test. The motor design was modified to eliminate the mixer baffles, thereby relying only on the aft injectors to produce the mixing. The motor was tested for 10.8 sec at a thrust of 4723 lb and a chamber pressure of 281 psia. The motor delivered a specific impulse of 309.8 sec (1000/14.7) or 90% of theoretical without using mixing baffles. Characteristic velocity (c^*) was 6227 ft/sec or 92.8% of theoretical.

(U) Fuel grain regression was as predicted with only slight injector effect, shown in figure 77, increasing the regression rate near the injector.

(U) The nozzle used on this test incorporated a single material (impregnated carbon cloth-phenolic) without the usual ATJ graphite insert. The nozzle throat shown in figure 78 survived without significant dimensional change as did the expansion skirt. However, the higher thermal conductivity of the carbon cloth material resulted in the delamination of a fiberglass reinforcing layer as shown in this figure. Improved nozzle design would, therefore, incorporate an insulation reinforced with carbon cloth on the interior.

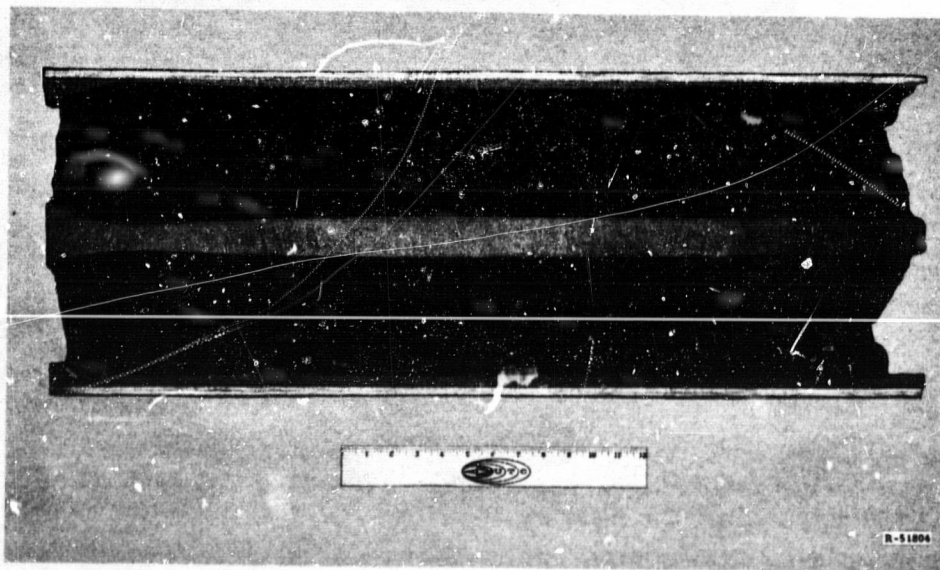


Figure 77A. (U) Fuel Grain from Motor 007 After Test

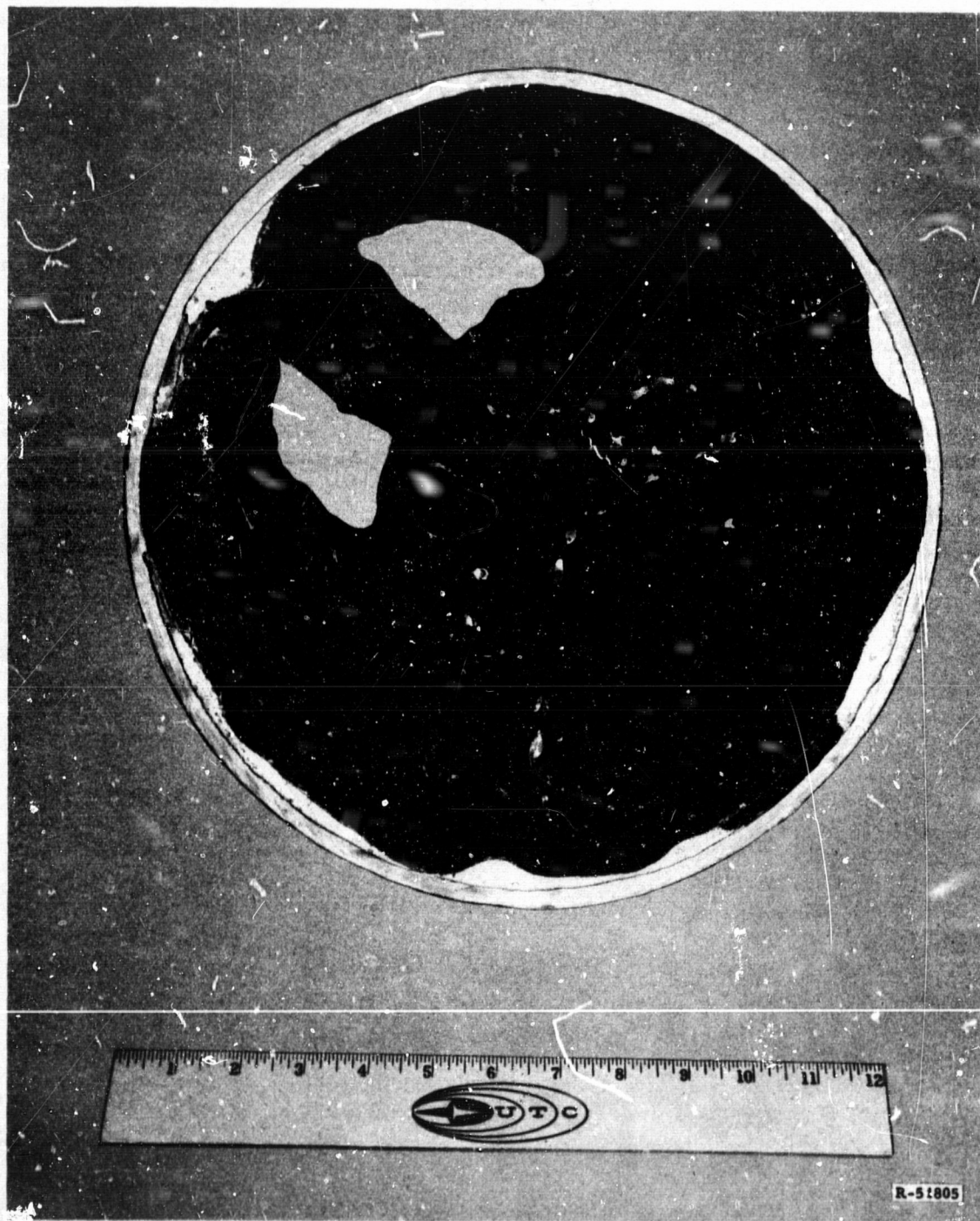


Figure 77B. (U) Fuel Grain from Motor 007 After Test



Figure 78A. (U) Carbon Cloth-Phenolic Nozzle



R-51787

Figure 78B. (U) Carbon Cloth-Phenolic Nozzle

1.5 QUALITATIVE PREDICTION OF THE RELIABILITY AND MAINTAINABILITY OF SPACE-STORABLE MOTORS

(U) Based on experimental data presently available, an estimate can be made of the relative reliability and maintainability of space-storable hybrid rocket motors should they be reduced to operational use utilizing the technology acquired under this program. This specific program has been primarily concerned with developing technology relative to the thrust chamber assembly (TCA), which includes the oxidizer valve, injectors, fuel grain, and nozzle. Of these components, the two most significant items pertinent to the reliability and maintainability of hybrids are the injectors and fuel grain; the remaining components being based on state of the art liquid and solid rocket technology.

(U) The primary injectors used in the full-scale motors have injector port openings approximately 0.4 in. in diameter. This relatively large opening is expected to lead to greatly simplified maintenance and increased reliability. Injector openings of this size are virtually immune to plugging by particles in the oxidizer supply and from manufacturing defects.

(U) The HFX 2081 and HFX 2084 fuels developed under this program do not sustain combustion in the absence of oxidizer; therefore, there is little or no possibility of inadvertent ignition or fire and no possibility of detonation. In addition, because the hybrid burning process is controlled predominantly by liquid flow, the solid grain surface does not determine the combustion pressure. Therefore, unlike solid propellants, cracks or voids in a hybrid fuel grain do not lead to faster or uncontrollable burning. During this program, numerous HFX 2084 fuel grains containing voids and cracks have been fired without affecting the operation of the motor.

2.0 PREPACKAGED HYBRID PROPELLANT SYSTEMS (PHASE II)

(C) This investigation was initiated to investigate potential prepackaged hybrid propellant systems that may have application in tactical missiles. The investigation has resulted in the evaluation of five fuel systems in forty 5-in. motor tests and fifty 3.5-in. motor tests. One of the fuel systems was also tested in three 12-in. motor tests. One of the fuel systems was also tested in three 12-in. motor tests using ClF_3 and ClO_3F . As a result of this experimental work, a fuel system containing TFTA, boron, AP, and binder has been selected for further evaluation under Contract No. AF 04(611)-10789 and for use in 5000-lb-thrust motor tests to be conducted under that contract.

(U) The investigation has consisted of evaluation and selection of candidate propellants, formulations and processing studies, 3.5-in. and 5.0-in. motor tests to evaluate the fuels, and the six 12.0-in. motor tests with three filament-wound test motors of the type described in paragraph 1.3.

2.1 PREPACKAGED HYBRID PROPELLANT STUDIES

(U) Several hybrid propellant combinations were selected for study for application in typical tactical air-launched missile systems. In order that these propellants be consistent with the requirements of the missile, certain criteria must be met. The propellants must deliver relatively high specific impulse and possess a high-temperature bulk density adequate to obtain the total impulse requirement (200,000 lb-sec) within vehicle weight and volume limitations. The fuel must not sustain combustion on termination of oxidizer flow because multiple start operation is required. The propellants should provide smooth and reproducible hypergolic ignition and efficient combustion, and should produce an exhaust plume which possesses favorable radar attenuation and reflection properties.

(C) Propellant investigations were initiated with a fuel system consisting of TAZ, boron, AP, and binder. Of the available propellants, this fuel, with an oxidizer consisting of a mixture of ClF_5 , ClO_3F , and BrF_5 , showed the most promise of fulfilling the requirements of a prepackaged hybrid propulsion system.

(C) Based on information obtained from formulations work and subscale motor testing, several compositions of the selected fuel formulation were evaluated for further development. A primary fuel system was chosen as

CONFIDENTIAL

the ultimate goal with emphasis on obtaining high specific impulse. Alternatives were considered to cover each of the possible development problems anticipated. These alternatives include the substitution of TFTA for TAZ, aluminum for boron, and the substitution of ClO_3F in the oxidizer for reduced AP loading in the fuel. The factors which necessitate consideration of these alternatives are discussed in paragraph 2.2.1. Table V lists the fuel systems, in the order of decreasing performance, that are in preliminary development. As problems are overcome or are found to be non-existent, development work on the respective alternative fuels will be discontinued. In the event of any serious problem, timely development of an alternative fuel is ensured.

2.1.1 Propellant Evaluation

(U) A preliminary survey was made to determine which candidate storable propellant systems offer significant performance gains over current pre-packaged propellants. Only those propellants suitable for application in advanced tactical missiles and considered to be state of the art for the 1965 to 1968 period were studied. The initial candidate propellant systems are listed in table VI.

TABLE V

HYBRID PROPELLANT COMBINATIONS SELECTED FOR EVALUATION

	Type of Fuel	Fuel Composition	Oxidizer	O/F	I_{sp}	ρI_{sp} sec
A	Pelletized	33 TAZ/20 B/ 27 AP/20 binder	ClF_5	2.3	294	495
B	Pelletized	22 TFTA/20 B/ 38 AP/20 binder	ClF_5	2.3	293	494
C	Homogeneous	35 TAZ/20 B/ 15 AP/30 binder	90 ClF_5 / 10 ClO_3	2.5/ 2.9	293	479
D	Pelletized	60 TFTA/20 B/ 20 binder	75 ClF_5 / 25 ClO_3F	3.5	297	468
E	Homogeneous	45 TFTA/20 B/ 35 binder	75 ClF_5 / 25 ClO_3F	3.5	295	461
F	Pelletized	22 TFTA/20 Al/ 38 AP/20 binder	ClF_5	1.5	289	486
G	Homogeneous	35 TFTA/20 Al/ 15 AP/30 binder	80 ClF_5 / 20 ClO_3F	2.2	288	455

CONFIDENTIAL

TABLE VI
THEORETICAL PERFORMANCE OF STORABLE HYBRID-PROPELLANT SYSTEMS

	<u>Fuel Composition</u>	<u>Oxidizer</u>	<u>O/F</u>	<u>Isp sec</u>	<u>pIsp at 77° F</u>	<u>pIsp at 165° F</u>
Nonsustaining Fuels						
1.	35 TAZ/30 B/15 AP/20 PBD	BrF ₅	4.0	242.5	540*	508*
2.	40 TAZ/40 B/20 PBD	80 BrF ₅ /20 ClO ₃ F	4.8	256.0	516	466
3.	35 TAZ/30 B/15 AP/20 PBD	ClF ₅	3.0	287.0	484	444
4.	60 LiH/20 B/20 Butyl**	70 ClF ₅ /20 BrF ₅ /10 ClO ₃ F	6.0	296.0	468	430
5.	40 TAZ/40 B/20 PBD	80 ClF ₅ /20 ClO ₃ F	3.6	293.5	480	429
6.	33.2 Li/46.8 Al/12 PBD/8 PS	55 ClF ₅ /35 BrF ₅ /10 ClO ₃ F	4.5	279.6	482	421
7.	Li/LiH/PBD (HFx 2083)	70 ClF ₅ /30 ClO ₃ F	3.75	308.7	405	375
Self-Sustaining Fuels						
8.	55 B/30 AP/15 HC434	BrF ₅	5.3	240.5	565	530
9.	55 B/30 AP/15 HC434	ClF ₅	3.5	285.2	503	445

* O/F = 5.0

** Pressed grain

(C) These two propellant systems were subjected to further study to determine which system (or systems) showed the greatest potential for performance, versatility, and rapid development. Results of these studies showed the most promising propellant system to be a combination of one or more of the interhalogen oxidizers (ClF_5 , BrF_5 , and ClO_3F) with a TAZ/boron/AP/binder fuel. This system offers high specific impulse, an adequate bulk density, and can be formulated to maximize specific impulse or density impulse or to optimize to a combination of those quantities. In its initial formulation, this propellant system offers the following capabilities: For weight-limited missile systems, where maximum specific impulse is required, the TAZ/boron/AP/binder system oxidized by a $\text{ClF}_5/\text{ClO}_3\text{F}$ mixture will provide a specific impulse of 294 sec; for volume-limited systems requiring high density fuels and an engine restart capability, the TAZ/boron/AP/binder system could be oxidized with BrF_5 to produce 540 g-sec/cc density impulse at 77° F and 508 g-sec/cc at 165° F; for other applications, where high specific impulse is required, the oxidizer composition could be varied to produce specific impulse levels between 243 and 298 sec, while density impulse can be maintained between 540 g-sec/cc and 480 g-sec/cc as tradeoffs are being made.

(U) All of these propellants are storable over the required -65° to +165° F temperature range. Most tactical missile propulsion systems cannot tolerate the production of an exhaust plume that will attenuate or reflect radar signals; therefore the use of the lithium-lithium hydride (fuel No. 7, table V) fuels is questionable. However, this fuel is of special interest for weight-limited vehicles, where high specific impulse is required.

2.1.2 Temperature Effects

(U) The effects of temperature on propellant selection include its effects on density and vapor pressure of the oxidizer and its effects on thermal stability of the fuel within the limits of -65° to +165° F.

(U) No significant problems are anticipated with any effects of temperature on oxidizer vapor pressure or thermal stability. The vapor pressure of all three oxidizers originally considered for this program present no problems at the system operating pressures. The vapor pressure, critical pressure, and temperature for the three oxidizers are shown in table VII and figure 79.

(U) Temperature effects on the stability of the fuel system is not considered to be a problem because differential thermal analysis (DTA) tests conducted with each of the fuel system constituents have indicated that all are stable to temperatures in excess of 392° F.

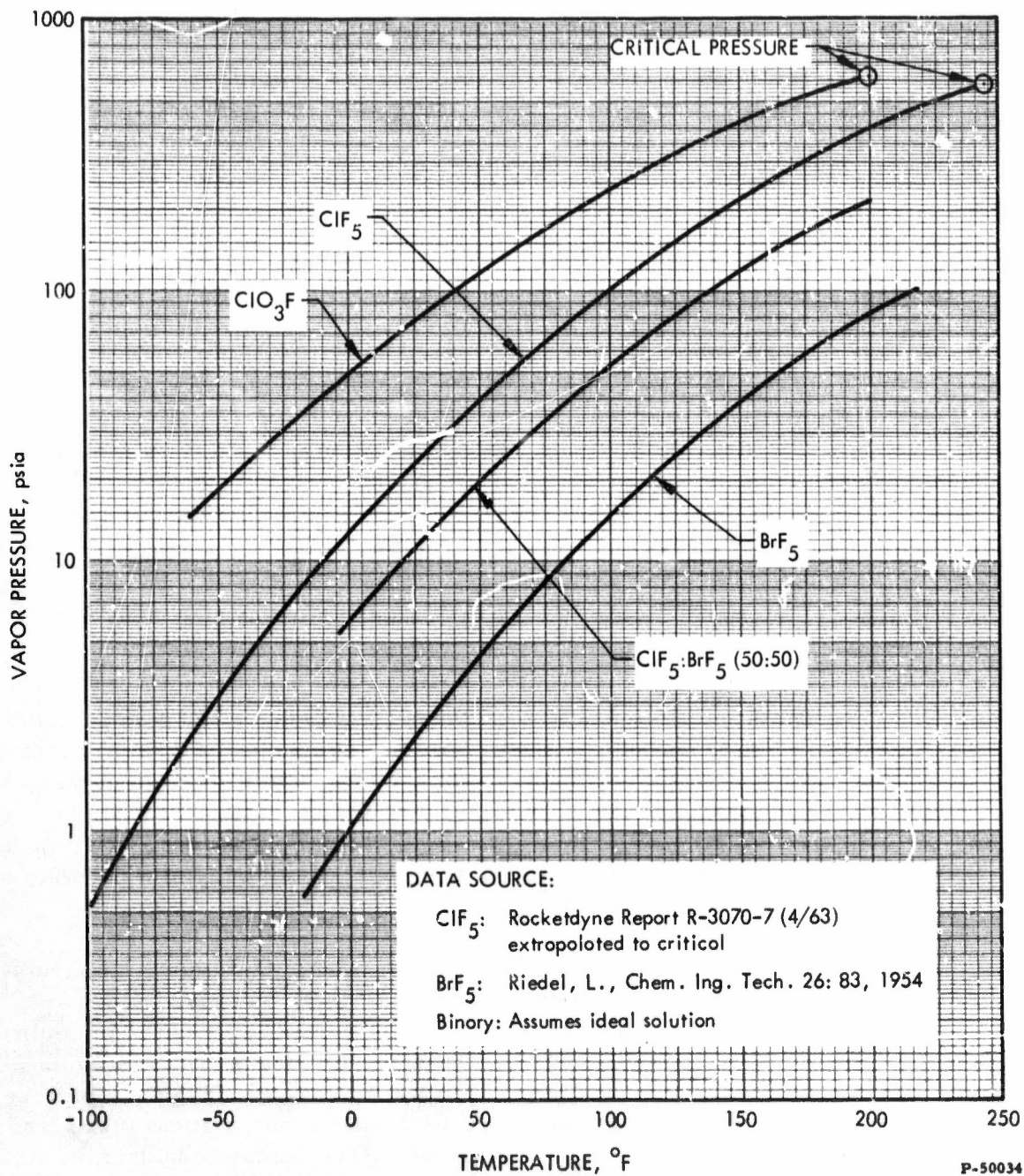


Figure 79. (U) Estimated Oxidizer Vapor Pressures

TABLE VII
OXIDIZER PHYSICAL PROPERTIES

<u>Parameter</u>	<u>Oxidizer</u>		
	<u>ClF₅</u>	<u>BrF₅</u>	<u>ClO₃F</u>
Boiling point, °F	8	105	-53
Freezing point, °F	-153	-80	-231
Critical pressure, psia	605	624	778
Critical temperature, °F	246	386	203
Heat of formation,* kcal/mole	-58	-109.8	-10.1
Density at 77° F, g/cc	1.74	2.47 ¹	1.42
Density at 165° F, g/cc	1.55	2.28	1.13

* Liquid at 77° F

(U) The effects of temperature on propellant density is an important consideration in the selection of propellants for prepackaged hybrid systems because a reduction in propellant volume yields a minimum tank weight and reduces aerodynamic drag. The density of the oxidizer at the highest operational temperature reached by the propellants during storage or flight is the most significant consideration for design purposes because this value will dictate the minimum tank size.

(C) The effects on density of ClF₅, BrF₅, and ClO₃F with temperature are shown in figure 80; however, adequate density impulse levels are possible with both ClF₅ and BrF₅ at elevated temperatures. The addition of ClO₃F to the oxidizer system is attractive for use with fuels containing hydrocarbon binders because such a mixture provides oxygen to oxidize the carbon. This will maximize specific impulse for a given fuel blend. The major disadvantage to the addition of ClO₃F is the reduction in bulk density. When used in quantities of less than 20 to 30% of the total oxidizer at temperatures up to 165° F, ClO₃F significantly improves performance while maintaining a reasonable value of density impulse. However, for use at higher operating temperatures and in higher percentages, additional investigation is required to compare the value of increased specific impulse with the added vehicle weight accompanying a lower oxidizer bulk density.

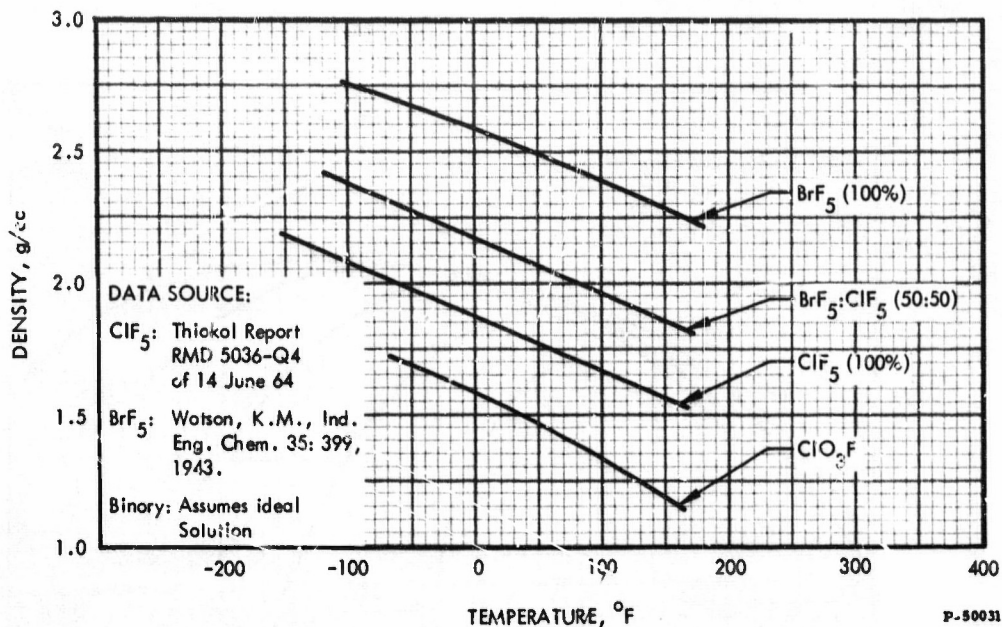


Figure 80. (U) Effect of Temperature on Oxidizer Density

2.1.3 Fuel Components

2.1.3.1 Ammonium Perchlorate

(C) The alternative method for providing oxygen to the system is the addition of AP (NH_4ClO_3) in the fuel system. Maximum theoretical performance is obtained when the oxygen content is sufficient to oxidize all carbon to carbon monoxide (CO).

(C) Parametric studies were made to determine the effects of AP loading on specific impulse and density impulse. These studies showed that the optimum AP loading resulted in a specific impulse of 294 sec and density impulse of 495 sec. The theoretical performance curves from this study are shown in figure 81. Based on these studies, a fuel containing 33% TAZ/20% boron/27% AP/20% binder (Fuel A, table V) was selected for use with ClF_5 .

(C) The addition of the required amount of AP to a fuel blend would result in self-sustained combustion. However, subscale motor tests described in paragraph 2.2 indicate that nonsustaining fuel grains can be formulated with pelletized AP. These tests indicate that the maximum AP loading in an homogeneous nonsustaining fuel blend is 15%. However, because the

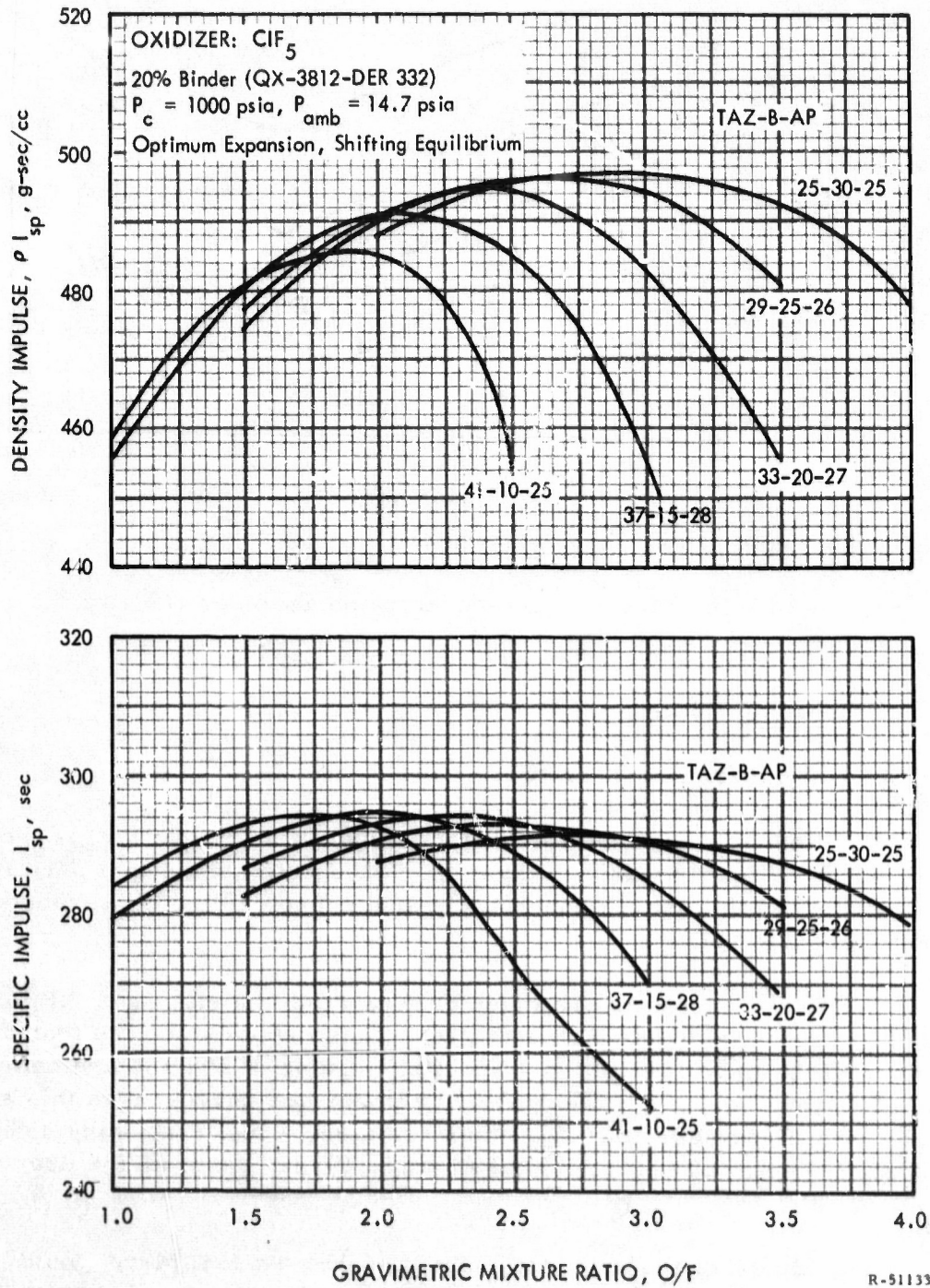


Figure 81. (U) Performance of Four-Component Fuels

maximum AP loading in nonsustaining fuels is a function of particle size, fuel development with coarse-particle AP should allow a significant increase in the AP loading of the optimum homogeneous fuel blend. Based on these results, a fuel system (Fuel C, table V) containing 35% TAZ/20% boron/15% AP/30% binder was selected as the optimum homogeneous fuel blend.

2.1.3.2 Nitrogen-Containing Additives

(C) Crystalline materials that are high in nitrogen have been used in several hybrid fuel systems developed at UTC. These additives increase the fuel regression rate and the hydrogen-carbon and nitrogen-carbon ratios, a desirable change for systems using interhalogen oxidizers. Besides being high in hydrogen and nitrogen, these materials all have a positive heat of formation and high heats of combustion. This indicates that the material would tend to decompose relatively easily, supplying significant quantities of working fluid (especially nitrogen) along with sufficient energy to augment the specific impulse. The interhalogen oxidizers do not oxidize carbon readily; therefore the low carbon content of these additives is attractive in hybrid fuel systems used on this program.

(C) Three nitrogen-containing additives have been under investigation: TAZ, THA, and TFTA. However, investigation of THA has been discontinued for this application because of the high-temperature fuel stability. Initial fuel development work used TAZ as the nitrogen additive. However, TAZ has become unavailable because of supplier problems, and substitution of another nitrogen additive has been made. This alternative additive is TFTA. Initial calculations indicated that the performance levels would be comparable, but some uncertainties existed in the heat of formation. The values in question were heats of combustion and heats of formation obtained from Food Machinery and Chemical Corporation (FMC). *

(U) The heats of combustion and formation were verified experimentally at UTC (see appendix III) by oxygen bomb calorimeter tests, and physical properties were studied. Results of the studies described in appendix III showed that TFTA was a good substitute for TAZ. In addition, TFTA was found to be insensitive to impact and less toxic. Thermal stability also was good over the required temperature range.

* Annual Progress Report, 1 June 1961 to 31 August 1962, Contract No. AF 04(611)-5689. Food Machinery and Chemical Corporation.

2. 1. 3. 3 Metal Additives

(C) Two metal additives, aluminum and boron, are being used in the development of high-density fuels. Theoretical performance calculations indicate that boron-containing fuels deliver a higher specific impulse and density impulse than aluminum-containing fuels. Because of the relatively higher performance and favorable radar reflection and attenuation properties of boron fuels, only boron is being seriously considered for use in full-scale motor development. Aluminum fuels provide a high level of performance and will provide operating motor environmental conditions comparable to those of boron systems; therefore, aluminum fuels were retained as a possible substitute fuel for motor development tests.

2. 1. 3. 4 Fuel Binders

(C) Since interhalogen oxidizers, in general, are poor oxidizers for carbon-containing fuels, it has been found desirable to minimize the carbon content and increase the oxygen content of the binder. This consideration has resulted in a change in the choice of binders from the R-45 hydrocarbon binder, which contains 86% carbon and 10% oxygen, to a binder designated as QX 3812, which contains 61.5% carbon and 26% oxygen.

(C) Experimental results indicate that an increase in solids loading by 10% has been achieved as an added benefit. The area of binder formulations will be the subject of continued investigation on Contract No. AF 04(611)-10789, both with respect to improving the stoichiometry and solids loading of hybrid fuels.

2. 1. 4 Formulation and Processing

(U) The objectives of the formulations studies conducted during this program were to determine the maximum solids loading that can be contained in a castable fuel system and to develop techniques for processing the fuels. The formulations which proved castable were then tested in 3.5-in. motors.

2. 1. 4. 1 Solids Loading

(U) The maximum achievable loading for nonpelletized castable fuels varies from 60 to 80%, depending on the constituents and their respective particle sizes. It appears that elemental boron is limited to a loading of 60% in binder alone where coarse boron is used. In similar fashion, TFTA and TAZ are limited to approximately the same percentage. Thus, the combined TFTA and boron loading limit in binder is also 60% or approximately 2:1 solids to binder ratio. Lower loading ratios result

with finer particle sizes. The addition of AP to the fuel does not appear to alter the relative ratios of boron-to-binder or TAZ-to-binder. Therefore, at present, the level of maximum loading achievable in a four-component fuel system in a homogeneous mix is established when the TAZ or TFTA and boron percentage is approximately twice that of the binder. To compensate for this, a technique in processing of the TFTA has been developed in which the material is precompacted. This precompacted or lightly pressed TFTA is then broken into random distribution of particles, which enables considerably higher solids loading in the fuel.

(U) By selectively pelletizing or compacting the fuel components, it is possible to attain 80% solids loading and still retain castability. Experience in formulation and testing of pelletized motors have demonstrated the feasibility of pelletizing. When AP and TFTA are pelletized together, the resultant pellet is impact sensitive. However, AP and TFTA can be used when pelletized separately. When TFTA/boron/AP pellets are used, poor combustion behavior of the boron resulted as was evidenced by glowing, unburned boron particles being ejected through the nozzle. It is apparent that AP must be pelletized separately if combustion efficiency is to be obtained. By a judicious distribution of the four fuel components throughout both the matrix and the pellets, efficient combustion should be attainable.

2.1.4.2 Processing

(C) During the investigation of four component fuels containing TFTA, a scaleup in processing batch sizes was required from 8-lb laboratory size batches used for 3.5-in. motor tests to 80-lb production batch sizes used for 5.0-in. motor tests. As a consequence of this rapid scaleup, problems were encountered in the processing of a four-component fuel system (35% TFTA/20% boron/15% AP/30% binder) for the initial subscale fuel evaluation tests.

(U) These problems were manifested by soft cure or noncure behavior of the fuel and by gross swelling or gassing of the fuel at the usual cure temperature of 160° F. Concurrently, a fire occurred that destroyed eight 5-in. motors and badly damaged a cure oven. The nature of the circumstances surrounding the incident tend to indicate either an autoignition of the fuel or an ignition of the gaseous mixture in the oven that resulted from a gradual fuel degradation at elevated temperatures.

(U) In an effort to locate and describe the source of the problem, an extensive compatibility study has been carried out using the four-component fuel system involved in the incident. The components were aluminum powder ("as received"), AP, TFTA, and the binder (QX 3812 resin/cured

with DER 332 resin). During this study, the following factors were considered to be of prime importance:

- A. The purity of TFTA
- B. Vacuum treating of the QX 3812 resin
- C. The chemical equivalence ratio of QX 3812/DER 332
- D. The compatibility of components alone and in combination at both 160° and 195° F.

Fuel samples were mixed in each possible combination of ingredients using binder curative (QX 3812/DER 332) in three equivalence ratios:

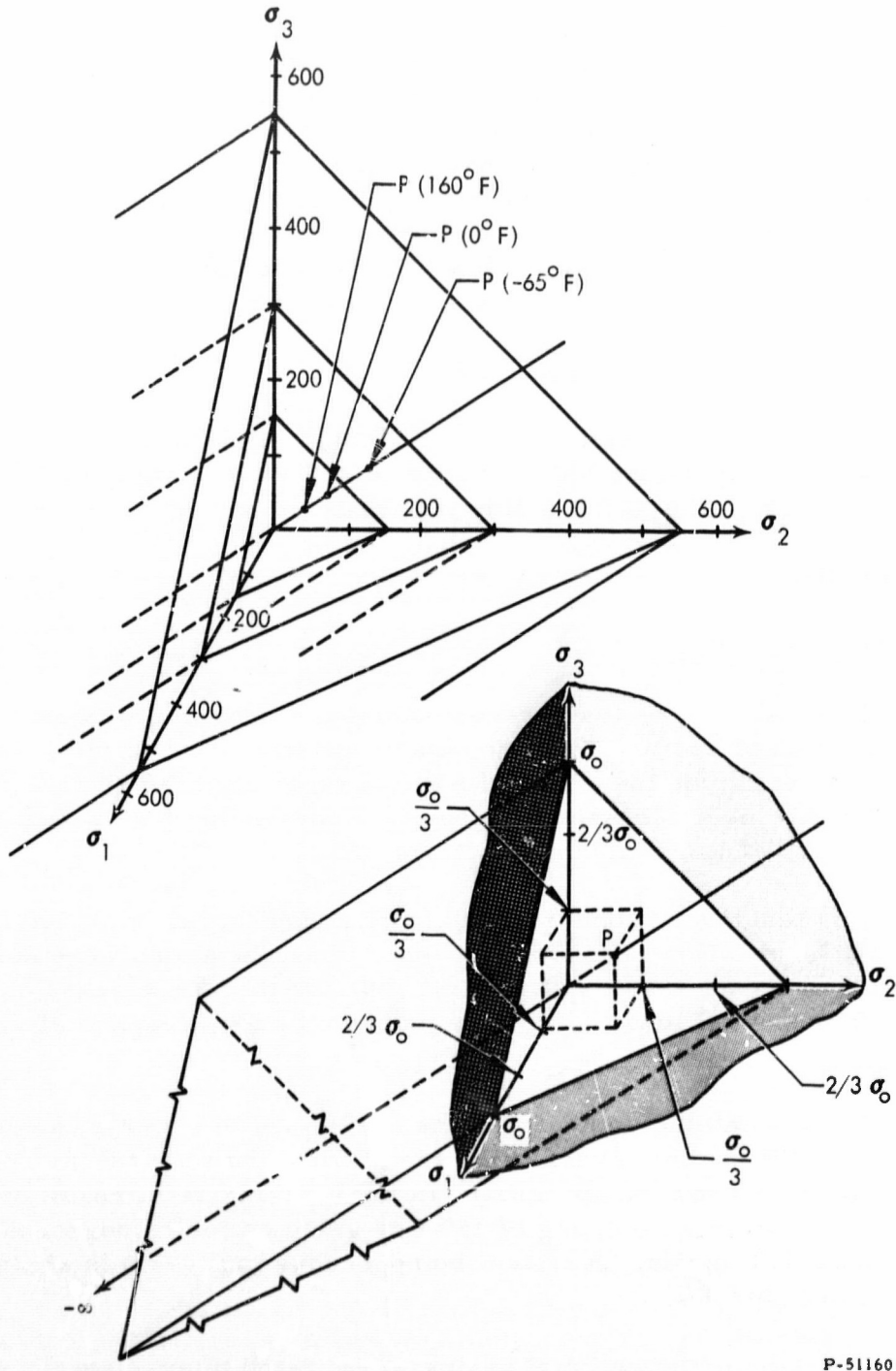
- A. 1.0/0.7
- B. 1.0/0.9
- C. 1.0/1.1

These fuel samples were cured at 160° and 200° F. The results of these processing studies are shown in figure 82.

(U) The following conclusions can be drawn from these tests:

- A. The TFTA must be free of impurities to avoid both outgassing and soft cure.
- B. Increased fuel stability is obtained when the QX 3812/DER 332 equivalence ratio is 1.0/1.1.
- C. Incompatibilities at elevated temperatures are minimized when the QX 3812 binder resin has been vacuum treated prior to fuel mixing.
- D. Minor incompatibility exists between the solid oxidizer (AP) and the nitrogen additive fuel (TFTA) in long-term storage at 195° F.

(U) Particular emphasis was placed on making astute observations with regard to cure behavior and sample swelling or gassing so that trends might be established, indicating the primary sources of difficulty. As a result of this study, fuel processing was altered to include a complete degassing of binder components in the presence of the powdered metal.



P-51160

Figure 82. (U) Fuel Compatibility Samples

Also, the order of component addition to the fuel mix was modified so that the AP was the last constituent added. Fuel curing temperatures of 135° to 170° F have ensured a good, gas-free, well cured fuel grain. A qualitative acceptability test has been developed to ensure the purity of TFTA after duct workup. The test consists of washing the TFTA with a non-oxidizing liquid until the wash liquids are no longer alkaline to methyl-red indicator. By employing these various techniques that have developed as a result of this study, it has been possible to prepare forty 5-in. motors and three 12-in. test motors with single fuel grains weighing 130 lb. Further studies in this general area will be directed toward seeking a binder system that will increase thermal stability of the fuel at temperatures above 200° F.

2.2 SUBSCALE MOTOR TEST PROGRAM

(U) Candidate fuel systems were evaluated in two subscale motor sizes. A 3.5-in. motor (figure 83) was used to screen fuel samples from laboratory-mixed batches. A 5.0-in. motor (figure 84) was used to characterize the regression rate behavior of fuels that had previously been screened in the 3.5-in. motor.

2.2.1 3.5-In. Motor Tests

(U) Fifty-six motor tests were conducted during this program in the investigation of prepackaged propellant systems. These tests were conducted to determine the effect of AP loading on regression rate, to determine the AP level necessary to reach the threshold of self-sustaining combustion, and to evaluate pelletized fuels.

(U) The tests were conducted at chamber pressures from 500 to 1250 psia using ClF_3 at a flow rate of 0.3 lb/sec. Test durations were nominally 12 sec. The data shown in figure 85 indicate that the regression rate is a function of the AP loading and is augmented by the presence of TFTA and TAZ.

(U) Self-sustaining combustion has been found to occur with homogeneous fuels with AP loading levels in excess of 20%, and the presence of other fuel ingredients lowers the maximum AP loading. As a result of these tests a maximum AP loading of 15% was selected for homogeneous non-pelletized fuel blends. A typical homogeneous fuel grain is shown after testing in figure 86.

(U) Thirteen pelletized fuel grains were tested to evaluate the concept of pelletizing to obtain high AP and TFTA or TAZ loading in a nonsustaining fuel grain. Initial tests with fuels containing pellets of TFTA demonstrate that smooth and uniform regression is possible with pelletized fuels, as shown in figure 87.

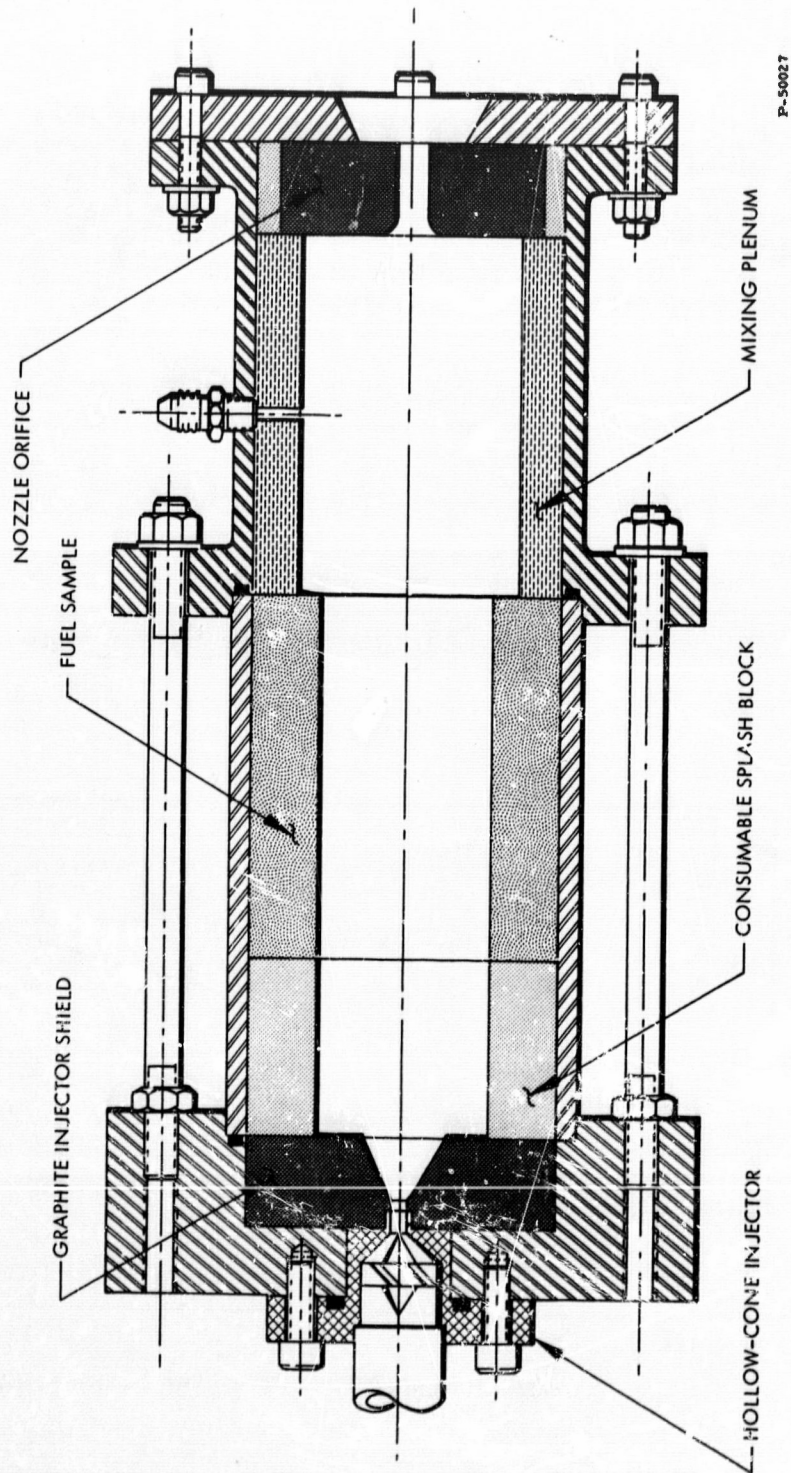
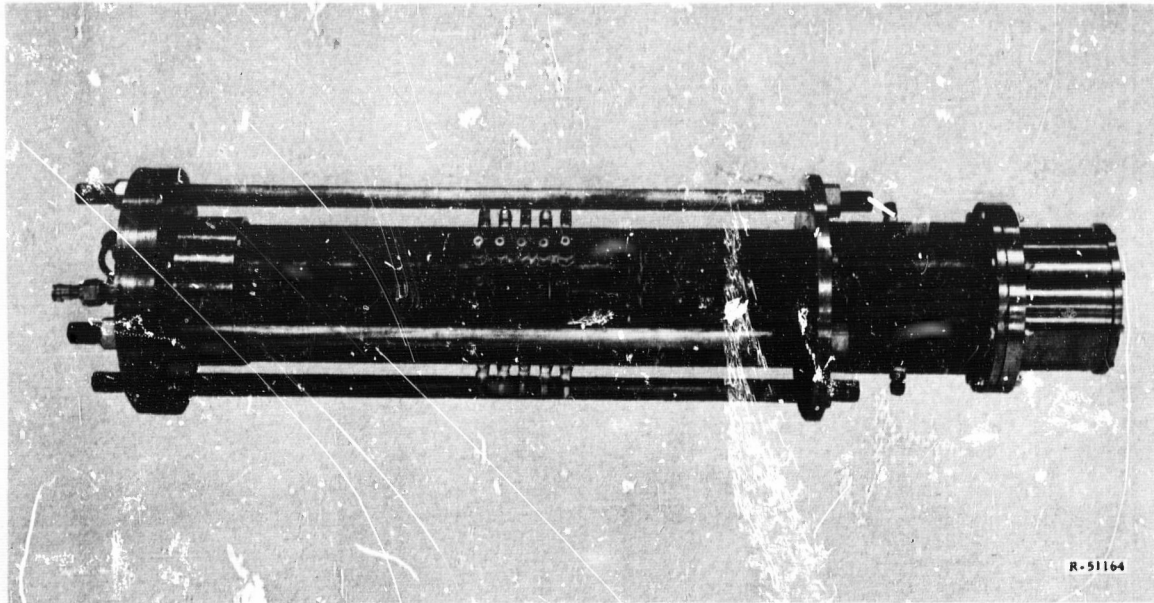
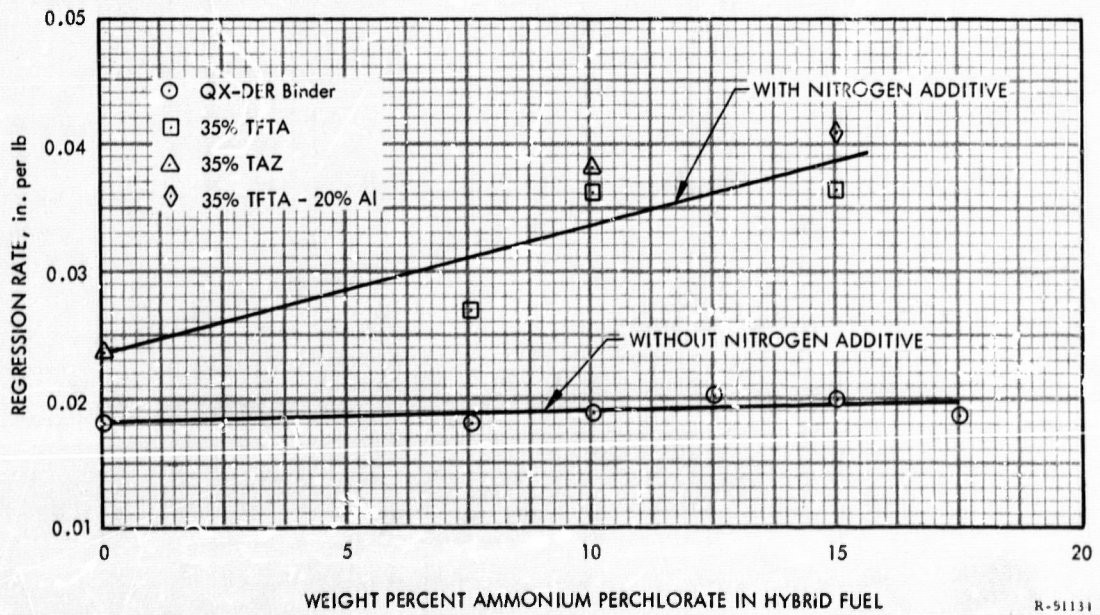


Figure 83. (U) 3.5-In. Hybrid Motor



R-51164

Figure 84. (U) 5.0-In. Hybrid Motor



R-51131

Figure 85. (U) Effect of AP Loading on Fuel Regression Rate

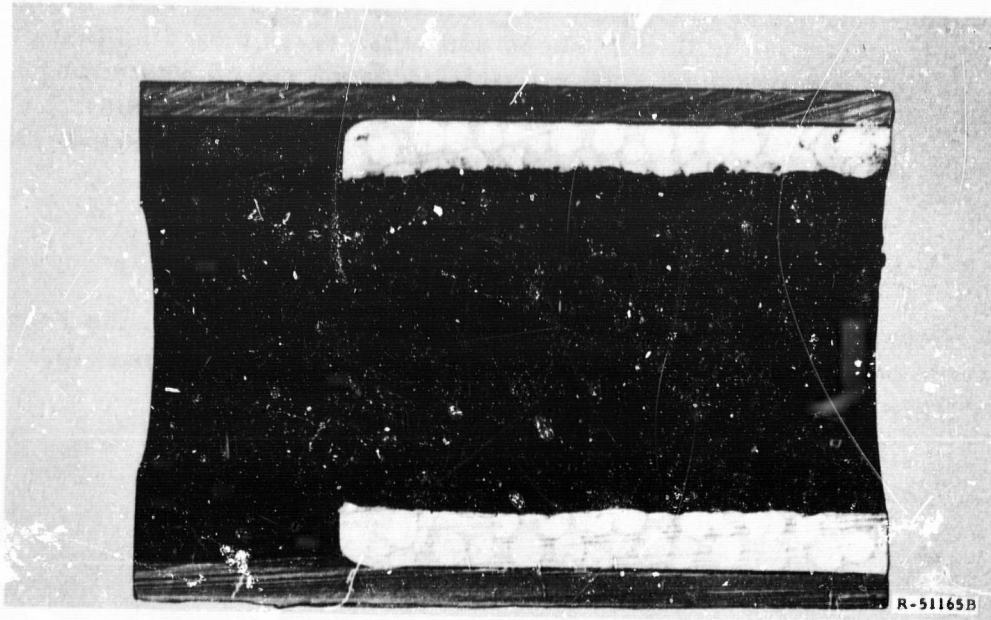


Figure 86. (U) 3.5-In. Homogeneous Fuel Grain After Test



Figure 87. (U) 3.5-In. Pelletized Fuel Grain After Test

(C) The 3.5-in. fuel grains were formulated and tested with 20% TFTA/15% boron/45% AP/20% binder in which the TFTA and AP were in the form of 1/4-in. -diameter pellets. These and other tests indicated that pelletizing was feasible and that it may be possible to develop a nonsustaining pelletized fuel that contains as much as 45% AP. It was felt that the motor size was influencing the data; therefore, the pelletized concept was transferred to a 5.0-in. motor for more complete evaluation.

2.2.2 5.0-In. Motor Tests

(C) Forty 5.0-in. motor tests were conducted to evaluate the regression behavior of five fuel systems that are of interest to this program. The fuels included the following formulations:

- A. 35% TFTA/20% boron/15% AP/30% binder
- B. 35% TFTA/20% Al/15% AP/30% binder
- C. 22% TFTA/20% boron/38% AP/20% binder
- D. 22% TFTA/20% Al/38% AP/20% binder
- E. 45% TFTA/20% Al/35% binder

(C) The tests were conducted at chamber pressures from 200 psi to 1250 psi with oxidizer flow rates from 0.66 to 2.25 lb/sec. The tests were conducted to evaluate the regression behavior of the fuel systems with respect to oxidizer mass flux and combustion chamber pressure.

(U) These formulations represent the state of the art in castable pre-packaged hybrid fuels. Fuels A and B (above) contain the highest practical loading in a nonsustaining, homogeneous AP-loaded fuel grain. Aluminum has been substituted for boron in three formulations to provide a less expensive, but also slightly less energetic, ingredient. The use of aluminum in the selected fuel formulations will be limited to early motor development tests.

(U) Fuels C and D (above) represent the maximum performance attainable with the four components that must necessarily include pelletized AP to qualify as a nonsustaining fuel system.

(C) Fuel E (above) represents the fuel system that would produce a high-performance level (295 sec) without AP, but must use an oxidizer containing ClO_3F that provides a density impulse of 461 gm-sec/cc.

CONFIDENTIAL

(U) Twelve light-sensing probes (figure 88) were used in each motor test to characterize the burning fuel surface as a function of burning time. A computer program is presently being used to fit the probe data by a method of least-square error to an anticipated regression behavior that is expressed by the relation:

$$\dot{r} = a P_c^m G_o^n \quad (1)$$

This computer program was used with notable success with the Li/LiH/binder fuel system in Phase I of this program. Although it is of assistance in the evaluation of the fuel systems discussed here, its accuracy was diminished because of nonuniform burning of the pelletized fuels and by light transmission through TFTA crystals, which produced false signals.

(U) Analysis of the results of these tests is discussed in the following paragraphs. A summary of the tests is given in table 5 of appendix V.

(C) Eight 5.0-in. motor tests were conducted with the fuel system containing 35% TFTA/20% boron/15% AP/30% binder. This fuel used precompact TFTA to increase solids loading. The tests were conducted using ClF_3 at nominal flow rates of 0.6, 1.3, and 2.3 lb/sec. Nominal chamber pressures of 250, 500, and 750 psi were achieved.

(U) Although the computer program cannot accurately obtain an expression for the regression behavior, sufficient data was obtained to determine that no pressure sensitivity exists and that the behavior is reasonably well characterized by the relationship

$$\dot{r} = 0.155 G_o^{0.75}$$

It can be seen in figure 89 that all of the data obtained at each nominal flow rate is essentially unaffected by chamber pressure. The equation predicting fuel regression as a function of burning time produced the solid lines superimposed on the data. Because of data scatter, the above equation is not considered to be a completely accurate analysis of the fuel regression behavior, but would be sufficient to scaleup to full-scale motors for the purpose of verification.

(U) Six of the eight motor firings sustained combustion on termination of oxidizer flow rate. The data and postfire condition of the fuel grains from this and other tests suggest that the presence of boron decreases the

CONFIDENTIAL

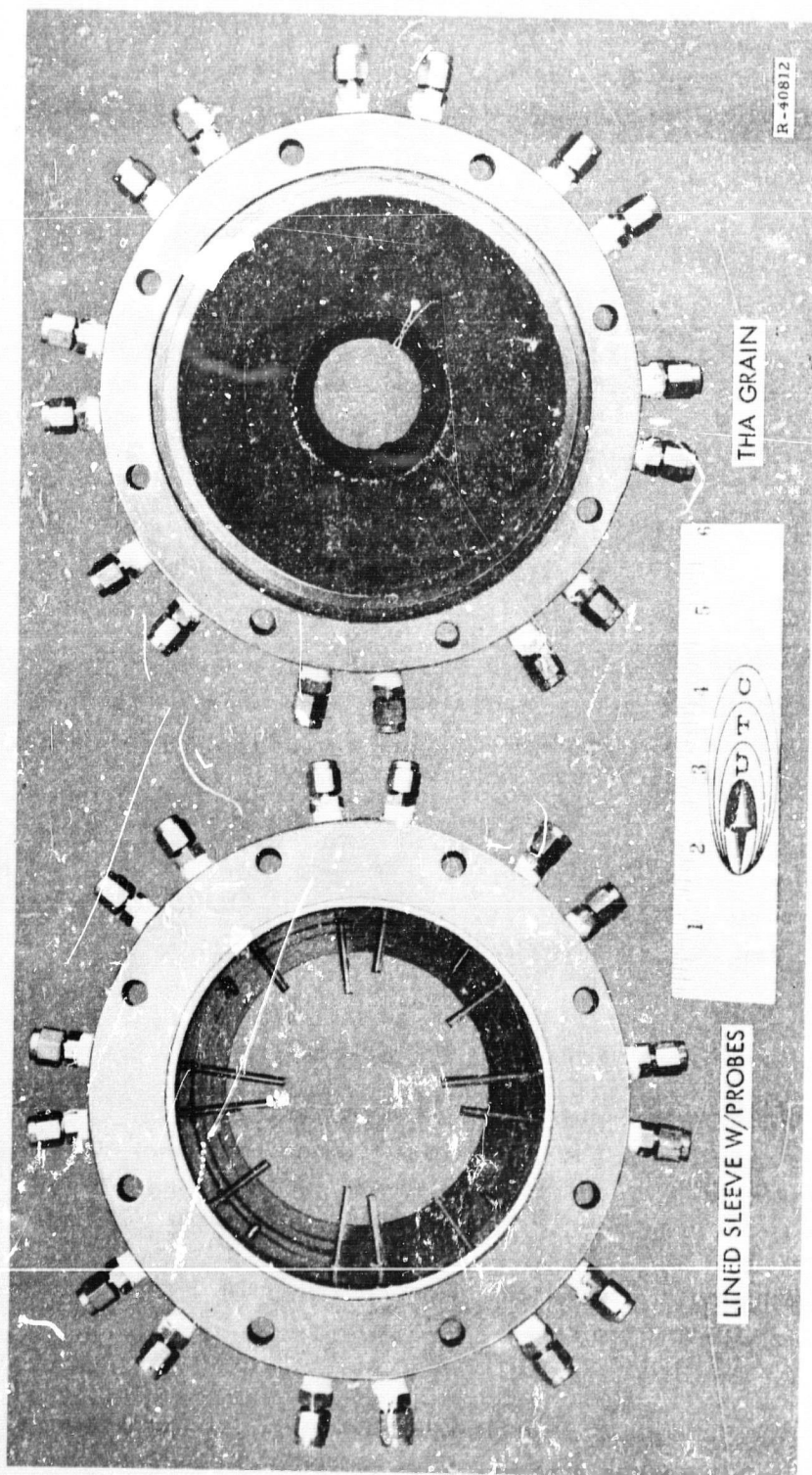


Figure 88. (U) Light Sensing Probes

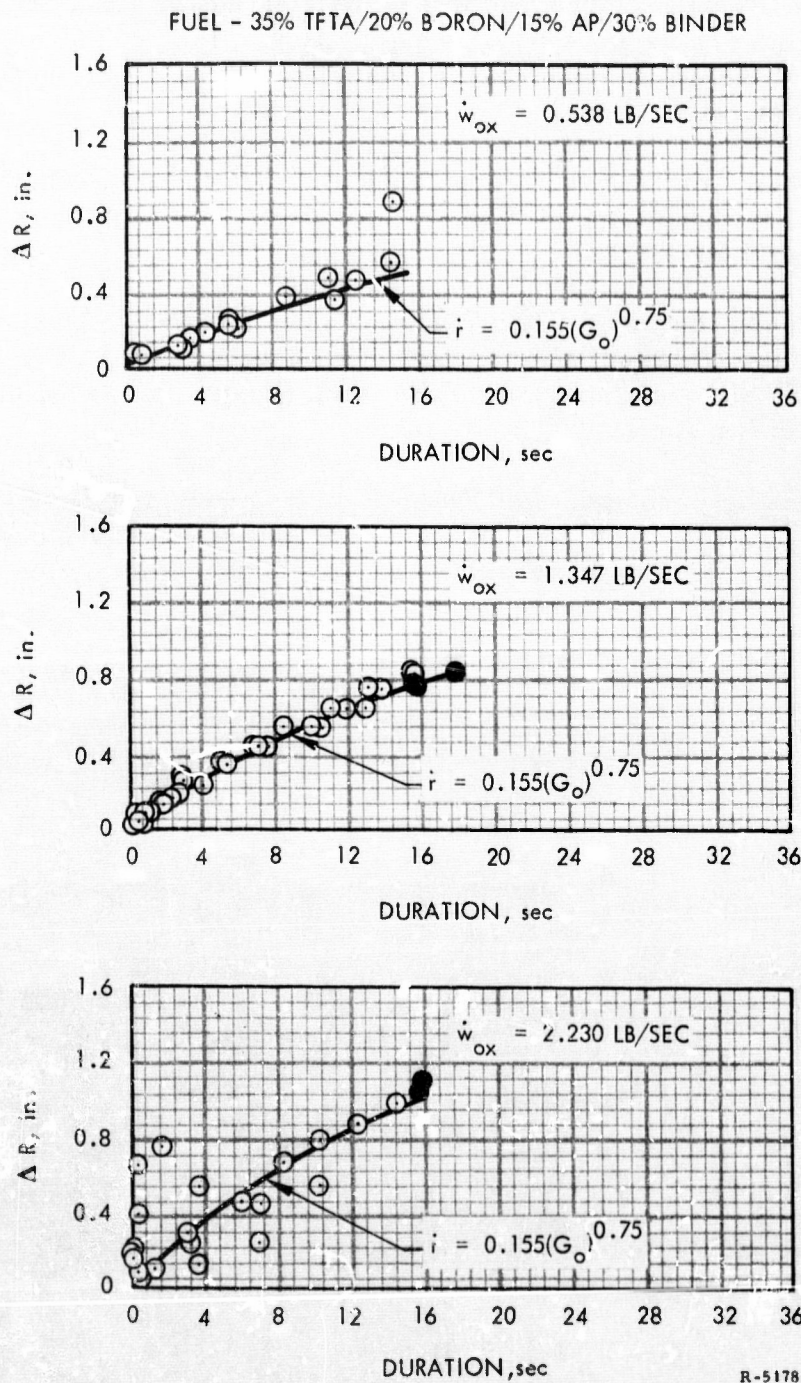


Figure 89. (C) Regression Behavior of Fuel Containing 35% TFTA/20% Boron/15% AP/30% Binder

CONFIDENTIAL

maximum AP level for nonsustaining fuels. In addition, the effective loading level of the AP is increased by compacting the TFTA. The two nonsustaining fuel grains were both at higher flow rates, which suggests that heat soak of the grain at lower regression rates may contribute to sustained combustion.

(C) Eight 5.0-in. motor tests were conducted with the fuel system (B) containing 35% TFTA/20% Al/15% AP/30% binder. A typical fuel grain after testing is shown in figure 90.

(U) In contrast to the fuel system (A) containing 35% TFTA/20% boron/15% AP/30% binder, this fuel did not sustain combustion after termination of oxidizer flow, although the only change in ingredients was the substitution of aluminum for boron.

(C) The regression probe data shown in figure 91 were not amenable to accurate analysis. However, the data indicate that no pressure dependency exists and that the regression behavior can be approximated by the relationship

$$\dot{r} = 0.14 G_o^{0.51}$$

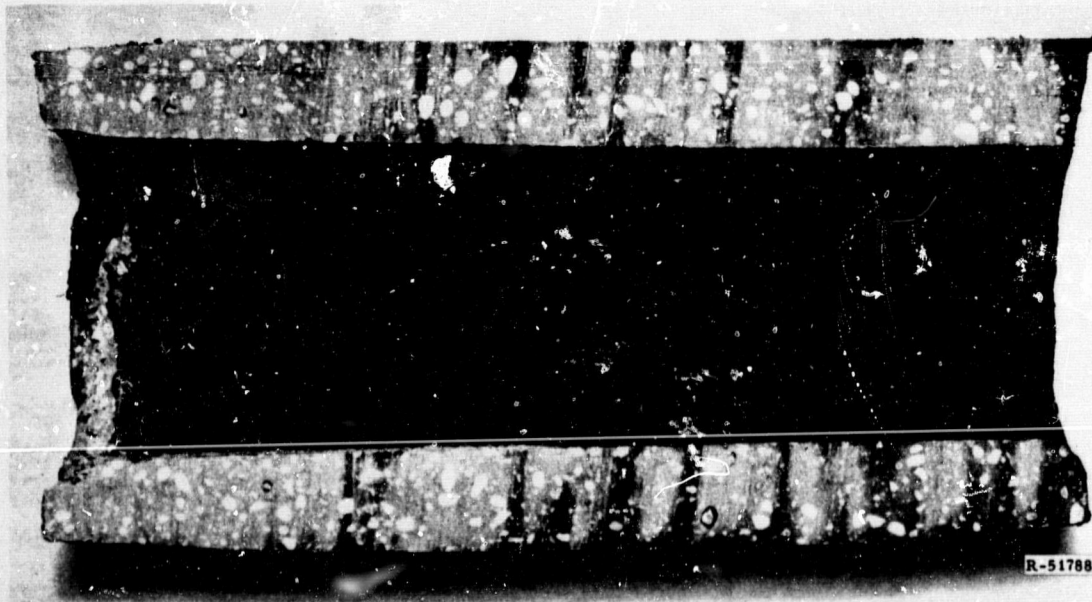


Figure 90. (U) Typical 5.0-In. Hybrid Fuel Grain After Test

CONFIDENTIAL

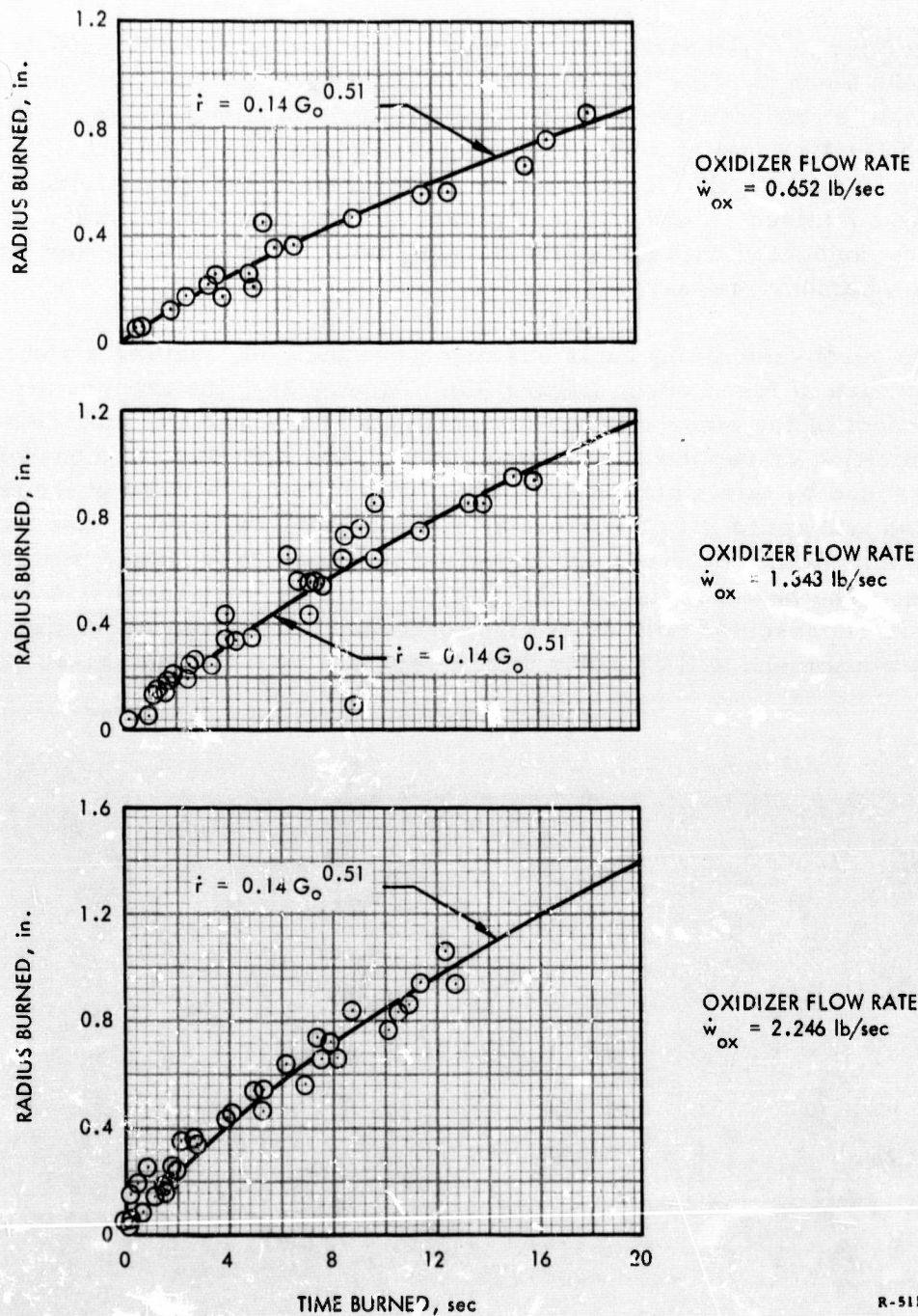


Figure 91. (C) Regression Behavior of Fuel Containing 35% TFTA/20% Al/15% AP/30% Binder

However, full-scale motor testing discussed in paragraph 2.3 indicates that this relationship is in error by 10 to 15%.

(C) The next fuel tested was the system (C) containing 22% TFTA/20% boron/38% AP/20% binder. This fuel requires pelletizing of AP and will deliver the optimum combination of specific impulse and density impulse. This test series, with the fuel system (D) containing 22% TFTA/20% Al/38% AP/20% binder, was intended to demonstrate the feasibility of pelletizing AP to prevent sustained combustion and obtain an optimum formulation. Eight tests were conducted with each formulation, with three oxidizer flow rates and three chamber pressures.

(U) The boron-containing fuels sustained combustion, leaving a sintered, hard structure of fused boron (figure 92). Apparently, the transpiration cooling effect of the other combustion products in the grain is sufficient to prevent melting or vaporization of the boron. The sustained combustion may be caused by this sintered structure, which stores energy in the form of heat and transmits it to the grain after shutdown. It appears that the boron content in the matrix is an important factor in producing a sintered structure. The boron content in the matrix of these fuel grains was 50%, although it represented only 20% of the total fuel. Investigation of the sintering phenomena will continue under Contract No. AF 04(611)-10789.

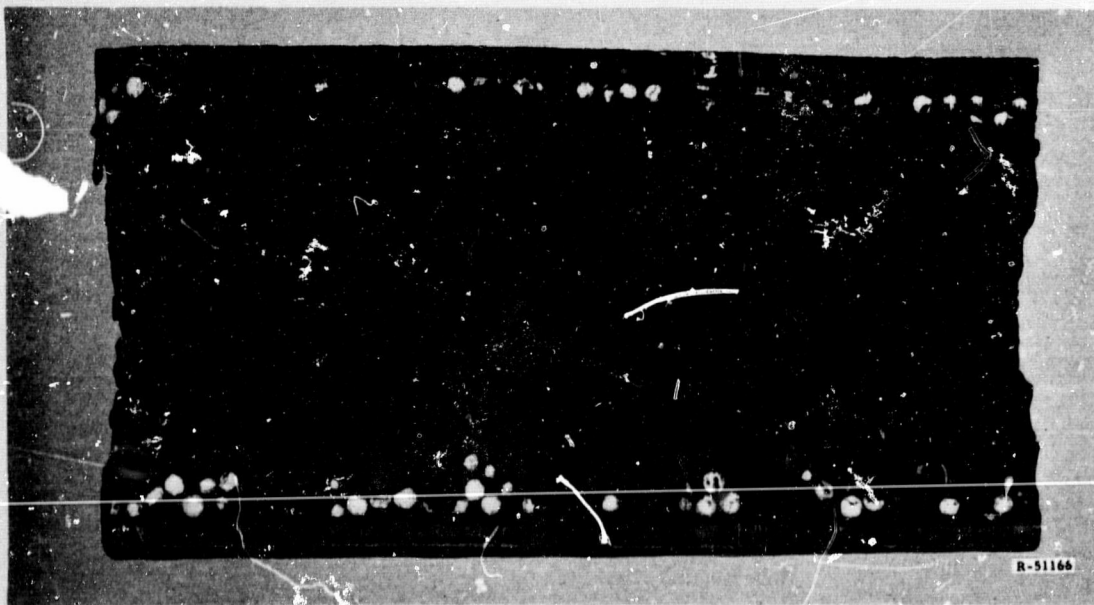


Figure 92. (U) 5.0-In. Fuel Grain, Postfire,
Containing Boron and Pelletized AP

(C) The fuel system (D) containing 35% TFTA/20% Al/15% AP/20% binder also uses pelletized AP. In the eight tests conducted, the tendency toward sustained combustion of the boron fuels was not exhibited with aluminum fuel. These tests demonstrated that nonsustaining fuels are feasible with a relatively high loading of AP if the AP is pelletized. No pressure-sensitive regression behavior is evident in three tests conducted at an oxidizer flow rate of 2.25 lb/sec. Figure 93 shows the fuel grains after testing. The difference in burned web indicates a slight pressure sensitive behavior, which can be expressed by the following proportionality when considering only the pressure extremes:

$$\bar{r} \propto P_c^{0.24}$$

At lower flow rates, any existing pressure-sensitive behavior is hidden in the limited accuracy of the data. This result is caused by the relative size of any pressure effect produced as compared to the diameter of the AP pellets, which is the limitation in data accuracy.

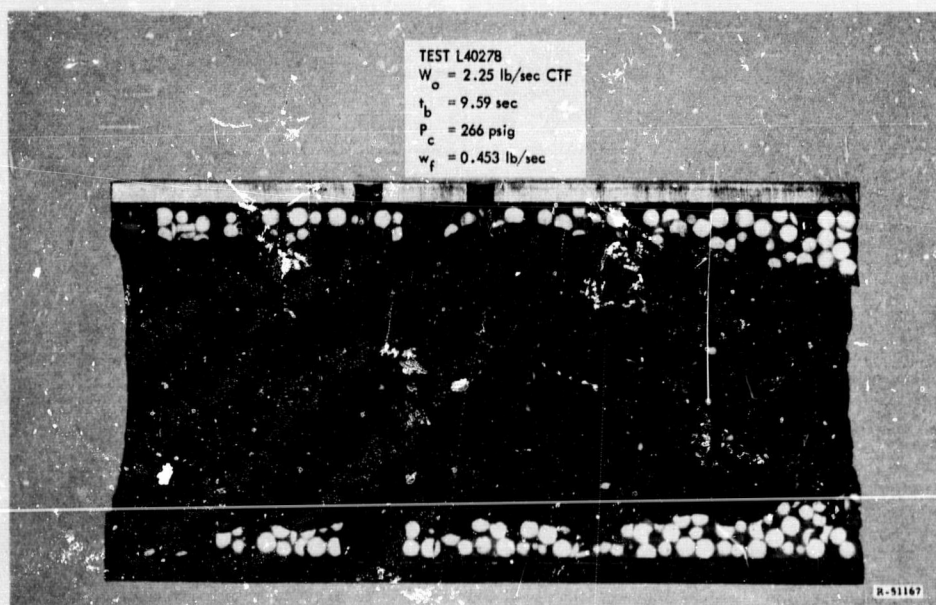


Figure 93. (U) Pressure Effects on Pelletized Hybrid Fuels
(Sheet 1 of 2)

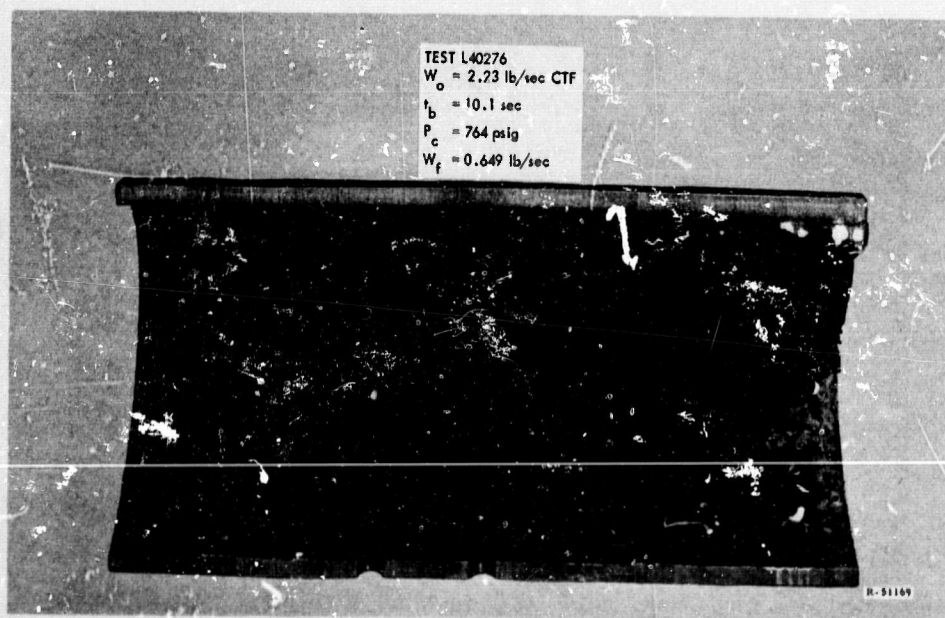
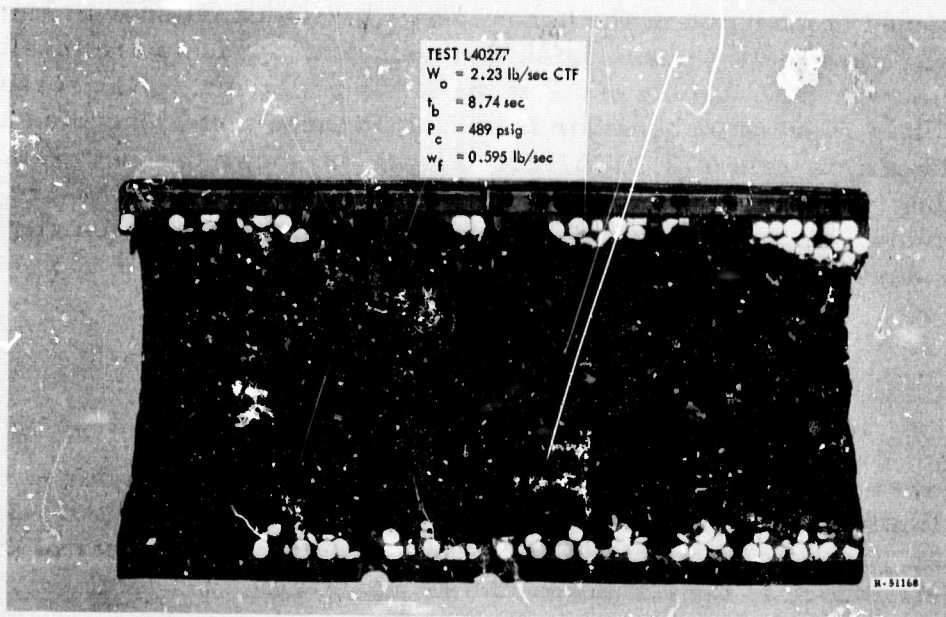


Figure 93. (U) Pressure Effects on Pelletized Hybrid Fuels
(Sheet 2 of 2)

CONFIDENTIAL

(U) Similarly, the fuel regression behavior as a function of oxidizer mass flux is inconsistent when comparing the behavior at different flow rates. However, the extremes in average regression rate at common chamber pressures can be expressed by the following proportionality

$$\bar{r} \propto G_o^{0.52}$$

These relationships cannot be used to accurately predict fuel flow rates, but they do represent approximate pelletized fuel behavior and can be used in preliminary motor test calculations.

(U) No attempt was made to fit this data to a form of the anticipated behavior $\dot{r} = a P_c^m G_o^n$ because it must deal in instantaneous rather than average regression rates, and precise knowledge of the fuel port area during the test is not known. These tests indicate that pelletized fuels are entirely feasible. Although fuel regression was not uniform (figure 94), separation of the AP pellets by a coating should produce a uniform regression profile in the grain.

(C) The fuel system (E) consisting of 45% TFTA/20% Al/35% binder uses precompacted TFTA and is intended for use with an oxidizer containing ClO_3F . The test results shown in figure 95 indicate that it burns with a relatively low regression rate (0.04 in./sec) as compared to 0.07 in./sec for the four-component fuel and 0.12 in./sec for the pelletized fuels. The tests indicate that a low degree of regression rate sensitivity to oxidizer mass flux and very little, if any, sensitivity to chamber pressure.

(U) The regression behavior is smooth and uniform as shown in figure 96. Precise determination of the mathematical relationship for regression is limited by the compacted TFTA grains which are translucent and produce false signals. These errors, coupled with the low rate of regression, can produce completely erroneous trends in the behavior of the fuel. However, the regression rate was found to be insensitive to chamber pressure and related to oxidizer mass flux by the expression, $\dot{r} \propto G_o^{0.30}$, when the extremes in average regression rate are evaluated.

2.3 TWELVE-IN. MOTOR TESTS

(U) Six tests were conducted with three 12-in. filament-wound motors of the basic design discussed in paragraph 1.4. The tests were conducted to evaluate processing techniques, regression behavior, fuel utilization, and relative performance of multiple component fuels. In addition, the tests were used to evaluate lightweight nozzles and injector designs.

CONFIDENTIAL

FUEL - 22% TFTA/20% ALUMINUM/38% AP/20% BINDER
WITH PELLETIZED AP

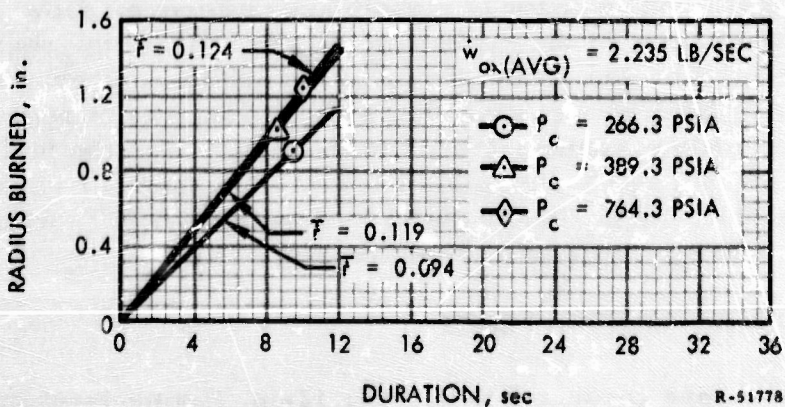
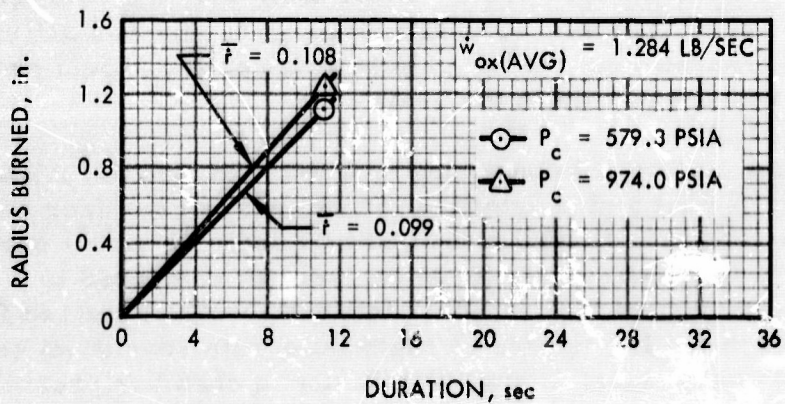
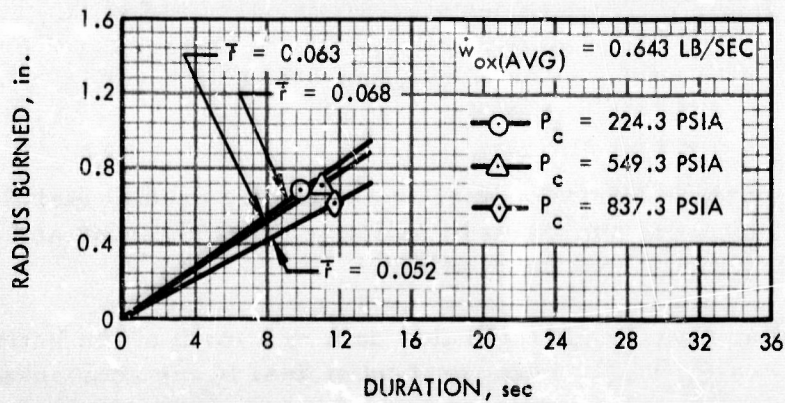


Figure 94. (C) Regression Behavior of Fuel Containing 22% TFTA / 20% Al / 38% AP (Pelletized) / 20% Binder

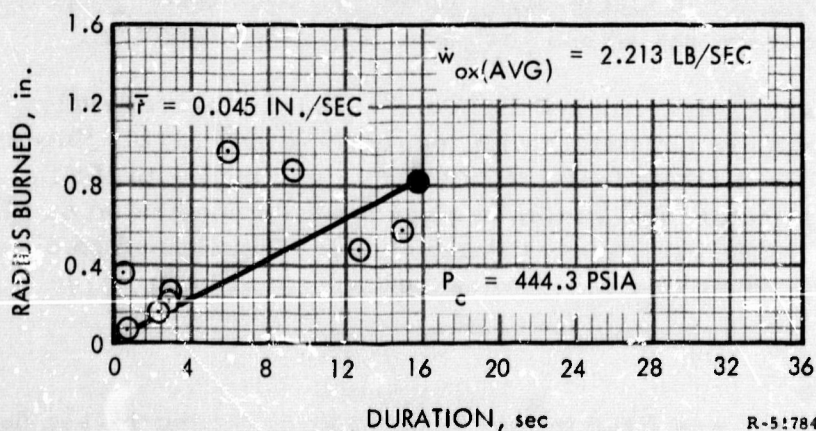
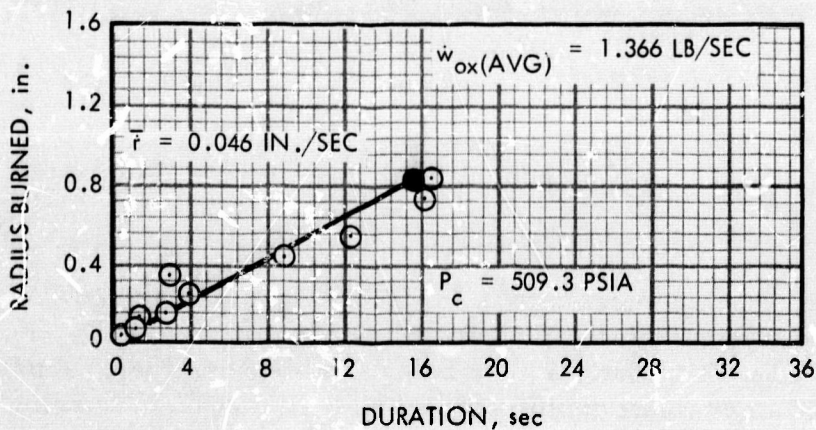
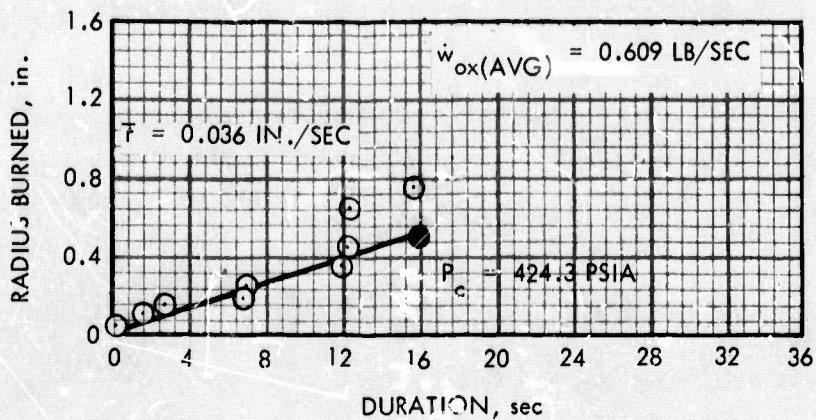


Figure 95. (C) Regression Behavior of Fuel Containing 45% TFTA (Compacted) / 20% Al / 35% Binder

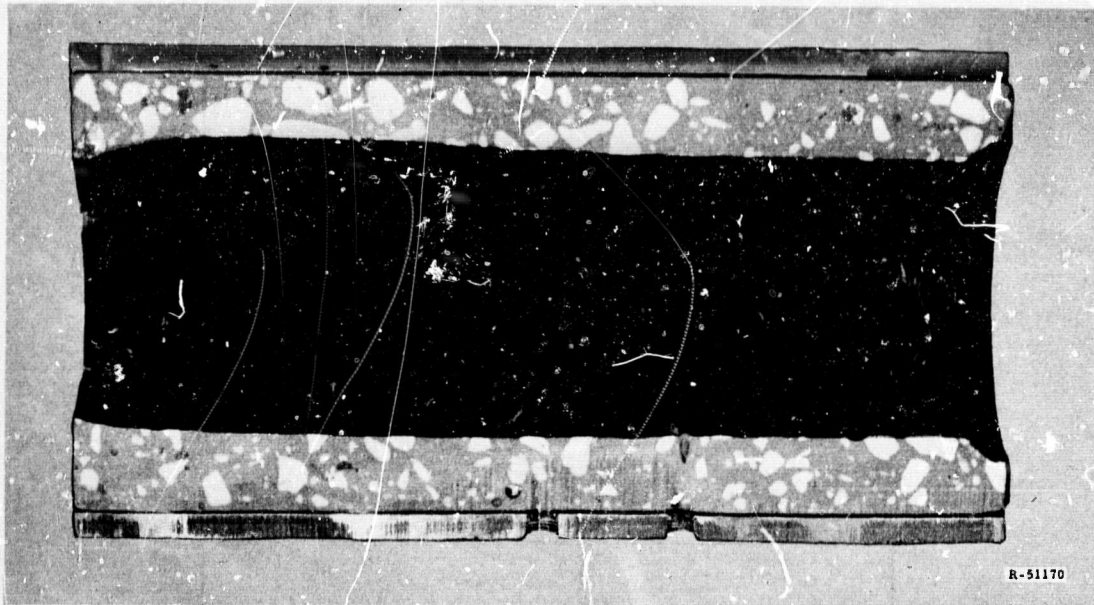


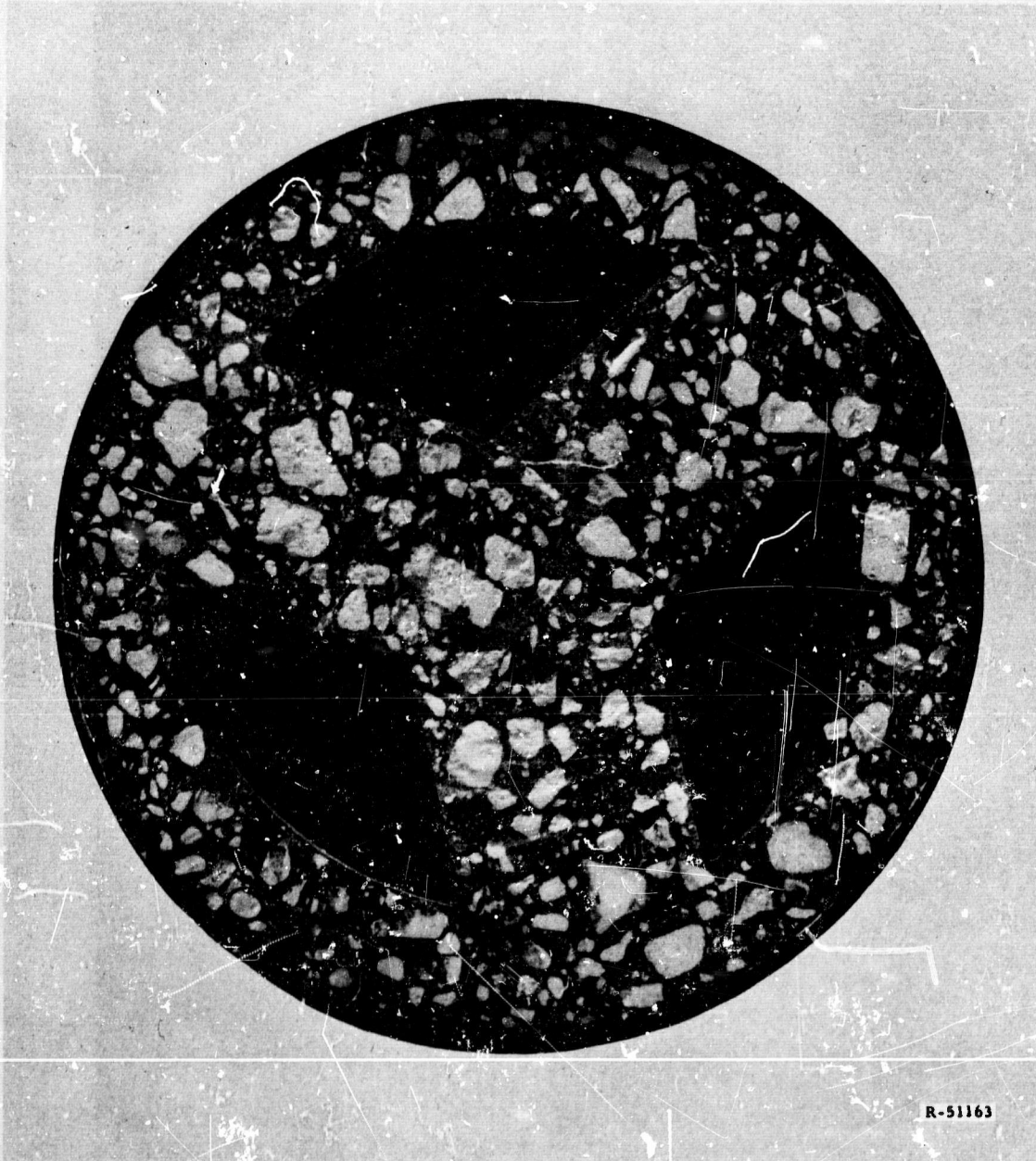
Figure 96. (U) Three-Component Fuel System with Compacted TFTA

(C) The fuel system consisted of 35% TFTA (compacted)/20% Al/15% AP/30% binder. A typical 12-in. fuel grain is shown in figure 97. Four tests were conducted with motor No. 008 using ClF_3 as oxidizer. These tests were designed to evaluate motor behavior as a function of burning time. The two remaining tests were designed to evaluate fuel utilization and motor performance in single-start 30-sec duration tests. The oxidizer used in these tests was an 82% ClF_3 and 18% ClO_3F mixture.

(U) The test results indicate that relative performance levels were attained, which are consistent with test data for the Li/LiH/binder fuel and FLOX. Predictable fuel utilization was obtained with the first motor. Lightweight injectors and nozzle designs were demonstrated on all three motor tests. However, motors No. 009 and 010 sustained combustion on termination of oxidizer flow. No change had been made in the fuel formulation.

2.3.1 Motor No. 008

(C) This motor was fired in four tests of 5, 5, 5, and 15-sec duration. The motor configuration (figure 98) was identical to those used in Phase I. A conventional hollow-cone injector, splash block, and mixer assembly were used. The motor was ignited with ClF_3 at a flow rate of 12.65 lb/sec, of which 1.0 lb/sec was injected through the aft injector. After each test,



R-51163

Figure 97. (U) 12-In. Hybrid Fuel Grain

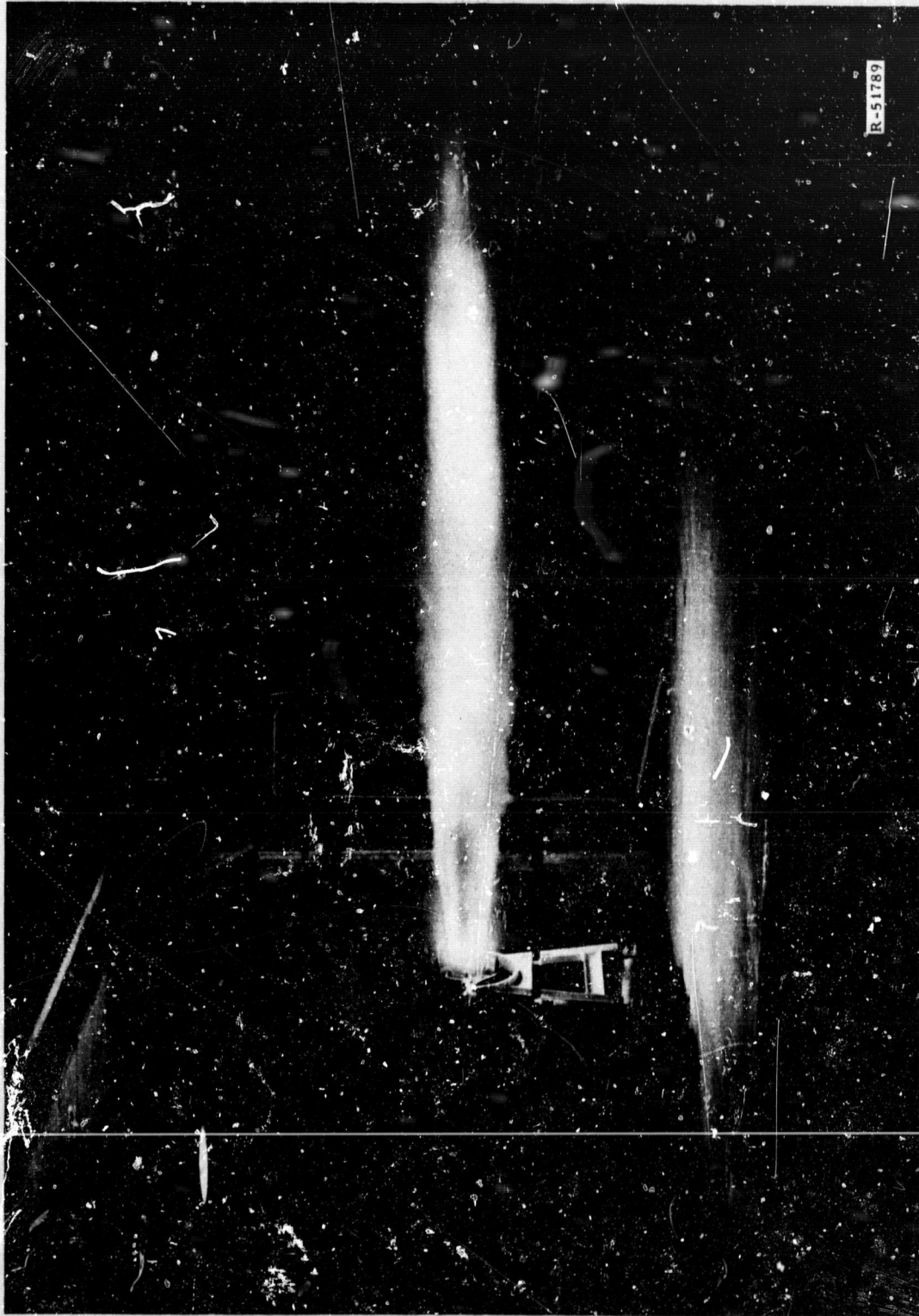


Figure 98. (U) 12-In. Hybrid Motor Firing

CONFIDENTIAL

the motor was removed from the test stand, weighed, and reinstalled for the subsequent firing. No difficulty was encountered in shutting down the motor. Internal inspection of the motor was conducted to evaluate the regression behavior as a function of test duration.

(C) The motor delivered relative performance levels from 90 to 95%, as shown in table VIII. The performance levels are entirely consistent with those obtained in 12-in. motor tests prior to Phase II.

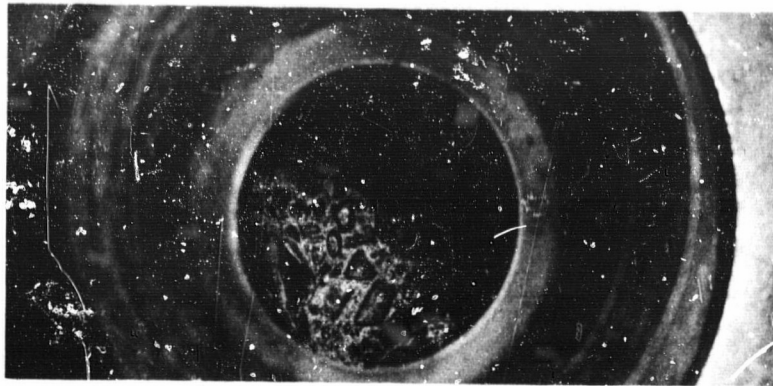
TABLE VIII
RELATIVE PERFORMANCE LEVELS

Test No.	Thrust (avg) lb	P_c psia	t_b sec	I_{sp} (1000/14.7) sec	Performance %
298	4079	245	4.86	251	95.4
299	3611	223	4.92	239	94.3
300	3402	214	5.02	229	91.3
301	2656	169	14.81	211	90.9

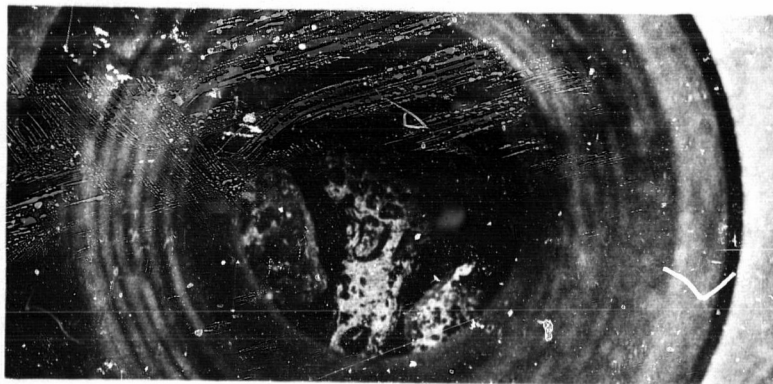
(C) The high performance levels compare favorably with the previous high of 94% obtained with the lithium fuel system and FLOX. The decay in performance with burning time is attributed to the erosion of the mixer lobes, which were nearly gone after the final test. The performance level at 30-sec duration (90.9%) is consistent with motor No. 007, which did not use a mixer but relied only on aft injection to induce mixing.

(U) The fuel flow rates and regression rates were slightly lower than predicted by the subscale data. The error in average regression rate amounts to approximately 15%, and probably results from inaccuracy of the 5.0-in. motor data. With the exception of a slight contouring near the injector, fuel regression was uniform and as predicted, both axially and laterally. The fuel grain is shown in figure 99, viewed through the nozzle after each test. The near complete fuel utilization is evident, as shown in figure 100. The only fuel remaining that could not be accounted for, as predicted, was a sliver of consumed fuel located at the head-end near the injector. The motor burned 82% of all fuel available, of which approximately 9% was left in the sliver and 9% was associated with the contoured

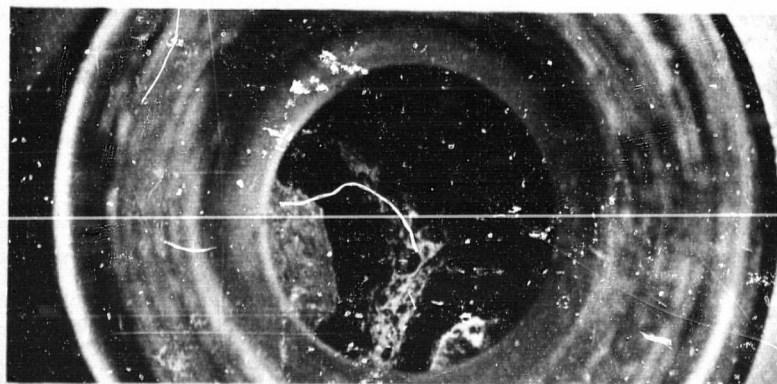
CONFIDENTIAL



5.0 SECONDS



10.0 SECONDS



15.0 SECONDS

R-5:792

Figure 99. (U) Photo Sequence of Motor 008 —
Fuel Grain After 5, 10, and 15 sec Duration

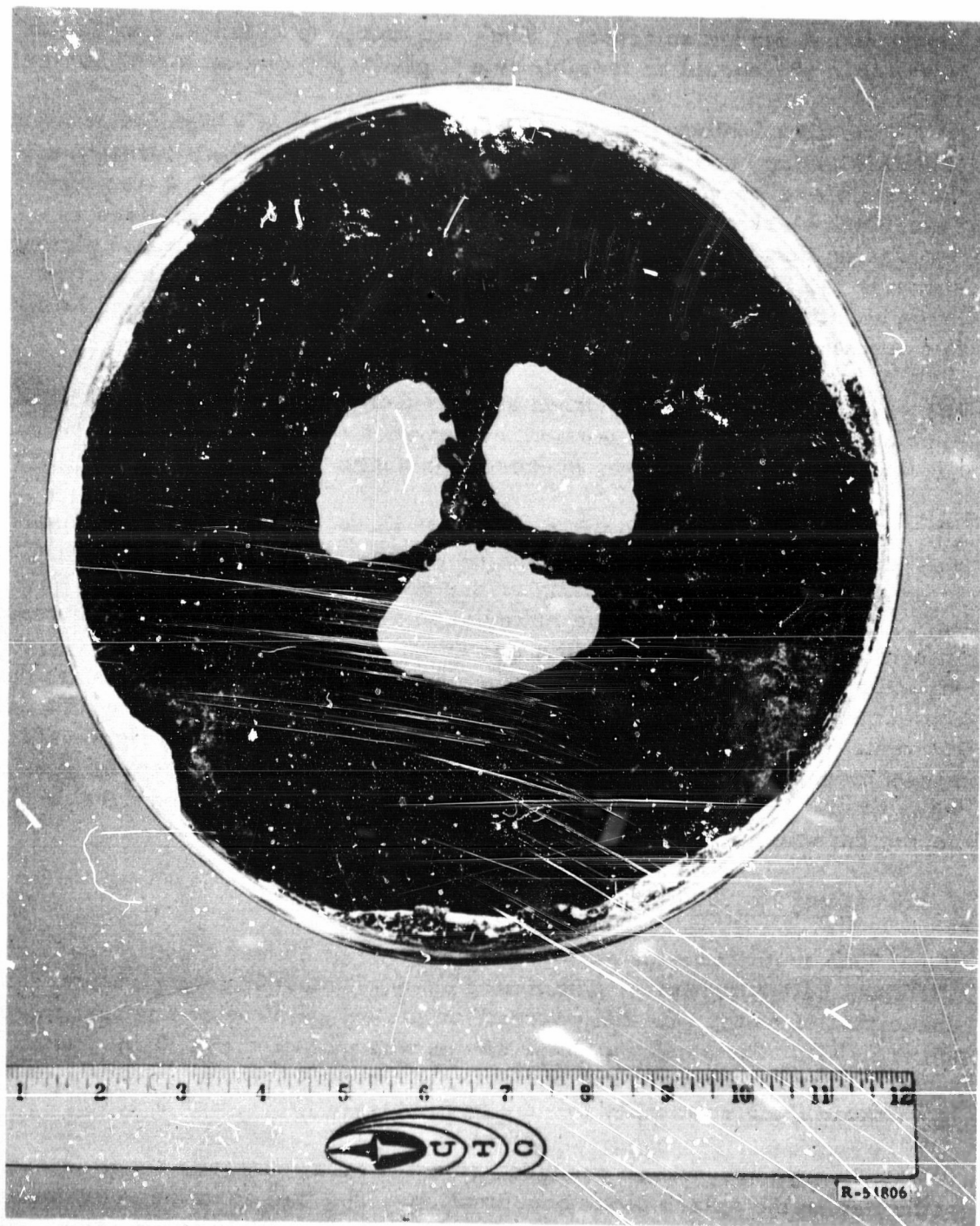


Figure 100. (U) Fuel Grain From Motor 008 After Test

CONFIDENTIAL

grain near the injector. The sliver loss can be reduced to approximately 3% in flight-configuration grain shapes by elimination of the splash block and proper design of injectors. Thus, an increase in fuel utilization to better than 95% should be feasible in a flight-configuration motor design.

(U) The splash block (figure 101) shows evidence of a significant quantity of PBAN having been consumed during the test. The PBAN insulation in the aft closure was completely consumed during the first 5.0-sec test. The splash block and aft closure insulation contributed to produce a decreasing thrust indicated in table VIII. An illuminated exhaust plume shown in the first frames of a sequence-camera coverage indicate that large quantities of carbon in the form of PBAN were consumed in the first few seconds of operation.

(U) The mixer assembly shown sectioned in figure 102 sustained little erosion in the cylindrical portion, which accumulated only 0.3 in. of char, but the ceramic-foam mixer spokes were nearly consumed.

(U) A carbon-cloth phenolic nozzle with an ATJ graphite nozzle insert was used in each test. In this test, as in the others, the nozzle throat dimensions remained essentially unchanged during the motor test. However, high conductivity of the material in the nozzle skirt assembly resulted in complete charring of the skirt and burning of the overwrap glass-epoxy structure. Although the nozzle remained intact throughout the test sequence, the completely charred carbon-cloth material delaminated in handling after the test. The reconstructed nozzle, shown with the mixer in figure 102, shows no erosion in the carbon-phenolic skirt. A carbon-phenolic liner, when combined with a lightweight insulator, should result in a durable nozzle capable of surviving the required duty cycle.

2.3.2 Motor No. 009

(C) This motor was tested in a single firing of 30-sec duration with a ClF_3 and ClO_3F mixture. The motor used an internal configuration identical to that of motor No. 008, except for the substitution of a poppet injector (figure 103). The poppet injector design was qualified in 5.0-in. motor tests, and the successful use of lightweight poppet injector in these tests has proved their suitability for use in full-scale propulsion systems.

(C) The injector, which produces an axial spray pattern, resulted in a reduction in the splash block consumption. The fuel sustained combustion on shutdown, prohibiting accurate determination of fuel consumption. The sustained combustion is attributed to several factors, including a higher flame temperature with ClO_3F in the oxidizer and a longer test duration.

CONFIDENTIAL

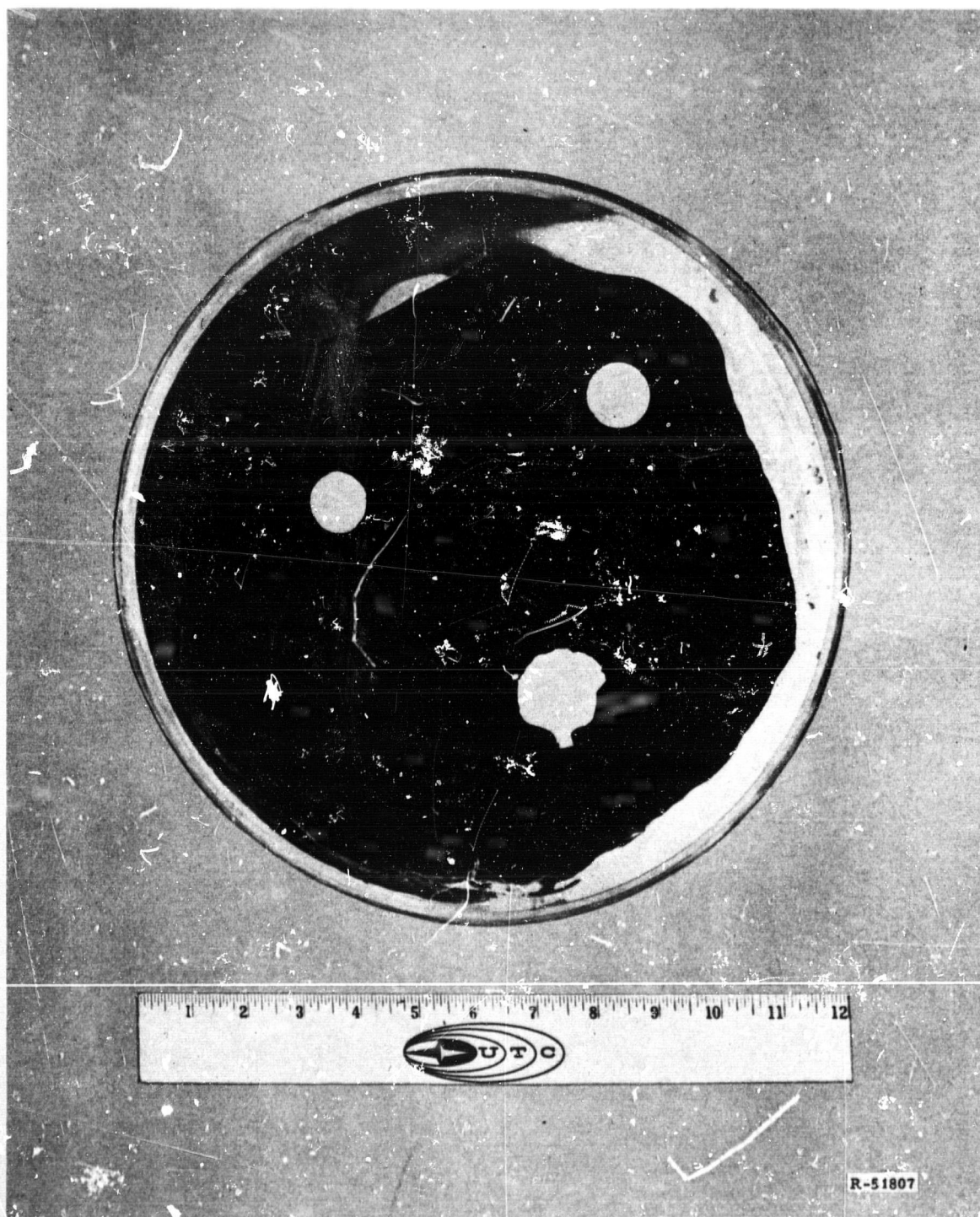


Figure 101. (U) Splash Block From Motor 008 After Test

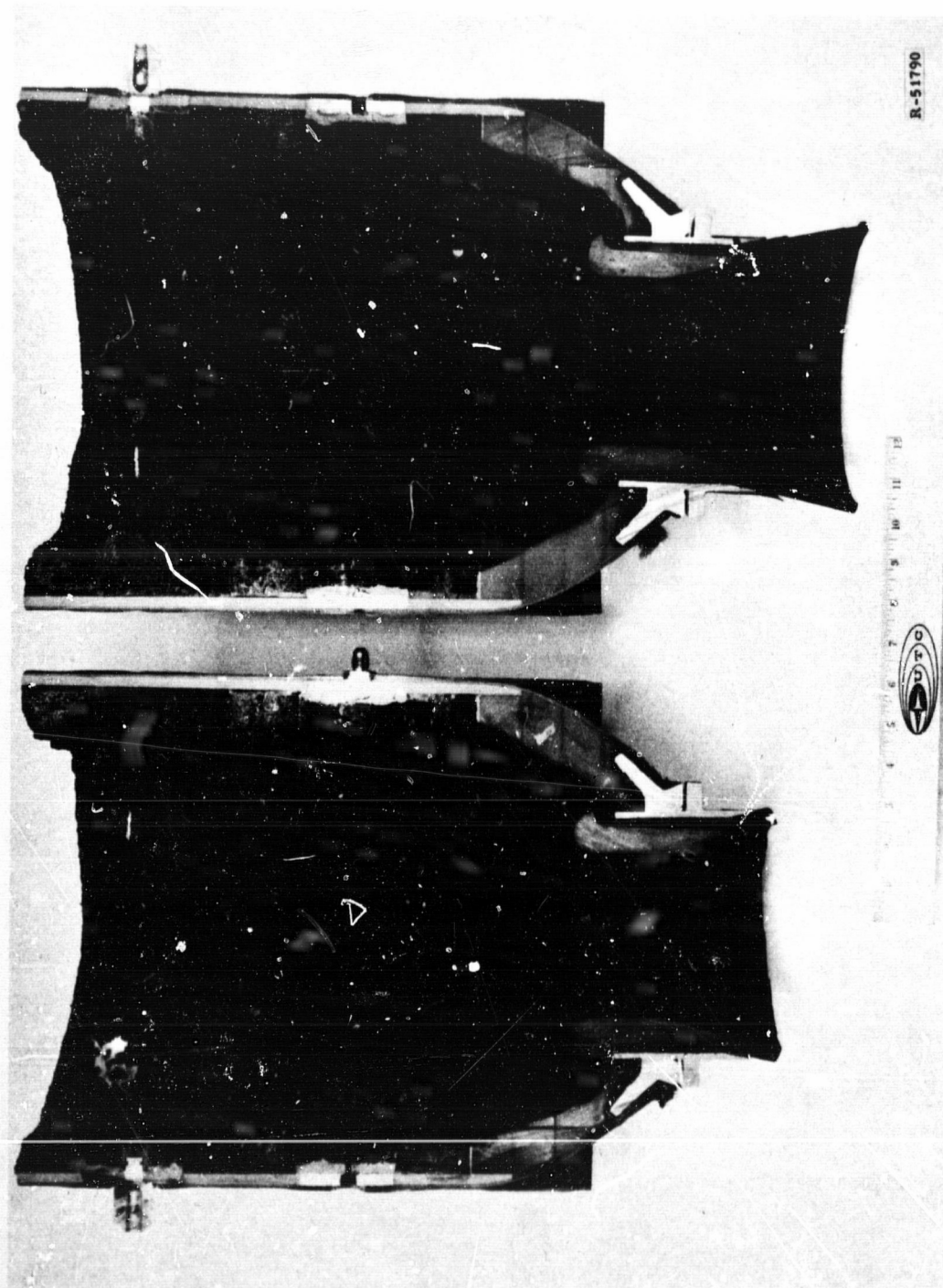


Figure 102. (U) Mixer Assembly From Motor 008 After Test

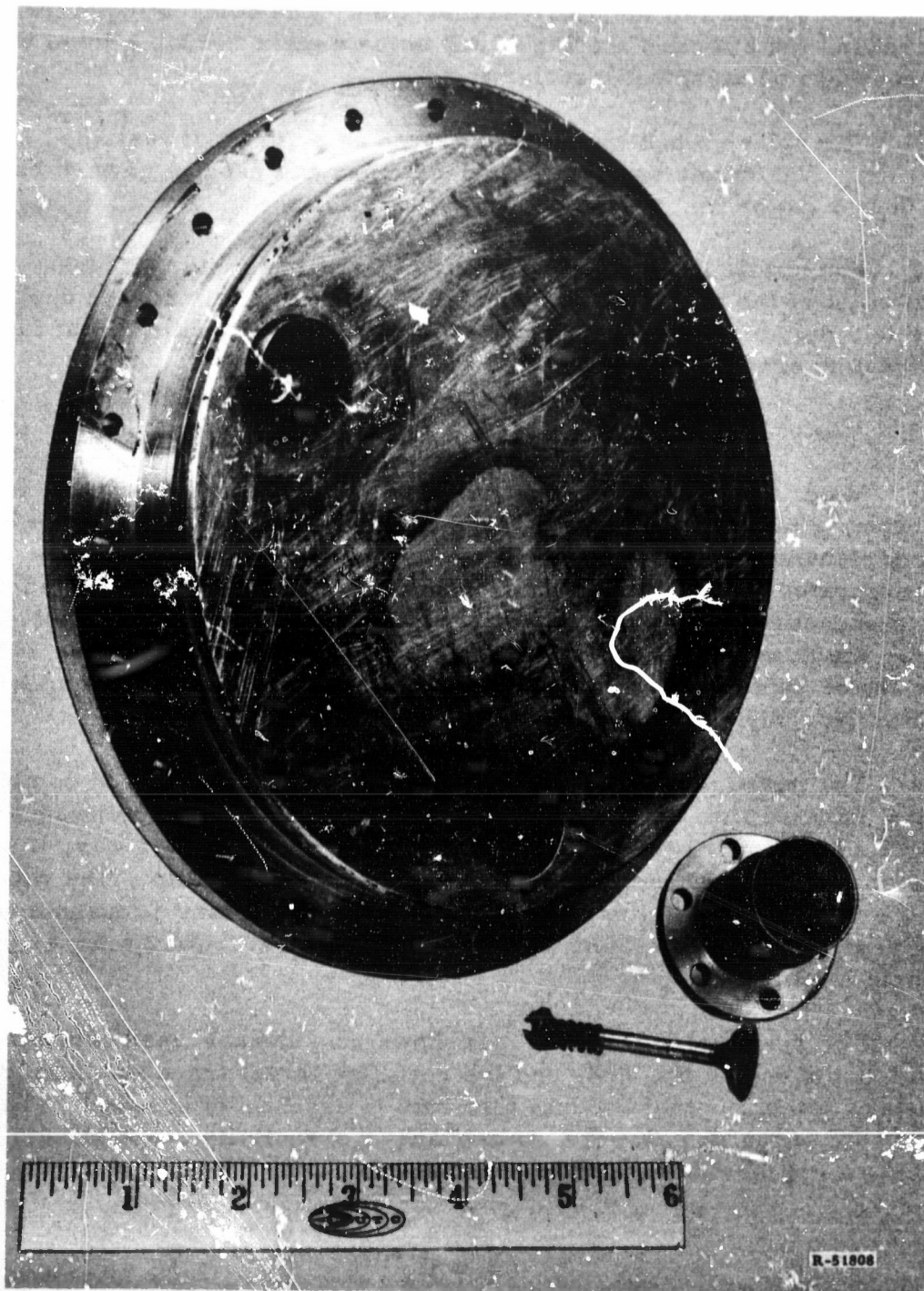


Figure 103. (U) Poppet Injector Assembly

The fact that it sustained, in contradiction to 5.0-in. subscale motor test data, is attributed to the TFTA compaction. The compacting of TFTA increased the effective loading of AP in the matrix to 23%, a level which is known to be marginally sustaining.

(U) The splash block was badly charred as a result of sustained combustion. The mixer section sustained a char and erosion pattern comparable to that of motor No. 008.

(U) The nozzle assembly was identical to that of motor No. 008. The exit skirt of the nozzle was ejected after approximately 20-sec duration due to a delamination failure. However, the ATJ graphite throat insert showed no erosion after 30 sec of firing.

2.3.3 Motor No. 010

(U) Motor No. 010 incorporated a minor design change in the mixer section, which included a graphite-phenolic three-lobe mixer and a ceramic-foam plenum wall, which was reduced in thickness to 0.50 in. The mixer incorporated a graphite cloth, impregnated with a refractory-filled high-char phenolic resin system. To provide the best resistance to hot-gas flow, the mixer was fabricated with the cloth lamination oriented 90° to the motor centerline. The motor used the poppet injector used with motor No. 009.

(U) The motor was fired for a 30-sec duration and sustained combustion after oxidizer flow termination. However, after this test some fuel was retained by purging the motor with liquid nitrogen. In this way, it was possible to observe the posttest condition of the fuel grain. The condition of the grain indicated that the sustained combustion may propagate from the rear of the motor, being forced by radiant heat from the mixer and nozzle assembly.

(U) The splash block (figure 104) shows considerably less consumption than that of motor No. 008, and the resulting thrust trace was noticeably flatter, indicating that the fuel flow rate is essentially constant. The fuel flow rate of the three-spoke grain shape is essentially constant with a fuel having a regression rate proportionality of

$$\dot{r} \propto G_o^{0.5}$$

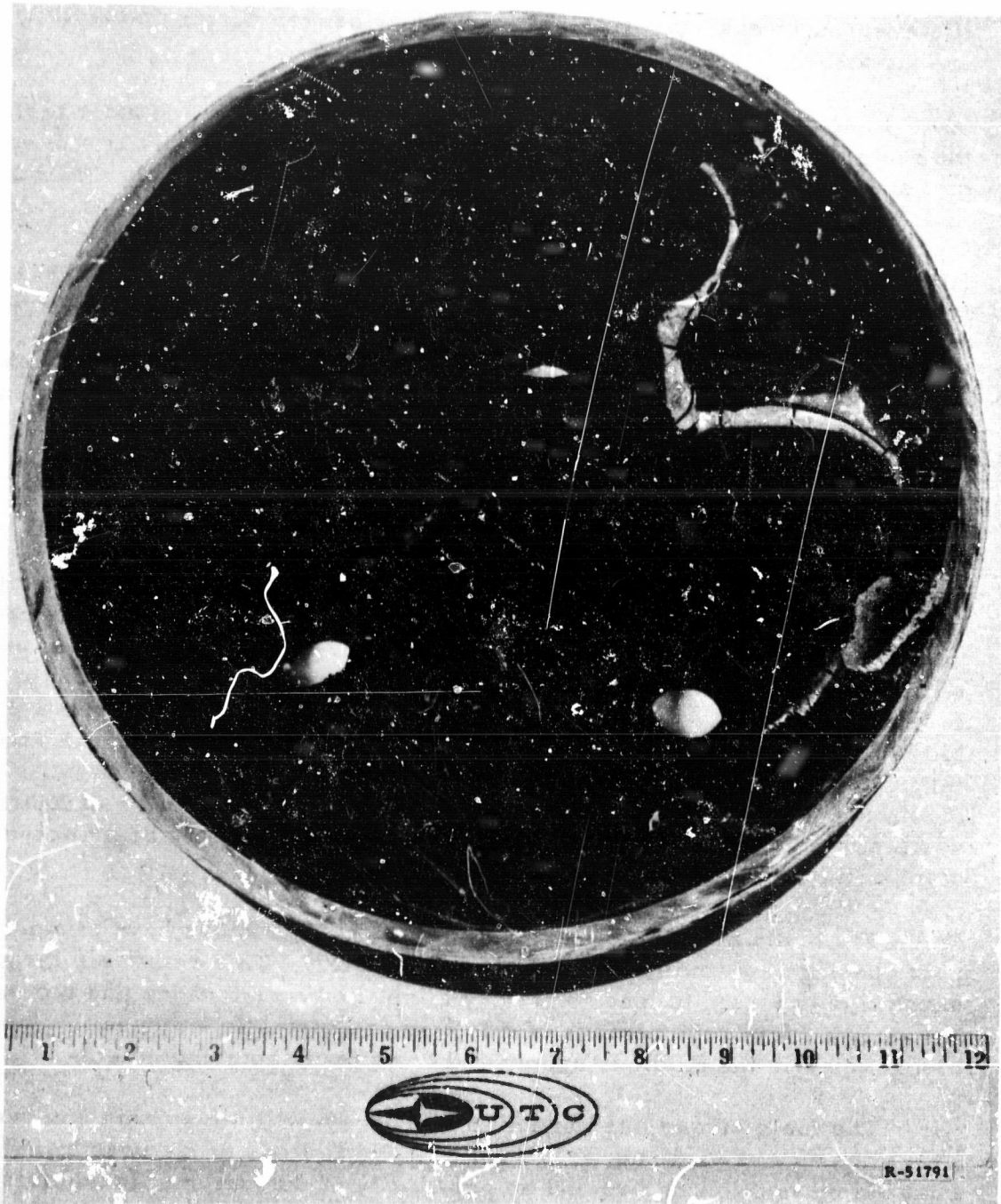


Figure 104. (U) Splash Block From Motor 010 After Test

CONFIDENTIAL

(U) The mixer baffle shown in figures 105 and 106 survived without significant erosion, although delamination occurred. The thinned mixer section shows a char depth of 0.3 after 30-sec duration. The nozzle assembly was identical to the previous tests and endured the test in a similar manner. However, the weakened structure was easily broken during dismantling operations.

(C) In spite of fuel lost during the sustained burning period after test, the motor delivered a specific impulse of 223 sec (1000/14.7) at a pressure of 250 psi. The performance level was 89% of the theoretically attainable, in spite of the fuel lost after motor shutdown.

(U) Motor No. 010 was to have been tested at two thrust levels, representing 100% and 50% thrust using the full-scale dual manifold hollow-cone injector shown in figure 107. However, late-developing injector leaks prevented use of the injector on this program. Single-element dual-manifold injectors similar to this one have been successfully tested under Contract No. AF 04(611)-10789.

2.4 QUALITATIVE PREDICTION OF THE RELIABILITY AND MAINTAINABILITY OF STORABLE PREPACKAGED MOTORS

(U) Based on experimental data presently available, an estimate can be made of the relative reliability and maintainability of earth-storable prepackaged hybrid rocket motors should they be reduced to operational use, utilizing the technology acquired under this program. This specific program has been primarily concerned with developing technology relative to the thrust chamber assembly (TCA), which includes the oxidizer valve, injectors, fuel grain, and nozzle. Of these components, the two most significant items pertinent to the reliability and maintainability of hybrids are the injectors and fuel grain, the remaining components being based on state of the art liquid and solid rocket technology.

(U) The primary injectors used in the full-scale motors have injector port openings approximately 0.4 in. in diameter. This relatively large opening is expected to lead to greatly simplified maintenance and increased reliability. Injector openings of this size are virtually immune to plugging by particles in the oxidizer supply and from manufacturing defects.

(U) The fuels investigated under this program will not sustain combustion in the absence of oxidizer; as a result, there is little or no possibility of inadvertent ignition or fire and no possibility of detonation. In addition, since the hybrid burning process is controlled predominantly by liquid flow, the solid grain surface does not determine the combustion pressure. Therefore, unlike solid propellants, cracks or voids in a hybrid fuel grain do not lead to faster or uncontrollable burning.

CONFIDENTIAL

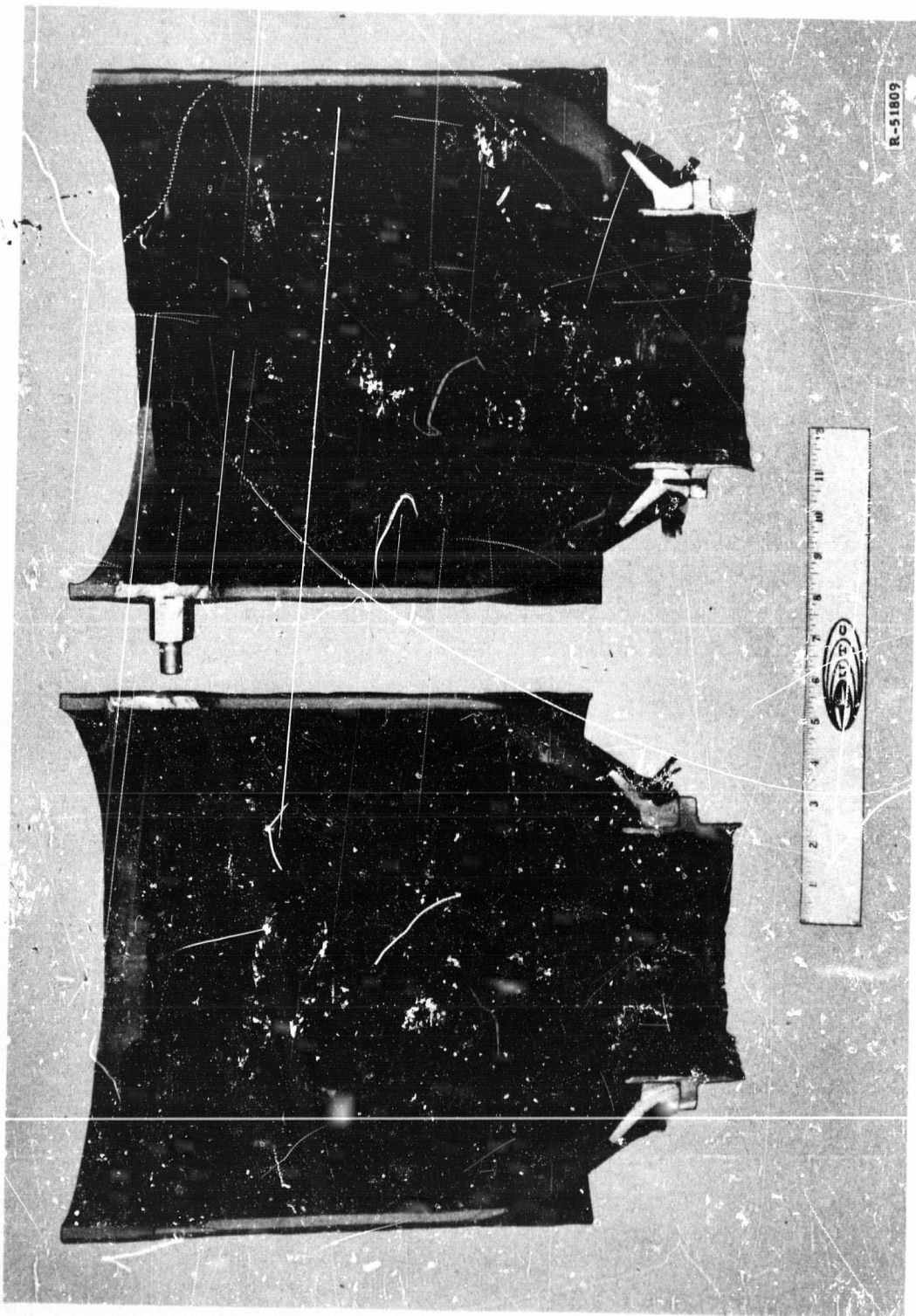
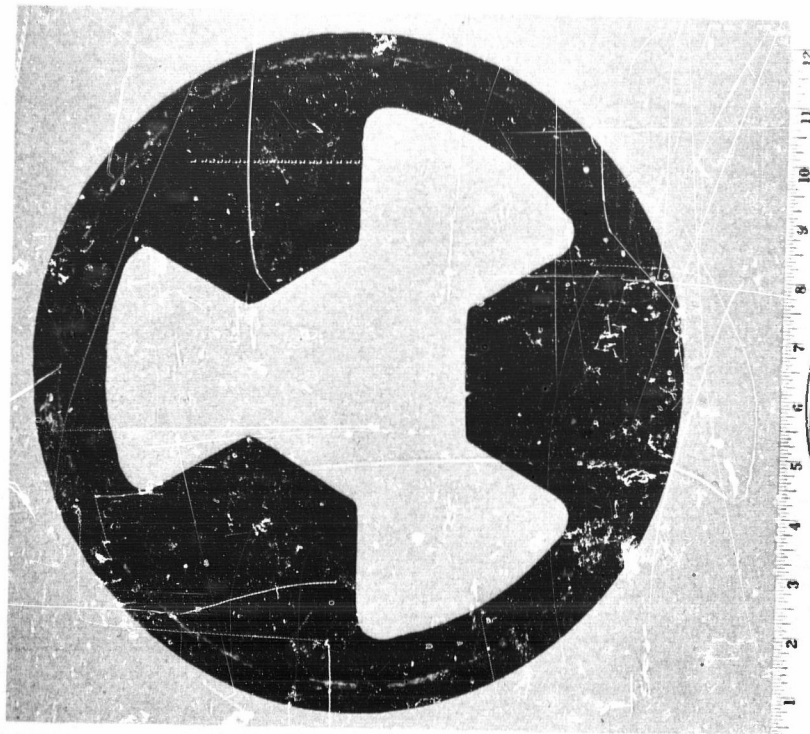


Figure 105. (U) Mixer Assembly From Motor 010 After Test



R-51811

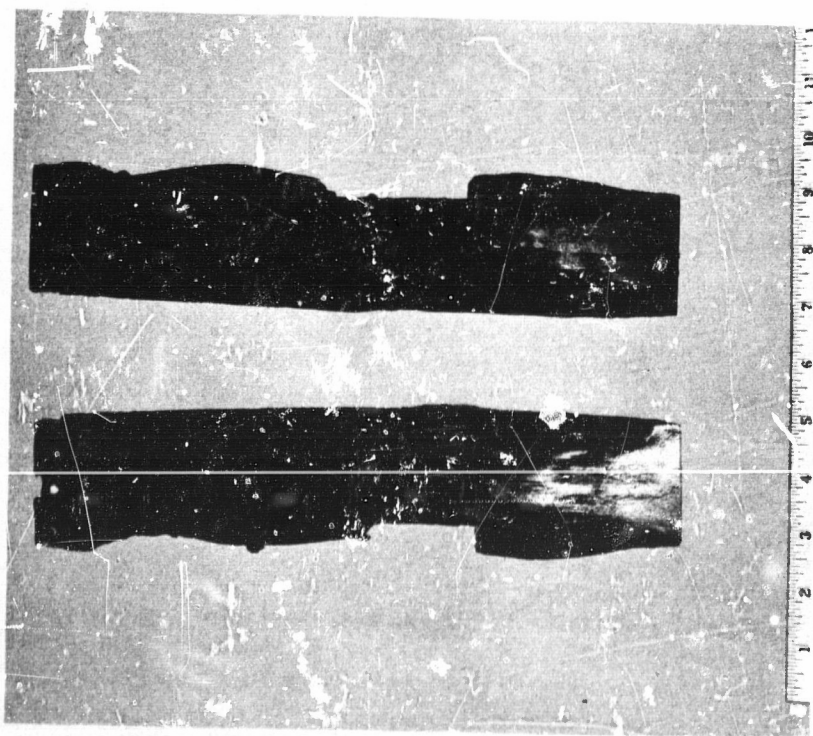


Figure 106. (U) Phenolic Mixer Baffle After Test

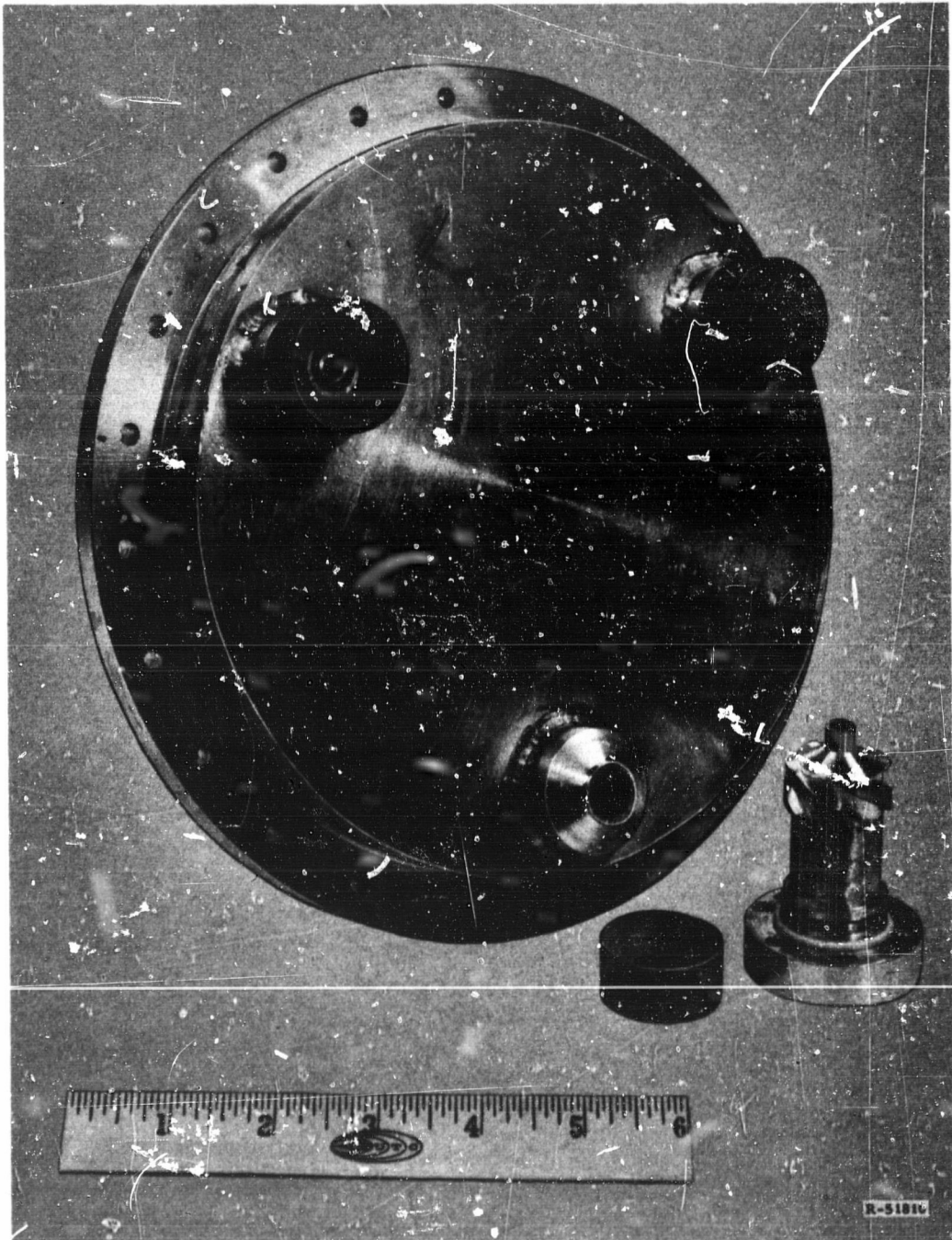


Figure 107. (U) Dust Orifice Injector Assembly

AFRPL-TR-65-184

APPENDIX I
IMPLICATIONS OF PRESSURE-SENSITIVE
HYBRID FUEL SYSTEMS

(U) The implications of pressure-sensitive fuel systems include the possibility of developing a fuel system that would be throttleable with primary oxidizer injection only. Conventional hybrid fuels require aft-end injection of oxidizer during throttling to maintain a constant mixture ratio.

(U) A pronounced pressure sensitivity has been observed with hybrid fuels containing THA and TAZ. Data from motor firings conducted on programs sponsored by UTC indicated that the regression rate of these fuels is dependent upon combustion chamber pressure (P_c) raised to some exponent (m). The conventional dependency of regression rate on oxidizer mass flux also exists, which leads to the assumption that the total regression behavior is expressed by

$$\dot{r} = a P_c^m (G_o')^n \quad (1)$$

where:

- \dot{r} = regression rate, in./sec
- a = constant
- P_c = combustion chamber pressure, psia
- G_o' = instantaneous oxidizer mass flux (\dot{w}_{ox}/A_p), lb/sec-in²
- \dot{w}_{ox} = oxidizer flow rate, lb/sec
- A_p = instantaneous grain port area, in²

The implications of this dependency include the possibility of developing a fuel system that would be throttleable with forward-end oxidizer injection only. Conventional hybrid fuels require aft-end oxidizer injection during throttling to maintain optimum mixture ratio.

(U) If it is assumed that motor thrust is a linear function of total propellant flow rate, that constant mixture ratio (O/F) is maintained, and that the regression rate relationship (equation 1) is applicable, then the thrust of hybrid motors with pressure-sensitive fuels is expressed by:

$$F_n = I_{sp} (\dot{w}_{ox} + \dot{w}_f) \quad (2)$$

in which

$$\dot{w}_f = \rho L P_b \dot{r} \quad (3)$$

where:

- F_n = motor thrust, lb
- ρ = fuel density, lb/in.³
- L = grain length, in.
- \dot{w}_f = fuel flow rate, lb/sec
- P_b = burning perimeter of the fuel grain.

Substituting equation 1 into the above yields:

$$F_n = I_{sp} \dot{w}_{ox} + a p L \left(\frac{P_b}{(A_p)^n} \right) \cdot P_c^m \cdot \dot{w}_{ox}^n \quad (4)$$

If combustion efficiency is assumed constant over the entire throttling range, chamber pressure can be expressed as a linear function of total propellant flow rate:

$$P_c = \frac{c^* (\dot{w}_{ox} + \dot{w}_f)}{A_t g}$$

where:

- c^* = characteristic exhaust velocity, ft/sec
- A_t = nozzle throat area, in.²
- g = gravitational constant.

Substituting the above equation for chamber pressure yields

$$F_n = I_{sp} \left[\dot{w}_{ox} + a p L \left(\frac{P_b}{(A_p)^n} \right) \left(\frac{c^*}{A_t g} \right)^m (\dot{w}_{ox} + \dot{w}_f)^m (\dot{w}_{ox})^n \right]$$

then

$$F_n = I_{sp} \left[\dot{w}_{ox} + \dot{w}_{ox}^{(m+n)} a_p L \frac{P_b}{(A_p)^n} \left(\frac{c^*}{A_t g} \right)^m \left(1 + \frac{1}{O/F} \right)^m \right] \quad (2)$$

where all factors except oxidizer flow are constant.

(U) The above relationship describes motor thrust as a linear function of forward-end oxidizer flow rate only if the sum of the exponents ($m + n$) is equal to 1.0.

(U) Because of grain design consideration, the G_o ' exponent (n) should be equal to or less than 0.5. Therefore, a throttleable hybrid motor using pressure-sensitive fuels is feasible if the pressure exponent (m) is greater than 0.5.

AFRPL-TR-65-184

APPENDIX II
METHOD FOR DETERMINING REGRESSION RATE
EQUATION FOR PRESSURE-SENSITIVE FUEL SYSTEM

(U) The method by which a regression rate characterization equation is obtained consists of determining the exponents m and n and the coefficient a of the anticipated form of the equation

$$\dot{r} = a P_c^m G_o^n \quad (1)$$

where

- \dot{r} = regression rate, in./sec
- a = coefficient
- P_c = chamber pressure, psi
- G_o = oxidizer mass flux, lb/sec-in.²
- m = pressure exponent
- n = oxidizer mass flux exponent.

(U) For a particular test with a constant oxidizer flow rate and virtually constant chamber pressure, for a cylindrical grain

$$\dot{r} = a P_c^m (G_o')^n = a P_c^m \left(\frac{\dot{w}_{ox}}{A_p} \right)^n = a P_c^m \left(\frac{\dot{w}_{ox}}{\pi R^2} \right)^n \quad (2)$$

Because R is now the only variable,

$$\dot{r} = CR^{-2n} \quad (3)$$

where C is a constant, including the other terms. Therefore,

$$\ln \dot{r} = -2n \ln R = \ln C \quad (4)$$

(U) By taking the differences in ΔR and time between probe data points, average values of regression rate ($\Delta R/\Delta t$) can be determined. By a method involving the calculation of least square error, the values of the terms n and C in equation 4 can be determined to fit the data best.

(U) Integration of equation 3 results in

$$R^{2n+1} = R_0^{2n+1} + C(2n+1)t \quad (5)$$

where R is the instantaneous port radius corresponding to the time (t) and R_0 is the initial port radius. By substituting the determined values of n into equation 5 with measured values of initial and final fuel port measurements and burning time, the value of C can be determined.

(U) Because C is a function of $(P_c)^m$, the values of C between any two tests can be used to determine the value of the exponent, m , with the following relationship:

$$\frac{C_1}{C_2} = \left(\frac{P_{c1}}{P_{c2}} \right)^m \quad (6)$$

Since $C = a P_c^m (w_{ox}/\pi)^n$ and all terms are now known except a , it can be calculated and included in the fuel characterization equation

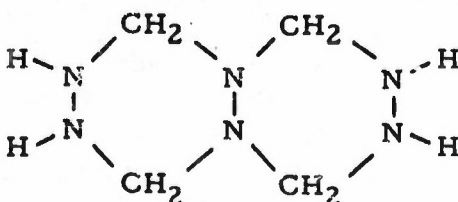
$$\dot{r} = a P_c^m G_o^n \quad (7)$$

APPENDIX III
THERMOCHEMISTRY OF A HIGH-NITROGEN
PROPELLANT INGREDIENT

THERMOCHEMISTRY OF A HIGH-NITROGEN
PROPELLANT INGREDIENT

INTRODUCTION

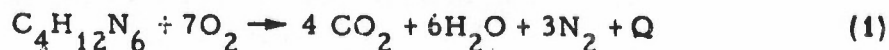
(C) On the basis of an estimated heat-of-formation value of tetraformal-trisazine (TFTA) ranging from +27 to +120 kcal/mole (depending on the assigned bond energies) and the inexpensive nature of the starting material used in synthesizing the amine, TFTA appears to be a similarly energetic but more economical substitute for propellant ingredients such as THA, TAG, and TAZ. However, the theoretical potential of TFTA as a propellant ingredient depends to a large extent upon the heat of formation assigned to the compound. Owing to variations in the theoretical specific impulse which can be ascribed as a result of the uncertainties in the heat of formation estimated from bond energies, it is necessary to define the heat of formation from experimental heats of combustion to obtain a valid evaluation of the potential of this material. The structural formula for TFTA is shown below.



THEORETICAL CONSIDERATIONS

(C) The heat of formation of a compound can be derived from experimental heat-of-combustion data provided the concentrations and heats of formation of the combustion products are known. The concentrations of the combustion products can be determined by direct chemical analysis or computed from the empirical formula of the compound, assuming complete reaction. The latter technique can be successfully applied to oxygen bomb calorimetry of organic compounds where combustion is generally stoichiometric, yielding water, carbon dioxide, and nitrogen.

(C) For TFTA, the complete combustion reaction (i. e. , the lowest energy state) under bomb conditions is:



where Q is the energy change of the combustion reaction under constant-volume and constant-pressure conditions, as $\Delta n(g) = 0$.

From Hess' Law, the heat of formation of TFTA utilizing equation 1 becomes:

$$\Delta H_f = 4\Delta H_f\text{CO}_2(g) + 6\Delta H_f\text{H}_2\text{O}(l) + 3\Delta H_f\text{N}_2(g) - 7\Delta H_f\text{O}_2(g) - Q. \quad (2)$$

Substituting known heat-of-formation values for the appropriate terms, equation 2 reduces to the following:

$$\Delta H_f = -786.1 - Q. \quad (3)$$

APPARATUS AND TECHNIQUE

(C) Combustions were conducted in a standard stainless steel oxygen bomb (Parr Instrument Company) immersed in demineralized water in a cylindrical 7-liter silvered Dewar flask. Extending through holes in an aluminum-encased polystyrene foam lid were a metal stirrer, a glass-sheathed platinum resistance thermometer, the igniter wires, and two calibration heaters wired in parallel.

(C) The sample was ignited by passing an electrical current supplied by a standard Parr transformer through a short length of fuse wire between electrodes inside the bomb. Temperatures of the calorimeter water bath were determined from measurements with a platinum resistance thermometer using a Mueller bridge.

(C) The heat capacity of the calorimeter was determined electrically by passing a known current through heaters of known resistance for a measured time period and then following the temperature rise of the system.

(C) Corrections made for the observed heat rise during combustion included those for nitrogen oxides, the oxidation of the nichrome fuse wire, and the heat leak of the calorimeter.

PROCEDURE

(C) A 0.1- to 0.2-g sample of TFTA was weighed in the combustion cup to an accuracy of ± 0.1 mg. The cup was placed in the bomb, and a 10-cm length of nichrome fuse wire was installed between the electrodes in such a manner that the wire rested about 1-mm above the sample. Five ml of demineralized water were added to the bomb to absorb nitrogen oxides formed in the combustion. The bomb was then closed, pressurized slowly to 25 to 30 atm with oxygen, and placed in the bottom of the Dewar flask. The electrical leads were attached and approximately 4 liters of demineralized water were added, covering the bomb and immersing the stirring paddle, the resistance thermometer, and the calibration heaters. Stirring was commenced at a predetermined constant rate such that equilibration time between ignition and attainment of the final drift rate was a minimum. Periodic temperature measurements were made until a steady initial drift rate was observed. At the end of this period, the firing circuit was energized. Temperature measurements were taken during the heat-release period and attainment of the new steady state and continued at intervals to determine the drift rate at the higher temperature.

(C) In a similar manner, the heat rise was then determined during a 1-min electrical calibration period, during which time the average current flow through the heaters was determined from the voltage drop across a standard resistance.

(C) Three corrections were made for the observed heat generated in each experiment. The first correction was made on the basis of nitrogen oxides formed in the combustion (instead of molecular nitrogen as assumed in equation 1) and from atmospheric nitrogen initially in the bomb before pressurization. This correction was determined by titrating the bomb washings with standard alkali after combustion. The total acidity found was assumed to be nitric acid, and a subtractive correction of 13.6 cal/millimole of nitric acid was made on the observed heat release.

(C) A second subtractive correction was applied to the observed heat release to account for the oxidation of the nichrome fuse wire. As the known caloric value of this type of fuse is 2.3 cal/cm, the length of unburned fuse was measured and the number of calories liberated by the oxidized portion subtracted from the total heat released.

(C) In those cases where the initial and final drift rate periods had unequal slopes, the true temperature rise for the reaction was determined by subtracting a heat-leak correction employing the average slope of the two drift lines and the time separating these steady states from the observed equilibrium temperature rise. A time-temperature curve in which this correction was not necessary is shown in figure III-1.

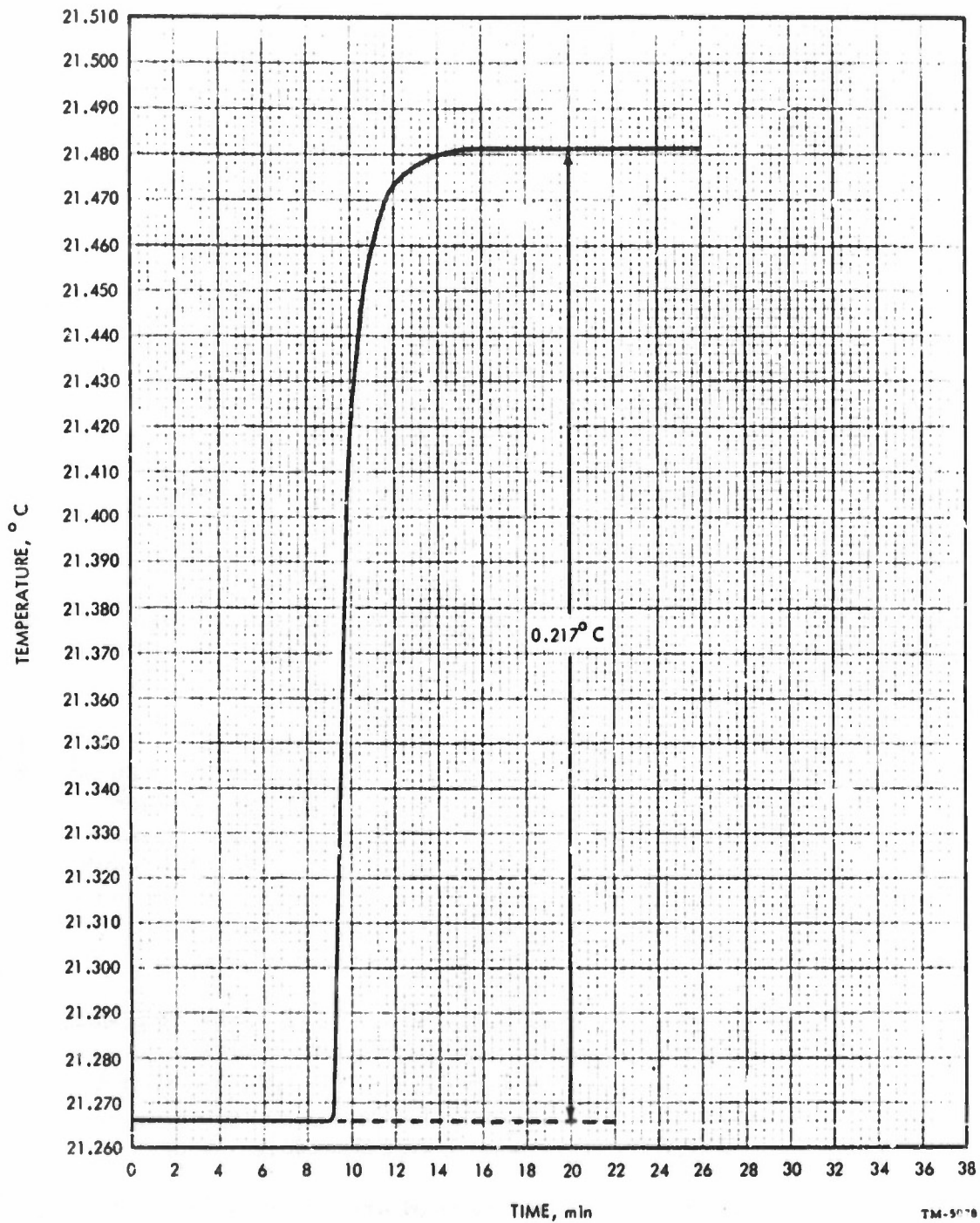


Figure 'II-1. (C) TFTA Combustion, Run No. 9

MATERIALS

(C) All materials were used as received. * Samples designated by A were recrystallized from water; those designated by B were washed after preparation with methanol, while C samples were extensively extracted with methanol after preparation. The infrared spectrum of the C samples was equivalent to the published spectrum for TFTA. **

RESULTS

(C) The results of the combustion experiments in terms of observed heat generation, the corrections made, and derived heat-of-formation values are summarized in table III-1.

DISCUSSION

(C) As can be noted from table I, there is a wide discrepancy in the experimentally derived heat-of-formation value of sample A in comparison to the values obtained for samples B and C. This discrepancy is consistent with the theory that sample A is of different composition than the other samples, and the wide variation from theoretical supports the hypothesis that sample A is not entirely TFTA. Before combustion, sample A had a strong odor of ammonia whereas samples B and C were odorless. The combustion reaction of sample A appeared to proceed at a different rate from that of sample B or C, and a sharp, audible detonation occurred in the latter case but not the former. Inspection of the bomb interior after the combustion of sample A revealed the presence of small amounts of a yellow liquid which was not present in the case of sample B or C. Finally, the amount of nitric acid formed per gram of sample A was approximately one-half that of sample B or C.

(C) The slightly more endothermic heat-of-formation values of sample C compared to sample B may be rationalized by assuming that the additional washing in methanol removed small amounts of impurities.

(C) Two separate cross-checks indicated that combustion occurred to the same extent in all of the combustion reactions with sample C. First, the amount of nitric acid produced from a combustion should be directly

* Materials were prepared and provided by Dr. E. G. Vessel.

** "Development of High-Nitrogen Polymers," Annual Progress Report 1 June 1960 to 31 May 1961, Contract AF 04(611)-5689, Food Machinery and Chemical Corporation, Inorganic Research and Development Department, Princeton, N. J., 1961.

TABLE III-1
EXPERIMENTAL RESULTS

	Run No.								
	1	2	3	4	5	6	7	8	9
Sample history	A	A	B	B	C	C	C	C	C
Weight of sample, gm	0.2182	0.2380	0.1853	0.1503	0.1685	0.1607	0.1884	0.1731	0.1549
Moles of sample $\times 10^{-3}$	1.513	1.650	1.285	1.042	1.169	1.114	1.307	1.200	1.074
C_p calorimeter, kcal/degree	4.465	4.452	4.396	4.3545	4.4879	4.4754	4.4643	4.4111	4.3895
$\Delta t_{corrected}$, °C	0.245	0.271	0.257	0.211	0.232	0.219	0.258	0.242	0.217
Kcal released	1.094	1.206	1.1297	0.9188	1.0412	0.9800	1.1518	1.0675	0.9525
Fuse correction, cal	12	17	9	10.5	14.5	4.5	7.5	11	10
HNO_3 correction, cal	5	6	10	7.1	8.8	6.3	9.4	9	8.1
Corrected kcal released	1.077	1.183	1.1107	0.9012	1.0179	0.9672	1.1349	1.0475	0.9344
m:moles HNO_3 /weight of sample	1.81	1.77	3.97	3.40	3.78	3.77	3.61	3.76	3.80
Reaction temperature, °C	20.4	21.3	21.1	22.0	21.4	21.5	21.2	21.1	21.4
ΔH_R , kcal/mole	-711.8	-717.0	-864.4	-865.0	-870.7	-868.2	-868.3	-872.9	-870.0
$\Delta H_{combustion}$, kcal/gm	-4.936	-4.971	-5.994	-5.996	-6.041	-6.019	-6.024	-6.051	-6.032
ΔH_f , kcal/mole	-74.3	-69.1	+78.3	+78.9	+84.6	+82.1	+82.2	+86.8	+83.9

A. Sample recrystallized from water
 B. Sample as prepared
 C. Sample as prepared, but additionally washed with MeOH

proportional to the sample size. Secondly, the derived heat-of-formation value should be quite sensitive to variations in the extent of combustion. The consistency of the nitric acid values and derived heats of formation are indicative of complete combustion in each experiment.

(C) The heat of formation results of runs 5 through 9 can be interpreted with a precision of $+83.9 \pm 1.7$ kcal/mole at 21.3°C . The heat of combustion results can be similarly interpreted as -6.033 ± 0.012 kcal/g at 21.3°C .

(C) To obtain an indication of the accuracy of the above results, a sample of standard benzoic acid having a National Bureau of Standards certified heat-of-combustion value of -6.318 kcal/g was burned under identical conditions to that of TFTA. A 1.1640 -g pellet of the standard benzoic acid liberated 7.368 kcal in a calorimetric system of 4.3646 kcal/degree heat capacity, resulting in a heat-of-combustion value of -6.350 kcal/g. The difference between the two heat-of-combustion values can be expressed as 0.00163 kcal difference/kcal liberated. Applying this correction to the average heat-of-formation value of TFTA gives an accuracy limitation of $+83.9 \pm 1.5$ kcal/mole.

AFRPL-TR-65-184

APPENDIX IV
ASSEMBLY DRAWING OF
12-IN. FILAMENT-WOUND HYBRID MOTOR

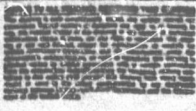
22

21

20

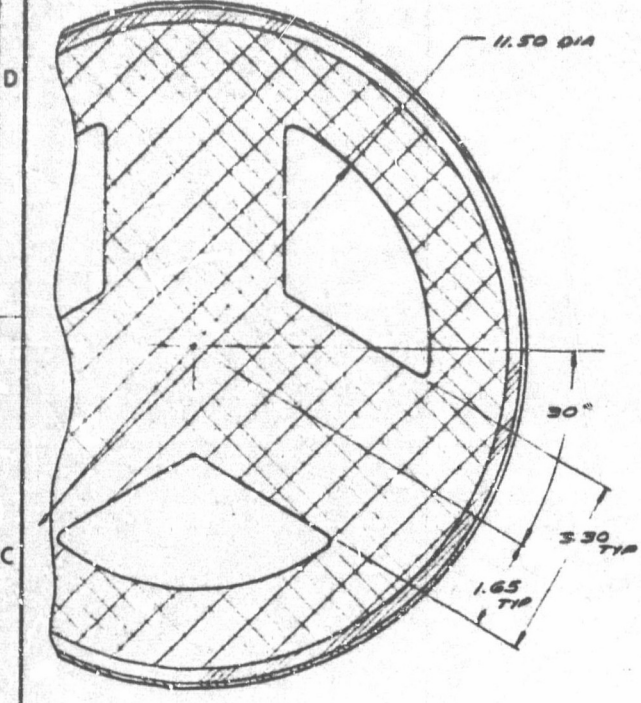
19

18

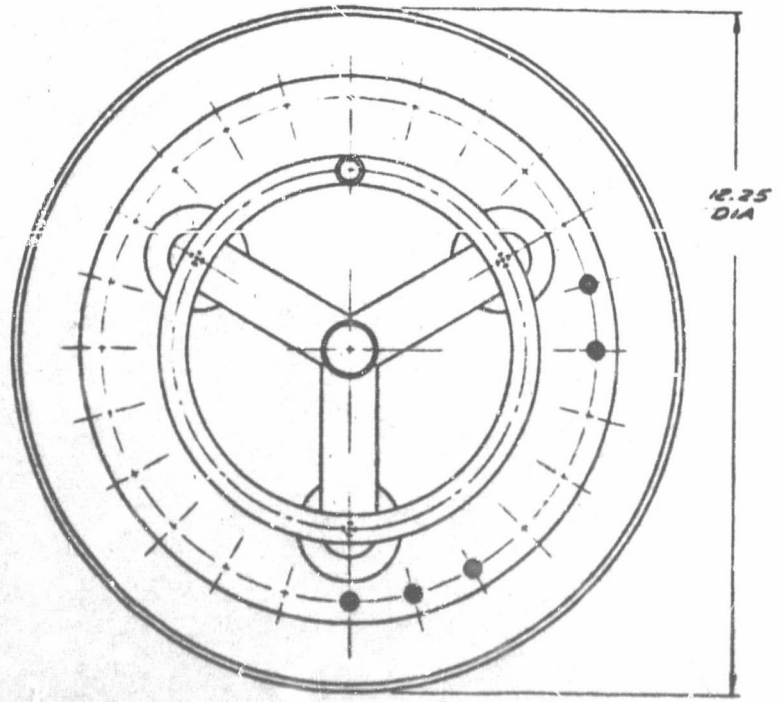
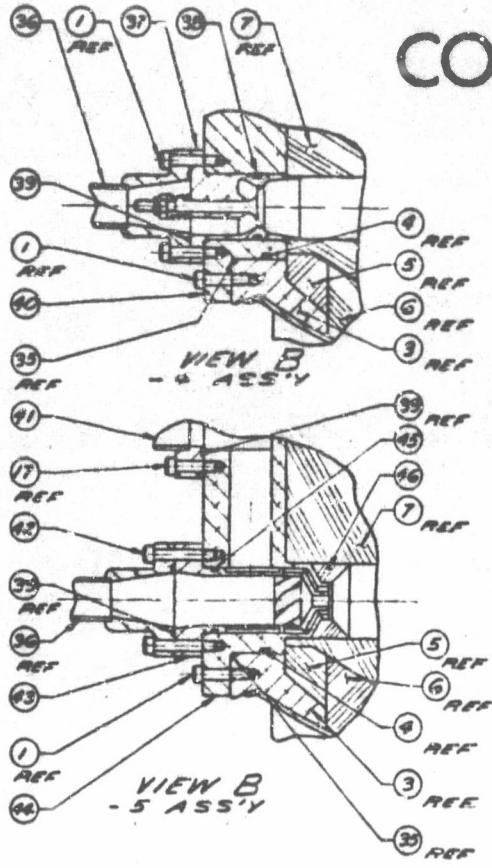


CONFIDE

AFRPL-TR-



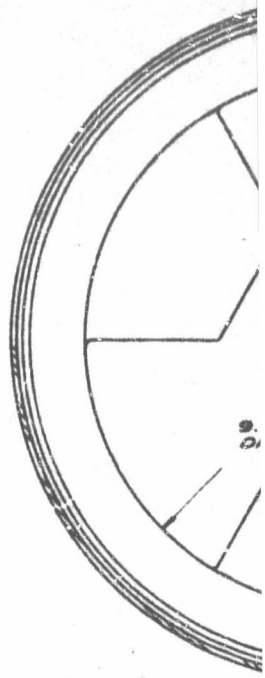
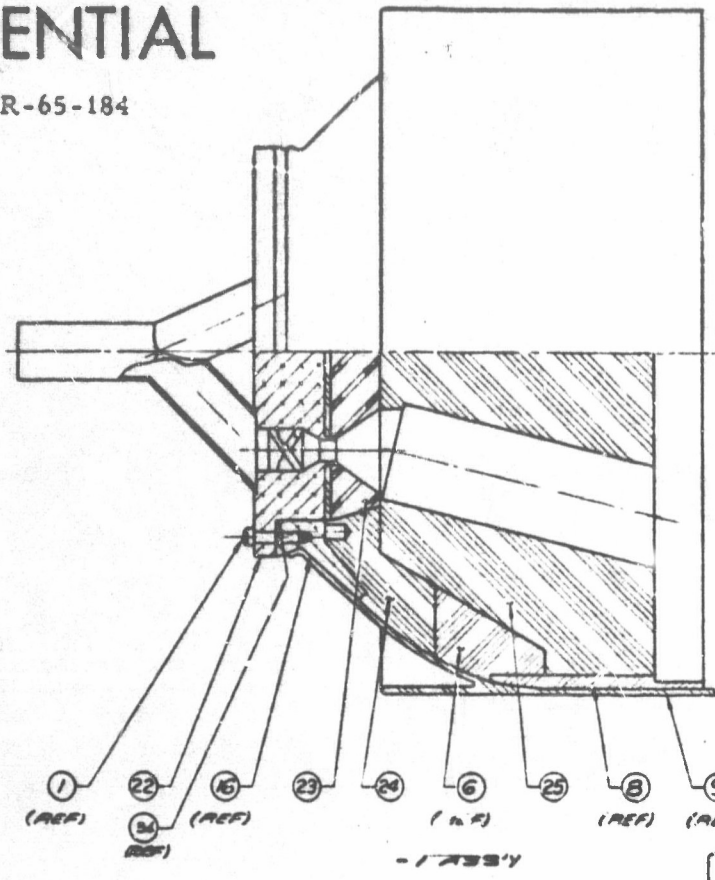
SECTION A-A



5

CONFIDENTIAL

AFRPL-TR-65-184



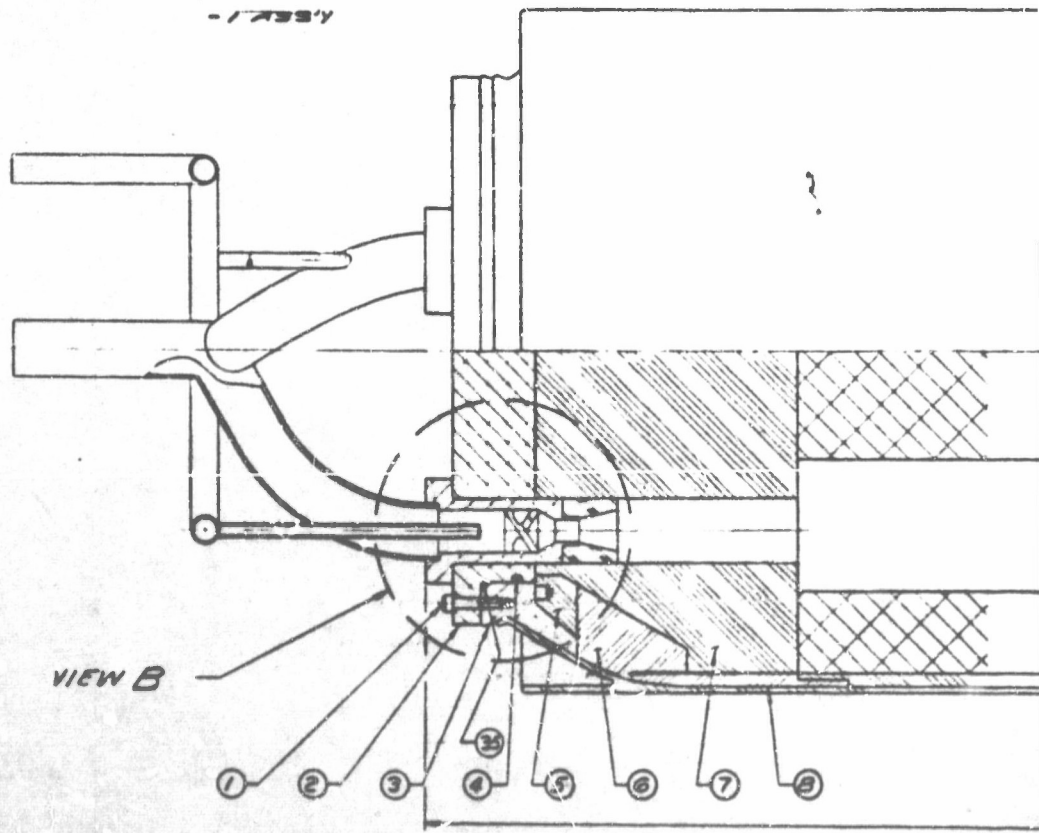
- 4 REF
- 5 REF
- 6 REF
- 3 REF
- 29 REF
- 13 REF
- 16 REF
- 7 REF

- 5 REF
- 6 REF
- 9 REF
- 3 REF
- 30 REF

12.25 DIA

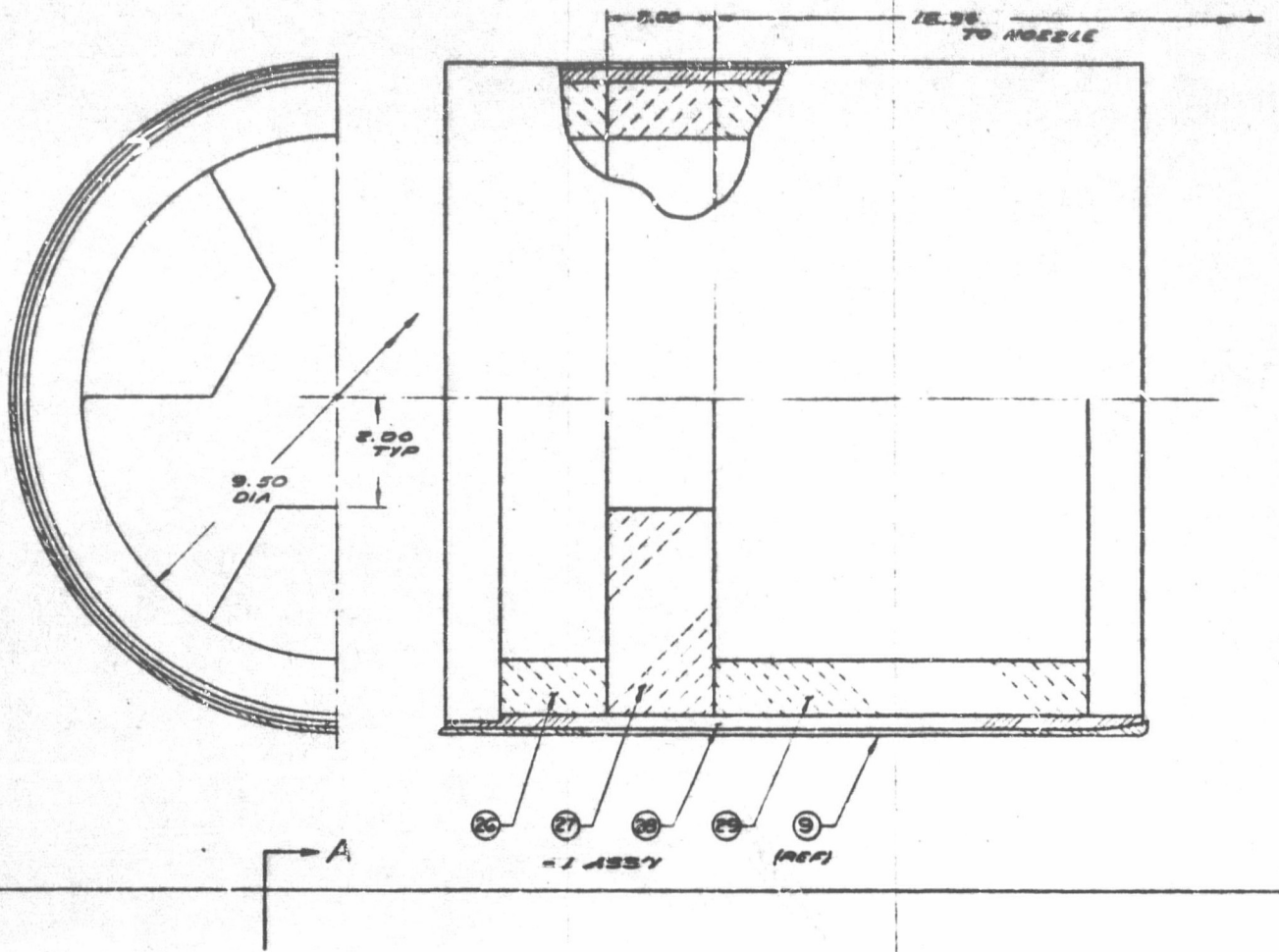
4

VIEW B

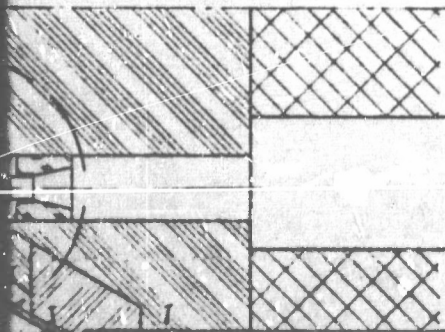


7300-227A

15 14 13 12 11 10



3



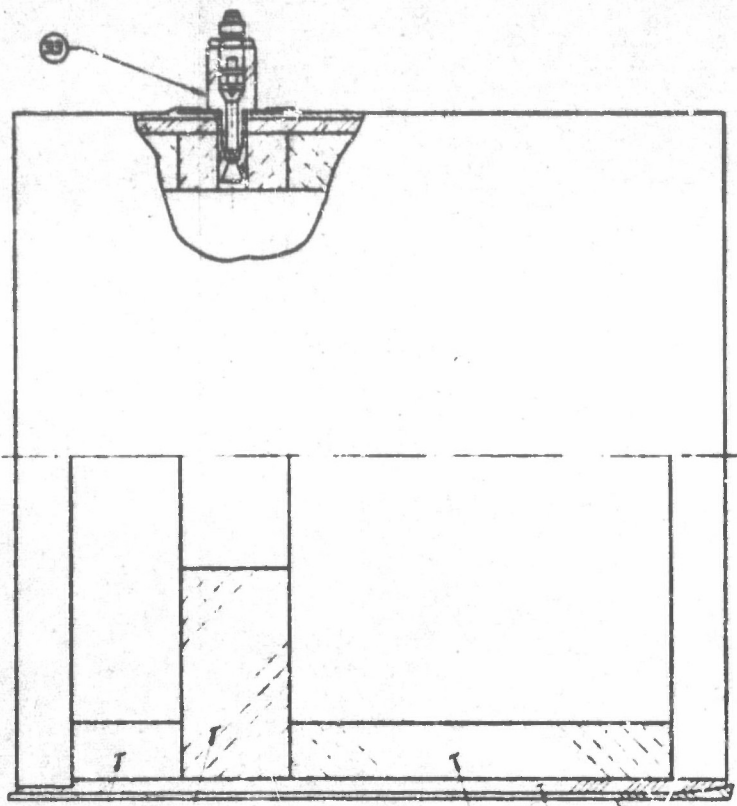
13-1332

13-1332

7306-227A

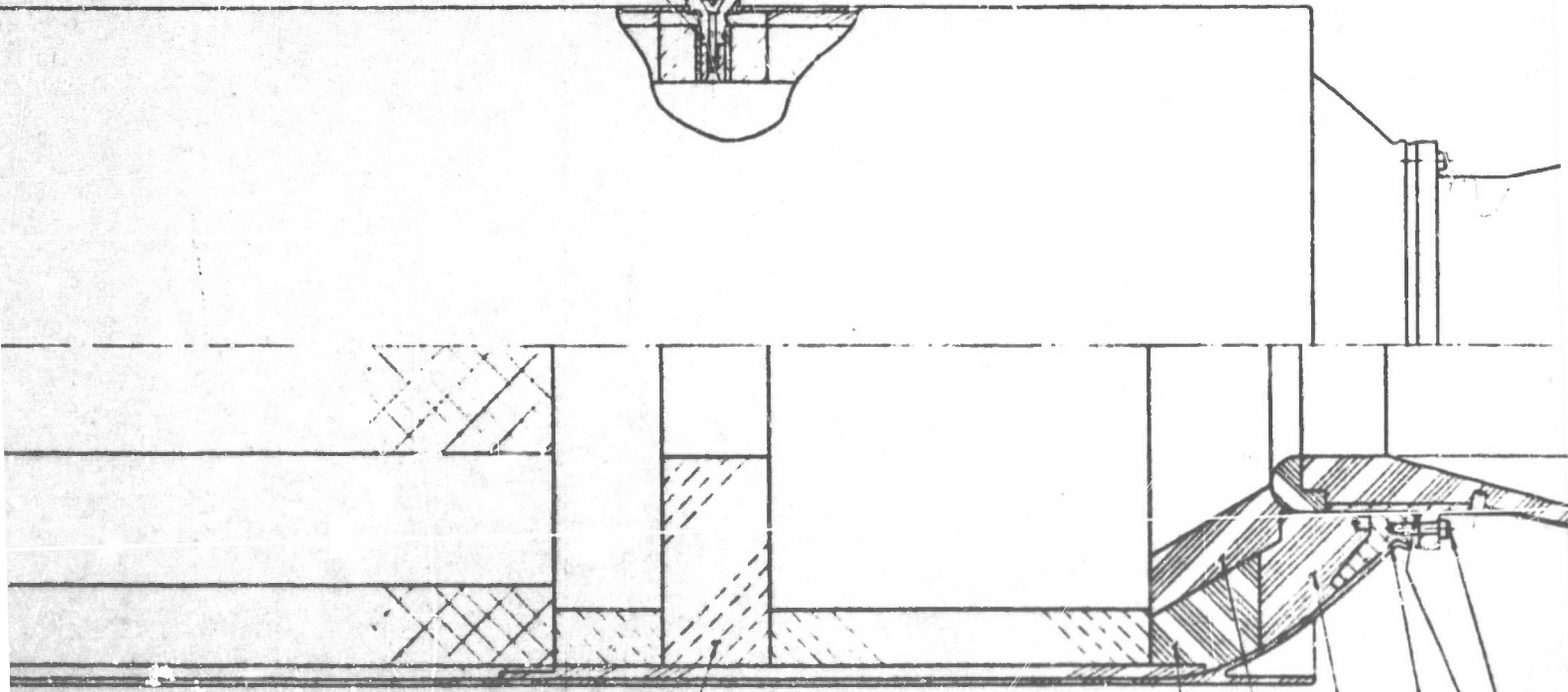
15 14 13 12 11 10

10 | 9 | 8 | 7 | 6



39
26 (REF) 27 (REF) 30 31 32 27 (REF) 26 (REF) 9 (REF)

17.94



2

13 14 15 16 17 18

7300-227

10 | 9 | 8 | 7 | 6 | 5

AFRFL-TR-65-184

APPENDIX V
SUMMARY OF MOTOR TESTS

THROTTLEABLE MOTOR DEVELOPMENT STUDIES (PHASE I)
 TABLE V-1
 ENGINE RESEARCH TEST SUMMARY PRESSURE-SENSITIVE FUELS

Test No.	\dot{w}_{ox}	$\dot{w}_{f_{gav}}$	O/F _{gav}	P _{cav} psia	F _{av}	t _b sec	$\dot{w}_{f_{misc}}$	\dot{w}_t	R _o	R _F
Fuel: 50% THA/50% Binder										
Oxidizer: FLOX										
L6-0211	0.26	0.172	1.51	99	83	26.6	0.025	0.457	0.927	2.010
L6-0212	0.26	0.168	1.54	46	60	40.6	0.017	0.445	—	—
L6-0213	0.26	0.152	1.64	446	108	18.5	0.031	0.443	1.002	1.667
L6-0214	0.25	0.392	0.64	710	139	8.4	0.014	0.656	0.984	1.667
L6-0216	1.10	0.228	4.83	100	233	20.3	0.054	1.382	0.991	1.963
L6-0217	1.09	0.222	4.91	133	254	18.4	0.050	1.362	0.985	1.873
L6-0218	1.10	0.269	4.09	234	313	14.3	0.054	1.423	0.987	1.811
L6-0219	1.10	0.397	2.77	378	264	11.4	0.070	1.567	0.971	1.946
L6-0220	1.67	0.279	5.99	116	335	14.6	0.070	2.019	0.906	1.927
L6-0221	1.67	0.304	5.50	192	379	11.1	0.072	2.046	0.878	1.786
L6-0222	1.67	0.283	5.90	272	407	9.1	0.086	2.039	0.937	1.573
L6-0223	1.69	0.298	5.68	397	446	8.3	0.089	2.077	0.951	1.587
L6-0224	0.74	0.181	4.09	58	142	18.5	0.038	0.959	0.970	1.772
L6-0225	0.74	0.190	3.89	120	178	17.5	0.043	0.973	0.972	1.743
L6-0226	0.74	0.205	3.61	278	228	16.4	0.050	0.995	0.995	1.736
L6-0227	0.74	0.203	3.65	361	240	15.5	0.043	0.986	0.997	1.759
L6-0229	0.74	0.176	4.20	60	141	20.3	0.038	0.954	1.006	1.792
L6-0230	0.74	0.225	3.29	134	183	19.2	0.043	1.008	1.006	1.871
L6-0231	0.74	0.233	3.18	474	237	18.4	0.043	1.016	1.008	1.932
L6-0232	0.75	0.229	3.28	516	243	17.5	0.044	1.023	1.006	1.902
L6-0233	0.26	0.148	1.76	79	91	24.75	0.051	0.459	1.000	1.751
L6-0234	0.75	0.213	3.52	369	237	17.66	0.055	1.018	1.004	1.843
L6-0239	1.13	0.297	3.80	500	339	15.01	0.066	1.493	0.998	1.981
L6-0240	1.65	0.325	5.08	586	450	13.02	0.074	2.049	1.002	1.930
L6-0291	0.282	0.289	0.98	382	93	2.12	0.019	0.590	0.375	0.705
L6-0292	0.283	0.193	1.46	404	99	4.08	0.022	0.498	0.375	0.790
L6-0293	0.281	0.181	1.55	407	95	8.24	0.027	0.489	0.375	1.095
L6-0294	0.283	0.170	1.66	442	104	16.22	0.027	0.480	0.375	1.430
Fuel: 50% THA/50% Binder										
Oxidizer: Liquid Oxygen										
L6-0279	0.58	0.081	7.16	30	56	19.81	0.017	0.678	1.0	1.331
L6-0280	0.59	0.101	5.84	71	91	18.80	0.026	0.717	1.0	1.453
L6-0281	0.59	0.154	3.83	270	134	17.88	0.041	0.785	1.0	1.683
L6-020	0.56	0.174	3.23	337	153	16.13	0.038	0.772	1.0	1.601

THROTTLEABLE MOTOR DEVELOPMENT STUDIES (PHASE I)
TABLE V-2
TEST SUMMARY INJECTOR AND MIXER EVALUATION PROGRAM

Test No.	Injector Tests											Injector
	Fuel	Oxidizer	P _{cav} psia	F _{av} lb	t _b sec	W _{ox} lb/sec	W _{He} lb/sec	O/F	D _p in.	Motor No.		
L6-0250	HFX 2084	FLOX	-	-	14	0.5	-	2.61	2	002	Variable-area hollow cone (checkout)	
L6-0255	HFX 2084	FLOX	230	302	12	1.2	-	2.65	2	003	Solid cone	
L6-0256	HFX 2084	FLOX	187	115	12	0.5	-	2.72	2	004	Variable-area hollow cone (40°)	
L6-0257	HFX 2084	FLOX	58	39	20	0.2	0.011	1.46	2	005	Aerated hollow cone	
L6-0258	HFX 2084	FLOX	48	27	20	0.2	0.008	1.47	2	006	Aerated hollow cone	
L6-0259	HFX 2084	FLOX	315	404	12	1.5	-	2.48	2	007	Showerhead	
L6-0264	HFX 2084	FLOX	89	66	15	0.5	-	4.27	2	008	Variable-area hollow cone (20°)	
L6-0265	HFX 2084	FLOX	73	78	15	0.5	-	3.67	2	009	Variable-area poppet	
L6-0266	HFX 2084	FLOX	44	-	20	0.2	0.0026	3.52	2	010	Aerated hollow cone	
L6-0267	HFX 2084	FLOX	49	-	20	0.2	0.0014	2.20	2	011	Aerated hollow cone	
L6-0260	HFX 2084	FLOX	49	-	20	0.2	0.0014	2.27	2	012	Aerated solid cone	
L6-0283	HFX 2084	FLOX	45	-	30	0.02	0.0014	1.00	2	024	Aerated solid cone	
L6-0284	HFX 2084	FLOX	45	-	30	0.02	0.0014	1.33	2	023	Aerated hollow cone	
L6-0285	HFX 2084	FLOX	96	80	20	0.5	-	3.07	2	022	Variable-area hollow cone (30°)	
L6-0307	HFX 2084	FLOX	262	348	15	1.5	-	2.52	2	021	Impinging streams	

Miscellaneous Tests										
Test No.	Fuel	Oxidizer	P _c psia	F _{av} lb	t _b sec	W _{ox} lb/sec	O/F	D _p in.	Motor No.	Objective
L6-02	HFX 2084	FLOX	321	48	16	1.95	2.34	2	-	Magnesia-asbestos/phenolic mixer
L6-0236	HFX 2084	FLOX	232	358	5	1.3	2.44	3 Spoke	-	Stop-start demonstration
L6-0237	HFX 2084	FLOX	220	336	5	1.3	2.44	3 Spoke	-	Stop-start demonstration
L6-0238	HFX 2084	FLOX	219	336	5	1.3	2.44	3 Spoke	-	Stop-start demonstration
L6-0241	HFX 2084	FLOX	200	280	15	1.0	2.76	3 Spoke	001	Spray-ring aft injector

THROTTLEABLE MOTOR DEVELOPMENT STUDIES (PHASE I)

TABLE V-3

FULL-SCALE MOTOR TEST SUMMARY HIGH-ENERGY PROPELLANT SYSTEM

Test No.	Motor No.	\bar{P} , c. psia	F , lb	\dot{W}_{ox} lb/sec	t_B sec	W_f lb/sec	ϵ	O/F	Remarks
L6-0215	-	500	5170	14.3	8.0	4.84	2.95		Cartwheel grain, steel case
L6-0246	001	177-17	4310-80	10.3	20.0	-	3.0	-	Throttled, glass case
L6-0247	001	215-69	4690-1760	13.5-4.0	8.5	-	3.0	-	Throttled
L6-0252	002	269	5777	12.4	13.5	-	3.0	-	Full thrust performance
L6-0295	003	285	4800	12.6	1.4	-	3.0	-	Aft injector failure
L6-0309	003	257	4388	12.2	1.6	-	3.0	-	Aft injector failure
L6-0320	004	302-51	4500-750	14.3-1.8	14.4	-	1.0	-	Throttled, constant aft flow
L6-0360	005	-	-	-	29.5	-	1.0	-	Data lost, low thrust
L6-0376	005	32	209	1.4	61.0	0.71	1.0	1.97	Low-thrust performance
L6-0477	006	347-38	5213-393	17.1-1.3	13.4	-	1.0	-	Throttled, constant aft flow
L6-0494	007	281	4724	14.2	12.0	4.23	3.0	3.36	OF ₂ performance

PREPACKAGED HYBRID PROP

TABLE

3.5-IN. MOTOR FUEL

Test No.	P _c psia	Firing Duration	Oxidizer Flux	O/F Ratio	Regression Rate	Fuel Density	Added N ₂ %	Metal %	Added O ₂ %	Binder %
L4-0236	463	12.6	0.067	8.53	0.012	0.033	-	-	-	100 R/TDI
H15A14	560	11.9	0.089	14.5	0.015	0.035	-	-	-	100 R/TDI
L4-0237	848	0.02	0.089	-	-	0.038	-	-	-	100 QX/DER
H15A11	600	12.2	0.090	11.4	0.019	0.036	-	-	-	100 QX/DER
L4-0238	729	12.8	0.092	7.05	0.022	0.038	85 TAZ	-	-	65 R/TDI
H15A15	770	12.3	0.091	11.0	0.024	0.042	35 TAZ	-	-	65 QX/DER
L4-0239	825	7.3	0.098	-	-	0.040	35 TFTA	-	-	65 QX/DER
H15A13	583	12.0	0.090	14.5	0.014	0.036	-	-	7.5 AP	92.5 R/TDI
H15A10	560	12.1	0.091	11.0	0.018	0.040	-	-	7.5 AP	92.5 QX/DER
L4-0240	724	12.7	0.090	6.09	0.027	0.041	35 TAZ	-	7.5 AP	57.5 R/TDI
H15A16	925	1.3	0.089	-	-	0.043	35 TAZ	-	7.5 AP	57.5 QX/DER
L4-0241	646	13.0	0.093	5.97	0.027	0.044	35 TFTA	-	7.5 AP	57.5 QX/DER
H15A12	575	12.5	0.092	12.5	0.016	0.035	-	-	10 AP	90 R/TDI
H15A9	656	11.9	0.090	9.81	0.019	0.040	-	-	10 AP	90 QX/DER
L4-0242	741	1.5	0.091	3.99	0.038	0.042	35 TAZ	-	10 AP	55 R/IDI
H15A17	845	12.3	0.093	4.61	0.039	0.047	35 TAZ	-	10 AP	55 QX/DER
L4-0243	625	1.1	0.094	-	-	0.040	35 TFTA	-	10 AP	55 R/TDI
L4-0244	486	12.8	0.094	8.46	0.020	0.040	35 TFTA	-	10 AP	55 R/TDI
L4-0245	774	12.6	0.091	5.48	0.037	0.036	35 TFTA	-	10 AP	55 QX/DER
H15A4	638	9.7	0.090	9.26	0.023	0.038	-	-	12.5 AP	87.5 R/TDI
H15A5	645	12.3	0.090	9.64	0.021	0.040	-	-	12.5 AP	87.5 QX/DER
L4-0246	774	4.7	0.091	-	-	0.042	35 TAZ	-	12.5 AP	52.5 R/TDI
H15A28	750	0.4	0.090	-	-	0.045	35 TAZ	-	12.5 AP	52.5 QX/DER
H15A19	735	4.1	0.092	-	0.039	0.043	35 TFTA	-	12.5 AP	52.5 QX/DER

2 CONFIDENTIAL

TABLE V-4

AFRPL-TR-65-184

MOTOR FUEL EVALUATION TESTS

L4-0245	774	12.6	0.091	5.48	0.037	0.036	35	TFTA	-	10 AP	55 QX/DER
H15A4	638	9.7	0.090	9.26	0.023	0.038	-	-	-	12.5 AP	87.5 R/TDI
H15A5	645	12.3	0.090	9.64	0.021	0.040	-	-	-	12.5 AP	87.5 QX/DER
L4-0246	774	4.7	0.091	-	-	0.042	35	TAZ	-	12.5 AF	52.5 R/TDI
H15A28	750	0.4	0.090	-	-	0.045	35	TAZ	-	12.5 AP	52.5 QX/DER
H15A19	735	4.1	0.092	-	0.039	0.043	35	TFTA	-	12.5 AP	52.5 QX/DER
H15A3	697	1.4	-	-	-	0.039	-	-	-	15 AP	85 R/TDI
H15A6	563	12.0	0.089	9.70	0.020	0.041	-	-	-	15 AP	85 QX/DER
L4-0247	700	12.3	0.091	5.02	0.035	0.043	35	IAZ	-	15 AP	50 R/TDI
H15A24	944	10.8	0.091	2.43	0.064	0.042	35	TAZ	-	15 AP	50 QX/DER
L4-0248	691	12.8	0.092	5.26	0.040	0.039	35	TFTA	-	15 AP	50 QX/DER
H15A2	643	11.5	0.092	15.4	0.023	0.038	-	-	-	17.5 AP	82.5 R/TDI
H15A7	635	12.2	0.090	10.4	0.019	0.042	-	-	-	17.5 AP	82.5 QX/DER
H15A1	927	4.6	0.091	7.88	0.021	0.039	-	-	-	20 AP	80 R/TDI
H15A8	560	12.3	0.090	16.0	0.011	0.042	-	-	-	20 AP	80 QX/DER
H15A25	675	11.9	0.094	3.77	0.033	0.048	30	TFTA	15 B	20 AP	35 QX/DER
H15A26	950	11.9	0.094	2.59	0.0623	0.048	30	TFTA	15 A1	20 AP	35 QX/DER
H15A29	850	12.3	0.094	2.63	0.0605	0.048	30	TFTA	15 A1	20 AP	35 QX/DER
H15A27	762	8.6	0.092	2.68	0.073	0.040	30	TFTA	25 B	15 TMETN	30 QX/DER
H15A31	908	12.3	0.099	3.41	0.052	0.043	42	TFTA	20 A1	13 TMETN	25 QX/DER
L4-J228	620	9.8	0.091	5.59	0.029	0.044	47	TFTA	-	-	53 QX/DER
L4-0230	490	9.7	0.088	6.97	0.019	0.038	-	-	50 B	-	50 R/TDI
L4-0229	1175	0.9	0.096	-	-	0.042	18	TFTA	27 B	-	55 R/TDI
L4-0231	454	19.2	0.091	4.62	0.038	0.042	-	-	25 B	25 AP	50 R/TDI
L4-0232	542	19.4	0.091	4.29	0.036	0.048	-	-	30 B	30 AP	40 R/TDI
L4-0235	683	14.5	0.092	5.32	0.045	0.036	31	TAZ	26 B	4 AP	39 R/TDI
L4-0234	490	19.6	0.097	5.57	0.034	0.040	29	TAZ	25 B	4 AP	42 R/TDI
L4-0224	595	5.4	0.228	9.12	-	0.039	29	TAZ	25 B	4 AP	42 R/TDI
L4-0225	527	5.2	0.242	9.18	0.051	0.039	29	IAZ	25 B	4 AP	42 R/TDI
L4-0226	975	1.0	0.245	-	-	0.038	29	TAZ	25 B	4 AP	42 R/TDI
L4-0227	610	9.8	0.236	11.4	0.046	0.038	29	IAZ	25 B	4 AP	42 T/TDI
H15A18	882	12.1	0.095	3.52	0.048	0.046	31	TFTA	26 B	13 AP	30 QX/DER
L4-0233	243	14.8	0.094	3.33	0.056	0.042	29	TFTA	31 B	21 AP	19 R/TDI
H15A23	-	0.1	-	-	-	-	31	TFTA	22 B	21 AP	26 QX/DER
H15A22	-	0.2	-	-	-	-	42	TFTA	16 B	18 AP	24 QX/DER
H15A21	-	0.1	-	-	-	-	21	TFTA	12 B	46 AP	21 QX/DER
H15A32	210	6.9	0.092	1.61	0.093	0.055	21	TFTA	16 A1	39 AP	24 QX/DER
H15A20	730	12.1	0.094	7.09	0.028	0.043	79.5	TFTA	-	-	20.5 QX/DER

PREPACKAGED HYBRID PROPELLANT STUDIES (PHASE II)

TABLE V-5

TEST SUMMARY
5-IN. FUEL CHARACTERIZATION TESTS

Test No.	P _c psia	F lb	w _{ox} lb/sec	w _{total} lb/sec	c* ft/sec	I _{sp} sec	O/F Ratio	t _b sec	
L4-0262	364	124	0.65	1.06	3989	117	1.56	12.8	} 35% TFTA/20% Al/ 15% AP/30% QX 3812 (Precompacted TFTA)
L4-0263	664	120	0.66	1.03	4005	117	1.80	15.3	
L4-0264	371	246	1.33	1.71	4651	144	3.50	12.8	
L4-0265	724	265	1.35	1.71	4758	155	3.79	15.8	
L4-0266	943	268	1.35	1.72	4587	156	3.61	13.0	
L4-0267	359	382	2.23	2.64	4612	145	5.44	12.8	
L4-0268	724	415	2.24	2.71	4698	153	4.72	12.9	
L4-0269	1044	412	2.25	2.70	5056	153	5.04	12.9	
L4-0271	224	130	0.65	1.21	4190	107	1.19	10.0	} 20% TFTA/23% Al/ 34% AP/23% QX 3812 (TFTA and AP Pelletized)
L4-0272	549	178	0.64	1.15	5024	155	1.26	11.2	
L4-0273	837	175	0.63	1.08	5411	162	1.41	11.9	
L4-0274	579	315	1.33	1.91	5232	165	2.27	11.4	
L4-0275	974	305	1.24	1.83	5368	167	2.12	11.4	
L4-0276	764	521	2.23	2.94	5043	177	3.12	10.1	
L4-0277	489	410	2.23	2.88	4517	143	3.38	8.7	
L4-0278	266	350	2.25	2.76	4416	127	4.42	9.6	
L4-0279	454	163	0.65	1.07	4623	153	1.52	12.0	} 20% TFTA/22% B/ 35% AP/23% QX 3812 (TFTA and AP Pelletized)
L4-0280	608	155	0.66	1.01	4511	154	1.89	12.9	
L4-0281	187	177	1.36	1.68	3506	106	4.28	15.9	
L4-0282	359	205	1.35	1.69	4145	121	4.04	15.8	
L4-0283	551	230	1.37	1.70	4532	135	4.07	15.8	
L4-0284	344	285	2.23	2.65	3681	108	5.31	12.9	
L4-0285	524	355	2.23	2.66	4351	133	5.09	12.9	
L4-0286	620	365	2.23	2.68	4347	136	4.90	12.9	
L4-0288	632	140	0.65	0.90	4645	156	2.57	18.9	} 34% TFTA/19% B/ 15% AP/22% QX 3812 (Precompacted TFTA)
L4-0289	1094	128	0.63	0.93	4687	138	2.14	15.6	
L4-0290	544	242	1.33	1.67	5286	145	3.92	17.8	
L4-0291	719	245	1.35	1.73	5165	142	3.58	15.8	
L4-0292	826	226	1.35	1.74	4985	130	3.47	15.9	
L4-0293	452	378	2.23	2.61	4599	145	5.80	15.8	
L4-0294	789	392	2.23	2.63	5821	149	5.58	15.9	
L4-0295	719	235	2.24	4.84	1667	49	0.86	1.8	
L4-0270	444	320	2.22	2.50	3244	126	7.79	15.9	} 45% TFTA/20% Al/ 35% QX 3812 (Precompacted TFTA)
L4-0287	509	225	1.37	1.63	4870	138	5.10	15.9	
H18A-1	424	129	0.61	0.75	4652	172	4.29	16.0	

PREPACKAGED HYBRID PROPELLANT STUDIES (PHASE II)

TABLE V-6

FULL SCALE MOTOR TEST SUMMARY
PREPACKAGED STORABLE PROPELLANT SYSTEM

Test No.	Motor No.	F _c , psia	F, lb	W _{ox}		t _B , sec	ε	O/F	Remarks
				lb/sec	lb/sec				
L4-0298	008	245	4079	13.7	5.96	4.9	3.0	2.30	-
L4-0299	008	224	3611	13.7	4.88	4.9	3.0	2.81	-
L4-0300	008	214	3403	13.7	4.68	5.0	3.0	2.93	-
L4-0301	008	169	2657	12.8	3.54	14.8	3.0	3.62	-
L4-0302	009	181	2939	13.9	-	30.2	3.0	-	Fuel sustained
L4-0303	010	192	3042	13.5	-	30.0	3.0	-	Fuel sustained

U. S. DEPARTMENT OF THE INTERIOR
BUREAU OF MINES CP-3
4800 FORBES AVENUE,
PITTSBURGH, PA. 15213
ATTN: M. M. DOLINAR, REPTS LIBRARIAN
EXPLOSIVES RESEARCH CENTER(1) 1A

NAT'L AERONAUTICS & SPACE ADMIN.
MANNED SPACECRAFT CENTER CP-10
P. O. BOX 1537
HOUSTON, TEXAS 77001 6A

ATTN: LIBRARY (1)

CENTRAL INTELLIGENCE AGENCY CP-6
2430 E STREET, N.W.
WASHINGTON, D.C. 20505 2A

ATTN: OCD, STANDARD DIST. (1)

OFFICE OF THE DIRECTOR OF DEFENSE
RESEARCH AND ENGINEERING CP-7
WASHINGTON, D.C. 20301
ATTN: DR. H.W. SCHULZ, OFFICE OF
ASST. DIR. (CHEM. TECHNOLOGY) 3A
(1)

NAT'L AERONAUTICS & SPACE ADMIN.
LANGLEY RESEARCH CENTER CP-12
LANGLEY AIR FORCE BASE
VIRGINIA 23365 7-9A

ATTN: LIBRARY (3)

NAT'L AERONAUTICS & SPACE ADMIN.
LEWIS RESEARCH CENTER CP-8
21000 BROOKPARK ROAD
CLEVELAND, OHIO 44135 4A

ATTN: LIBRARY (1)

NAT'L AERONAUTICS & SPACE ADMIN.
WASHINGTON, D.C. 20546 CP-13

ATTN: OFFICE OF TECHNICAL INFO.
& EDUCATIONAL PROGRAMS
CODE ETL (1) 10A

JOHN F. KENNEDY SPACE CENTER CP-9
NAT'L AERONAUTICS & SPACE ADMIN. 5A
COCOA BEACH, FLORIDA 32931

ATTN: LIBRARY
(1)

SCIENTIFIC AND TECH. INFO.
FACILITY CP-14
P. O. BOX 5700
BETHESDA, MARYLAND

ATTN: NASA REPRESENTATIVE (2) 11-12A

COMMANDING OFFICER CP-15
BALLISTIC RESEARCH LABORATORIES
ABERDEEN PROVING GROUND,
MARYLAND 21005

ATTN: AMIBR 1 (1)

13A

U. S. ARMY MISSILE COMMAND CP-29
REDSTONE SCIENTIFIC INFO. CENTER
REDSTONE ARSENAL, ALABAMA 35808

ATTN: CHIEF, DOCUMENT SECTION (4)

19A
20A
21A
22A

COMMANDING OFFICER CP-21
U.S. ARMY RESEARCH OFFICE (DURHAM)
BOX CM, DUKE STATION
DURHAM, NORTH CAROLINA 27706 (1)

14A

COMMANDING GENERAL CP-30
WHITE SANDS MISSILE RANGE
NEW MEXICO 88002
ATTN: TECHNICAL LIBRARY (1)

23A

COMMANDING OFFICER CP-23
FRANKFORD ARSENAL
PHILADELPHIA, PENNSYLVANIA 19137

ATTN: PROPELLANT AND EXPLOSIVES
SECTION, 1331 (1)

15A

BUREAU OF NAVAL WEAPONS CP-34
DEPARTMENT OF THE NAVY
WASHINGTON, D. C. 20360

ATTN: DLI-3 (2)

24A
25A

COMMANDING OFFICER CP-25
PICATINNY ARSENAL
DOVER, NEW JERSEY 07801

ATTN: LIBRARY (1)

16A

BUREAU OF NAVAL WEAPONS CP-35
DEPARTMENT OF THE NAVY
WASHINGTON, D. C. 20360

ATTN: RMMP-2 (2)

26A
27A

BUREAU OF NAVAL WEAPONS CP-37
DEPARTMENT OF THE NAVY
WASHINGTON, D. C. 20360

ATTN: RHMP-4 (1)

28A

COMMANDING OFFICER CP-26
PICATINNY ARSENAL
LIQUID ROCKET PROPULSION LABORATORY
DOVER, NEW JERSEY 07801

ATTN: TECHNICAL LIBRARY (2)

17-18A

BUREAU OF NAVAL WEAPONS
DEPARTMENT OF THE NAVY
WASHINGTON, D. C. 20360

CP-38

ATTN: RRRE-6

(1)

29A

COMMANDING OFFICER
U. S. NAVAL PROPELLANT PLANT
INDIAN HEAD, MARYLAND 20640

CP-46

ATTN: TECH. LIBRARY
(2)

42-43A

COMMANDER
U. S. NAVAL MISSILE CENTER
POINT MUGU, CALIFORNIA 93041

CP-40

ATTN: TECH. LIBRARY

(2)

30A 31A

COMMANDING OFFICER
OFFICE OF NAVAL RESEARCH
1030 E. GREEN STREET
PASADENA, CALIFORNIA 91101
(1)

CP-51

44A

COMMANDER
U. S. NAVAL ORDNANCE LAB.
WHITE OAK
SILVER SPRING, MARYLAND 20910

CP-42

ATTN: LIBRARY

(2)

32A 33A

COMMANDER
U. S. NAVAL ORDNANCE TEST STATION
CHINA LAKE, CALIFORNIA 93557

CP-43

ATTN: CODE 45

(5)

34A 38A

DEPT. OF THE NAVY
OFFICE OF NAVAL RESEARCH
WASHINGTON, D.C. 2036

CP-52

ATTN: CODE 429
(1)

45A

COMMANDER (CODE 753)
U. S. NAVAL ORDNANCE TEST STATION
CHINA LAKE, CALIFORNIA 93557

CP-44

ATTN: TECH. LIBRARY
(2)

39A 40A

DIRECTOR (CODE 6180)
U. S. NAVAL RESEARCH LAB.
WASHINGTON, D. C. 20390

CP-53

ATTN: H.W. CARHART
(1)

46A

SUPERINTENDENT
U. S. NAVAL POSTGRADUATE SCHOOL
NAVAL ACADEMY
MONTEREY, CALIFORNIA 93900
(1)

CP-45

41A

DIRECTOR
SPECIAL PROJECTS OFFICE
DEPARTMENT OF THE NAVY
WASHINGTON, D.C. 20360
(1)

CP-55

47A

COMMANDING OFFICER CP-56
U. S. NAVAL UNDERWATER ORDNANCE
STATION
NEWPORT, RHODE ISLAND 02844

ATTN: W. W. BARTLETT

(1) 48A

AFRPL (RPR) CP-64
EDWARDS, CALIFORNIA 93523

(1)
(2)

72-73A

RTD (RTNP) CP-58
BOLLING AFB
WASHINGTON, D.C. 20332

(1)

49A

AIR FORCE ROCKET PROPULSION LAB.
EDWARDS, CALIFORNIA 93523 CP-65

ATTN: RPM
(1)

74A

ARNOLD ENG. DEVELOPMENT CENTER
AIR FORCE SYSTEMS COMMAND CP-59
TULLAHOMA, TENNESSEE 37389
ATTN: AEOIM
(1)

50A

HEADQUARTERS, U. S. AIR FORCE
WASHINGTON, D. C. 20330 CP-68
ATTN: AFRSTD (1)

75A

DEFENSE DOCUMENTATION CENTER
CAMERON STATION CP-61
ALEXANDRIA, VIRGINIA 22314
(20)

51-70A

OFFICE OF RESEARCH ANALYSIS (OAR)
HOLLOMAN AFB, NEW MEXICO 88330
CP-69

ATTN: RRRT
(1)

76A

AFRPL (RPCL) CP-62
EDWARDS, CALIFORNIA 93523 (1)

71A

AIR FORCE OFFICE OF SCIENTIFIC RES.
WASHINGTON, D. C. 20333 CP-71

ATTN: SREP, DR. J. P. NASI
(1)

77A

WRIGHT-PATTERSON AFB CP-78
OHIO 45433

ATT: AFML (MAAE)

78A

AEROPROJECTS, INC. CP-87
310 EAST ROSEDALE AVENUE
WEST CHESTER, PENNSYLVANIA 19380

ATTN: C. D. MCKINNEY
(1)

85A

AEROJET-GENERAL CORPORATION CP-83
P. O. BOX 296
AZUSA, CALIFORNIA 91703

ATTN: LIBRARIAN
(1)

79A

AEROSPACE CORPORATION CP-88
P. O. BOX 95085
LOS ANGELES, CALIFORNIA 90045

ATT; LIBRARY DOCUMENTS (2)

86A
87A

AEROJET-GENERAL CORPORATION CP-84
11711 SOUTH WOODRUFF AVENUE
DOWNEY, CALIFORNIA 90241

ATTN: P. M. WEST LIBRARIAN
(1)

80A

ALLIED CHEMICAL CORPORATION CP-91
GENERAL CHEMICAL DIVISION
P. O. BOX 405
MORRISTOWN, NEW JERSEY 07960
ATTN: SECURITY OFFICE

88A

AEROJET-GENERAL CORPORATION CP-85
P. O. BOX 1947
SACRAMENTO, CALIFORNIA 95809

ATTN: TECHNICAL LIBRARY 2484-2015A
(3)

81A-83A

CELANESE CORPORATION OF AMERICA CP-92
BOX 3049
ASHEVILLE, NORTH CAROLINA 28802

(1)

89A

AERONUTRONIC DIV. PHILCO CORP. CP-86
FORD ROAD
NEWPORT BEACH, CALIFORNIA 92600

ATTN: DR. L. H. LINDER, MGR.
TECH. INFO. DEPT. (1)

84A

AMERICAN CYANAMID COMPANY CP-93
1937 W. MAIN STREET
STAMFORD, CONNECTICUT 06902

ATTN: SECURITY OFFICER
(1)

90A

IIT RESEARCH INSTITUTE CP-98
TECHNOLOGY CENTER
CHICAGO, ILLINOIS 60616

ATTN: C. L. HERSH,
CHEMISTRY DIVISION (1)

ARO, INC. CP-99
ARNOLD ENGRG. DEV. CENTER
ARNOLD AF STATION, TENNESSEE 37389

ATTN: DR. B. H. GOERTHERT
CHIEF SCIENTIST (1) 92A

ATLANTIC RESEARCH CORPORATION
SHIRLEY HIGHWAY AND EDSALL ROAD
ALEXANDRIA, VIRGINIA 22314 CP-101

ATTN: SECURITY OFFICE FOR LIBRARY
(2) 93-94A

BATTELLE MEMORIAL INSTITUTE CP-103
505 KING AVENUE
COLUMBUS, OHIO 43201

ATTN: REPORT LIBRARY, ROOM 6A
(1) 95A

BELL AEROSTSTEMS
BOX 1
BUFFALO, NEW YORK 14205

ATTN: T. REINHARDT
(1) 96A

THE BOEING COMPANY CP-108
AERO SPACE DIVISION
P. O. BOX 3707
SEATTLE 24, WASHINGTON (1)
ATTN: R. PEERENBOOM, LIBRARY PROCESS
SUPT. (1190) 97A

CHEMICAL PROPULSION INFORMATION
AGENCY CP-114
APPLIED PHYSICS LABORATORY
8621 GEORGIA AVENUE
SILVER SPRING, MARYLAND 20910
(3) 98A
99A
100A

FMC CORPORATION CP-115
CHEM. RESEARCH & DEV. CENTER
P. O. BOX 8
PRINCETON, NEW JERSEY 08540 (1)
101A

DOUGLAS AIRCRAFT CO., INC. CP-122
SANTA MONICA DIVISION
3000 OCEAN PARK BOULEVARD
SANTA MONICA, CALIFORNIA 90405
ATTN: MR. J. L. WAISMAN
(1) 102A

THE DOW CHEMICAL COMPANY CP-123
SECURITY SECTION
BOX 31
MIDLAND, MICHIGAN 48641
ATTN: DR. R. S. KARPIUK,
1710 BUILDING

(1) 103A

HERCULES POWDER COMPANY CP-142
RESEARCH CENTER
WILMINGTON, DELAWARE 19899
ATTN: DR. HERMAN SKOLNIK, MANAGER
TECHNICAL INFORMATION DIV.

108A

E. I. DUPONT DENEMOURS AND COMPANY
EASTERN LABORATORY CP-125
GIBBSTOWN, NEW JERSEY 08027

ATTN: MRS. ALICE R. STEWARD

104A

INSTITUTE OF DEFENSE ANALYSES
400 ARMY-NAVY DRIVE CP-146
ARLINGTON, VIRGINIA 22202
ATTN: CLASSIFIED LIBRARY
(1)

109A

ESSO RESEARCH AND ENGINEERING CO.
SPECIAL PROJECTS UNIT CP-126
P. O. BOX 8
LINDEN, NEW JERSEY 07036

ATTN: MR. D. L. BAEDER

(1)

105A

JET PROPULSION LABORATORY CP-147
4800 OAK GROVE DRIVE
PASADENA, CALIFORNIA 91103

GENERAL DYNAMICS/ASTRONAUTICS
P.O. BOX 1128 CP-133
SAN DIEGO, CALIFORNIA 92112

ATTN: LIBRARY & INFO. SERVICES
(1) (129-00)

106A

LOCKHEED PROPULSION COMPANY CP-152
P. O. BOX 111
REDLANDS, CALIFORNIA 92374

(1)

110A

HERCULES POWDER COMPANY CP-138
ALLEGANY BALLISTICS LABORATORY
P. O. BOX 210
CUMBERLAND, MARYLAND 21501

ATTN: LIBRARY

(1)

107A

ATTN: MISS BELLE BERLAD,
LIBRARIAN

(3)

111A

112

113

GUARDT CORPORATION
4 SATICOY STREET CP-155
2013, SOUTH ANNEX
NUYS, CALIFORNIA 91404

114A

SPACE TECHNOLOGY LABORATORY, INC.
1 SPACE PARK CP-165
REDONDO BEACH, CALIFORNIA 90200

ATTN: STL TECH. LIB. DOC.
ACQUISITIONS

(2) 123A
124A

ESOTA MINING & MANUFACTURING CO.
BUSH AVENUE CP-159
PAUL, MINNESOTA 55106
: CODE 0013 R&D
H. C. ZEMAN
SECURITY ADMINISTRATOR

115A
116A

TEXACO EXPERIMENT INCORPORATED
P. O. BOX 1-T CP-187
RICHMOND, VIRGINIA 23202

ATTN: LIBRARIAN
(1)

125A

ANTO RESEARCH CORPORATION
ON LABORATORY CP-161
ETT, MASSACHUSETTS 02149

117A

THIOKOL CHEMICAL CORPORATION
ALPHA DIVISION, HUNTSVILLE PLANT
HUNTSVILLE, ALABAMA 35800 CP-189

ATTN: TECHNICAL DIRECTOR
(1)

126A

NORTH AMERICAN AVIATION, INC.
SPACE & INFORMATION SYSTEMS DIV.
12214 LAKEWOOD BOULEVARD
DOWNY, CALIFORNIA 90242
ATTN: W. H. MORITA CP-166

118A

ETDYNE CP-180
CANOGA AVENUE
GA PARK, CALIFORNIA 91304

: LIBRARY, DEPT. 596-306

119A
120A
121A

THIOKOL CHEMICAL CORPORATION
ELKTON DIVISION CP-192
ELKTON, MARYLAND 21921

ATTN: LIBRARIAN
(1)

127A

AND HAAS COMPANY CP-182
TONE ARSENAL RESEARCH DIV.
SVILLE, ALABAMA 35808

: LIBRARIAN

122A

THIOKOL CHEMICAL CORPORATION
REACTION MOTORS DIVISION CP-193
DENVER, NEW JERSEY 07834

ATTN: LIBRARIAN
(1)

128A

NAT'L AERONAUTICS & SPACE ADMIN.
WASHINGTON, D.C. 20546 CP-209

ATTN: R. W. ZIEM (RPS)
(1)

134A

THIOKOL CHEMICAL CORPORATION
ROCKET OPERATIONS CENTER CP-194
P. O. BOX 1640
OGDEN, UTAH 84401

ATTN: LIBRARIAN (1)

129A

NAT'L AERONAUTICS & SPACE ADMIN.
GODDARD SPACE FLIGHT CENTER CP-210
GREENBELT, MARYLAND 20771

ATTN: LIBRARY
(1)

135A

THIOKOL CHEMICAL CORPORATION
WASATCH DIVISION CP-195
P. O. BOX 524
BRIGHAM CITY, UTAH 84302

ATTN: LIBRARY SECTION (2)

130-131A

GENERAL ELECTRIC COMPANY CP-211
APOLLO SUPPORT DEPT.
P. O. BOX 2500
DAYTONA BEACH, FLORIDA 32015
ATTN: C. DAY (1)

136A

UNITED AIRCRAFT CORPORATION CP-201
CORPORATION LIBRARY
400 MAIN STREET
EAST HARTFORD, CONNECTICUT 06118

ATTN: MR. DAVID REX (1)

132A

AFSC (CLT/ CAPT. S. W. BOWEN)
ANDREWS AIR FORCE BASE CP-229
WASHINGTON, D. C. 20332
(1)

137A

UNITED AIRCRAFT CORPORATION CP-202
PRATT & WHITNEY P.L.A., RS. & DEV.
CENTER
P. O. BOX 2691
WEST PALM BEACH, FLORIDA 33402
ATTN: LIBRARY (1)

133A

ROCKET RESEARCH CORPORATION CP-231
520 SOUTH PORTLAND STREET
SEATTLE, WASHINGTON 98108

(1)

138A

DENVER SEMINARY CP-232
(UNIVERSITY OF DENVER)
UNIVERSITY PARK
P.O. BOX 10127
DENVER, COLORADO 80210
ATTN: SECURITY OFFICE (1) 139A

CALLERY CHEMICAL COMPANY CP-111
RESEARCH AND DEVELOPMENT
CALLERY, PENNSYLVANIA 16024
ATTN: DOCUMENT CONTROL 145A
(1)

AFFTC (FTBAT-2)
EDWARDS AIR FORCE BASE
CALIFORNIA
ATTN: TECHNICAL LIBRARY (1) 140A

ETHYL CORPORATION CP-127
P. O. BOX 3091
BATON ROUGE, LOUISIANA 70805
(1) 145A

NAT'L AERONAUTICS & SPACE ADMIN.
LANGLEY RESEARCH CENTER
LANGLEY AIR FORCE BASE
VIRGINIA 23365
ATT: ER. C. E. NICHOLS (1) 143A

HYNES RESEARCH CORPORATION CP-144
308 BON AIR AVENUE
DURHAM, NORTH CAROLINA 27704
(1) 147A

AIR UNIVERSITY LIBRARY
MAXWELL AFB, ALABAMA 36112
(1) 142A

LOS ALAMOS SCIENTIFIC LABORATORY
UNIVERSITY OF CALIFORNIA CP-154
P.O. BOX 1663
LOS ALAMOS, NEW MEXICO 87544
(1) 148A

DIRECTOR 141A
ADVANCED RESEARCH PROJECTS AGENCIES
WASHINGTON, D. C. 20301 (1)

GLIN MATHIESON CHEMICAL CORP. CP-168
MARION, ILLINOIS 62959

CATEGORY 2
AIR FORCE ROCKET PROPULSION LAB.
EDWARD, CALIFORNIA 93523
CP-63
ATTN: RPCS (1)

ATTN: RESEARCH LIBRARY
BOX 508
(1) 149A

144A

OLIN MATHIESON CHEMICAL CORP. CP-169
RESEARCH LIBRARY 1-K-3
275 WINCHESTER AVENUE
NEW HAVEN, CONNECTICUT 06511
ATTN: MAIL CONTROL ROOM
(1) MISS LAURA M. KAJUTI

150A

THIokol CHEMICAL CORPORATION
SPACE BOOSTER DIVISION CP-190
BRUNSWICK, GEORGIA 31520

156A

ATTN: LIBRARIAN
(1)

PENNSALT CHEMICALS CORP. CP-170
TECHNOLOGICAL CENTER
900 FIRST AVENUE
KING OF PRUSSIA, PENNSYLVANIA 19406

151A

(1)

CALIFORNIA INSTITUTE OF TECHNOLOGY
1201 E. CALIFORNIA BLVD. CP-221
PASADENA, CALIFORNIA

ATTN: SECURITY OFFICER
(1)

157A

PURDUE UNIVERSITY CP-174
LAFAYETTE, INDIANA 47907

152A

ATTN: M. J. ZUCROW
(1)

DEPARTMENT OF COMMERCE CP-234
OFFICE OF EXPORT CONTROL
WASHINGTON, D.C.

ATTN: CHIEF, CHEMISTRY & FUELS SEC.
PAUL M. TERLIZZI (1)

158A

NORTH AMERICAN AVIATION CP-181
ROCKETDYNE DIVISION
MC GREGOR PLANT
MC GREGOR, TEXAS 75657

153A

(1)

SHELL DEVELOPMENT COMPANY CP-183
1400 53RD STREET
EMERYVILLE, CALIFORNIA 94608
(1)

154A

TEXACO INC. CP188
P. O. BOX 509
BEACON, NEW YORK 12508

ATTN: Dr. R. E. CONARY, Mgr.
(1)

155A

<p>Air Force Flight Test Center, Edwards AF Base, Calif. Rpt. No. AFRPL-TR-65-184. AN INTEGRATED RESEARCH EFFORT ON HIGH-ENERGY HYBRID PROPELLANTS (U) Final report, Oct 1965, 178 p., incl illus., tables. Confidential Report</p> <p>A lightweight 12-in. hybrid test motor has been developed which is capable of delivering 5000-lb thrust for 20-sec duration and up to 90-sec duration at reduced thrust. The motor is capable of multiple restarts and can be throttled over a wide ratio while maintaining a constant mixture ratio. The propellant system and binder have demonstrated their suitability to space-storable mission requirements.</p>	<p>I. AFSC Project 305804 II. Contract AF 04(611)-8516 III. C. W. Vickland</p>
---	--

<p>Air Force Flight Test Center, Edwards AF Base, Calif. Rpt. No. AFRPL-TR-65-184. AN INTEGRATED RESEARCH EFFORT ON HIGH-ENERGY HYBRID PROPELLANTS (U) Final report, Oct 1965, 178 p., incl illus., tables. Confidential Report</p> <p>A lightweight 12-in. hybrid test motor has been developed which is capable of delivering 5000-lb thrust for 20-sec duration and up to 90-sec duration at reduced thrust. The motor is capable of multiple restarts and can be throttled over a wide ratio while maintaining a constant mixture ratio. The propellant system and binder have demonstrated their suitability to space-storable mission requirements.</p>	<p>I. AFSC Project 305804 II. Contract AF 04(611)-8516 III. C. W. Vickland</p>
---	--

<p>Air Force Flight Test Center, Edwards AF Base, Calif. Rpt. No. AFRPL-TR-65-184. AN INTEGRATED RESEARCH EFFORT ON HIGH-ENERGY HYBRID PROPELLANTS (U) Final report, Oct 1965, 178 p., incl illus., tables. Confidential Report</p> <p>A lightweight 12-in. hybrid test motor has been developed which is capable of delivering 5000-lb thrust for 20-sec duration and up to 90-sec duration at reduced thrust. The motor is capable of multiple restarts and can be throttled over a wide ratio while maintaining a constant mixture ratio. The propellant system and binder have demonstrated their suitability to space-storable mission requirements.</p>	<p>I. AFSC Project 305804 II. Contract AF 04(611)-8516 III. C. W. Vickland</p>
---	--

<p>Air Force Flight Test Center, Edwards AF Base, Calif. Rpt. No. AFRPL-TR-65-184. AN INTEGRATED RESEARCH EFFORT ON HIGH-ENERGY HYBRID PROPELLANTS (U) Final report, Oct 1965, 178 p., incl illus., tables. Confidential Report</p> <p>A lightweight 12-in. hybrid test motor has been developed which is capable of delivering 5000-lb thrust for 20-sec duration and up to 90-sec duration at reduced thrust. The motor is capable of multiple restarts and can be throttled over a wide ratio while maintaining a constant mixture ratio. The propellant system and binder have demonstrated their suitability to space-storable mission requirements.</p>	<p>I. AFSC Project 305804 II. Contract AF 04(611)-8516 III. C. W. Vickland</p>
---	--

Formulations studies have resulted in the selection of a potential prepackaged hybrid propellant system which has high theoretical specific and density impulse levels. This fuel system has also been tested in the 12-in. motor.

Formulations studies have resulted in the selection of a potential prepackaged hybrid propellant system which has high theoretical specific and density impulse levels. This fuel system has also been tested in the 12-in. motor.

Formulations studies have resulted in the selection of a potential prepackaged hybrid propellant system which has high theoretical specific and density impulse levels. This fuel system has also been tested in the 12-in. motor.

Formulations studies have resulted in the selection of a potential prepackaged hybrid propellant system which has high theoretical specific and density impulse levels. This fuel system has also been tested in the 12-in. motor.

Air Force Flight Test Center, Edwards AF Base, Calif.
 Rpt. No. AFRPL-TR-65-184. AN INTEGRATED RESEARCH
 EFFORT ON HIGH-ENERGY HYBRID PROPELLANTS (U) III. C. W. Vickland
 Final report, Oct 1965, 178 p., incl illus., tables.
 Confidential Report

A lightweight 12-in. hybrid test motor has been developed which is capable of delivering 5000-lb thrust for 20-sec duration and up to 90-sec duration at reduced thrust. The motor is capable of multiple restarts and can be throttled over a wide ratio while maintaining a constant mixture ratio. The propellant system and binder have demonstrated their suitability to space-storable mission requirements.

Air Force Flight Test Center, Edwards AF Base, Calif.
 Rpt. No. AFRPL-TR-65-134. AN INTEGRATED RESEARCH
 EFFORT ON HIGH-ENERGY HYBRID PROPELLANTS (U) III. C. W. Vickland
 Final report, Oct 1965, 178 p., incl illus., tables.
 Confidential Report

A lightweight 12-in. hybrid test motor has been developed which is capable of delivering 5000-lb thrust for 20-sec duration and up to 90-sec duration at reduced thrust. The motor is capable of multiple restarts and can be throttled over a wide ratio while maintaining a constant mixture ratio. The propellant system and binder have demonstrated their suitability to space-storable mission requirements.

Air Force Flight Test Center, Edwards AF Base, Calif.
 Rpt. No. AFRPL-TR-65-184. AN INTEGRATED RESEARCH
 EFFORT ON HIGH-ENERGY HYBRID PROPELLANTS (U) III. C. W. Vickland
 Final report, Oct 1965, 178 p., incl illus., tables.
 Confidential Report

A lightweight 12-in. hybrid test motor has been developed which is capable of delivering 5000-lb thrust for 20-sec duration and up to 90-sec duration at reduced thrust. The motor is capable of multiple restarts and can be throttled over a wide ratio while maintaining a constant mixture ratio. The propellant system and binder have demonstrated their suitability to space-storable mission requirements.

Air Force Flight Test Center, Edwards AF Base, Calif.
 Rpt. No. AFRPL-TR-65-134. AN INTEGRATED RESEARCH
 EFFORT ON HIGH-ENERGY HYBRID PROPELLANTS (U) III. C. W. Vickland
 Final report, Oct 1965, 178 p., incl illus., tables.
 Confidential Report

A lightweight 12-in. hybrid test motor has been developed which is capable of delivering 5000-lb thrust for 20-sec duration and up to 90-sec duration at reduced thrust. The motor is capable of multiple restarts and can be throttled over a wide ratio while maintaining a constant mixture ratio. The propellant system and binder have demonstrated their suitability to space-storable mission requirements.

Formulations studies have resulted in the selection of a potential prepackaged hybrid propellant system which has high theoretical specific and density impulse levels. This fuel system has also been tested in the 12-in. motor.

Formulations studies have resulted in the selection of a potential prepackaged hybrid propellant system which has high theoretical specific and density impulse levels. This fuel system has also been tested in the 12-in. motor.

Formulations studies have resulted in the selection of a potential prepackaged hybrid propellant system which has high theoretical specific and density impulse levels. This fuel system has also been tested in the 12-in. motor.

Formulations studies have resulted in the selection of a potential prepackaged hybrid propellant system which has high theoretical specific and density impulse levels. This fuel system has also been tested in the 12-in. motor.